Vol. 281, No. 3, September 24, 1993
Completing Volume 281

ISSN 0003-2670

Special issue
BIOSENSORS

ANALYTICA CHIMICA ACTA

An international journal devoted to all branches of analytical chemistry

ELSEVIER

ANALYTICA CHIMICA ACTA

Scope. *Analytica Chimica Acta* publishes original papers, preliminary communications and reviews dealing with every aspect of modern analytical chemistry. Reviews are normally written by invitation of the editors, who welcome suggestions for subjects. Preliminary communications of important urgent work can be printed within four months of submission, if the authors are prepared to forego proofs.

Submission of Papers

Americas

Prof. Harry L. Pardue
Department of Chemistry
1393 BRWN Bldg, Purdue University
West Lafayette, IN 47907-1393
USA

Tel:(+1-317) 494 5320
Fax:(+1-317) 496 1200

Computer Techniques

Prof. J.T. Clerc
Universität Bern
Pharmazeutisches Institut
Baltzerstrasse 5, CH-3012 Bern
Switzerland

Tel:(+41-31) 654171
Fax:(+41-31) 654198

Prof. Sarah C. Rutan
Department of Chemistry
Virginia Commonwealth University
P.O. Box 2006
Richmond, VA 23284-2006
USA
Tel:(+1-804) 367 1298
Fax:(+1-804) 367 8599

Other Papers

Prof. Alan Townshend
Department of Chemistry
The University
Hull HU6 7RX
Great Britain

Tel:(+44-482) 465027
Fax:(+44-482) 466410

Prof. Willem E. van der Linden
Laboratory for Chemical Analysis
Department of Chemical Technology
Twente University of Technology
P.O. Box 217, 7500 AE Enschede
The Netherlands
Tel:(+31-53) 892629
Fax:(+31-53) 356024

Prof. Paul Worsfold
Dept. of Environmental Sciences
University of Plymouth
Plymouth PL4 8AA
Great Britain

Tel:(+44-752) 233006
Fax:(+44-752) 233009

Submission of an article is understood to imply that the article is original and unpublished and is not being considered for publication elsewhere. *Anal. Chim. Acta* accepts papers in English only. There are no page charges. Manuscripts should conform in layout and style to the papers published in this issue. See inside back cover for "Information for Authors".

Publication. *Analytica Chimica Acta* appears in 16 volumes in 1994 (Vols. 281–296). *Vibrational Spectroscopy* appears in 2 volumes in 1994 (Vols. 6 and 7). Subscriptions are accepted on a prepaid basis only, unless different terms have been previously agreed upon. It is possible to order a combined subscription (*Anal. Chim. Acta* **and** *Vib. Spectrosc.*).
Our p.p.h. (postage, packing and handling) charge includes surface delivery of all issues, except to subscribers in the U.S.A., Canada, Australia, New Zealand, China, India, Israel, South Africa, Malaysia, Thailand, Singapore, South Korea, Taiwan, Pakistan, Hong Kong, Brazil, Argentina and Mexico, who receive all issues by air delivery (S.A.L.–Surface Air Lifted) at no extra cost. For Japan, air delivery requires 25% additional charge of the normal postage and handling charge; for all other countries airmail and S.A.L. charges are available upon request.

Subscription orders. Subscription prices are available upon request from the publisher. Subscription orders can be entered only by calendar year and should be sent to: Elsevier Science Publishers B.V., Journals Department, P.O. Box 211, 1000 AE Amsterdam, The Netherlands. Tel: (+31-20) 5803 642, Telex: 18582, Telefax: (+31-20) 5803598, to which requests for sample copies can also be sent. Claims for issues not received should be made within six months of publication of the issues. If not they cannot be honoured free of charge. Readers in the U.S.A. and Canada can contact the following address: Elsevier Science Publishing Co. Inc., Journal Information Center, 655 Avenue of the Americas, New York, NY 10010, U.S.A. Tel: (+1-212) 6333750, Telefax: (+1-212) 6333990, for further information, or a free sample copy of this or any other Elsevier Science Publishers journal.
Advertisements. Advertisement rates are available from the publisher on request.

US mailing notice – Analytica Chimica Acta (ISSN 0003-2670) is published biweekly by Elsevier Science Publishers (Molenwerf 1, Postbus 211, 1000 AE Amsterdam). Annual subscription price in the USA US$ 3035.75 (subject to change), including air speed delivery. Second class postage paid at Jamaica, NY 11431. *USA Postmasters*: Send address changes to Anal. Chim. Acta, Publications Expediting, Inc., 200 Meacham Av., Elmont, NY 11003. Air freight and mailing in the USA by Publication Expediting.

ANALYTICA CHIMICA ACTA

An international journal devoted to all branches of analytical chemistry

(Full texts are incorporated in CJELSEVIER, a file in the Chemical Journals Online database available on STN International; Abstracted, indexed in: Aluminum Abstracts; Anal. Abstr.; Biol. Abstr.; BIOSIS; Chem. Abstr.; Curr. Contents Phys. Chem. Earth Sci.; Engineered Materials Abstracts; Excerpta Medica; Index Med.; Life Sci.; Mass Spectrom. Bull.; Material Business Alerts; Metals Abstracts; Sci. Citation Index)

VOL. 281 NO. 3 CONTENTS SEPTEMBER 24, 1993

Special issue articles on Biosensors
(Guest Editor: M. Aizawa)

(Continued overleaf)

Contents (continued)

SPECIAL ISSUE

BIOSENSORS

Analytica Chimica Acta, 281 (1993) 451
Elsevier Science Publishers B.V., Amsterdam

PREFACE

It was in 1983 that the *First International Meeting on Chemical Sensors* (IMCS) was held at Fukuoka, Japan. In accordance with the IMCS, both the terms chemical sensors and biosensors have been recognized throughout the world, which has led to the formation of a "sensor world". Many researchers in the field of chemical sensors, specifically biosensors, have actively created their own community, seemingly outside the "analytical chemistry world".

The International Meeting on Chemical Sensors has made a trip around the world during the last 9 years, with the fourth meeting being held in Tokyo in 1992. In 1990 the First Biosensor Symposium was held in Singapore, which was followed by the Second Symposium in Geneva in 1992. This continuing research activity with respect to biosensors is reflected in this special issue of *Analytica Chimica Acta*.

The term "biosensor" has been widely recognized since the early 1980s. Since the mid-1960s a unique combination of enzymatic molecular recognition and electrochemical determination has been intensively investigated to create a variety of enzyme electrodes. The author proposed calling these enzyme electrodes "bioelectrochemical sensors" from the viewpoint of sensor technology. It did not take long to realize that such a sensor could not be limited to electrochemical determinations. Mosbach reported an enzyme thermistor in which molecular recognition depended on an enzyme and determination on a thermistor. This clearly indicated that a new term based on wider concept should be created, and the "biosensor" was therefore proposed.

The science and technology of biosensors have developed widely in interdisciplinary fields including bioscience, biotechnology, electronics, electrochemistry, clinical chemistry, medical electronics, analytical chemistry and bioelectronics. This has been an important decade for crystallizing various unique sensing principles and for integrating advanced technologies developed in the different fields. Semiconductor process technology has been introduced to fabricate microsensing devices, which is closely related to the successful implementation of field effect transistor (FET) structures to ion sensors. Ion-sensitive FETs (ISFETs) have provided enzymes with signal transduction to form semiconductor-based biosensors. Micromachining technology seems promising to bring a breakthrough in biosensor technology. A major breakthrough in the practical application of biosensors came with the introduction of a disposable glucose sensor produced using screen-printing techniques. This new trend has opened the door to producing biosensors on a mass scale, and to apply biosensors in wider areas.

It is also noted that many different sensing principles have been proposed for designing biosensors. Not only electrochemical but also optical, acoustic and thermometric sensing technologies have been used to determine molecular recognition of biomolecules such as enzymes and antibodies with extremely high sensitivity in various forms. From the viewpoint of basic science, increasing interest has attracted many researchers to investigate molecular phenomena, specifically protein molecular phenomena, on solid surface, and to manipulate a single protein molecule on a solid surface. The accomplishments in such exploratory research will lead to the next generation of biosensors.

Professor Masuo Aizawa
Department of Bioengineering,
Tokyo Institute of Technology,
Nagatsuta, Midori-ku, Yokohama 227,
Japan

Analytica Chimica Acta, 281 (1993) 453–459
Elsevier Science Publishers B.V., Amsterdam

Polyferrocenes as mediators in amperometric biosensors for glucose

S.P. Hendry [1], M.F. Cardosi [2] and A.P.F. Turner

Cranfield Biotechnology Centre, Cranfield Institute of Technology, Cranfield, Bedfordshire MK43 OAL (UK)

E.W. Neuse

Department of Chemistry, University of the Witwatersrand, Johannesburg (South Africa)

(Received 8th May 1992; revised manuscript received 16th October 1992)

Abstract

This paper describes the first successful application of polymeric ferrocenes as mediators in amperometric biosensors. The results have implications for the design of stable biosensors and bioelectronic devices involving electron transfer from oxidoreductases to electrode surfaces. The behaviour of two ferrocene polymers in enzyme electrodes was explored and a distinctive pH profile was noted. It is suggested that changes in either the enzyme conformation or the polymer in response to hydrogen ion concentration may explain the difference in behaviour between monomeric and polymeric ferrocenes.

Keywords: Amperometry; Biosensors; Enzymatic methods; Enzyme electrodes; Ferrocenes; Glucose; Glucose oxidase

The use of mediated electrochemistry offers a generic route to the construction of a range of enzyme electrodes capable of detecting important analytes [1–3]. A commercial glucose monitor shaped like a pen and using a disposable ferrocene-mediated enzyme electrode [4,5] was launched in 1987 and it is likely that pocket-sized analytical devices for metabolites such as cholesterol, alcohol and lactate will be commercially available in the near future. In addition, opportunities exist for simultaneous measurement by several enzyme electrodes in one device [6] and for continuous in vivo monitoring [7,8]. Mediated electrochemistry has also been applied to great effect with immunoassays [9,10], nucleic acid probes [11], the detection of general bacterial contamination [12,13], monitoring toxic gases [14] and in organic-phase biosensors [15].

Ferrocene and its derivatives have proved to be particularly useful as mediators for amperometric enzyme electrodes [4,6,8,14,16–24]. Other mediators, however, such as tetracyanoquinodimethane (TCNQ) [25,26] and tetrathiafulvalene (TTF) [27,28] offer viable alternatives for incorporation into single-use biosensors, although the toxicity of the latter two mediators limits their applicability in vivo. Ferrocene has been suggested for use as a haematinic agent and toxicological data are available. No contraindications have appeared to data for the use of ferrocene in humans at reasonable dosage levels. Ferrocene-mediated enzyme electrodes reported to date,

Correspondence to: A.P.F. Turner, Cranfield Biotechnology Centre, Cranfield Institute of Technology, Cranfield, Bedfordshire MK43 OAL (UK).

[1] Present address: Biomedical Sensors Ltd., George Street, High Wycombe, Buckinghamshire HP11 2RZ (UK).

[2] Present address: University of Paisley, Department of Biology, High Street, Paisley PA1 2BE (UK).

however, have had relatively short lifetimes in continuous use largely due to either loss of enzyme or its denaturation [6]. Loss of ferrocene also undoubtedly occurs [29], especially during the first day of operation, but the significance of this for long-term stability depends on the precise construction of the sensor. It is essential to develop an understanding of the molecular mechanism involved in order to engineer the properties of future devices. This is particularly critical for the success of continuous in vivo biosensors.

Monomeric mediators such as ferrocene were initially conceived of as functioning as a result of an element of mobility [4,29]. Ferrocene is essentially insoluble in aqueous solutions, but once oxidised at an electrode it was postulated that the resulting ferricinium ion could diffuse to the redox centre of the enzyme where it would act as an artificial electron acceptor. Once reduced to the insoluble form the mediator would return to the electrode. The mobility of the mediator in such a system would inevitably be a source of long-term instability due to loss of ferricinium ions from the immediate vicinity of the electrode. Significantly, increasing the molecular weight of the mediator should decrease this possible loss [30], but with a consequent impairment to the rate of diffusion during the electron shuttling process. If, however, mediation were to occur with the mediator remaining attached to either the electrode, the enzyme or both, it would be feasible to construct a "bridge" between the enzyme's redox centre and an electrode. Recent work in our laboratory has shown that polypyrrole functionalised with ferrocenecarbonyl chloride accepts electrons from glucose oxidase yielding approximately one third of the current achieved with 1,1′-dimethylferrocene-modified carbon electrodes [31]. The alternative approach involving modification of the enzyme with mediator molecules has been extensively investigated by Heller and others (e.g., [32]) with very promising results. Another interesting attempt to reduce loss of mediator involved the synthesis of monoalkylated ferrocenes with long alkyl chains [30]. These insoluble mediators were dispersed in micelles and retained at the sensor surface behind a dialysis membrane.

In an oral presentation [33], we reported that contrary to previous indications [34] polyferrocenes could act as mediators in amperometric biosensors. Below we report in detail the use of poly(ferrocenylenemethylene) and methoxyphenyl-substituted polyferrocene, which both act as good mediators with glucose oxidase at carbon electrodes. The ability of polymeric mediators to effect electron transfer between an enzyme and an electrode suggests that it may be feasible to connect more intimately these two principal components. Even in the absence of a direct link between the enzyme and the electrode, manipulation of the molecular weight of the mediator offers the opportunity simply to enhance retention in various electrode matrices or behind membranes [30]. It is hoped that such a molecular strategy in the design of mediated enzyme electrodes will lead to more stable and reproducible devices.

EXPERIMENTAL

Synthesis of poly(ferrocenylenemethylene) and methoxyphenyl-substituted polyferrocene

The synthesis of poly(ferrocenylenemethylene) (Cpd 1) and methoxyphenyl-substituted polyferrocene (Cpd 2) (see Fig. 1) consisted of the condensation of ferrocene with an aldehyde; R is equal to hydrogen and a 2-methoxyphenyl moiety, respectively. The condensations were carried out as previously described [35,36] with ferrocene employed in a slight to moderate excess over the stoichiometry required.

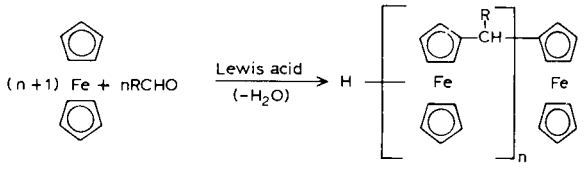

Fig. 1. The synthesis of Cpd 1 and Cpd 2 consisted of the condensation of ferrocene with an aldehyde. The general reaction is the condensation of ferrocene with the aldehyde, RCHO, in which R may represent aliphatic, aromatic or heterocyclic groups.

The purity of the polymers was very high as the materials were obtained by fractional precipitation. In addition, the polymer was reprecipitated prior to use. Hence the content of monomeric ferrocene should effectively have been zero as the monomer is very soluble in the mother liquors and remains dissolved when the polymer precipitates. Rigorous washing was also used to remove any traces of adsorbed monomer. In addition, the second reprecipitation served to purify the polymer further. In neither the first nor the second reprecipitated material was any monomeric ferrocene detected by thin-layer chromatography (TLC). The poly(ferrocenylenemethylene) had an average chain length (n) of 12–14 monomer units as determined by vapour pressure osmometry.

Construction of electrodes

Electrodes were constructed as described previously [4,37] to facilitate comparison of polyferrocene-modified electrodes with ferrocene-based sensors.

Enzyme immobilisation was effected as described previously [6] using sodium periodate-modified glucose oxidase. First, the carbon electrodes were dipped in a solution of hexadecylamine in chloroform (1 mg ml^{-1}) for 15 min. The electrodes were allowed to air dry. The polyferrocene mediators were deposited as 5-μl aliquots (20 mg mediator per ml of toluene) onto the surface of the electrode and allowed to dry. This was repeated until a total of 20 μl of polymer solution had been deposited. The electrodes were then allowed to dry thoroughly and were then placed into the periodate-modified glucose oxidase solution for 90 min. The electrodes were then transferred into a solution of adipic dihydrazide (2.5 mg ml^{-1} in acetate buffer, pH 5.5) for 15 min.

Apparatus

The sensors were evaluated using a BBC 32K micro-computer (Acorn, Cambridge) via a programmable biosensor interface (Artek, Olney, UK), with an Ag/AgCl reference electrode [37]. A three-electrode system was employed to obtain temperature profiles. This consisted of a precision potentiostat (Ministat, HB Thompson and Associates, Newcastle upon Tyne) and the current was recorded on a flat-bed chart recorder (Euroscribe Recorder, Gallenkamp, London) via a resistance board (JJ Junior, JJ Instruments, Southampton). A calomel electrode was used as a reference and the auxiliary electrode was platinum wire (0.46 mm diameter).

The sensors were immersed in buffer (15 ml) which was usually a 20 mM phosphate buffer, pH 7.0, contained in a 20-ml glass water-jacketed cell (Soham Scientific, Ely, UK) thermostated at 25 $\pm$ 0.5°C. Unless stated otherwise, the sensors were poised at 250 mV versus the saturated calomel electrode.

Buffers and reagents

The standard buffer used was 20 mM sodium phosphate, pH 7.0, containing 0.1 M KCl. The buffers used for the pH profiles all contained 0.1 M KCl and were as follows: pH 4.0, 20 mM citric acid–Na_2HPO_4; pH 4.4, 20 mM citric acid–Na_2HPO_4; pH 5.0, 20 mM citric acid–Na_2HPO_4; pH 5.8, 20 mM sodium phosphate; pH 6.3, 20 mM sodium phosphate; pH 7.0, 20 mM sodium phosphate; pH 7.5, 20 mM sodium phosphate; pH 8.0, 20 mM sodium phosphate; pH 9.4, 20 mM Na_2CO_3.

Buffers used in the three-electrode systems lacked 0.1 M KCl. Glucose was introduced into the system by injection of known volumes of 1.0 M D-glucose which had been stored overnight to allow equilibration of α and β-anomers. All chemicals were of analytical-reagent grade (BDH, Analar, Atherstone, UK).

RESULTS AND DISCUSSION

Direct current cyclic voltammetry

The d.c. cyclic voltammograms of poly(ferrocenylenemethylene) and methoxyphenyl-substituted polyferrocene-modified carbon electrodes (not shown) demonstrated that each mediator was capable of undergoing reduction and oxidation between 0 and 700 mV vs. SCE. Cpd 1-modified electrodes exhibited a well defined oxidation peak at 650 mV vs. SCE. A reductive

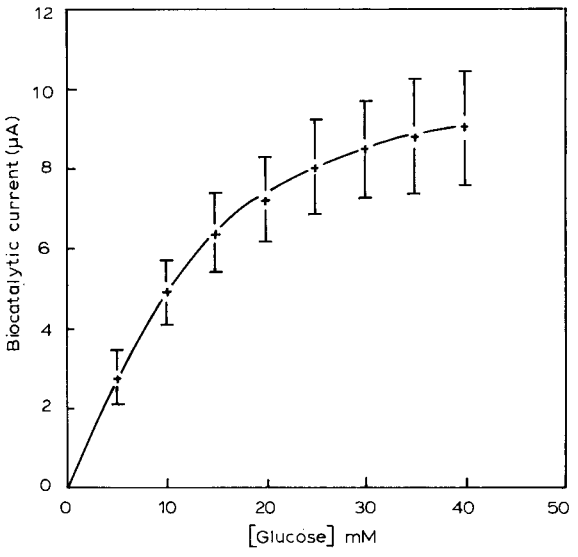

Fig. 2. Response of Cpd 1-modified glucose oxidase electrodes to additions of glucose. The error bars represent standard deviations between 5 electrodes.

peak was also present at 500 mV vs. SCE. The peak separation of 150 mV indicated an ideal kinetic behaviour. Electrodes modified with Cpd 2, on the other hand, gave less well defined oxidation peaks over the potential window of interest. A reductive wave was present with the peak potential occurring at 0.1 V vs. SCE. In neither case could cyclic voltammograms of homogeneous solutions of mediator be obtained as both mediators were insoluble in suitable aqueous solvents. Constant cycling of the potential demonstrated that neither mediator lost any significant electrochemical activity with repeated oxidation/reduction (results not shown).

Poly(ferrocenylenemethylene) (Cpd 1) electrodes: calibration curve

The electrodes responded in the range 0–40 mM glucose (Fig. 2). The response of the electrodes was rapid, typically taking 60 s to reach 90% of the steady-state response after a glucose addition. The standard deviation ($n = 5$) error bars (Fig. 2) showed that the electrodes were reasonably reproducible even though the fabrication technique was crude. The half-life decay time at saturating glucose concentrations (66 mM) was 22 h, but this was variable due to disparate enzyme and/or mediator loading on the electrodes caused by the inconsistent nature of the carbon foil.

pH profile of the Cpd 1 electrodes. The effect of pH on the anodic current of the electrodes was investigated over the pH range 5.0–9.0 (Fig. 3). The electrodes had a pH optimum in the strongly alkaline region of pH ca. 9.0. This value was extremely high compared to previously described mediated systems [4,6,24,25,27]. It was considered that this was a reflection of the steric interaction of the polyferrocene with the glucose oxidase.

Effect of temperature on Cpd 1 electrodes. The effect of temperature on the electrodes was investigated between 0 and 50°C, at saturating glucose concentration, using Cpd 1 as mediator. When the electrodes were maintained at higher temperatures thermal denaturation became significant. Figure 4 shows an Arrhenius plot for a typical Cpd 1-modified glucose oxidase electrode. From this graph the activation energy for the reaction was calculated as 34.1 kJ mol^{-1} illustrating that the activation energy is independent of mediator (cf. [4,25,27]).

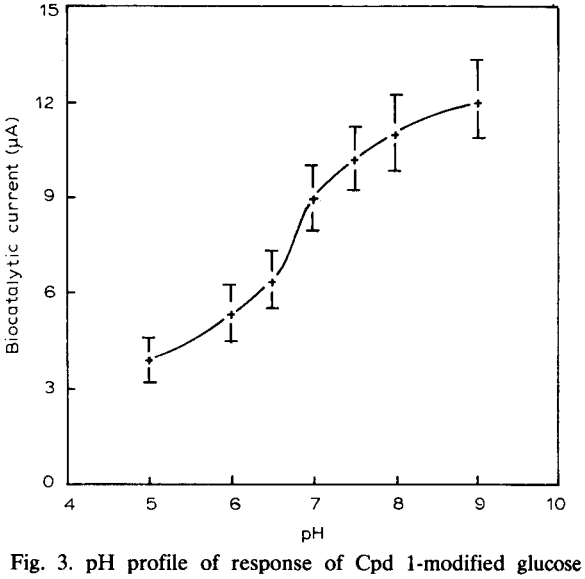

Fig. 3. pH profile of response of Cpd 1-modified glucose oxidase electrodes to additions of glucose. The error bars represent standard deviations between 5 electrodes.

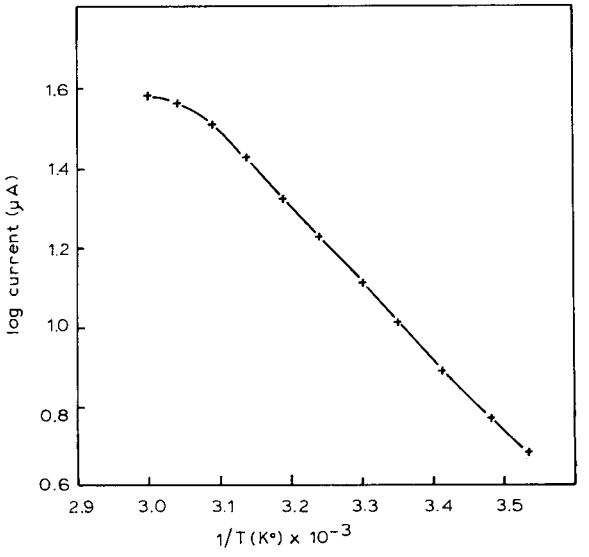

Fig. 4. Arrhenius plot for a typical Cpd 1 enzyme electrode at 66 mM glucose.

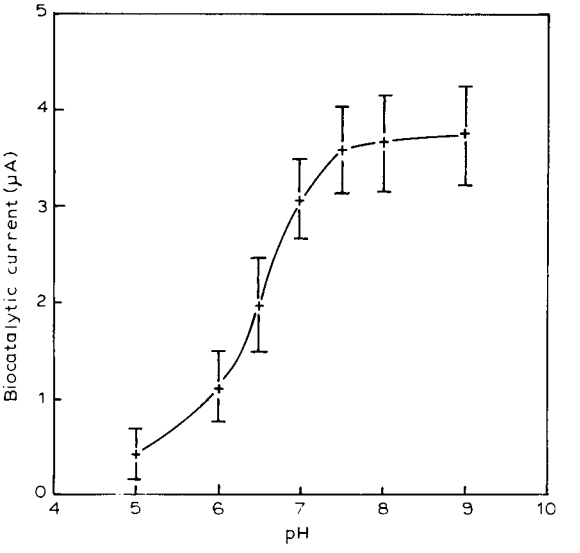

Fig. 6. pH profile of response of Cpd 2-modified glucose oxidase electrodes at 66 mM glucose. The error bars represent the standard deviations between 5 electrodes.

Methoxyphenyl-substituted polyferrocene (Cpd 2): calibration curve

These electrodes gave smaller currents (Fig. 5) than the Cpd 1-mediated electrodes (Fig. 2) and were saturated at slightly lower glucose concentrations (30 mM). The response time was typically 2 min to reach 90% steady-state current. The standard deviations ($n = 5$) shown in Fig. 5 were similar to the Cpd 1 electrodes. An explanation for the lower saturation is that the methoxyphenyl-substituted polyferrocene was a slightly less efficient electron acceptor than the poly(ferrocenylenemethylene), hence the enzyme would not have been turned over as fast and a lower apparent K_m would have resulted. The half-life decay time of the electrodes at saturating glucose concentrations (66 mM) was ca. 22 h, but again it was variable. If electrodes were stored in 20 mM buffer, pH 7.5 at 4°C after initial use, calibration curves after 22 h were similar to those of fresh electrodes.

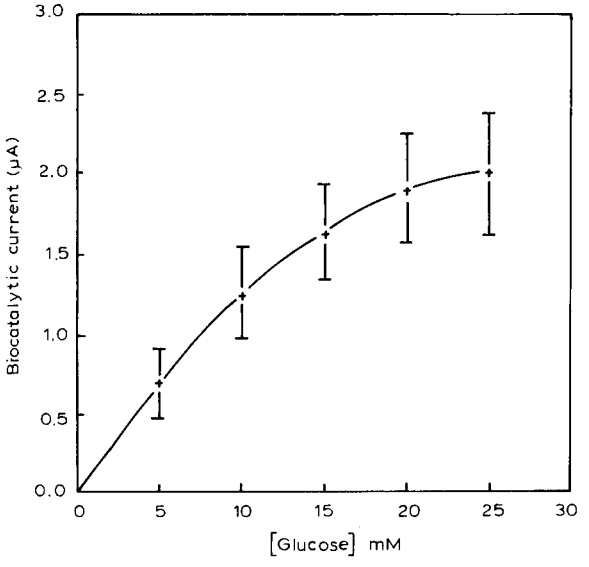

Fig. 5. Response of Cpd 2-modified glucose oxidase electrodes to glucose. The error bars represent the standard deviations between 5 electrodes.

pH profile of Cpd 2 electrodes. The effect of pH on the anodic current of the electrodes at 66 mM glucose was investigated in the range 5.0–9.0 (Fig. 6). The profile was similar to the Cpd 1 profile (Fig. 3) with an optimum in the alkaline region. This suggested that this phenomenon was a general effect due to the polymeric nature of the mediator.

Effect of temperature on Cpd 2 electrodes. The Q_{10} (reaction rate following an increase of 10°C, within the linear portion of the temperature re-

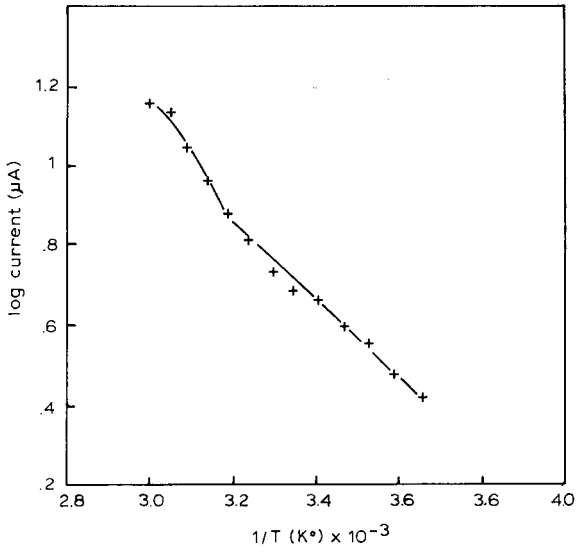

Fig. 7. Arrhenius plot of a typical Cpd 2-modified glucose oxidase electrode.

sponse curve, divided by the original rate) for the reaction was 1.33, which was similar to previous results. An Arrhenius plot for a typical methoxyphenyl-substituted polyferrocene-modified electrode is shown in Fig. 7. The activation energy for this reaction was calculated as 31.2 kJ mol^{-1} which was in accord with the activation energies calculated for other mediated reactions.

Conclusions

Although it has been demonstrated previously that both ferrocene moieties can be incorporated into polymers [38] and polymeric films can be derivatised with ferrocene [31] this paper demonstrated that polyferrocenes themselves are capable of acting as mediators, shuttling electrons between glucose oxidase and a carbon electrode. Current to glucose concentration ratios were much smaller than for ferrocene [4], TTF [27] and TCNQ [25] mediated electrodes. This could be explained in two ways, i.e., less efficient electron transfer or smaller diffusion coefficients for the polymer compared to monomeric mediators. From the Stokes–Einstein equation, it is possible to account for the smaller currents obtained on the basis of difference in rates of diffusion. This does not, however, explain the difference between Cpd 1 and Cpd 2. It is more likely that the polymers are simply less effective electron acceptors for glucose oxidase than monomeric mediators. The size of the polymers presumably hinders their access to the redox site of the enzyme. This is supported by the pH profiles obtained for the polymer-modified electrodes showing pH optima in the alkaline region. When a protein is subjected to variations in pH various side groups of amino acids change ionisation state. This can cause the protein to alter slightly its quaternary structure [39,40]. At alkaline pH, therefore, glucose oxidase may become a more relaxed molecule. Thus one can envisage that access to the redox site would be easier for a polymeric molecule under alkaline conditions. An alternative explanation is that the conformation of the polymeric mediator responds to pH change, thus affecting its ability to access the enzyme redox site.

The pH profiles obtained using the polyferrocenes also indicate that neither hydrogen peroxide nor monomeric ferrocene was involved in the sensors' response to glucose. Oxidation of hydrogen peroxide at the relatively low potentials used is unlikely to have been sufficient to produce the observed currents and would in any case have been associated with a pH optimum of 5.5 with oxygen as the electron acceptor for glucose oxidase. Monomeric mediators are known to increase the pH optimum of enzyme electrode to ca. 7.5 [4,6,24,25,27], but the pH profile observed with the polymeric mediators reported in this paper is quite distinct form monomeric mediation. Additional evidence against the involvement of ferrocene monomers is the high purity of the polymers used.

While the observed currents may have been smaller with polymeric compared to monomeric mediators, glucose assays in the clinically relevant range are entirely feasible using this type of electrode. Further work is now required to explore the possibility of anchoring either one of both ends of the mediator to the electrode and the enzyme, respectively. If such a molecular wire could be fabricated it would not only enhance stability but facilitate the remainder of the electrode surface being insulated from the sample

thus drastically reducing electrochemical interference. A simpler strategy to exploit polymeric mediators would be to reduce loss of mediator form enzyme electrodes by modification of the pore size of a conducting matrix or by use of a suitable membrane [30]. These approaches are currently under investigation in our laboratory.

REFERENCES

1 A.P.F. Turner, I. Karube and G.S. Wilson (Eds.), Biosensors: Fundamentals and Applications, Oxford University Press, Oxford, 1989.
2 A.P.F. Turner and S.P. Hendry, in D.L. Wise (Ed.), Bioinstrumentation: Research, Development and Applications, Butterworths, Stoneham, MA, 1990, pp. 1461–1500.
3 M.F. Cardosi and A.P.F. Truner, in A.P.F. Turner (Ed.), Advances in Biosensors, JAI Press, London, 1991, pp. 125–169.
4 A.E.G. Cass, G. Davis, G.D. Francis, H.A.O. Hill, W.J. Aston, I.J. Higgins, E.V. Plotkin, L.D.L. Scott and A.P.F. Turner, Anal. Chem., 56 (1984) 667.
5 D.R. Mattthews, E. Bown, A. Watson, R.R. Holman, J. Steemson, S. Hughes and D. Scott, Lancet, April (1987) 778.
6 S.L. Brooks, R.E. Ashby, A.P.F. Turner, M.R. Calder and D.J. Clarke, Biosensors, 3 (1987) 45.
7 J.C. Pickup, G.W. Shaw and D.J. Claremont, Biosensors, 4 (1989) 109.
8 M.F. Cardosi and A.P.F. Turner, in K.G.M.M. Alberti and L.P. Krall (Eds.), The Diabetes Annual, Vol. 6, Elsevier, Amsterdam, 1991, pp. 271–301.
9 M.F. Cardosi, S.W. Birch, C.J. Stanley, A. Johannsson and A.P.F. Turner, Am. Biotechnol. Lab., 7 (1989) 50.
10 J.V. Bannister, I.J. Higgins and A.P.F. Turner, in L.J. Blum and P.R. Coulet (Eds.), Biosensors: Principles and Applications, Marcel Dekker, New York, 1991, pp. 47–61.
11 M.E.A. Downs, P.J. Warner, J.C. Fothergill and A.P.F. Turner, Biomaterials, 9 (1988) 66.
12 G. Ramsay and A.P.F. Turner, Anal. Chim. Acta, 215 (1988) 61.
13 A.P.F. Turner, M. Allen, B.H. Schneider, A.S. Swain and F. Taylor, Int. Biodeterior., (1989) 137.
14 A.P.F. Turner, W.J. Aston, J. Bell, J. Colby, G. Davis, I.J. Higgins and H.A.O. Hill, Anal. Chim. Acta, 163 (1984) 161.
15 F. Schubert, S. Saini and A.P.F. Turner, Anal. Chim. Acta, 245 (1991) 133.
16 E.J. D'Costa, A.P.F. Turner and I.J. Higgins, Biosensors, 2 (1986) 71.
17 J.M. Dicks, W.J. Aston, G. Davis and A.P.F. Turner, Anal. Chim. Acta, 182 (1986) 103.
18 G. Jönsson, L. Gorton and L. Pettersson, Electroanalysis, 1 (1989) 49.
19 K. Yokoyama, E. Tamiya and I. Karube, Anal. Lett., 22 (1989) 2949.
20 J. Wang, L.-H. Wu, Z. Lu, R. Li and J. Sanchez, Anal. Chim. Acta, 228 (1990) 251.
21 H. Okuma, H. Takahashi and S. Sekimukai, Anal. Chim. Acta, 244 (1991) 161.
22 P.D. Sánchez, A.J.M. Ordieres, A.C. Garcia and P.T. Blanco, Electroanalysis, 3 (1991) 281.
23 L. Chen, M.S. Lin, M. Hara and G.A. Rechnitz, Anal. Lett., 24 (1991) 1.
24 S.K. Beh, G.J. Moody and J.D.R. Thomas, Analyst, 116 (1991) 459.
25 S.P. Hendry and A.P.F. Turner, Horm. Metab. Res., 20 (1988) 37.
26 J. Kulys and E.J. D'Costa, Biosens. Bioelectron., 6 (1991) 109.
27 A.P.F. Turner, S.P. Hendry and M.F. Cardosi, in Biosensors, Instrumentation and Processing, The World Biotech Report, Vol. 1, No. 3, Online, London, 1987, pp. 125–137.
28 G. Palleschi and A.P.F. Turner, Anal. Chim. Acta, 234 (1990) 459.
29 W. Schuhmann, U. Löffler, H. Wohlschläger, R. Lammert, H.-L. Schmidt, H.-D. Weimhöfer and W. Göpel, Sensors, Actuators, B1 (1990) 571.
30 U. Löffler, H.-D. Wiemhöfer and W. Göpel, Biosens. Bioelectron., 6 (1991) 343.
31 J.M. Dicks, S. Hattori, I. Karube, A.P.F. Turner and T. Yokozawa, Ann. Biol. Clin., 47 (1989) 607.
32 M.V. Pishko, A.C. Michael and A. Heller, Anal. Chem., 63 (1991) 2268.
33 A.P.F. Turner, S.P. Hendry, M.F. Cardosi and E.W. Neuse, Diabet. Med., 5(2) (1988).
34 G. Davis, Ph.D. Thesis, University of Oxford, 1984.
35 E.W. Neuse and K. Koda, J. Organomet. Chem., 4 (1965) 475.
36 E.W. Neuse and E. Quo, Bull. Chem. Soc. Jpn., 39 (1966) 1508.
37 A.P.F. Turner, Methods Enzymol., 137 (1988) 90.
38 N.C. Foulds and C.R. Lowe, Anal. Chem., 60 (1988) 2473.
39 H.R. Mahler and E.H. Cordes, Biological Chemistry, Harper and Row, New York, 1971.
40 R. Wilson and A.P.F. Turner, Biosens. Bioelectron., 7 (1992) 165.

Analytica Chimica Acta, 281 (1993) 461–466
Elsevier Science Publishers B.V., Amsterdam

Miniature electrochemical glucose biosensors

M. Koudelka-Hep, D.J. Strike and N.F. de Rooij
Institute of Microtechnology, University of Neuchâtel, Breguet 2, 2000 Neuchâtel (Switzerland)

(Received 2nd April 1992; revised manuscript received 8th September 1992)

Abstract

Glucose-oxidase-based sensors were realized using three techniques of immobilizing thin layers of enzyme over a three-thin-film electrode transducer. Sensors with chemically crosslinked membranes, completed by an outer diffusion-limiting membrane, were characterized with consideration of the basic requirements of an implantable device. Thus, e.g. a negligible loss of the activity was observed when the sensors were sterilized by a 2.5 MRad dose of gamma radiation. On the other hand, the sensors with the electrochemically deposited membranes were particularly suitable, e.g. with respect to response time, etc., for flow-injection analysis measurements.

Keywords: Biosensors; Flow injection; Enzymes; Glucose biosensor; Glucose oxidase

Silicon-based technology offers considerable practical advantages for the fabrication of electrochemical cells and electrodes. Of these advantages the most commonly exploited is the ease with which various electrode geometries, including arrays, can be reproducibly fabricated. Besides the use of such microfabricated structures as transducers for electrochemical (bio)sensors [1–4] their interest to other fields of electrochemistry has been demonstrated [5].

Our particular interest lies in the development and characterization of glucose electrodes, primarily for in vivo glucose monitoring and flow-injection analysis (FIA) of glucose for bioprocess control. Using thin film and photolithography techniques the transducer part, in both cases a three-electrode microcell, was realized on a silicon substrate. The transducer was completed by an enzymatic membrane formed either by chemical crosslinking of glucose oxidase (GOD) with bovine serum albumin (BSA) using glutaraldehyde, or by electrochemical (co)deposition of the enzyme using either entrapment with polypyrrole (PPy), or a direct galvanostatic co-deposition of GOD and BSA. The former method is used when a relatively thick enzymatic membrane has to be deposited over the whole transducer surface while the latter techniques allow spatially controlled deposition exclusively onto the working electrode. Obviously the choice of the enzyme immobilization method depends on the required sensor characteristics concerning response, life-time and especially useful concentration range. We have found chemical co-crosslinking to be well suited for the in vivo devices where an additional outer diffusion-limiting polyurethane (PU) membrane is used to complete the sensor and we are currently investigating the suitability of the electrochemical depositions for sensors to be used in FIA and batch measurements.

Following a brief description of the fabrication of the transducer, this paper will deal mainly with

Correspondence to: M. Koudelka-Hep, Institute of Microtechnology, University of Neuchâtel, Breguet 2, 2000 Neuchâtel (Switzerland).

the membrane deposition technology and pertormance characteristics of three sensors types.

EXPERIMENTAL

Chemicals

For the in vivo sensor GOD (from *Aspergillus niger*) was obtained from Calbiochem (250 IU/mg), whilst for the electrochemical depositions Sigma grade VII (145 U/mg) was used. BSA (fraction V) was obtained from Calbiochem. All other chemicals were obtained from Merck. The glucose measurements and the galvanostatic depositions were made in 5.3 mM potassium phosphate buffer, pH 7.2, containing 2.5 mM potassium chloride and 0.115 M sodium chloride. For the PPy–GOD depositions 100 mM potassium phosphate buffer, pH 7, containing 10 mM sodium perchlorate was used.

Transducer

The first generation of transducers, which we have described in detail elsewhere [6], was realized by photolithographic lift-off patterning of two thin-film metallic layers, i.e. Pt (1500 Å) and Ag (1 μm) deposited by electron beam evaporation onto the Si–SiO_2–Al_2O_3 substrate. Intermediary Ti adhesion layers of 200 Å for Pt and 500 Å for Ag were used to improve the adhesion of the noble metal layers to the oxide layer. The resulting on-chip microcell was composed of Pt working and counter electrodes and an Ag/AgCl reference electrode and had overall dimensions of 0.55 mm × 3 mm × 0.38 mm (Fig. 1). The individual chips were mounted on printed circuit boards, wire bonded and encapsulated, leaving only the active area exposed. After the epoxy encapsulation, the band-type Pt working electrode had a length of 1000 μm and a width of 100 μm.

To avoid inaccuracies in the definition of the surface of the working electrode caused by relying on the epoxy encapsulant the second generation of transducers, although preserving the same electrode geometry as the first, used a silicon nitride passivation layer and polysilicon interconnections.

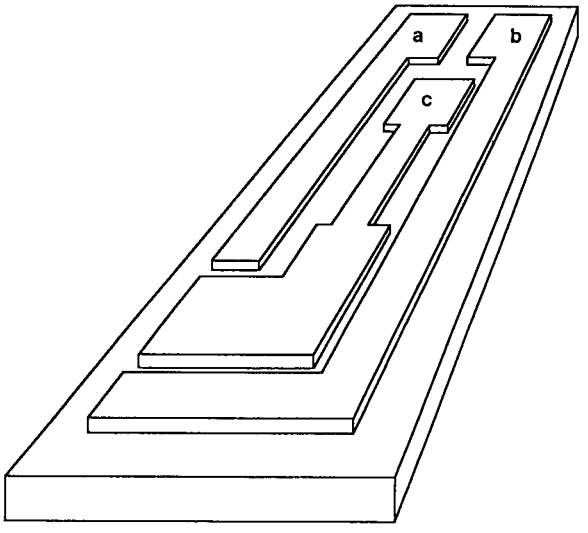

Fig. 1. Schematic representation of the transducer: (a) Pt working and (b) counter electrodes, (c) Ag/AgCl reference electrode. Overall dimensions 0.55 mm × 3 mm × 0.38 mm.

Enzymatic membrane deposition

In vivo sensor (chemical crosslinking). GOD was immobilized using glutaraldehyde as a crosslinking agent and bovine serum albumin BSA (fraction V) as a carrier protein. A 3-μl volume of solution containing GOD (50 mg/ml), BSA (80 mg/ml) and glutaraldehyde (2.5%) was deposited on the transducer surface and left for two hours at room temperature to crosslink.

Electrochemical deposition. (i) Galvanostatic co-deposition of GOD and BSA. The deposition of the enzyme for these sensors closely followed that of Johnson [7], i.e. galvanostatically at a current density of 5 mA/cm^2. The duration of the deposition ranged from 30 s to 4 min. The proteins were deposited from buffer (pH 7.2) containing between 5 and 10% (w/w) protein, i.e. GOD and BSA. The sensor was rinsed in deionized water and then crosslinked in a 2.5% glutaraldehyde solution, in buffer, for 30 min. A Pt wire counter electrode and the on-chip reference were used during the protein deposition. The counter electrode was placed as close as possible to the working electrode. Prior to the deposition the working electrode was treated by cyclic voltammetry in 0.5 M H_2SO_4 at 50 mV/s. Four cycles were made.

the first, second and last being over the range −0.25 to 1.2 V whilst for the third the anodic limit was extended to 2.0 V. The sequence began at −0.25 V and ended at 0.2 V. For this treatment an external counter electrode and an external reference electrode were used.

(ii) PPy–GOD. GOD was entrapped in PPy following a procedure based on that of Yon Hin et al. [8]. The electrochemical growth of the polymer was from 0.1 M potassium phosphate, pH 7.0, containing 10 mM sodium perchlorate, 0.1 M pyrrole and 2.4 mg/ml glucose oxidase. The deposition was performed at 800 mV vs. SCE and a charge of 68 μC was passed.

Outer diffusion-limiting membrane for the in vivo sensor

To render the sensor response less sensitive to fluctuations in oxygen tension [9] it was coated with a thin polyurethane membrane. This was deposited by dipcoating from a 1 + 9 (v/v) mixture of dimethylformamaide (DMF) and tetrahydrofuran (THF) containing 5% polyurethane (donated by Japan Erastran). The solvent was allowed to evaporate to give a thin transparent film.

In most cases the sensors were stored in 10 mM phosphate buffer solution at 4°C, however dry storage at room temperature is also possible providing the electrodes are allowed about 15 min to rehydrate before use. The dimensions of the ready-to-use device, determined solely by the availability of the support, were initially 2 mm (width) by 1.5 cm (length). Recently, the width of the support has been reduced to 0.6 mm.

Instrumentation

All electrochemical measurements were performed using either an IBM EC 225 voltammetric analyser or EG&G 273A potentiostat/galvanostat. For the in vivo measurements, an in-house built potentiostat was used. The working potential for the peroxide detection was 0.65 V vs. SCE. The flow injection system was composed of a Model MV-CA4 peristaltic pump (Ismatec), a rotary injection valve (Ig Instrumenten Gesellschaft) and a Perspex flow-through cell (on loan from Ciba-Geigy).

RESULTS AND DISCUSSION

In vivo sensors using chemically crosslinked GOD and BSA

There are several crucial points of the sensor fabrication that have to be rigorously controlled to achieve reasonably reproducible sensors. While the transducer fabrication process and the enzymatic membrane deposition cause no particular problem, the polyurethane membrane deposition is much harder to control. This results from the coating technique used, i.e. dipcoating, which although straightforward is generally difficult to perform reproducibly. Unfortunately, it is the only technique available for coating the polyurethane membrane over the full length of the sensor. Because some of the most important functional parameters of the sensor are determined by the transport properties of this outer polyurethane membrane, careful control of the deposition is of critical importance.

Several membrane compositions have been investigated and a 5% PU solution in 1 + 9 (v/v) DMF and THF was found to give the best results. Allowing for several attempts at the deposition to be needed on occasion, a 90% yield of sensors having satisfactory functional characteristics was obtained. The definition of "satisfactory" functional characteristics, although limited by the present state of the sensor development, is based on the general requirements for an implantable glucose sensor. Besides the obvious requirements concerning stability and miniaturization, the linear response range (0–15 mM), response time (< few minutes) and a minimized influence of changes in oxygen tension on the sensor response are the most important prerequisites [10]. Table 1 gives the in vitro values (mean ± S.D.) of some important sensor parameters, determined in a

TABLE 1

In vitro characteristics of the glucose sensor ($n = 35$)

Linear range	≤ 18 mM at $p_{O_2} \geq 37$ mmHg
Sensitivity	2.5 ± 0.9 nA/mM
Background current (at 0 mM)	1.1 ± 0.2 nA
Temperature coefficient	5%/°C at 18 mM
95% response time	180 ± 4 s at 18 mM

phosphate–saline physiological solution at 37°C ($n = 35$).

Furthermore, the sensor response is pH-(tested in the range 6–8) and stir-independent. It should be noted that decreasing the p_{O_2} from 37 to 15 mmHg shortens the upper linear limit of linearity ($\leq$ 14 mM) and also increases the response time (t_{95} about 300 s at 14 mM).

The effect of two interfering substances was investigated at what is supposed to be their maximum physiological plasma concentrations [11] with the glucose concentration kept constant at 5 mM. A 2–4% increase in the sensor output was observed upon the addition of 0.2 mM of ascorbic acid to the 5 mM glucose solution. However, the same amount of acetaminophen, i.e. 0.2 mM, caused an increase of approximately 35% in the sensor current. Thus, if acetaminophen was present in the tissue at the upper limit of its plasma physiological concentration range it would be a major interferent on the sensor response.

An important additional feature of in vivo sensors is their capacity of being sterilized. Among different methods sterilization using a 2.5 MRad dose of gamma radiation was chosen. Because of the possible loss of the sensitivity resulting from the sterilization, sensors having a slightly higher sensitivity (3.3 ± 1.3 nA/mM compared to 2.5 ± 0.9 nA/mM) have been prepared. Following the sterilization, which was performed in dry state, the sensors were rehydrated for several hours in 10 mM phosphate buffer solution and then tested. Surprisingly only a slight loss of sensitivity was observed, all other characteristics, i.e. linear range, background current and response time remained unchanged. Table 2 gives the mean sensitivity values, determined intermittently over a period of more than 50 days. In between the measurements, the sensors were stored in a phosphate buffer solution at 4°C.

The possibility of sensor sterilization as well as a reasonable storage stability over the period investigated can be thus added to the sensor performance characteristics.

Several series of sensors have been implanted subcutaneously in normal rats. It has been shown that, over a short-term study of several hours, it was possible to obtain a reasonable correlation between the measured plasma and the calculated apparent subcutaneous glucose concentration [12]. Recent results of longer-term (several days) studies, in which the implanted sensors were calibrated and tested intermittently, have shown that 80% of sensors could be used for 4 days with good correlations between the plasma and the apparent subcutaneous glucose concentrations over the concentration range investigated (2–16 mM).

TABLE 2

Storage stability of sterilized sensors

Day	Sensitivity [nA/mM] (Mean ± S.D., $n = 6$)
Prior to sterilization	3.3 ± 1.3
After sterilization	
0	2.6 ± 1.1
7	2.7 ± 0.8
9	2.7 ± 0.8
11	3.0 ± 0.8
17	2.7 ± 0.5
25	2.9 ± 0.5
42	2.7 ± 0.7
49	2.6 ± 0.5
55	2.9 ± 0.5

Electrochemically deposited GOD

Among different strategies for immobilizing enzymes, the electrochemical techniques present important advantages when a spatially well controlled enzyme deposition has to be performed. The enzyme can be deposited either with a polymer matrix [8,13–16] or alone [7,17,18]. Here we will describe glucose sensitive enzyme electrodes prepared by immobilizing GOD in a PPy matrix, or by galvanostatic co-deposition with BSA.

When, after the various protein depositions, the electrodes were examined under a light microscope it was found that both the electrostatic and the PPy depositions gave uniform deposits that were localized on the working electrode. This demonstrates the possibility of localized enzyme depositions, for example for multi-analyte sensors, as Yon Hin et al. have recently shown with PPy [8].

Figure 2 shows the typical glucose response curves for the two types of electrochemically de-

posited GOD, as well as that of an unmodified transducer. Comparison with the unmodified transducer indicates that both of the GOD deposits were enzymatically active. The typical 95% response time for these electrodes was 10–20 s for the electrodes modified with galvanostatically deposited protein and 30–50 s for the PPy–GOD electrodes. We have investigated several membrane compositions for the galvanostatic deposition, and have found that a membrane deposited out of a solution of 5% GOD–5% BSA, over a two-minute period gave the optimal balance of enzyme consumption against sensor response. Higher GOD concentrations or longer deposition times did not significantly improve the size of the glucose response. We have found that the relative positions of the working and counter electrodes during the depositions are important, with closer spacing appearing to result in higher responses to glucose. We are currently investigating this effect.

With the PPy–GOD depositions we have found that, for our electrodes, a membrane thickness corresponding to 68 mC/cm^2 appears to be the optimal compromise between convection noise and the size of the glucose response, both of which fall with increasing membrane thickness. Also we have found that the amount of enzyme used here (2.4 mg/ml) seems to be optimal since the size of the response falls with either increasing or decreasing the amount. These effects are similar to those reported by Fortier [13]. In general we have found that the PPy electrodes gave smaller glucose responses than the galvanostatic electrodes. Our current densities are comparable with those reported in the literature, although our K_m values are somewhat lower. The galvanostatically deposited films behaved favorably when tested under FIA conditions (Fig. 3).

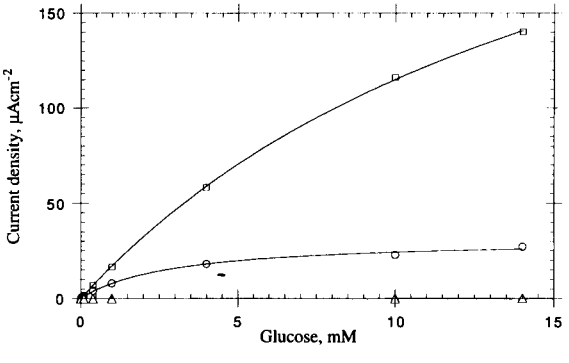

Fig. 2. The glucose response of the electrodes utilizing electrochemically deposited GOD, recorded in unstirred solution, at 37°C. (□) GOD and BSA, deposited out of phosphate buffer containing 5% GOD and 5% BSA (w/w), over a 2-min period at a current density of 5 mA/cm^2; (○) PPy–GOD, deposited out of phosphate buffer containing 0.1 M pyrrole and 2.4 mg/cm^3 GOD. The deposition potential was 800 mV (vs. SCE) and the total charge passed was 68 mC/cm^2; (△) unmodified transducer.

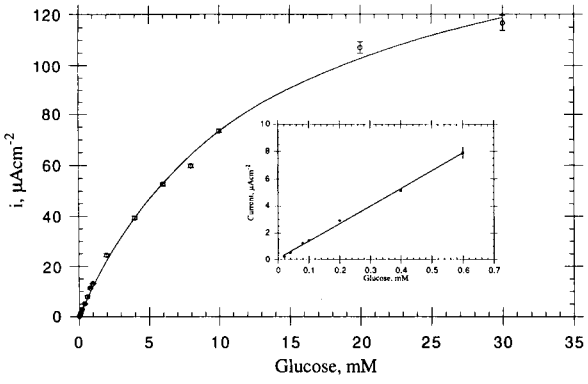

Fig. 3. The glucose response of the galvanostatically deposited GOD and BSA described in Fig. 2 recorded under FIA conditions. The flow-rate was 1.0 cm^3/min, the injection volume was 100 μl and the recordings were made at room temperature. The insert shows the linear portion of the response (r = 0.999). Each point is the mean of 5 injections.

These results strongly indicate that for simple GOD-based electrodes the galvanostatic deposition procedure may be superior to the PPy entrapment. However, in other situations PPy may be advantageous since it offers many opportunities for chemical modifications, for example with appropriate catalysts, e.g. ferrocene [19], displays rejection of certain potential interferences based on both charge and size [20,21] and shows potentially important interactions with GOD [22].

Conclusions

The glucose sensor technology described here allows some of the essential requirements for

both implantable and non-implantable sensors use to be met. For the former, the small size (0.55 mm width) of the three thin-film electrode transducer is of obvious importance. The ease of the transducer microfabrication allows these devices to be disposable, which is convenient for many applications. Nevertheless, it should be mentioned that the biggest problem which impedes still wider use of these transducers is the time-consuming, hand-made encapsulation procedure as well as the enzyme deposition step. The enzyme deposition could be greatly facilitated by the electrochemical deposition techniques which could allow large numbers of electrodes to be modified in parallel, and may become a valuable alternative to photolithographic-based techniques [23]. Both of the electrochemical deposition processes described appear promising, and although the direct deposition is considerably simpler to perform than the PPy-based technique, it may be that the latter will prove to be the more versatile, particularly with regard to the properties described above.

The enzyme deposition using the classical chemical crosslinking is, in our hands, still favoured for the production of in vivo sensors. Besides having favorable in vitro characteristics with regard to sensitivity, linear range, life-time and sensitivity to changes in p_{O_2}, the ruggedness of the sensor in undergoing gamma irradiation sterilization with a negligible loss of sensitivity is of great importance.

The authors would like to thank Mme S. Pochon and Mr G. Mondin for their technical assistance, Ciba Geigy for the loan of the FIA flow-through cell, and the National Science Foundation and the Committee for the Promotion of Applied Research for funding the work. The in vivo measurements were performed in the group of Prof. B. Jeanrenaud at the Laboratories of Metabolic Research, University of Geneva.

REFERENCES

1 K. Yokoyama, E. Tamiya and I. Karube, Anal. Lett., 22 (1989) 2949.
2 A. Hintsche, G. Neumann, I. Dransfeld, J. Kampfrath, B. Hoffmann and F. Scheller, Anal. Lett., 22 (1989) 2175.
3 I. Takatsu and T. Moriizumi, Sensors Actuators, 11 (1987) 309.
4 G. Urban, G. Jobst, F. Kohl, A. Jachimowicz, F. Olcaytug, O. Tilado, P. Goiser, G. Nauer, F. Pittner, T. Schalkhammer and E. Mann-Buxbaum, Biosensors Bioelectron., 6 (1991) 555.
5 R.W. Murray, R.E. Dessy, W.R. Heineman, J. Janata and W.R. Seitz (Eds.), Chemical Sensors and Microinstrumentation, ACS Symposium Series, Vol. 403, American Chemical Society, Washington, DC, 1989.
6 S. Gernet, M. Koudelka and N.F. de Rooij, Sensors Actuators, 18 (1989) 59.
7 K.W. Johnson, Sensors Actuators, B5 (1991) 85.
8 B.F.Y. Yon Hin, R.S. Sethi and C.R. Lowe, Sensors Actuators, B1 (1990) 550.
9 M. Shichiri, R. Kawamori, Y. Aymasaki, M. Nomura, N. Hakui and H. Abe, Diabetologia, 246 (1983) 179.
10 A.P.F. Turner, I. Karube and G. Wilson (Eds.), Biosensors — Fundamentals and Applications, Oxford University Press, Oxford, 1987.
11 J.W. Shaw, D.J. Claremont and J.C. Pickup, Biosensors Bioelectron., 6 (1991) 401.
12 M. Koudelka, F. Rohner-Jeanrenaud, J. Terrettaz, E. Bobbioni-Harsch, N.F. de Rooij and B. Jeanrenaud, Biosensors Bioelectron., 6 (1991) 31.
13 G. Fortier, E. Brassard and D. Bélanger, Biosensors Bioelectron., 5 (1990) 473.
14 C. Malitesta, F. Palmisano, L. Torsi and G. Zambonin, Anal. Chem., 62 (1990) 2735.
15 M. Shaolin, X. Huaiguo and Q. Bidong, J. Electroanal. Chem., 304 (1991) 7.
16 P.N. Bartlett, P. Tebbutt and C.H. Tyrell, Anal. Chem., 64 (1992) 138.
17 Y. Ikariyama, S. Yamauchi, T. Yukiashi and H. Ushioda, J. Electrochem. Soc., 136 (1989) 702.
18 J. Wang and L. Angnes, Anal. Chem., 64 (1992) 456.
19 N.C. Foulds and C.R. Lowe, Anal. Chem., 60 (1988) 2473.
20 A. Witkowski, M.S. Freund and A. Brajter-Toth, Anal. Chem., 63 (1991) 622.
21 W. Schuhmann, Sensors Actuators, B4 (1991) 41.
22 S.-I. Yabuki, H. Shinohara and M. Aizawa, J. Chem. Soc. Chem. Commun., (1989) 945.
23 S. Nakamoto, N. Ito, T. Kuriyama, J. Kimura, Sensors Actuators, 13 (1988) 165.

Analytica Chimica Acta, 281 (1993) 467–473
Elsevier Science Publishers B.V., Amsterdam

Electropolymerized 1,3-diaminobenzene for the construction of a 1,1′-dimethylferrocene mediated glucose biosensor

Robert J. Geise [1], Sheila Y. Rao and Alexander M. Yacynych
Rutgers, The State University of New Jersey, Department of Chemistry, New Brunswick, NJ 08903 (USA)

(Received 10th April 1992)

Abstract

An electron-mediated glucose biosensor was constructed from spectroscopic-grade graphite electrodes in three steps. A non-conducting electropolymerized film serves to screen out electroactive interferents and prevents electrode fouling. The electron mediator 1,1′-dimethylferrocene is adsorbed on, and retained by the polymer film-modified electrode. Glucose oxidase is then crosslinked with glutaraldehyde on the modified electrode. This yields a biosensor with linear glucose response (2–76 mM) at +150 mV vs. SCE, and little or no interference from oxygen, with a lifetime of up to four months.

Keywords: Biosensors; Diaminobenzene; Dimethylferrocene mediated glucose biosensor; Electron mediator; Electropolymerized films; Glucose biosensor

The first generation of oxidase enzyme-based, electrochemical biosensors used oxygen as the electron acceptor [1,2]. However, oxygen becomes a limiting factor in the enzymatic reaction at high substrate concentrations, due to its limited solubility in aqueous solutions. This limits the upper linear range of the biosensor. To overcome problems associated with low ambient oxygen concentration, the second generation of biosensors used electron mediators as substitutes for oxygen. They mediate the electron transfer in the regeneration of the enzyme to the active form by oxidizing the reduced prosthetic group, e.g., $FADH_2$. Electron mediators also reduce the working potential of the biosensor, thus decreasing interferences, noise, and background current.

Originally, electron mediators were added to the sample solution [3,4], but ideally, they should be confined to the sensing layer to give a self-contained biosensor. However, confining the mediator to the sensing layer has proved to be a challenging task. Two divergent factors must be reconciled, the mediator must be confined to the surface of the biosensor so that it does not leach into the solution. Yet it must be mobile enough to interact with the active site of the enzyme and the electrode surface. Often when a mediator is covalently immobilized to prevent leaching, it does not have sufficient mobility to interact with the active site of the enzyme.

Desirable factors for electron mediators include:

(1) Confining the mediator to the sensing layer at the electrode.

Correspondence to: A.M. Yacynych, Rutgers, The State University of New Jersey, Department of Chemistry, New Brunswick, NJ 08903 (USA).
[1] Present address: International Specialty Products, 1361 Alps Rd., Wayne, NJ 07470 (USA).

(2) Completely reversible redox behavior and a moderate oxidation potential, but not so low as to have interference from oxygen reduction. With higher oxidation potentials, the biosensor requires a longer time to establish baseline, background current and noise are higher, and the number of interferents electrolyzed increases.

(3) The mediator should be stable in both its oxidized and reduced forms.

(4) The electron transfer rates between the mediator and the enzyme, and between the mediator and the electrode, should be as fast as possible.

(5) The mediator should not react with oxygen or any other species present in the sample solution.

(6) Oxidation of the reduced enzyme by the mediator, not by oxygen, should be favored. This minimizes, or eliminates, interference from ambient oxygen.

The use of electron mediators has several advantages: the dependence on low ambient oxygen concentration is decreased or eliminated. This extends the linear response of the biosensor, and also prevents the problem of signal fluctuations with changes in oxygen concentration. A lower working potential is possible because the mediator, and not hydrogen peroxide, is sensed. At a lower working potential there is less interference from electroactive species, such as acetaminophen, ascorbate and urate. The enzyme is not deactivated by hydrogen peroxide, which is no longer produced, or at least has been decreased (if there is competition from oxygen). The limitations include a more complex reaction at the sensor, and additional constraints on construction due to the incorporation of the mediator.

Developing electrochemical enzyme biosensors with surface-confined electron mediators has been the focus of much research. In 1984, ferrocene adsorbed on graphite with immobilized glucose oxidase was the first use of an electron- mediated biosensor [5]. A linear response to glucose, in deoxygenated solution, was obtained over a 1–30 mM range. Jonsson and Gorton used N-methylphenazium ion [6] and ferrocene modified with an "aromatic anchor" [7] as adsorbed mediators. Foulds and Lowe [8] synthesized ferrocene-modified pyrrole by amide linkage of *N*-(3-aminopropyl) pyrrole with ferrocene carboxylic acid. The ferrocene-modified pyrrole was then electropolymerized onto the electrode surface, and glucose oxidase was entrapped in the film during electropolymerization.

Research incorporating mediators and enzymes into carbon paste for use as biosensors is attractive because the sensor can be renewed as needed by stripping off "used" carbon paste to expose a "fresh" sensing surface. Ferrocene derivatives have been mixed into carbon paste with glucose oxidase [9,10], and with xanthine oxidase [11], to yield glucose and hypoxanthine biosensors, respectively. This has also been done with galactose, glycolate, and amino acid oxidases [12]. Gorton et al. [13] have used mediator-modified carbon paste electrodes with dehydrogenase enzymes. Others have used modified carbon paste as a "robust" sensor by placing macroscopic membranes over the surface [14]. Another approach of confining a mediator to the sensing surface is by entrapment in micelles held in place by a dialysis membrane [15]. Adsorbed or entrapped quinones have also been used as mediators [16,17].

Bregg and Heller [18] have described using "electrical wires" to connect the active site of the enzyme to the electrode surface. The wires are redox polymers, such as poly(vinylpyridine), which are complexed or covalently bound to the electrode surface. Hale and co-workers [19,20] have used "polymeric relay systems" for electrical communication between enzyme and carbon paste electrode. These systems use ferrocene-modified poly(ethylene oxide) [19] or polysiloxanes [20] for a glucose biosensor. These polymers have also been used for glutamate biosensors [21]. Bartlett et al. [22] have covalently attached ferrocenes to glucose oxidase yielding mediator-modified enzyme.

Another approach to the problem of communication between enzyme and electrode is direct electron transfer, thus eliminating the need for mediators. Ikeda et al. [23] had success with direct communication between carbon paste electrodes and fructose, alcohol and gluconate dehydrogenase enzymes. Also, conducting salts

(organic metals) such as *N*-methylphenazinium tetracyanoquinodimethanide (NMP + $TCNQ^-$) have been used as electrode materials in the hope of achieving direct electron transfer [24]. While direct electron transfer was observed for enzymes containing flavin mononucleotide (FMN) [25], for flavin oxidases (e.g., glucose oxidase and xanthine oxidase), the oxidation of the prosthetic group is mediated by ions of the dissolved conductive salt [26].

The mediated enzymatic reaction is shown in Fig. 1. The electrode is poised at a potential to oxidize the mediator. For ferrocene mediators this would form the ferricinium ion. Glucose is oxidized at the active site of glucose oxidase and the flavin prosthetic group, FAD, is reduced to $FADH_2$. The mediator oxidizes the $FADH_2$, reactivating the enzyme, and in the process it is reduced to a neutral ferrocene. The ferrocene is then oxidized at the electrode surface to regenerate the ferricinium ion. The resulting current is directly proportional to the glucose concentration.

We sought to address the problems associated with electron mediated biosensors through the use of a construction sequence of a self-regulating electropolymerized film, followed by adsorption of a ferrocene derivative, and the immobilization of glucose oxidase. Previous work has shown that these films are effective in protecting the electrode surface from fouling species (i.e., proteins), and also serve to block electroactive interferents [27–29]. This method of construction resulted in a mediated biosensor with excellent stability and lifetime compared to previously reported mediator-based biosensors. There was no interference from oxygen, and the response was linear to 76 mM glucose. It was possible to use a lower working potential (+150 mV vs. SCE) when compared to hydrogen peroxide-based biosensors. Also, the biosensor did not respond to physiological concentrations of acetaminophen, urate and ascorbate, which are electroactive interferents, nor was protein fouling a problem because of the polymer film. The electropolymerized film provided a high degree of stability for a ferrocene-based biosensor by retaining the mediator within the sensing layer. Results will show that electropolymerized, non-conducting films retain the ferrocene mediator and show no loss of either ferrocene or enzymatic activity for up to 100 days.

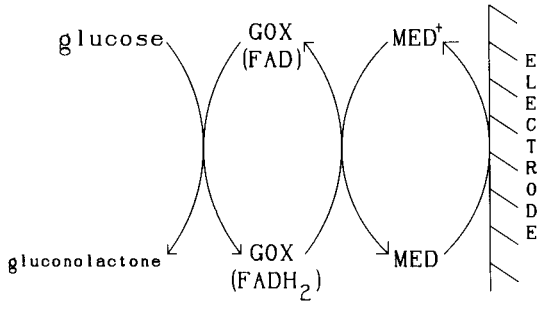

Fig. 1. Schematic of the mediated enzymatic reaction at the electrode surface.

EXPERIMENTAL

Apparatus

All experiments were done using either an EG&G Princeton Applied Research (Princeton, NJ) Model 264A potentiostat or a Model 174 potentiostat. A three-electrode system was used with a saturated calomel reference electrode (SCE) (Fisher, Springfield, NJ), a platinum mesh was the auxiliary electrode, and spectroscopic-grade graphite rods were used as the working electrodes for biosensor construction.

Materials

1,3-Diaminobenzene, 99+% (Aldrich) was purified by sublimation. Phosphate buffer (0.1 M) was prepared with distilled-deionized water using ACS certified potassium phosphate salts (Fisher, Springfield, NJ). The pH was adjusted to 7.4 with concentrated phosphoric acid or potassium hydroxide. Other chemicals used were 1,1'-dimethylferrocene (Lancaster Synthesis, Windham, NH), L-ascorbic acid, 99% (Aldrich), 4-acetamidophenol, 98% (Aldrich), uric acid (Aldrich) and β-D(+)-glucose and bovine serum albumin (Sigma, St. Louis, MO). Hydrogen peroxide solutions were prepared in phosphate buffer by making appropriate dilutions of a 30% solution

(Baker, Phillipsburg, NJ). Glucose oxidase was from Sigma (Type II from *Aspergillus Niger*) and glutaraldehyde, 25% (wt.%) was from Aldrich.

Procedure

Working electrodes were constructed by sealing spectroscopic-grade graphite rods in glass tubing with epoxy. Copper wire was epoxyed to the graphite and extended outside the glass tube for electrical connection. The electrodes were sanded flush and polished by normal methods, the result were disk electrodes.

1,3-Diaminobenzene (DAB) was electropolymerized onto the electrode from a 3 mM solution in phosphate buffer using cyclic voltammetry. The potential was cycled between +0.00 V and +0.80 V at 5 mV s^{-1} for twelve cycles.

A saturated solution of 1,1'-dimethylferrocene (1,1'-DMF) in ethanol was then adsorbed onto an inverted polymer-modified electrode by using three successive drops (approximately 10 μl each), and each was allowed to air dry before applying the next drop. The electrode was then rinsed in distilled-deionized water. Glucose oxidase (GOX) was immobilized on the electrode by crosslinking with glutaraldehyde. A solution containing 5000 units ml^{-1} GOX was prepared by dissolving approximately 0.40 g GOX (25 000 units g^{-1}) in 1 ml phosphate buffer (0.1 M; pH 6.5). 1 ml of 25% glutaraldehyde was then added and the solution was mixed. The enzyme solution (approximately 20 μl) was placed onto an inverted electrode for 0.5 h. The electrode surface was then rinsed with cold phosphate buffer.

The determination of glucose was carried out in a test solution that was prepared to closely resemble a serum sample: 3% (w/v) bovine serum albumin, 0.4 mM urate, 0.1 mM ascorbate, 0.2 mM acetaminophen, and 6 mM glucose in pH 7.4 phosphate buffer. A glucose calibration curve was generated by adding aliquots of glucose stock solution to phosphate buffer with stirring. The electrode response to the test solution was measured, and the glucose concentration was determined by linear regression.

The experiments were performed in "batch" mode with stirring. The biosensor was placed in 20.00 ml of phosphate buffer together with the SCE reference and platinum mesh auxiliary, the potential was applied and the response allowed to come to baseline. The required amount of glucose or interferent was added to the solution to generate a glucose calibration curve and to test the response of interferents.

RESULTS AND DISCUSSION

Modification order of the electrode surface

The three components which comprise the sensing layer are the electropolymerized film [poly(1,3-DAB)], electron mediator (1,1'-DMF), and immobilized enzyme (GOX). These can be applied to the electrode surface in different order. The use of an ethanol solution of the mediator (MED), precludes applying components in order of film/GOX/MED, GOX/MED/film, or GOX/film/MED because of the deactivating effect of ethanol on the enzyme. Applying components in the order MED/GOX/film yielded a biosensor that responded poorly to increasing glucose concentrations. The order MED/film/GOX was not investigated. The response of a biosensor with film/GOX and no mediator is negligible, which indicates that the mediator is required under these operating conditions, +150 mV vs. SCE. However, the order of film/MED/GOX [poly(1,3-DAB)/1,1'-DMF/GOX] yields a very effective glucose biosensor.

Performance of poly(1,3-DAB) / 1,1'-DMF / GOX biosensor

Figure 2 shows a typical strip chart recorder output for such a biosensor. There is no measurable response to 0.1 mM ascorbate (acetaminophen is not electroactive at +150 m V vs. SCE), and the response to aliquots of glucose are fast (90% response < 20 s) and show little noise. Typical responses for biosensors that measure hydrogen peroxide are usually noisier making measurement difficult, which compromises precision and accuracy. There is excellent linearity over an extended range ($r = 0.9950$ for 2–76 mM glucose) in deoxygenated buffer. This extended

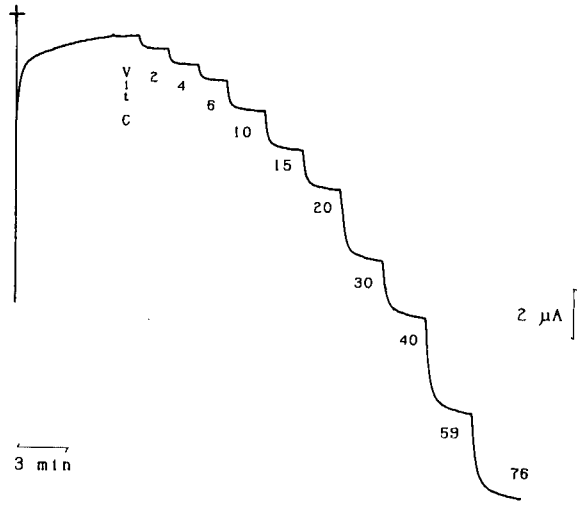

Fig. 2. Strip chart recorder output of a glucose calibration curve (mM glucose additions). Spectroscopic-grade graphite electrode modified with poly(1,3-DAB)/1,1'-DMF/GOX at +150 mV vs. SCE in a deoxygenated solution.

linear response, encompassing the clinical and diabetic ranges, eliminates the need to dilute samples and allows direct measurement.

The electron mediation probably occurs by charge transfer from ferrocene to ferrocene, which is shown in Fig. 3. The electron mediator is represented by the circles with hexagons. This proposed structure demonstrates how the mediator could be in contact with the active site of the enzyme, as well as the electrode surface through a network of ferrocenes.

Ideally, one would prefer a biosensor that is effective at ambient oxygen concentrations, to avoid the work involved in removing oxygen from the system. The competition between ambient oxygen and ferrocene mediator for the oxidation of $FADH_2$ is of major importance if the biosensor is to be used in the presence of oxygen. The regeneration of the oxidized, active form of the enzyme by the mediator must be preferred over oxidation by ambient oxygen, because the oxygen produces hydrogen peroxide, which is not detected at the low working potential. The result, depending on the extent of interference by oxygen, is a decrease in response or no response to glucose.

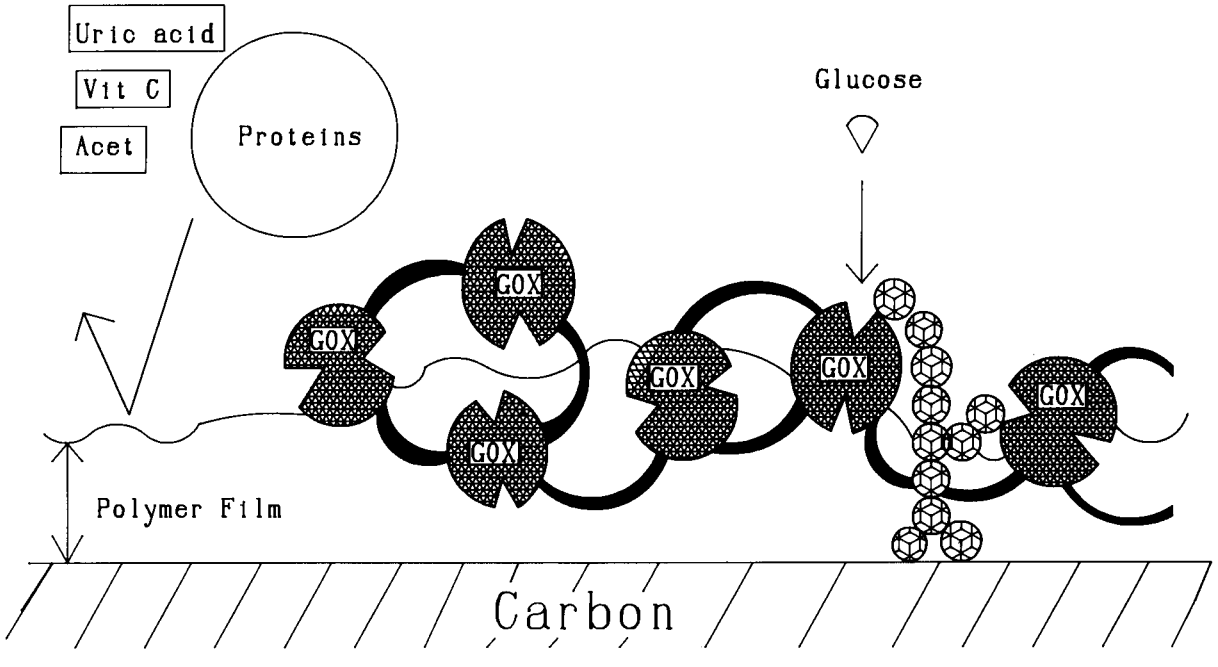

Fig. 3. Proposed schematic showing components of sensing layer at electrode surface. Ferrocene mediator is indicated by circles with hexagons.

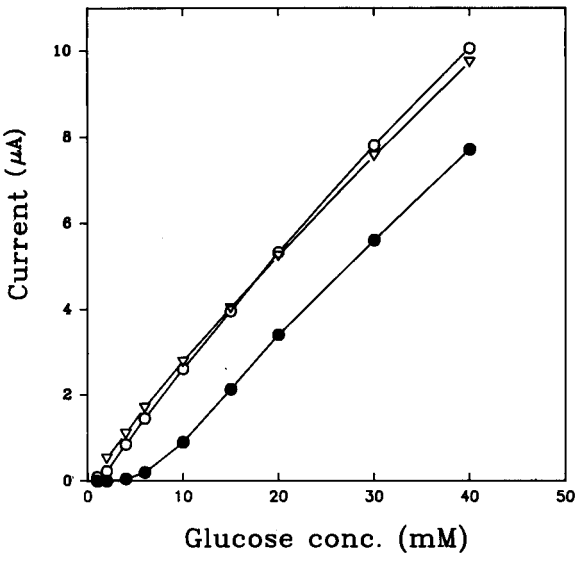

Fig. 4. Glucose calibration curves under conditions of deoxygenation (open triangles), ambient oxygen (open circles), and saturated oxygen (closed circles). Graphite electrode modified same as Fig. 2 at +150 mV vs. SCE.

Figure 4 shows that for 1,3-DAB/1,1'-DMF/GOX biosensor, the mediator reaction, not the oxygen reaction, proceeds virtually exclusively. This is evidenced by the ambient oxygen and deoxygenated glucose calibration curves being superimposed. Any competition from oxygen would produce hydrogen peroxide instead of reduced mediator. Hydrogen peroxide cannot be oxidized at the working potential, thus a decreased response would be observed. With the solution saturated with oxygen, there is little response up to 6 mM glucose, indicating that oxygen, now at a greater concentration, competes with the mediator. However, above this concentration, the slope (sensitivity) of the curve becomes the same as the other two calibration curves, indicating that oxygen no longer competes and is not an interferent. This should not be a practical problem, because measurements under saturated oxygen conditions are rare.

TABLE 1

Determination of glucose in a 6 mM test solution
[C rod with 1,3-DAB/1,1'-DMF/GOX. Test solution: 0.4 mM uric acid, 0.2 mM acetaminophen, 0.1 mM ascorbic acid, 3% (w/v) BSA and 6 mM glucose]

	C rod 56 (21 days)	C rod 30 (100 days)
Glucose calib. curve	$y = 0.23x + 0.14$	$y = 0.19x + 0.09$
2–40 mM: +150 mV	$r = 0.9989$	$r = 0.9992$
Glucose calib. curve	$y = 0.25x + 0.31$	$y = 0.18x - 0.07$
2–40 mM: +100 mV	$r = 0.9967$	$r = 0.9988$
Test solution +100 mV	5.4 mM	6.6 mM
Glucose calib. curve	$y = 0.22x + 0.16$	$y = 0.18x + 0.09$
2–40 mM: +150 mV	$r = 0.9992$	$r = 0.9984$

TABLE 2

Long term performance of glucose biosensors
(Response at +150 mV vs. SCE in deoxygenated buffer. Carbon rods modified same as Fig. 2)

Electrode	Response to 6 mM glucose (μA)	Slope (μA/mM) ($\bar{x} \pm$S.D.) Initial	Final	Days
28	1.51±0.27	0.19 (0.22±	0.17 0.04)	72
29	1.71±0.23	0.22 (0.24±	0.19 0.03)	93
30	1.10±0.12	0.15 (0.19±	0.19 0.02)	129

Determination of glucose in a test solution

The effectiveness of the biosensor in determining glucose in a test solution was studied. Table 1 summarizes the performance of two biosensors tested after 21 and 100 days, respectively. Calibration curves were run at +150 mV vs. SCE before and after the biosensor was exposed to the test solution to check whether its performance and precision was affected by protein fouling. The slopes and correlation coefficients for both runs agree well, proving that the film has prevented protein fouling. A calibration curve was also generated at +100 mV to minimize a slight interference caused by uric acid, and neither sensitivity (slope) nor linearity suffered. Responses to a test solution of 6 mM glucose were typically within ±10% at +100 mV vs. SCE.

Long term performance of poly(1,3-DAB) / 1,1'-DMF / GOX biosensors

These biosensors showed excellent long-term stability stored in buffer at 4°C. Table 2 gives the

long term performance of three biosensors. The usual current response to 6 mM glucose is about 2 μA. The sensitivity of the biosensors, as indicated by the slope of the response (2–40 mM), is also stable. For electrodes 28 and 29 the mean slope value is higher than both initial and final values because the sensitivity actually increased slightly after the start of the experiment, then decreased to the final value.

In contrast, control biosensors without film (mediator/GOX only), lose 25–50% of their absolute current response to 6 mM glucose and 30–55% of their sensitivity, over a 2–40 mM glucose range, within three days of construction due to leaching of the mediator from the surface.

In conclusion, a ferrocene-mediated glucose biosensor was constructed by modifying a spectroscopic-grade graphite electrode with three components. These components, in order of application to the electrode surface, are a non-conducting polymer film, poly(1,3-DAB), 1,1'-dimethylferrocene, and immobilized glucose oxidase. These biosensors are easily and quickly constructed, show excellent linear range and long-term stability with no interference from ambient oxygen.

The authors thank Eugene R. Reynolds for constructing the spectroscopic-grade graphite electrodes.

REFERENCES

1 L.C. Clark and C. Lyons, Ann. N.Y. Acad. Sci., 102 (1962) 29.
2 G.G. Guilbault and G.J. Lubrano, Anal. Chim. Acta, 64 (1973) 436.
3 R.M. Ianniello, T.J. Lindsay and A.M. Yacynych, Anal. Chem., 54 (1982) 1980.
4 R. Szentrimay, P. Yeh and T. Kuwana, ACS Symp. Ser., 38 (1977) 143.
5 A.E.G. Cass, G. Davis, G.D. Francis, H.A.O. Hill, W.J. Aston, I.J. Higgins, E.V. Plotkin, L.D.L. Scott and A.P.F. Turner, Anal. Chem., 56 (1984) 667.
6 G. Jonsson and L. Gorton, Biosensors, 1 (1985) 355.
7 G. Jonsson, L. Gorton and L. Pettersson, Electroanalysis, 1 (1989) 49.
8 N.C. Foulds and C.R. Lowe, Anal. Chem., 60 (1988) 2473.
9 J. Wang, L. Wu, Z. Lu, R. Li and J. Sanchez, Anal. Chim. Acta, 228 (1990) 251.
10 A. Amine, J.M. Kauffmann and G.J. Patriarche, Talanta, 38 (1991) 107.
11 H. Okuma, H. Takahashi, S. Sekimukai, K. Kawahara and R. Akahoshi, Anal. Chim. Acta, 244 (1991) 161.
12 J.M. Dicks, W.J. Aston, G. Davis and A.P.F. Turner, Anal. Chim. Acta, 182 (1986) 103.
13 L. Gorton, G. Bremle, E. Csoregi, G. Jonsson-Pettersson and B. Persson, Anal. Chim. Acta, 249 (1991) 43.
14 S.K. Beh, G.J. Moody and J.D.R. Thomas, Analyst, 116 (1991) 459.
15 U. Loffler, H.D. Wiemhofer and W. Gopel, Biosensors Bioelectronics, 6 (1991) 343.
16 T. Ikeda, T. Shirashi and M. Senda, Agric. Biol. Chem., 52 (1988) 3187.
17 J. Hu and A.P.F. Turner, Anal. Lett., 24 (1991) 15.
18 B.A. Gregg and A. Heller, Anal. Chem., 62 (1990) 258.
19 P.D. Hale, H.L. Lan, L.I. Boguslavsky, H.I. Karan, Y. Okamoto and T.A. Skotheim, Anal. Chim. Acta, 251 (1991) 121.
20 P.D. Hale, L.I. Boguslavsky, T. Inaguki, H.I. Karan, H.S. Lee and T.A. Skotheim, Anal. Chem., 63 (1991) 677.
21 P.D. Hale, H.S. Lee, Y. Okamoto and T.A. Skotheim, Anal. Lett., 24 (1991) 345.
22 P.N. Bartlett, V.Q. Bradford and R.G. Whitaker, Talanta, 38 (1991) 57.
23 T. Ikeda, F. Matsushita and M. Senda, Biosensors Bioelectronics, 6 (1991) 299.
24 W.J. Albery, P.N. Bartlett and D.H. Craston, J. Electroanal. Chem., 194 (1985) 223.
25 J.J. Kulys, Biosensors, 2 (1986) 3.
26 J.J. Kulys and G.J.S. Svirmickas, Anal. Chim. Acta, 117 (1980) 115.
27 S.V. Sasso, Ph.D. Dissertation, Rutgers, The State University of New Jersey, New Brunswick, NJ, 1986.
28 R.J. Geise, J.M. Adams, N. Barone and A.M. Yacynych, Biosensors Bioelectronics, 6 (1991) 151.
29 S.V. Sasso, R.J. Pierce, R. Walla and A.M. Yacynych, Anal. Chem., 62 (1990) 1111.

Analytica Chimica Acta, 281 (1993) 475–481
Elsevier Science Publishers B.V., Amsterdam

Glucose quantitation using an immobilized glucose dehydrogenase enzyme reactor and a tris(2,2′-bipyridyl) ruthenium(II) chemiluminescent sensor

Alice F. Martin and Timothy A. Nieman

Department of Chemistry, University of Illinois, Urbana, IL 61801 (USA)

(Received 18th June 1992; revised manuscript received 10th September 1992)

Abstract

A flow-injection analysis detection method for glucose is presented which is based on oxidation of glucose by glucose dehydrogenase with concomitant conversion of NAD^+ to NADH followed by chemiluminescent detection of NADH. The glucose dehydrogenase is immobilized via glutaraldehyde crosslinking to controlled pore glass to form an immobilized enzyme reactor. The chemiluminescent reagent, tris(2,2′-bipyridyl)ruthenium(II) [$Ru(bpy)_3^{2+}$] is immobilized in a Nafion film coated on a platinum electrode to form a regenerable chemiluminescent sensor. The immobilized $Ru(bpy)_3^{2+}$ is oxidized to $Ru(bpy)_3^{3+}$ which then reacts with NADH produced by the enzyme reactor to yield light and $Ru(bpy)_3^{2+}$. $Ru(bpy)_3^{2+}$ is thus recycled and made available again. Conditions for optimum enzyme reactor efficiency and chemiluminescent detection are determined and reported for pH (about 6.5), flow-rate (2 ml min^{-1}), and NAD^+ concentration (1–2.5 mM). At the optimum conditions a working curve is constructed where the upper limit for glucose detection is dependant on NAD^+ concentration and lower detection limit is 10 μM glucose. Signal reproducibility is 1–2% relative standard deviation. The method is very selective for glucose; some interference is seen from uric acid, ascorbic acid and catechol as well as species (such as oxalate and aliphatic amines) already known to chemiluminesce with the $Ru(bpy)_3^{2+}$ sensor.

Keywords: Biosensors; Chemiluminescence; Flow injection; Enzyme reactor; Glucose quantitation; Immobilized enzyme

Immobilized enzyme reactors (IMER) have been used to selectively catalyze reactions of substrates of analytical interest for some time. Besides inherent selectivity and high efficiency they offer greater enzyme stability, reuseability, and are susceptible to few interferences. The use of oxidase enzymes, glucose oxidase in particular, is most common. Although a large number of dehydrogenase enzymes exist, there have been fewer analytical sensor applications involving these enzymes because the electron acceptor $NAD(P)^+$ must be added to the sample or immobilized along with the enzyme. For example, the reaction sequence of glucose dehydrogenase (GDH) begins with oxidation of β-D-glucose catalyzed by the enzyme with a simultaneous reduction of an equivalent amount of $NAD(P)^+$ followed by hydrolysis of δ-D-gluconolactone to D-gluconic acid.

$$\beta\text{-D-glucose} + NAD(P)^+ \overset{GDH}{\rightleftharpoons} \delta\text{-D-gluconolactone} + NAD(P)H + H^+$$

$$H_2O + \delta\text{-D-gluconolactone} \longrightarrow \text{D-gluconic acid}$$

Correspondence to: T.A. Nieman, Department of Chemistry, University of Illinois, 1209 W. California Street, Urbana, IL 61801 (USA).

For quantitation purposes, NADH is most often the molecule of interest since it can be detected directly by absorption, fluorescence, or electrochemical oxidation. The use of GDH immobilized enzyme reactors (GDH-IMER) to quantitate glucose has been illustrated with use of GDH attached to nylon support or controlled pore glass followed with NADH detection by absorbance [1–3] or electrochemical oxidation [4,5]. Direct electrochemical oxidation of NADH is the most common approach to NADH detection but there are drawbacks due to the high overpotential required, interfering side-reactions and electrode fouling. These problems have been minimized by various modified electrodes containing redox mediators [6,7].

The chemiluminescent reaction of tris(2,2′-bipyridyl)ruthenium(III), $Ru(bpy)_3^{3+}$, and NADH offers an alternative approach for NADH detection. The chemiluminescent (CL) reagent, $Ru(bpy)_3^{2+}$, has been used for quantitation of NADH [8], oxalate [8–10], aliphatic and alicyclic amines [11–14], amino acids and proteins [15–17]. The reaction occurs by the following scheme where the initial oxidation of $Ru(bpy)_3^{2+}$ to $Ru(bpy)_3^{3+}$ is facilitated electrochemically.

$$Ru(bpy)_3^{2+} \longrightarrow Ru(bpy)_3^{3+} + e^-$$

$$Ru(bpy)_3^{3+} \xrightarrow{\text{reductant}} \left[Ru(bpy)_3^{2+}\right]^*$$

$$\left[Ru(bpy)_3^{2+}\right]^* \longrightarrow Ru(bpy)_3^{2+} + h\nu$$

The electrogenerated chemiluminescence (ECL) intensity is then directly related to the amount of reductant, which is NADH in this case. The sensor described here employs $Ru(bpy)_3^{2+}$ immobilized in a Nafion membrane to create a regenerable ECL sensor [8]. This approach conserves the $Ru(bpy)_3^{2+}$ reagent as it is continuously recycled, and also makes the measurement relatively insensitive to pH changes [8].

The discussion which follows illustrates the quantitation of glucose concentrations by use of a GDH-IMER with CL detection of NADH. This is a model system in which other substrates of NAD^+ dependent enzymes could be quantitated. The operating conditions have been optimized, the analytical working range determined and a number of possible interferences tested.

EXPERIMENTAL

Reagents

Glucose dehydrogenase from *Bacillus megaterium* (EC 1.1.1.47), β-nicotinamide adenine dinucleotide from yeast (β-NAD, Grade III), and β-nicotinamide adenine dinucleotide, reduced form (β-NADH, Grade III) were purchased from Sigma (St. Louis, MO). Nafion (a 5% solution in a mixture of alcohols) and tris(2,2′-bipyridyl)-ruthenium(II) chloride hexahydrate [$Ru(bpy)_3^{2+}$] were purchased from Aldrich (Milwaukee, WI). The remaining sample solutions were prepared from reagent grade or better chemicals and purchased from commercial sources. Water for all solutions was purified using a Milli-Q water purification system (Millipore, Bedford, MA). Controlled pore glass (125–180 μm diameter, mesh 80/120) for enzyme immobilization was purchased from Electro-Nucleonics (Fairfield, NJ) and had 62 $m^2\ g^{-1}$ surface area and an average pore size of 250 Å.

Instrumentation

The work presented here was done with the flow-injection system shown in Fig. 1. An Altex Model 110A HPLC pump (Berkely, CA) was used to deliver a buffered carrier stream to the injector, GDH immobilized enzyme reactor column (GDH-IMER), and flow cell via 1/16″ × 0.01″ PTFE low pressure tubing (Rainin, Woburn, MA). Samples were introduced into the carrier stream with an Alcott Model 732 (Norcross, GA) injection valve filled and actuated by an Alcott Model 728 autosampler.

The flow cell was assembled from a conventional LCEC dual platinum electrode (Bioanalyti-

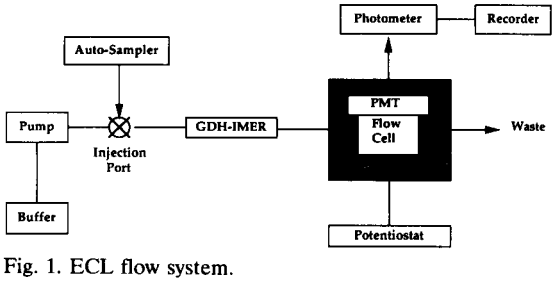

Fig. 1. ECL flow system.

cal Systems, West Lafayette, IN), a Plexiglas window for detection of chemiluminescent emission, and a 1.5-mm PTFE spacer for a cell volume of 125 μl. A screw-in Ag/AgCl reference electrode (Bioanalytical Systems) and a stainless-steel counter electrode tube at the cell exit completed the electrochemical cell. For all experiments the cell potential was held at 1300 mV vs. Ag/AgCl by a BAS 100 (Bioanalytical Systems) potentiostat.

Chemiluminescent emission was collected with a collimating lens placed between the Plexiglas window and a Hamamatsu R928 photomultiplier tube for detection. The anode current was converted to voltage and amplified using a Pacific Instruments Model 124 digital photometer (Concord, CA) and the final signal recorded using a strip chart recorder. All CL intensities reported are the net peak height above the background.

Electrode preparation

For each experiment the dual platinum electrode was polished with 0.05-μm alumina, sonicated and rinsed with methanol, and allowed to dry before casting the Nafion film. The surface was modified by pipetting 25 μl of 2.5% Nafion directly over the platinum electrodes. The 2.5% Nafion was prepared by dilution of the stock Nafion with 2-propanol–H_2O (1 : 1). After drying face up for 30 min, the film was soaked in 0.1 M H_2SO_4 for 1 h to allow the film to swell, then in 1.0 mM $Ru(bpy)_3^{2+}$ dissolved in 0.1 M H_2SO_4 for 30 min to load the $Ru(bpy)_3^{2+}$, and finally again in 0.1 M H_2SO_4 for 30 min. The same $Ru(bpy)_3^{2+}$ solution was used for each loading and is stable for several months without notable degradation [8]. The flow cell was then assembled, placed in a dark box with the photomultiplier tube, and the electrode potential applied with the buffered carrier stream flowing past the modified electrode. The $Ru(bpy)_3^{2+}$ sensor was allowed to equilibrate for at least 30 min prior to the first sample injection.

Enzyme immobilization

The procedure for immobilization of GDH on controlled pore glass (CPG) followed that developed previously in our lab [18,19]. The CPG was cleaned, silanized with an aminoalkyl silane, and reacted with 25% glutaraldehyde. The glutaraldehyde-labelled CPG (0.5 g) was mixed with 12 mg GDH dissolved in 10 ml 0.1 M phosphate buffer at pH 7.5 to complete enzyme immobilization via glutaraldehyde crosslinking. The enzyme-modified CPG was rinsed and packed as a wet slurry into a Plexiglas column (5.7 cm × 0.4 cm i.d.) and capped with nylon end fittings containing 20-μm stainless-steel frits. Between experiments the GDH-IMER was filled with phosphate buffer (pH 6.5) and stored at 4°C.

The efficiency of the enzyme column was monitored by comparing CL signals from 100 μM glucose with added NAD^+ and from 100 μM NADH. A complete reaction of glucose and equivalent conversion of NAD^+ to NADH by the column compared to an equivalent sample of NADH would then yield 100% conversion efficiency. For the results reported, the conversion efficiency of the GDH-IMER varied from 12 to 20%. The column efficiency is affected by the amount of immobilized enzyme and its activity as well as the chosen operating conditions. The reported efficiency is less than that which has been shown achievable with immobilized enzyme reactors but the conversion of NAD^+ to NADH was sufficient to report a useful and sensitive detection method for glucose.

Experimental conditions

Each experiment was carried out using a 0.1 M pH 6.5 potassium phosphate buffer carrier stream. For the pH study the flow system was altered so that the sample was injected into a carrier stream of water and mixed with 0.2 M potassium phosphate buffered at the appropriate pH just prior to the GDH-IMER column. The buffered carrier stream was changed for each pH tested. Samples of 100 μM NADH and 100 μM glucose (with 1.0 mM NAD^+) for this study were made from stock solutions and diluted with water. For the remaining experiments, all samples were made from stock solutions and diluted with buffer. The flow-rate for each experiment was 2.0 ml min^{-1} except for the flow-rate study. For the interference study, two samples of each test compound were made from a stock solution of 1 mM or

greater and diluted to 100 μM with buffer. The first contained test compound alone and the second contained test compound with 100 μM glucose and 1.0 mM NAD^+ added. As a control, 100 μM glucose (with 1.0 mM NAD^+) was injected after the two test compound solutions. Sample injections were made with an autosampler from 1-ml vials with three injections per vial every 2 to 3 min. All experiments were completed using a 45-μl injection loop with exception of the NAD^+ study which used a 100-μl injection loop with manual syringe injections. The peak width at half height was 6 s for a 100 μM NADH sample without the IMER in the flow system and 38 s with the inserted IMER.

RESULTS AND DISCUSSION

The basic goal of these experiments was to illustrate the use of a regenerable $Ru(bpy)_3^{2+}$ CL sensor for selective quantitation of substrates catalyzed by enzymes requiring NAD^+ as a cofactor. Glucose dehydrogenase (GDH) was the model enzyme chosen since it is very selective for glucose and a substrate of bioanalytical importance and commercial interest. The enzyme was immobilized on CPG via glutaraldehyde attachment because of its large surface area and simple procedure for enzyme coupling. Quantitation of glucose is achieved by passing the sample with added NAD^+ through the GDH-IMER and recording a CL signal at the $Ru(bpy)_3^{2+}$ sensor for the NADH produced. This signal is directly proportional to the glucose concentration.

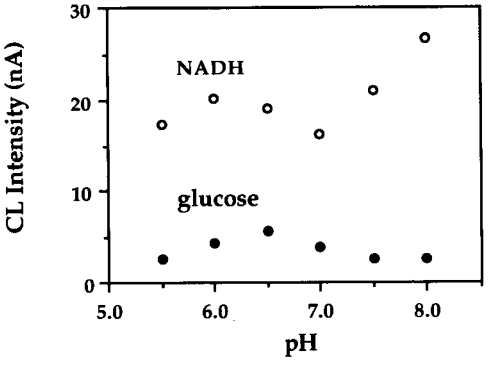

Fig. 2. Effect of pH on CL for 100 μM NADH and 100 μM glucose (with 1.0 mM NAD^+).

NADH has already been shown to be detected quantitatively with the $Ru(bpy)_3^{2+}$ sensor having a detection limit of 1 μM [8]. For the GDH reaction it was necessary to check for possible interferences from gluconic acid, the other enzymatic product, as well as glucose and NAD^+ which may be left unreacted after passing through the GDH-IMER. 1.0 mM glucose and 1.0 mM gluconic acid alone gave no signal. There was an observed signal for 1.0 mM NAD^+ but it was barely distinguishable from the baseline noise and was equivalent to the signal expected for 0.4 μM NADH; this miniscule signal could be due to trace NADH in the NAD^+.

pH and flow-rate

The operating pH was chosen by determining the combined optimum pH for GDH activity and for the $Ru(bpy)_3^{2+}$ sensor reaction with NADH. The pH maximum for other immobilized systems of GDH is somewhat broad, ranging from pH 7.0 to 8.0 [20]. For a similar system, Appelqvist et al. [4] immobilized GDH on CPG and coupled it to NADH detection by a chemically modified electrode. They chose a pH of 6.0 based on the optimum sensitivity of the modified electrode. For the system described here, CL from both 100 μM glucose (with 1.0 mM NAD^+) and 100 μM NADH were compared. For each pH tested, the samples were injected into a carrier stream of water and mixed with the appropriate buffer before passing through the column. Figure 2 shows the CL dependence on pH for the two samples. At pH 6.5 there is a net maximum for the combination of NADH CL and NADH production by the GDH-IMER. The change in NADH CL below pH 6.0 is not due to a drop in the sensor sensitivity but to a decreased stability of NADH in acidic solution. Although the CL increases slightly for NADH above pH 7.0, the amount of NAD^+ converted by the GDH-IMER decreases to a greater degree showing an overall decrease in CL for glucose. The remaining experiments were conducted at pH 6.5.

The optimum flow was determined in a similar manner. Figure 3 shows the CL dependence on

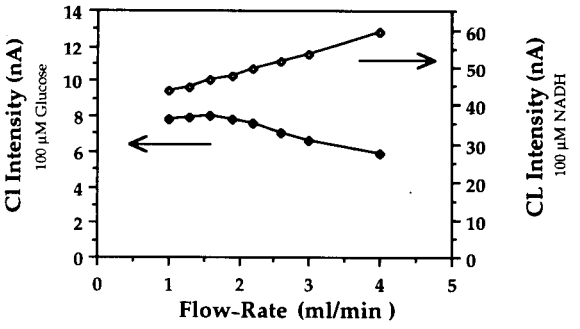

Fig. 3. Effect of flow-rate on CL for 100 μM NADH and 100 μM glucose (with 1.0 mM NAD^+).

flow-rate for both 100 μM NADH and 100 μM glucose (with 1.0 mM NAD^+). As the flow-rate increased, so did the measured signal for NADH. This behavior is reasonable because a greater rate of delivery of NADH to the sensor results in more photons s^{-1} being emitted. The extent of conversion of the NAD^+ to NADH will continuously decrease with increasing flow-rate (due to reduced time in the enzyme reactor). One would expect these opposing trends to yield a maximum in the CL intensity vs. flow-rate plot. This maximum is seen in Fig. 3 at about 1.5 ml min^{-1}. Overall, the signal varied little with flow-rate for the glucose concentration tested; a flow-rate of 2.0 ml min^{-1} was selected for the remaining experiments. The residence time in the enzyme reactor at this flow-rate was about 20 s.

NAD^+ concentration

The NAD^+ cofactor is necessary for the enzyme to carry out oxidation of glucose and must be added to the sample before analysis. Since NADH is the molecule detected by the $Ru(bpy)_3^{2+}$ sensor, the NAD^+ concentration used will influence the working range and sensitivity of glucose detection. This was illustrated by creating four different working curves for glucose, each with a different amount of NAD^+. These curves are shown in Fig. 4. A least squares fit for each curve showed a linear working range up to the point at which NAD^+ became the limiting reagent. For 1.0 mM NAD^+ this range extended beyond 1.0 mM glucose to 2.5 mM. This is understandable because the percent of glucose converted to gluconic acid (with concomitant consumption of NAD^+) by the enzyme was only about 17%. Thus, at higher glucose concentrations there is still additional cofactor available.

Over the 0–2 mM glucose range, the slope for each glucose curve increases with the NAD^+ concentration; this yields increased detection sensitivity at higher concentrations of NAD^+. Also note that for a given glucose concentration the CL signal is dependent on the amount of NAD^+ up to 2.5 mM NAD^+ but beyond that there is no additional increase in CL signal. This reveals an increased conversion efficiency with NAD^+ concentration which has also been observed by Appelqvist et al. [4]. This is reasonable in that both glucose and NAD^+ affect the reaction rate at low concentrations. Although 2.5 mM NAD^+ would seem the best choice for maximum CL, the remaining experiments were conducted with 1.0 mM NAD^+ to conserve on the expensive cofactor while still maintaining almost a 2-decade working range for glucose.

Glucose quantitation

To show the suitability of the method for analytical application the optimized conditions were used to create a glucose working curve and determine signal reproducibility. Figure 5 shows the signal relationship for glucose concentration from 10 μM to 5000 μM (with 1.0 mM NAD^+). The log linear working range extends from 10 μM to 2500 μM. Each point is a mean of three or more

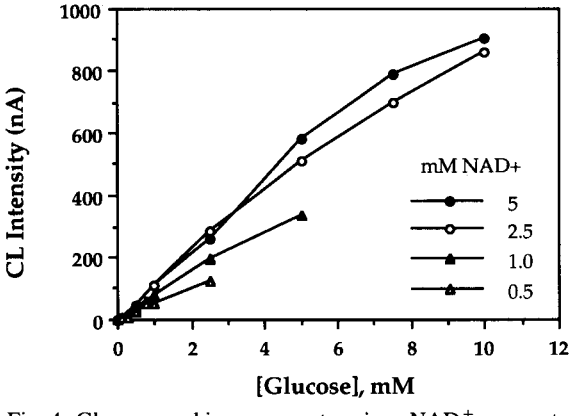

Fig. 4. Glucose working curves at various NAD^+ concentrations.

injections of a sample. The pooled estimate of the relative standard deviation is 1.7% over the 25 μM to 2500 μM log linear working range. For the log–log plot over the 10 to 2500 μM range the least squares slope is 1.06, the standard error estimate is 0.02, and the correlation coefficient is 0.9993. The signal reproducibility was tested by making 20 successive injections of 300 μM glucose. The relative standard deviation was 1.1% for this set of injections and is in agreement with the estimated precision for pooled data over the 25 to 2500 μM range. These data show the excellent precision available and applicability of the method for glucose quantitation.

Selectivity / interferences

The detection scheme presented is applicable for glucose detection in biological samples or food products. A number of sugars similar to glucose and analytes common in biological samples were tested to check for interferences either with the GDH-IMER or $Ru(bpy)_3^{2+}$ sensor. Two solutions of each test compound were made in phosphate buffer (pH 6.5). The first contained 100 μM test compound, the second, 100 μM test compound plus 100 μM glucose (with 1.0 mM NAD^+). Table 1 lists all compounds tested and the resulting signals given relative to the signal for 100 μM glucose injected between samples as a control. The detection system is quite selective for glucose but not exclusive. The small response by galactose and lactose alone is reasonable given possible glucose impurity in those sugars of cross reactivity of the enzyme. NADH, oxalate, proline and tripropylamine also give CL response when injected alone but are known analytes for the $Ru(bpy)_3^{2+}$ sensor and expected to give CL [8]. Uric acid and ascorbic acid give little or no signal alone but yield higher than expected signals when added to glucose. Further investigation showed a sample of either uric or ascorbic acid plus NADH also yields a higher signal than the NADH injected alone. If the enzyme column is removed this phenomena disappears. The results at this point have not been explained and are still under investigation. None of the species investigated inactivates the GDH-IMER. The only species seen to impair the $Ru(bpy)_3^{2+}$ sensor is catechol. After a catechol injection, the signal for glucose is cut by almost 1/3 and does not recover. A similar interference has been previously reported [8].

TABLE 1
Selectivities for various compounds

(Test compound CL signal: normalized to 1.00 for 100 μM glucose with 1.0 mM NAD^+)

Test compound (100 μM)	Test compound alone	Test compound + 100 μM glucose
Allantoin	0.00	1.00
Ascorbic acid	0.05	1.30
Catechol	0.00	0.67
Fructose	0.00	1.05
Galactose	0.08	1.06
Glucosamine	0.00	1.01
Glucuronic acid	0.00	1.04
Lactic acid	0.00	0.99
Lactose	0.04	1.00
Maltose	0.00	1.00
Mannose	0.00	1.03
NADH	3.73	3.70
Oxalate	1.38	2.12
Proline	0.44	1.32
Tripropylamine	8.80	9.04
Urea	0.00	1.10
Uric Acid	0.00	1.51
Xylose	0.00	1.01

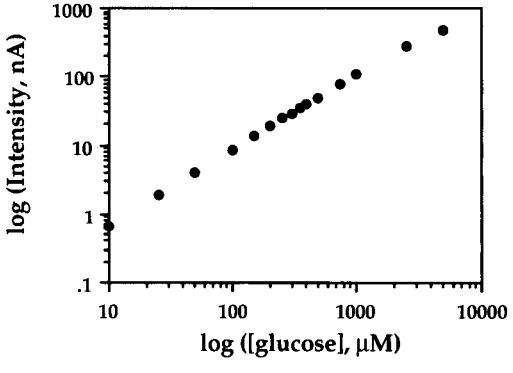

Fig. 5. Glucose working curve.

Conclusions

The work presented illustrates analytical utility of a detection method which couples the selectivity of an enzymic reaction to the sensitivity and

selectivity of a CL $Ru(bpy)_3^{2+}$ sensor. The use of glucose dehydrogenase in this system provides an example by which substrates of other NAD^+ dependant enzymes could be quantitated. Although the conversion efficiency for the GDH-IMER used in this work was not extremely high, the system can easily be improved. With greater enzyme capacity a higher conversion efficiency would be achieved and the detection limit would be correspondingly improved. Another drawback of the current system design is significant sample band broadening which occurs as it passes through the GDH-IMER. Reduction of the column diameter and CPG size would minimize this problem while increasing peak height and detection sensitivity as well as increasing sample throughput. Future directions of this work are to investigate the $NADH/Ru(bpy)_3^{3+}$ reaction for NAD^+ recycling with hopes of also immobilizing the NAD^+ and enzyme to form an enzyme modified electrode.

This work was supported, in part, by a grant from the Biotechnology Research and Development Corporation.

REFERENCES

1 E. Bisse and D.J. Vonderschmitt, FEBS Lett., 81 (1977) 326–330.
2 E. Bisse and D.J. Vondershmitt, FEBS Lett., 93 (1978) 102–104.
3 P.V. Sundaram, B. Blumenberg and W. Hinsch, Clin. Chem., 25 (1979) 1436–1439.
4 R. Appelqvist, G. Marko-Varga, L. Gorton, A. Torstensson and G. Johnsson, Anal. Chim. Acta, 169 (1985) 237–247.
5 G. Marko-Varga, R. Appelqvist and L. Gorton, Anal. Chim. Acta, 179 (1986) 371–379.
6 L. Gorton, G. Bremle, E. Csöregi, G. Jönsson-Pettersson and B. Persson, Anal. Chim. Acta, 249 (1991) 43–54.
7 L. Gorton, E. Csöregi, E. Domíngues, J. Emnéus, G. Jönsson-Pettersson and G. Marko-Varga, Anal. Chim. Acta, 250 (1991) 203–248.
8 T.M. Downey and T.A. Nieman, Anal. Chem., 64 (1992) 261–268.
9 I. Rubinstein, C.R. Martin and A.J. Bard, Anal. Chem., 55 (1983) 1580–1582.
10 N. Egashira, H. Kumasako and K. Ohga, Anal. Sci., 6 (1990) 903–904.
11 J.B. Noffsinger and N.D. Danielson, Anal. Chem., 59 (1987) 865–868.
12 J.B. Noffsinger and N.D. Danielson, J. Chromatogr., 387 (1987) 520–524.
13 N.D. Danielson, L. He, J.B. Noffsinger and L. Trelli, J. Pharm. Biomed Anal., 7 (1989) 1281–1285.
14 K. Uchikura and M. Kirisawa, Anal. Sci., 7 (1991) 803–804.
15 L. He, K.A. Cox and N.D. Danielson, Anal. Lett., 232 (1990) 195–210.
16 K. Uchikura and M. Kirisawa, Anal. Sci., 7 (1991) 971–973.
17 S.N. Brune and D.R. Bobbitt, Talanta, 38 (1991) 419–424.
18 K. Hool and T.A. Nieman, Anal. Chem., 59 (1987) 869–872.
19 C.A.K. Swindlehurst and T.A. Nieman, Anal. Chim. Acta, 205 (1988) 195–205.
20 E. Bisse, A. Scholer and D.J. Vonderschmitt, Appl. Biochem., 3 (1981) 176–182.

Analytica Chimica Acta, 281 (1993) 483–487
Elsevier Science Publishers B.V., Amsterdam

Ferrocene-attached L-lysine polymers as mediators for glucose-sensing electrodes

Seiichiro Iijima, Fumio Mizutani, Soichi Yabuki, Yoshio Tanaka, Michihiko Asai and Tatsuo Katsura

Research Institute for Polymers and Textiles, 1–1–4 Higashi, Tsukuba, Ibaraki 305 (Japan)

Shigeo Hosaka and Masaru Ibonai

Department of Industrial Chemistry, Faculty of Engineering, Kogakuin University, 1–24–2 Nishi-shinjuku, Shinjuku-ku, Tokyo 160 (Japan)

(Received 1st April 1992; revised manuscript received 15th September 1992)

Abstract

Two kinds of water-soluble polymers having ferrocenyl groups were prepared by the reactions of ferrocenoyl chloride with a homopolymer and a copolymer of L-lysine. The polymers acted as electron mediators between electrodes and the reduced form of glucose oxidase. Amperometric glucose-sensing electrodes were constructed by the simultaneous immobilization of each polymeric mediator and glucose oxidase near the surface of a glassy carbon electrode with a semipermeable membrane. The sensing-electrode using the ferrocene-attached L-lysine homopolymer was usable for the determination of glucose concentrations up to 6 mM.

Keywords: Amperometry; Biosensors; Enzymatic methods; Enzyme electrodes; Ferrocene; Glucose; Lysine polymers; Polymeric mediators

Enzyme-based biosensors have been developing rapidly in recent years. In the field of amperometric sensing electrodes with oxidoreductases, much effort is currently being directed at devising enzyme electrodes by the use of redox-active species such as ferrocenium ion and benzoquinone, which mediate the electron transfer between the redox site of an enzyme and the base electrode [1,2]. A membrane-type polymer [3,4] or a carbon paste [1,5], which contains an immobilized enzyme–mediator couple, is usually used for the construction of this type of enzyme electrode. When the mediator is macromolecular and water soluble, a unique and simple method is applicable to the construction; the mediator is entrapped near the base electrode surface together with an enzyme only by using a semipermeable membrane [4,6–8]. Leakage of the mediator and the enzyme into bulk solutions, which would preclude the use of these electrodes as implantable probes, can be avoided by this method, and the simplicity of the method may make it possible to apply a wide variety of oxidoreductases to the mediator-coupled sensing devices. Further, the electron transfer between two macromolecules, enzyme and mediator, is of interest in mimicking the biological electron transfer system, e.g., the cytochrome *c* oxidase–cytochrome *c* system. Ferrocene-attached bovine serum albumins have been reported previously [6,7]. Glucose-sensing electrodes were obtained by the immobilization of the macromolecular water-soluble mediators with glucose oxidase (GOD). This paper reports

Correspondence to: S. Iijima, Research Institute for Polymers and Textiles, 1–1–4 Higashi, Tsukuba, Ibaraki 305 (Japan).

the preparation of L-lysine homopolymer and copolymer having ferrocene moieties and their use as mediators for such a type of glucose-sensing electrode.

EXPERIMENTAL

Preparation of ferrocene-attached polymers

Ferrocene-attached poly-L-lysine (**1**) was prepared by the reaction of poly-L-lysine · HBr (Sigma P-1274, molecular weight based on viscosity 126200 [9]) with ferrocenoyl chloride [10], as follows. To a mixed solution of water (1 ml) and pyridine (5 ml) containing 225 mg of poly-L-lysine · HBr, 210 mg of ferrocenoyl chloride in 1 ml benzene were added at room temperature. After being allowed to stand for 6 h with stirring, the solvents were evaporated to ca. 1 ml under reduced pressure. The residues were extracted with dichloromethane and then with 0.1 M HCl. The extract with 0.1 M HCl was dialysed successively against 0.1 M sodium 3-(*N*-morpholino)-2-hydroxypropanesulphonate (MOPSO · Na) (pH 7.0) and 0.02 M MOPSO · Na (pH 7.0), and was then lyophilized. The resulting dark-brown powder (sample I, 1.02 g) was soluble in water.

Ferrocene-attached L-lysine copolymer (**2**) was prepared according to the procedure used for the preparation of **1** by using the copolymer of L-lysine · HBr, L-alanine, L-glutamic acid and L-tyrosine (molar ratio 34:45:14:7) purchased from Sigma (P-1278, molecular weight by low-angle laser light scattering 52000) instead of the poly-L-lysine · HBr. A dark-brown powder containing **2** (sample II) was obtained similarly through dialysis against MOPSO · Na buffers followed by lyophilization.

Electrochemical measurements

A standard three-electrode configuration was employed, with a platinum wire as the counter electrode and an Ag/AgCl electrode as the reference electrode. The cyclic voltammograms were measured by using a glassy carbon disc (Bioanalytical Systems) (area 7 mm^2) as the working electrode in 0.1 M sodium acetate buffer solution containing 0.2 M NaCl (pH 5.0), which was saturated with argon before the measurement. The enzyme electrodes constructed as described below were tested for their current responses to glucose under potentiostatic conditions, in the same acetate buffer solution that was bubbled with argon and stirred magnetically during the measurement.

Enzyme electrode construction

The enzyme electrode immobilizing **1** and GOD (Toyobo) by the use of a semipermeable membrane (Electrode Ia) was constructed as follows [7]. Sample I (5.0 mg) and GOD (2.0 mg) were placed on the surface of a glassy carbon disc electrode (Bioanalytical Systems) (area 7 mm^2) and then covered with a semipermeable cellulose membrane (Viskase Sales), which was held in place with rubber rings so that the mixed powder of sample I and GOD was sandwiched between the electrode and the membrane. The enzyme electrode was then soaked in 0.1 M sodium acetate buffer solution containing 0.2 M NaCl (pH 5.0). During the soaking period, a small amount (ca. 0.05 ml) of the buffer solution penetrated through the semipermeable membrane to dissolve the powder. As a result, the electrode had a mixed solution layer of **1** and GOD on the glassy carbon surface.

The enzyme electrode immobilizing **1** and GOD by the use of a photo-cross-linkable polymer (electrode Ib) was constructed as follows. A polymer layer including **1** and GOD was prepared by visible light irradiation of the mixed aqueous solution of sample I, GOD and a photo-cross-linkable poly(vinyl alcohol)-based polymer [11] according to the procedure described previously [12]. The polymer layer (thickness ca. 0.03 mm, iron content 0.6 μg) was placed on the surface of the glassy carbon electrode and then covered with a nylon mesh held in place with rubber rings so that the polymer layer contacted the electrode surface tightly.

The enzyme electrode immobilizing **2** and GOD by the use of a semipermeable membrane (electrode II) was constructed according to the procedure applied to the construction of electrode Ia. A mixture of 3.0 mg of sample II and 2.0

mg of GOD was used for the construction of electrode II.

RESULTS AND DISCUSSION

A ferrocene-attached L-lysine homopolymer (**1**) was prepared by the side-chain amide formation of poly-L-lysine with ferrocenyl chloride in a mixed solvent of pyridine and water. The aqueous extract of the reaction mixture was dialysed against 0.1 M MOPSO · Na (pH 7.0) and was lyophilized to afford a water-soluble powdered sample containing **1** (sample I). When the extract was dialysed against pure water, **1** became insoluble by lyophilization. Therefore, sample I, which contained some amount of the buffer species, was used for the following electrochemical experiments.

An aqueous solution of sample I showed absorptions around at 270, 350 and 450 nm, which indicated the introduction of ferrocenyl groups into the starting poly-L-lysine [13]. Its iron content was determined as 0.31% by atomic absorption spectrometry. Optical rotation measurements were made in order to determine the content of **1** in sample I. The optical rotation of the sample in a buffer solution (pH 5.0) was compared with that of the starting polymer solution of known concentration in the same buffer, and the poly(amino acid) concentration (mol g^{-1}) in sample I was calculated on the assumption that the ferrocenyl-group substitution does not affect substantially the optical rotatory power of poly-L-lysine molecules. From the iron and the poly(amino acid) concentrations, it was found that about 6% of the amino groups in poly-L-lysine molecules had reacted with ferrocenoyl chloride. The sample contained 13% of the ferrocene-attached poly-L-lysine as the weight of the free base form.

In the cyclic voltammogram measured for the pH 5.0 buffer solution of sample I, anodic and cathodic peaks were observed at 0.49 and 0.43 V, respectively; this indicated that the ferrocenyl groups bonded to poly-L-lysine molecules were electrochemically active. The half-wave potential of **1** (0.46 V) was similar to that of ferrocenecarboxylic acid (0.49 V), determined in the same buffer solution. The cyclic voltammogram of sample I solution in the presence of GOD is shown in Fig. 1 (line a), and was virtually identical with that measured in the absence of GOD. When glucose was added to the **1**–GOD solution, the shape of the voltammogram changed considerably, as shown in Fig. 1 (lines b–d). The anodic peak of **1** increased according to the concentration of the glucose added, whereas the cathodic peak gradually disappeared. This means that the polymer-attached ferrocenium–ferrocene redox couple mediates the electron transfer between GOD and the electrode as follows:

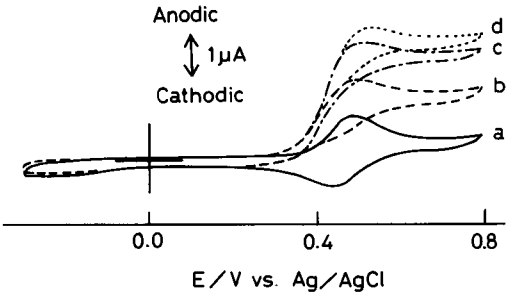

Fig. 1. Cyclic voltammograms of a pH 5.0 buffer solution containing sample I (7 mg ml^{-1}) and glucose oxidase (5 mg ml^{-1}) at different glucose concentrations: (a) 0, (b) 1, (c) 2 and (d) 3 mM. Potential scan rate, 50 mV s^{-1}. Sample I contains the ferrocene-attached L-lysine homopolymer (**1**) as described.

$$\text{glucose} + \text{GOD/FAD} \longrightarrow \text{gluconolactone} + \text{GOD/FADH}_2$$

$$\text{GOD/FADH}_2 + 2\text{Fc}^+ \longrightarrow \text{GOD/FAD} + 2\text{Fc} + 2\text{H}^+$$

$$2\text{Fc} \longrightarrow 2\text{Fc}^+ + 2\text{e}^-$$

where GOD/FAD and $GOD/FADH_2$ represent the oxidized and reduced form of flavin adenine dinucleotide within GOD, and Fc^+ and Fc are the oxidized (ferrocenium) and reduced form of the ferrocenyl group of **1**, respectively.

An enzyme electrode constructed by the simultaneous immobilization of **1** and GOD with a semipermeable membrane (electrode Ia) was tested for its response to glucose at an electrode potential of 0.5 V, i.e., a sufficiently high value for the oxidation of the ferrocenyl groups in **1**.

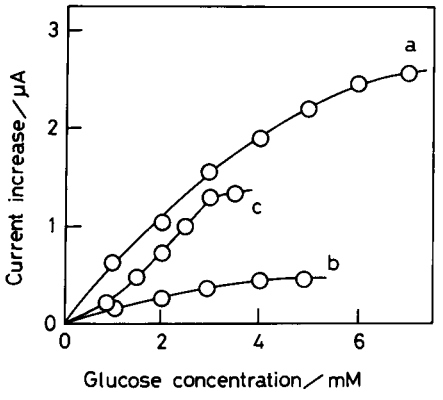

Fig. 2. Relationships between the steady-state current increase and the glucose concentration measured for (a) electrode Ia, (b) electrode Ib and (c) electrode II in a pH 5.0 buffer solution at electrode potential of 0.5 V vs. Ag/AgCl.

The addition of glucose caused an increase in current as expected, and the current reached a steady-state value within 10 min. The relationship between the steady-state current increase and the concentration of glucose is shown in Fig. 2 (line a). This line indicates that glucose concentrations up to ca. 6 mM can be measured by the modified electrode; this upper limit of glucose concentration is about twice those with the same type of enzyme electrodes using ferrocene-attached bovine serum albumin [6,7]. The relative standard deviation was 2.5% for ten successive measurements of 4 mM glucose.

An electrode immobilizing **1** and GOD by the use of a photo-cross-linkable polymer [11,12] (electrode Ib) was also constructed for comparison. As shown in Fig. 2 (line b), the response of electrode Ib to glucose was much lower than that of electrode Ia. With electrode Ib, the probability of collision of the mediator with GOD, and also that with the base electrode, does not seem large, because the molecules of **1** and GOD were confined by the network of the photo-cross-linked polymer. In electrode Ia, on the other hand, the polymeric mediator and GOD can diffuse freely in the solution between the semipermeable membrane and the base electrode, which would be responsible for the greater current increase with electrode Ia by glucose addition.

Another water-soluble polymer having ferrocenyl groups (**2**) was prepared by the reaction of the copolymer of L-lysine · HBr, L-alanine, L-glutamic acid and L-tyrosine with ferrocenoyl chloride. Similarly to **1**, a sample containing some amount of buffer species (sample II, iron content 0.050%) was used for the electrochemical measurements. According to the method applied to the analysis of sample I, it was found that about 14% of the amino groups in the copolymer molecules had reacted with ferrocenoyl chloride, and that sample II contained 2.2% of the ferrocene-attached L-lysine copolymer as the weight of the free base form.

In the cyclic voltammogram measured for a solution of sample II (pH 5.0), anodic and cathodic peaks were observed at 0.51 and 0.45 v, respectively, owing to the redox reactions of the ferrocenyl groups of **2**. An increase in the anodic peak and a decrease in the cathodic peak were observed when glucose was added to the solution in the presence of GOD. An enzyme electrode constructed by the co-immobilization of **2** and GOD with a semipermeable membrane (electrode II) also responded to glucose in a potentiostatic measurement at 0.5 V, as shown in Fig. 2 (line c). The current response of the enzyme electrode, however, reached a saturated value at a lower glucose concentration than that with electrode Ia. The relative standard deviation was 3.0% for ten successive measurements of 2 mM glucose.

Mediator **1** is expected to be positively charged at pH 5.0 because of the high pK_a of the backbone polymer, and there is the possibility of an attractive interaction between **1** and GOD, whose charge is negative at this pH [14,15]. It was found, in fact, that a precipitate was formed by the addition of **1** to a GOD solution of low ionic strength, due to complexation of GOD with **1**. Heller and co-workers [8,16–18] studied a series of polycationic redox polymers having quaternized pyridine groups, and found that electrostatic complex formation of GOD with the polycationic polymers is effective in increasing the rate of the electron transfer between GOD and the polymers. The high mediator ability of **1** suggests that such an electrostatic interaction is

important also for the mediator function of ferrocene-attached poly(amino acid)s.

REFERENCES

1 M. Senda and T. Ikeda, in D.L. Wise (Ed.), Bioinstrumentation, Butterworths, Boston, 1990, p. 189.
2 F. Mizutani and M. Asai, in D.L. Wise (Ed.), Bioinstrumentation, Butterworths, Boston, 1990, p. 317.
3 B.A. Gregg and A. Heller, Anal. Chem., 62 (1990) 258.
4 F. Mizutani and S. Yabuki, in S. Yamauchi (Ed.), Chemical Sensor Technology, Vol. 4, Kodansha, Tokyo, 1992, p. 167.
5 P.D. Hale, H.L. Than, L.I. Boguslavsky, H.I. Karan, Y. Okamoto and T.A. Skotheim, Anal. Chim. Acta, 251 (1991) 121.
6 F. Mizutani and M. Asai, Denki Kagaku, 56 (1988) 1100.
7 F. Mizutani and M. Asai, in I. Karube and R.D. Schmid (Eds.), Proceedings of the MRS International Meeting on Advanced Materials, Vol. 14, Material Research Society, Pittsburgh, 1989, p. 147.
8 M.V. Pishko, I. Katakis, S.-E. Lindquist, A. Heller and Y. Degani, Mol. Cryst. Liq. Cryst., 190 (1990) 221.
9 A. Yaron and A. Berger, Biochim. Biophys. Acta, 69 (1963) 397.
10 E.M, Acton and R.M. Silverstein, J. Org. Chem., 24 (1959) 1487.
11 K. Ichimura, J. Polym. Sci., Polym. Chem. Ed., 22 (1984) 281 7.
12 F. Mizutani, T. Yamanaka, Y. Tanabe and K. Tsuda, Anal. Chim. Acta, 177 (1985) 153.
13 Y.S. Sohn, D.N. Hendrickson and H.B. Gray, J. Am. Chem. Soc., 93 (1971) 3603.
14 B.E.P. Swoboda and V. Massey, J. Biol. Chem., 240 (1965) 2209.
15 H. Tsuge, M. Suzuki, N. Kito, Y. Nakanishi K. Ohashi and K. Aoki, Agric. Biol. Chem., 48 (1984) 19.
16 Y. Degani and A. Heller, J. Am. Chem. Soc., 111 (1989) 2357.
17 B.A. Gregg and A. Heller, J. Phys. Chem., 95 (1991) 5970.
18 B.A. Gregg and A. Heller, J. Phys. Chem., 95 (1991) 5976.

Analytica Chimica Acta, 281 (1993) 489–502
Elsevier Science Publishers B.V., Amsterdam

Amperometric enzyme electrodes for lactate and glucose determinations in highly diluted and undiluted media

Dorothea Pfeiffer, Frieder W. Scheller and Karen Setz

Max-Delbrück-Centre of Molecular Medicine, Department of Biosensors, Robert-Rössle-Strasse 10, O-1115 Berlin-Buch (Germany)

Florian Schubert

Physikalisch-Technische Bundesanstalt, Abbestrasse 2–12, W-1000 Berlin 10 (Germany)

(Received 9th October 1992; revised manuscript received 2nd December 1992)

Abstract

The combination of immobilized enzymes and amperometric electrodes to realize lactate and glucose probes for application to real samples is described. The paper concentrates on the design of lactate oxidase and glucose oxidase membranes for sensors in different areas of diagnostic relevance. Two types of membranes based on the same enzyme immobilization but characterized by different diffusion characteristics are presented.

Keywords: Amperometry; Biosensors; Blood; Enzyme electrodes; Glucose; Lactate

Enzymes are highly attractive tools for diagnostic purposes. They are applied in enzymatic test strips, in autoanalysers, as marker in immunoassays and in enzyme sensors. Enzyme sensors for more than 80 different substances have been described [1–3]. Enzymes have been coupled to electrochemical transducers, optodes, field-effect transistors, calorimetric sensors and piezoelectric devices. However, the enzyme sensors commercialized so far are almost exclusively based on amperometric transducers. Between fifteen and twenty analysers using enzyme electrodes are on the market worldwide. With the exception of the ExacTech (Medisense, Abingdon, UK, and Cambridge, MA, USA) glucose pen [4], the commercialized amperometric enzyme electrodes are enzyme sensors of the membrane type. Most of them measure glucose by means of the anodic oxidation of hydrogen peroxide at +600 mV according to

$$H_2O_2 \rightarrow O_2 + 2H^+ + 2e^- \quad (1)$$

giving a current signal that rises with increasing substrate concentration. The high positive potential applied leads to the anodic co-oxidation of reducing substances that are present in biological media. Various efforts have been made to eliminate these electrochemical disturbances. A cellulose acetate membrane developed by Newman [5] is used in the YSI glucose analyser (Yellow Springs Instruments, Yellow Springer, OH) to improve the selectivity of glucose analysis. However, the cellulose acetate membrane is not truly selective for H_2O_2, but only decreases the permeation of larger molecules. The glucose sensor incorporated in the Model 23 A (YSI) was found to be three times more sensitive to acetaminophen than to glucose [6]. Palleschi et al. [7] proposed the use of membranes with a molecular weight cut-off (MWCO) between 50 and 100 to

Correspondence to: D. Pfeiffer, MDC of Molecular Medicine, Department of Biosensors, Robert-Rössle-Strasse 10, O-1115 Berlin-Buch (Germany).

separate effectively H_2O_2 from larger molecules. However, this would diminish the sensitivity of the enzymatic probe and therefore hamper the analysis of diluted samples.

The prevalence of diabetes in industrialized countries amounts to ca. 4%. Therefore, the selective determination of blood glucose is of utmost importance for the screening and treatment of diabetes. The normal concentration of glucose in blood serum ranges between 4.2 and 5.5 mmol l^{-1} whereas a derailed metabolism may cause an increase to up to 40 mmol l^{-1} glucose.

The identification of lactic acidosis is of increasing interest in clinical chemistry with respect to the diagnosis of cardiac ischaemia, intraoperative monitoring during cardiovascular surgery and in sports medicine to control the energy state of trained sportsmen. The normal lactate value in blood is below 2.7 mmol l^{-1}. Extreme exercise and metabolic stress may cause an increase in lactate concentration to up to 30 mmol l^{-1}, resulting in critical metabolic situations. Only very few laboratory analysers for lactate analysis are on the market. Major efforts are therefore being made to develop a sensor-based lactate analyser that can be readily used at the bedside, providing the user with rapid and reliable lactate results without delay.

The aim of this paper is to demonstrate the potential of the amperometric enzyme electrode concept in application to real samples. Highly reliable glucose oxidase and lactate oxidase membrane electrodes have been established. Modification of the enzyme membrane system permits the application of the sensors in different areas of diagnostic relevance. Two types of device using different kinds of enzyme membranes, but based on the same enzyme immobilization, are presented.

EXPERIMENTAL

Reagents

Glucose oxidase (GOD, EC 1.1.3.4) from *Penicillium notatum* (50 U mg^{-1}) was purchased from Arzneimittelwerk Dresden (Dresden, Germany) and lactate oxidase (LOD, EC 1.1.3.2) from *Pediococcus species* (20 U mg^{-1}) from Boehringer (Mannheim, Germany). The following control sera were used: M + D Moni-Trol I and II from Baxter (Unterschleissheim, Germany), PK I, II and III from AWD Dresden (Dresden, Germany) and Validate-N from Organon Teknika (Eppelheim, Germany). The membranes used were a cellulose dialysis membrane (d = 15–20 μm, MWCO 12 000) obtained from Filmfabrik Wolfen (Wolfen, Germany), a cellulose acetate membrane (thickness 25 μm) supplied by Elkey Products (Worcester, MA) polycarbonate membranes (d = 10 μm, pore diameter 0.015 μm) obtained from Nucleopore (Tübingen, Germany), polycarbonate membranes (d = 10–30 μm, pore diameter > 0.03 μm), polyester membranes (d = 10–20 μm, pore diameter > 0.03 μm) and poly(vinylidene difluoride) membranes (d = 10 μm, pore diameter > 0.03 μm) supplied by Oxyphen (Dresden, Germany). Polyurethane K 8010 and the cross-linking agent Systanat were supplied by BASF (Schwarzheide, Germany). Whole blood samples for accuracy studies were taken from the diagnostic laboratories of a local hospital.

All other reagents used were of analytical-reagent grade.

Enzyme membranes

An amount of 10 mg of lyophilized glucose oxidase (GOD) or lactate oxidase (LOD) was suspended in 250 μl of a 5% solution of polyurethane in acetone and homogenized for 15 min in an ultrasonic bath (Sonorex TK 52; Bandelin Electronic, Berlin). A 5-μl volume of the suspension was spread over 0.2 cm^2 of the cellulose membrane [8]. For application to highly diluted samples, the enzyme layer was covered either with another cellulose dialysis membrane (GOD-NORM and LOD-NORM, respectively) or with a cellulose acetate membrane. For analysis of undiluted media the enzyme was covered with one or more polycarbonate, polyester or poly(vinylidene difluoride) layers and finally sandwiched by a second cellulose dialysis membrane (GOD-MOD and LOD-MOD, respectively). The membranes were stored dry at 4°C (GOD-NORM and GOD-MOD) or −20°C (LOD-NORM and LOD-MOD). GOD-NORM, LOD-NORM,

GOD-MOD and LOD-MOD membranes are now commercially available from BST Bio Sensor Technology (Berlin).

Apparatus

For flow analysis of highly diluted samples the enzyme membrane was used in the flow-through cell of a commercial instrument (enzyme chemical analyser, ESAT 6660 for glucose and ESAT 6661 for lactate; Prüfgeräte-Werk Medingen, Dresden, and Eppendorf, Hamburg) containing a Pt–Ag/AgCl electrode (Pt diameter 0.5 mm; Metra, Radebeul, Germany) polarized at +600 mV. Potassium chloride (0.10 M) was used as the electrolyte. The flow-rate was 1 ml min^{-1}. Alternatively, a modified flow-through cell (BST Bio Sensor Technology) containing a micro-Pt–Ag/AgCl electrode (Pt diameter 0.5 mm; Elbau, Berlin) was used, which allows the flow-rate to be reduced to 0.15 ml min^{-1}.

For STAT analysis the enzyme sandwich membrane is attached to the micro-Pt–Ag/AgCl electrode polarized at +600 mV and incorporated in a portable device (BIOSEN Lactate 2000, EKF Industrie Elektronik, Magdeburg). The first derivative of the current–time dependence of hydrogen peroxide oxidation was used as the measuring signal. In some membrane modification experiments the stationary-state current value of the hydrogen peroxide oxidation was recorded using a chart recorder (BD 112; Kipp & Zonen, Delft, Netherlands).

Measuring procedure

For diluted samples a hypotonic phosphate buffer solution (pH 7.0) with the composition 3 mmol l^{-1} KH_2PO_4, 10 mmol l^{-1} Na_2HPO_4 and 30 mmol l^{-1} KCl is applied for sample dilution (1:50) and for rinsing the sensor. Whole blood is diluted immediately after withdrawal. The buffer provides immediate haemolysis and complete inhibition of glycolysis. Hence the glucose concentration is stable over a period of 24 h. In order to prevent coagulation in the analysis of undiluted samples, 0.5 ml l^{-1} heparin is added to the rinsing solution.

The sensors are calibrated with solutions of 3, 6, 12 and 24 mmol l^{-1}. These solutions are diluted 1:50 with the background buffer for measurement in the ESAT 6660/6661 autoanalyser. The diluted standard solutions are stable for more than 10 days at room temperature. The concentration of glucose or lactate in undiluted solutions is stable for more than 150 days when the solutions are stored at 4°C.

RESULTS AND DISCUSSION

Diluted samples

Lactate. Lactate oxidase specifically catalyses the following reaction:

Lactate + oxygen →

pyruvate + hydrogen peroxide (2)

For the determination of lactate in diluted samples, lactate oxidase entrapped in polyurethane is sandwiched between two identical cellulose dialysis membranes. This type of membrane is designated LOD-NORM.

The enzyme loading test of the LOD-NORM membrane reveals a transient to diffusion-controlled response at about 2 U LOD cm^{-2}. Thus, with a loading of a 25-fold enzyme excess (50 U cm^{-2}) a high functional stability of the enzyme membrane can be expected.

Variation of the pH between 5.0 and 8.0 resulted in a nearly zero-order dependence for lactate concentrations of 0.01 and 0.2 mmol l^{-1}. This gives strong evidence for a diffusion controlled sensor response.

The measuring time of enzyme electrodes depends on the thickness and permeability of the diffusion layer and on the flow conditions in the vicinity of the sensor surface. The estimated characteristic diffusion time for the LOD-NORM membrane is $\tau = 30$ s ($d = 65$ μm). The LOD-NORM membrane was applied to a flow injection analysis system consisting of a palladium–gold-modified carbon electrode polarized at +450 mV [9]. An injection volume of 2.5 μl resulted in a peak width of 18 s at 1% of the maximum peak height. Thus, a measuring frequency of 200 h^{-1} with a serial precision below 1% for twenty successive injections of 1 mmol l^{-1} lactate was obtained.

Sensors equipped with the LOD-NORM membrane are characterized by a linear dI/dt – concentration dependence between 0.01 and 2.0 mmol l^{-1} lactate. With the ESAT 6661 commercial analyser lacate can be measured with lower detection limit of 0.6 mmol l^{-1} lactate and a measuring range up to 40 mmol l^{-1}. Taking in consideration a 1:50 dilution this corresponds to final concentrations of 0.012 and 0.8 mmol l^{-1} lactate, respectively.

The serial and day-to-day relative standard deviations (R.S.D.) obtained with the ESAT 6661 furnished with the LOD-NORM membrane are summarized in Table 1. The R.S.D. represent mean values of ten runs with $n = 21$.

The LOD-NORM membrane can be used for more than 3000 measurements during a period of 10 days. The membrane is stored in a dry state until use. It is stable for more than 1 year at −20°C, 40 days at room temperature and 20 days at 40°C.

The membrane possesses an excellent behaviour towards electrochemically interfering substances. There is no significant contribution of any important substance to the original lactate value up to pathological concentrations. Therefore, the results of lactate analysis using the LOD electrode in the ESAT 6661 agree well with those obtained by established methods, e.g., spectrophotometric analysis using lactate dehydrogenase:

$$y = (0.9907 \pm 0.004)x + (0.1666 \pm 0.002)\ \text{mmol}\,l^{-1}$$

$$r = 0.9923\ (n = 244),\ s_{xy} = 0.45\ \text{mmol}\,l^{-1}$$

where y is ESAT 6661 and x is spectrophotometric analysis.

To guarantee a high accuracy even with varying ambient temperature, the dependence of the sensor performance on the measuring temperature was studied. An increase in temperature from 25 to 37°C increased the measuring frequency by 10%. The serial precision was kept below 2%. The linear measuring range and the behaviour toward potentially interfering substances were also not changed. Similarly, the functional stability was not diminished. Routinely, the enzyme electrode can be thermostated at 37°C during the measuring phase and at room temperature during the stand by mode. The results correlate with those obtained at 25°C as follows:

$$y = (1.0035 \pm 0.02)x - (0.0094 \pm 0.0007)\ \text{mmol}\,l^{-1}$$

$$r = 0.9994\ (n = 30),\ s_{xy} = 0.25\ \text{mmol}\,l^{-1}$$

where y is 37°C and x is 25°C.

Glucose. Glucose oxidase (GOD) catalyses the oxidation of β-D-glucose to D-gluconolactone in the presence of an electron acceptor. Using the co-substrate oxygen, hydrogen peroxide is produced during glucose oxidation:

$$\beta\text{-D-glucose} + \text{oxygen} \rightarrow \text{D-glucono-}\delta\text{-lactone} + \text{hydrogen peroxide} \quad (3)$$

For the determination of glucose in diluted samples, glucose oxidase entrapped in polyurethane is sandwiched between two identical cellulose dialysis membranes. In analogy with the LOD

TABLE 1

Precision of lactate measurement using the ESAT equipment with a LOD-NORM membrane

Sample material	Declared value (mmol l^{-1})	R.S.D. (%)	
		Within-run	Day-to-day
Lactate solution	12.00	0.90	–
Lactate solution	6.00	1.25	–
Control serum	5.35	1.20	2.5
Control serum	9.90	0.67	–
Whole blood	10.01	0.30	–
Whole blood	19.34	1.80	–

membrane described above, this membrane type is designated GOD-NORM.

The enzyme loading test of the GOD-NORM membrane reveals a minimum activity of 1 U cm^{-2} to achieve maximum sensitivity with the glucose probe. The application of 50 U cm^{-2} is the basis for a diffusion-limited glucose electrode with a long lifetime.

Variation of the pH of buffer solution between 5 and 8 did not influence the sensitivity for glucose at concentrations below 0.14 mmol l^{-1}, which corresponds to the normal blood glucose value (considering a dilution of 1:50). This is in agreement with theoretical considerations for diffusion-controlled performance [10]. In contrast, at glucose concentrations above 1 mmol l^{-1} the pH–sensitivity profile exhibits a significant pH optimum close to 7.0. This points to a contribution of the enzyme kinetics to the sensor response.

Polyurethane was found to be high-temperature stable matrix. Whereas for GOD entrapped in gelatin 40°C was found [11], the optimum temperature of polyurethane-entrapped GOD is near 60°C [12].

The final thickness of the glucose oxidase diffusion layer ($d = 60$ μm) is less than that of the lactate oxidase membrane, owing to the higher specific activity of the glucose oxidase. The characteristic diffusion time for the GOD-NORM membrane at 25°C was determined to be $\tau = 24$ s ($D_{eff} = 2 \times 10^{-6}$ cm^2 s^{-1}). With a GOD-NORM-covered electrode in a stirred measuring cell 60 samples per hour can be analysed. However, when the same GOD-NORM membrane is incorporated in a flow system, the sample throughput can be increased. The segmented flow system of the ESAT 6660 enzyme chemical analyser allows a sample frequency of 120 h^{-1}, and the application in a flow-injection analysis system permits 300 samples per hour to be measured with an R.S.D. of 0.5% [13].

Sensors equipped with the GOD-NORM membrane are characterized by a linear concentration range between 0.01 and 2.5 mmol l^{-1} glucose. Similarly to lactate, with the ESAT 6660 commercial analyser glucose can be measured between 0.012 and 1 mmol l^{-1}. Taking into account a dilution of 1:50, this corresponds to glucose concentrations between 0.6 and 50 mmol l^{-1} in the sample.

The within-run and day-to-day precisions for different media using the GOD-NORM membrane in the ESAT 6660 are summarized in Table 2. The data represent the mean values of ten runs with $n = 21$ each. The whole blood precision was obtained by an alternating double analysis of 4.90 and 11.90 mmol l^{-1} glucose-containing samples. A high precision and no statistically significant carryover were obtained.

Recently, these results were supported by a European Multicentre Evaluation of the ESAT 6660 [14]. Following the European guidelines for the evaluation of analysers for clinical chemistry, in this study day-to-day precisions between 1.1 and 3.4% and within-run precisions between 0.35 and 1.45% using five different control materials were found.

Several reducing substances that are present in whole blood are anodically co-oxidizable with hydrogen peroxide and may contribute substantially to the current signal. Most prominent are drugs

TABLE 2

Precision of measurements using the GOD-NORM membrane in the ESAT 6660 analyser

Sample material	Declared value (mmol l^{-1})	R.S.D. (%)	
		Within-run	Day-to-day
Glucose solution	6.0	0.85	2.85
Glucose solution	12.0	0.50	2.55
Control serum PKI	3.05	1.60	3.10
Control serum PKII	5.08	1.25	2.35
Control serum PKIII	7.97	0.90	1.95
Whole blood	4.90/11.90	1.20	–

such as acetaminophen, acetylsalicylic acid and ascorbic acid and metabolites such as uric acid. Depending on the medication and metabolism, the concentration of these compounds may vary over a wide range.

Compared with the concepts described so far [5,7,15], a promising alternative might be the modification of the immobilization matrix in order to optimize the diffusion behaviour of the enzyme membrane. Table 3 shows the relative sensitivity of the GOD-NORM membrane to ascorbic acid, uric acid and acetaminophen as compared with that to glucose. The GOD-NORM membrane has a good specificity towards glucose as compared with potentially interfering substances. The maximum falsification of a whole blood sample with a normal glucose content of 5.5 mmol l^{-1} by the maximum physiological concentration (BIAS) would be 2.45% for uric acid, 1.1% for ascorbic acid and 4% for aetaminophen. This can still be improved upon by covering the GOD-NORM membrane with an additional cellulose acetate membrane.

In addition, no significant interference by 1 g l^{-1} galactose, 1 g l^{-1} fructose, 1 g l^{-1} xylose, 543 μmol l^{-1} bilirubin, 7 mmol l^{-1} triacylglycerol, 3.7 g l^{-1} haemoglobin, 155 g l^{-1} albumin, 36 g l^{-1} paraprotein or 16 mg l^{-1} isoniacid was observed [14].

The GOD-NORM membrane has been applied for up to 10000 measurements over a period of 30 days. The membrane can be stored in a dry state at 4°C for more than 1 year without any decrease in activity.

Both whole blood and serum can be used as sample material. The correlation with the glucose dehydrogenase–NAD^+ method for blood is

$$y = (1.003 \pm 0.006)x - (0.015 \pm 0.002) \text{ mmol}\,l^{-1}$$

$$r = 0.996\ (n = 196);\ s_{yx} = 0.12 \text{ mmol}\,l^{-1}$$

and that for serum is

$$y = (1.024 \pm 0.007)x - (0.019 + 0.0018) \text{ mmol}\,l^{-1}$$

$$r = 0.997\ (n = 260);\ s_{yx} = 0.11 \text{ mmol}\,l^{-1}$$

where y is ESAT 6660 and x is GDH-NAD^+ method.

Viscosity problems with blood samples caused by the lysis of leucocytes with counts of more than 50×10^9 l^{-1} applying a 1 mol l^{-1} NaCl-containing haemolysing solution described by Raabo [16] and Barlow and Harrison [17] were not observed with the basic buffer solution described above.

For measurements of urine glucose, a nitrocellulose-modified glucose oxidase membrane is employed in order to exclude electrochemically interfering uric acid [18]. The method correlates well with the hexokinase reference method:

$$y = (0.958 \pm 0.009)x + (0.149 \pm 0.085) \text{ mmol}\,l^{-1}$$

$$r = 0.995\ (n = 300);\ s_{yx} = 1.78 \text{ mmol}\,l^{-1}$$

where y is ESAT 6660 and x is HK method.

The accuracy has been rated as excellent for the analysis of dilute whole blood and as very good for the analysis of serum [14]. In these studies the ACP 5040 (Eppendorf, Hamburg) the Hitachi 737 (Boehringer) and the ASTRA (Beckman, Munich) were employed as reference methods.

TABLE 3

Sensitivity of GOD-NORM and cellulose acetate-modified GOD-NORM membranes toward interferences

Substance	Maximum physiological range (mM)	GOD-NORM [a]		GOD-NORM + CA [a]	
		RS [b]	(%)	RS [b]	(%)
Glucose	5.50	1.0		1.0	
Ascorbic acid	0.11	0.6	1.1	0.3	0.6
Uric acid	0.40	0.3	2.5	0.1	0.8
Acetaminophen	0.20	1.1	4.0	0.6	1.6

[a] GOD-NORM = cellulose–GOD-PU–cellulose membrane; GOD-NORM + CA = cellulose–GOD-PU–cellulose–cellulose acetate membrane. [b] RS = relative sensitivity.

In analogy with lactate, the GOD-NORM membrane was shown to permit glucose determination at 37.5°C. An increase in temperature from 25 to 37.5°C increased the measuring frequency by 8%. The behaviour toward potentially interfering substances and the linear measuring range were not changed. The serial precision was kept below 2%.

Similarly, the functional stability was not diminished. More than 80% of the initial sensitivity was retained over a period of 45 days (Fig. 1). Routinely, the enzyme electrode can be thermostated at 37.5°C during the measuring phase and at room temperature in the stand-by position.

The results of the determination of 143 whole blood samples analysed at 37.5°C (y) agree well with those obtained at a system temperature of 25°C (x):

$$y = (1.02 \pm 0.004)x + (0.022 \pm 0.008)\ \text{mmol}\,l^{-1}$$

$$r = 0.998\ (n = 143);\ s_{yx} = 0.32\ \text{mmol}\,l^{-1}.$$

Based on the excellent analytical performance of both enzyme systems, a GOD-NORM membrane-containing flow-through cell and a LOD-NORM membrane-containing flow-through cell were arranged in the same flow in series. In addition to the ESAT, a normal amperometric amplifier was applied as the second detection system.

The experiments used glucose- and lactate-containing mixtures. These are stable for more than 100 days at room temperature. Different concentrations of lactate (1.5, 3.0, 6.0 and 12.0 mmol l^{-1}) were added to 12 mmol l^{-1} glucose, giving a linear dependence for lactate. Further, the sensitivity of the glucose probe was not influenced (Fig. 2a). Analogous results were obtained with increasing concentrations of glucose in the presence of a constant amount of lactate (Fig. 2b).

The arrangement with two flow cells in series did not cause a deterioration of the precision. Both detectors exhibited a serial precision below 1.5% with 40 measurements of samples containing 12 mmol l^{-1} of the substances.

Further, there was no carry-over of hydrogen peroxide from the first enzymatic reaction to the second electrode and no influence of the second substrate on the first electrode with GOD at the

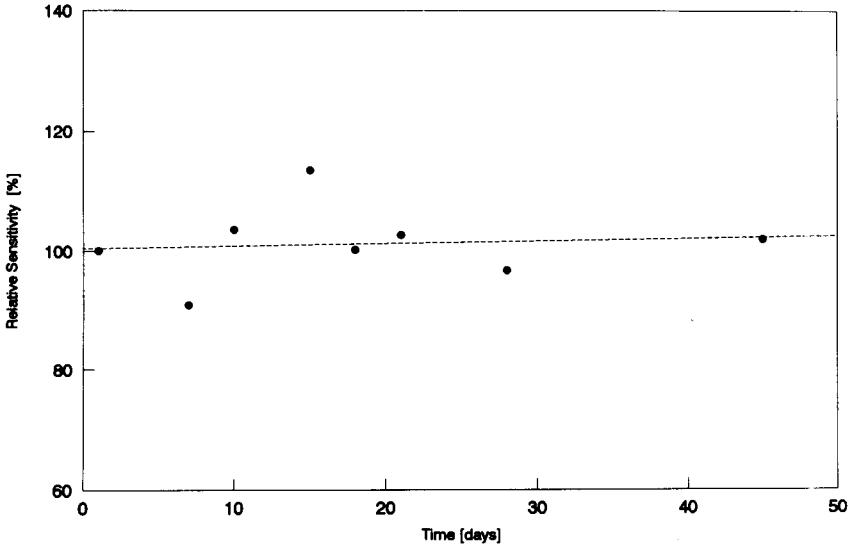

Fig. 1. Functional stability of the GOD-NORM membrane at an operational and storage temperature of 37°C. Glucose concentration, 12.00 mmol l^{-1}.

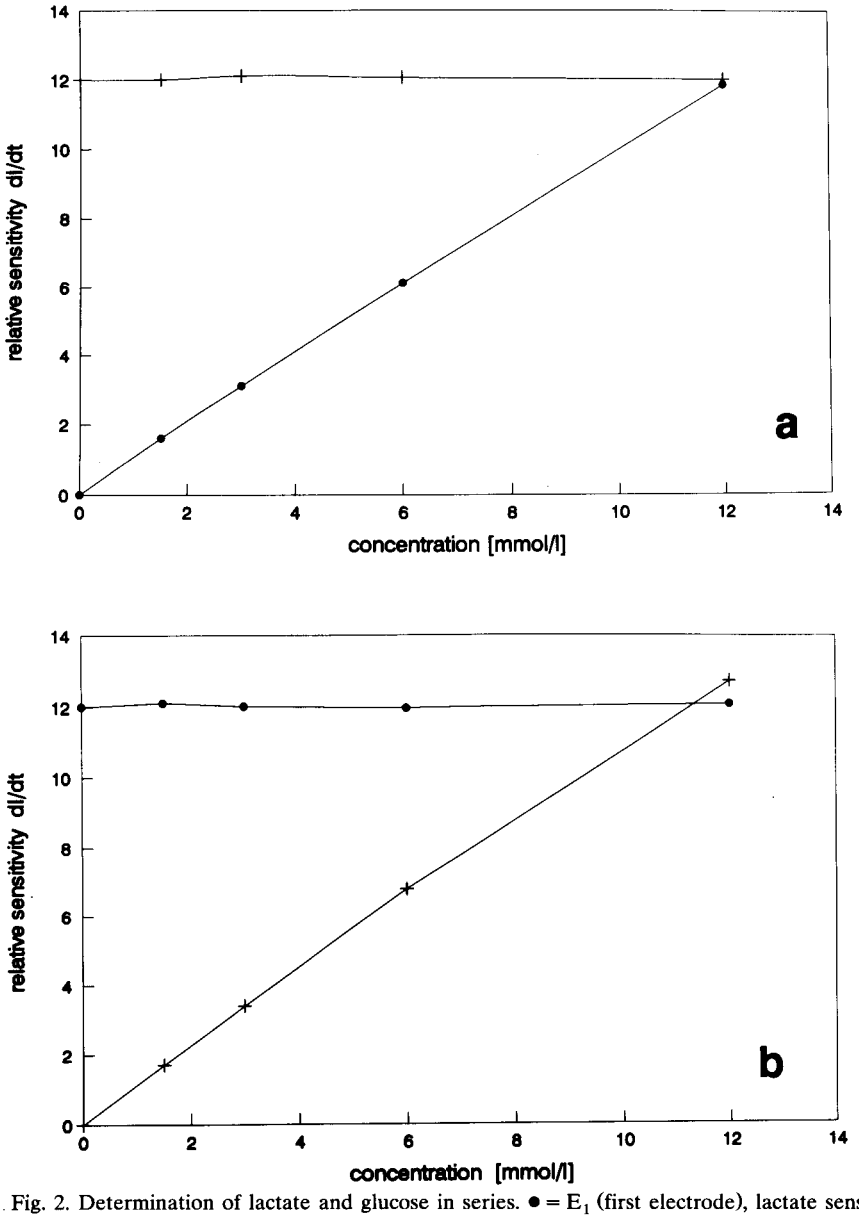

Fig. 2. Determination of lactate and glucose in series. ● = E_1 (first electrode), lactate sensor; + = E_2 (second electrode), glucose sensor. (a) Measurement of lactate in the presence of glucose; (b) measurement of glucose in the presence of lactate.

first and LOD at the second electrode, or in the reverse arrangement.

Undiluted samples

Lactate. To ensure a linear concentration range that allows the analysis of undiluted whole blood and serum, the diffusion behaviour of the lactate oxidase membrane was modified in such a way that the permeation of lactate is reduced significantly while oxygen permeation is promoted. As early as 1978 the extension of the linear concentration range from 2 up to 60 mmol l^{-1} glucose by covering a glucose sensor with an additional polyurethane membrane has been described [19].

Applying this principle, the optimum material for the diffusion barrier has been sought by membrane screening with respect to oxygen permeability, thickness and porosity.

The oxygen permeability of polycarbonate matrices impermeable to substrate was found to be 20 times larger than that of polyester and 30 times larger than that of poly(vinylidene difluoride). This is in agreement with Paul [20], who characterized the oxygen permeation differences in a similar way (polyethylene terephthalate, 0.03×10^{-10}; polycarbonate, 1.4×10^{-10} cm^2 s^{-1} $cmHg^{-1}$). Polycarbonate was therefore used in further experiments.

The optimization of the diffusion behaviour was based on a recently published mathematical model [21].

The experiments resulted in a polycarbonate membrane with a porosity below 0.025%. The membrane type incorporating the polycarbonate layer is designated LOD-MOD.

The incorporation of this diffusion barrier into the original LOD-NORM membrane enzyme membrane significantly increases the response time and decreases the corresponding current output. Using the selected polycarbonate membrane the response time is below 15 s and a complete measuring cycle takes less than 2 min.

Figure 3 shows the results of a loading test with the modified lactate oxidase membrane. The current values for 2.5 and 5.0 mmol l^{-1} lactate increase linearly with increasing enzyme loading between 0.025 and 0.2 U per membrane, corresponding to 0.1 and 0.8 U cm^{-2}. At higher LOD loadings the saturation value is attained. In accordance with theoretical considerations [22], the transient to the diffusion-controlled overall process is below that of the unmodified membrane because of the barrier effect of the perforated gas-permeable membrane.

To ensure an acceptable lifetime of the modified lactate oxidase membrane, an enzyme loading of 16 U cm^{-2} was applied.

Between pH 5 and 8 the sensitivity of the LOD-MOD-containing sensor did not change when samples containing 2.5 and 5.0 mmol l^{-1} lactate were measured. This is due to the diffusion-controlled process, and is in accord with results obtained with the diffusion-controlled unmodified lactate oxidase polyurethane membrane and with gelatin-entrapped lactate oxidase [23] and other enzyme sensors [24].

Recently, the modified lactate oxidase membrane was used with the commercial BIOSEN-Lactate 2000 portable pocket lactate device. Simple handling and low weight make the device

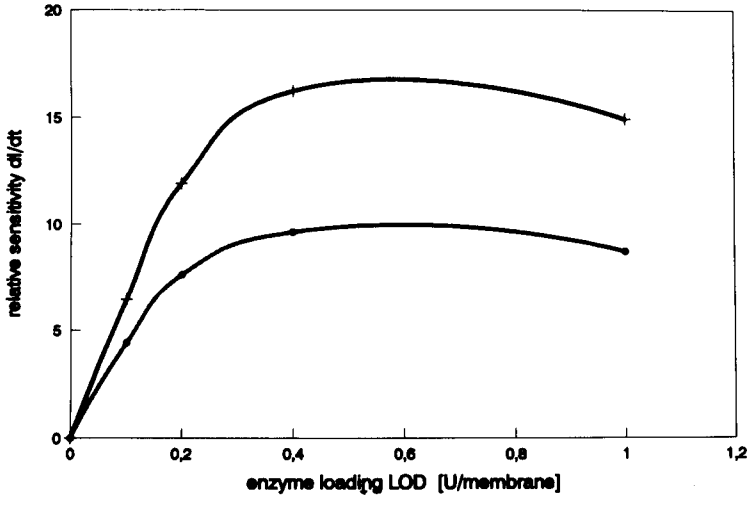

Fig. 3. Enzyme loading test with the modified lactate oxidase membrane (LOD-MOD). LOD-MOD: C–LOD–PC–C, where C = cellulose, PC = polycarbonate, LOD = lactate oxidase entrapped in polyurethane. Lactate: (●) 2.5 and (+) 5.0 mmol l^{-1}.

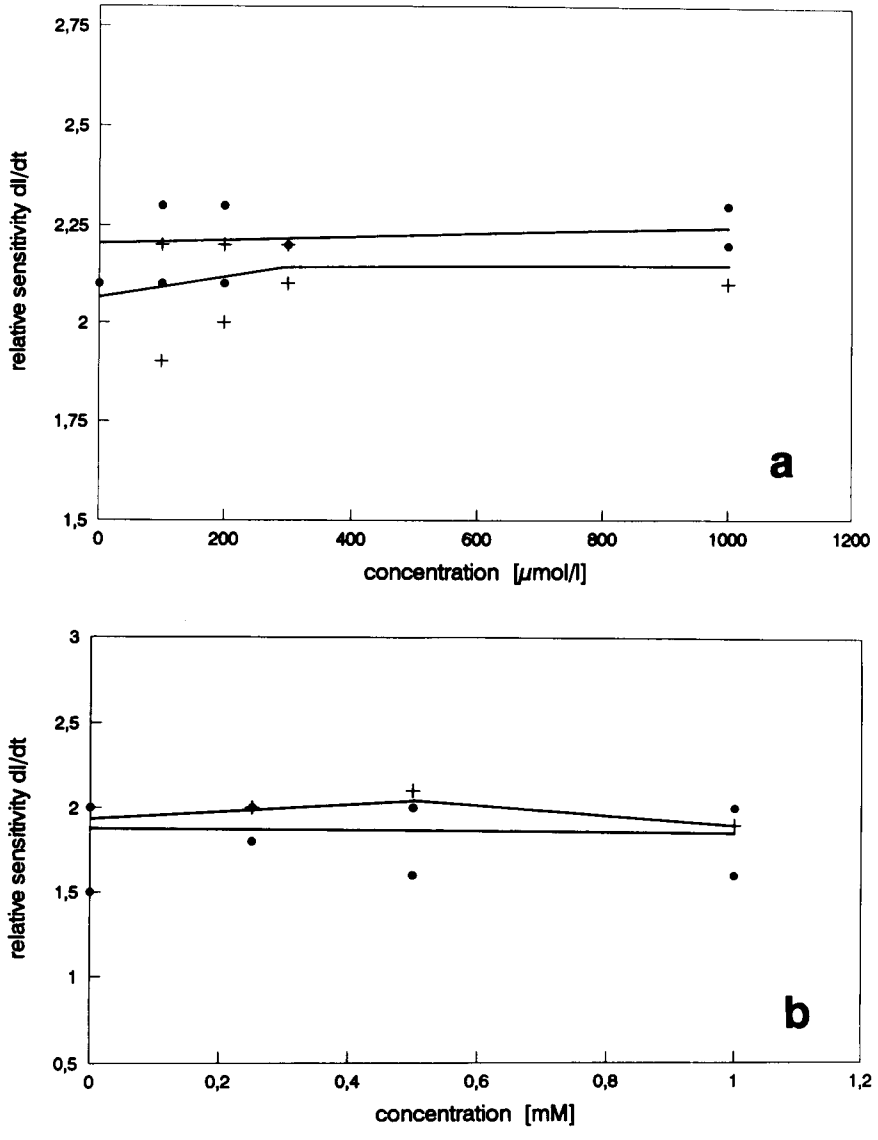

Fig. 4. Accuracy of the LOD-MOD membrane: behaviour toward reducing substances. (a) Contribution of ascorbic acid to the original blood lactate value. • = Whole blood; + = whole blood with increasing concentrations of ascorbic acid. (b) Contribution of acetaminophen to the original blood lactate value. • = Whole blood; + = whole blood with increasing concentrations of acetaminophen.

ideally suited for use in the physicians' or sports medicine consulting room and at sports facilities for exercise control and also in the operating theatre for intensive care. The application of the modified LOD membrane in this device results in the following analytical performance.

Using the modified membrane described, with an overall thickness of $d = 85$ µm, the linear range is up to 20 mmol l^{-1} lactate with a sensitivity of 15 nA $mmol^{-1}$ l^{-1}. The basic current is about 1 nA, which results in a detection limit of 0.1 mmol l^{-1}. The mathematical treatment of

TABLE 4

Accuracy of the lactate probe with the LOD-MOD membrane and undiluted clinical control serum

	c-lactate, declared (mmol l^{-1}) (UV-Boehringer)	c-lactate, BIOSEN-Lactate (mmol l^{-1})
MONI-TROL I (LTD-218)	1.40	1.51
Validate-N (4 y 743)	0.44	0.40
MONI-TROL II	4.90	5.00

c-lactate = lactate concentration.

substrate and cosubstrate concentration profiles shows a 90% decrease in the substrate concentration within the polycarbonate layer whereas the oxygen profile is not significantly affected between 0.2 and 20 mmol l^{-1} lactate.

The within-run precision as determined with 21 lactate solutions of 5.0 and 10.0 mmol l^{-1} is less than 3%. Analyses of 21 serum samples give serial R.S.D.s below 5%. The same was found for whole blood. When a 1.4 mmol l^{-1} lactate-containing clinical control serum was analysed over a period of 10 days, the precision from day to day was below 8%.

The results of serum analysis given in Table 4 demonstrate the accuracy of the sensor. The measured serum lactate values agree very well with the declared values.

Several substances co-oxidizable at +600 mV were investigated with respect to their interfering effect. As can be seen from Fig. 4a and 4b, ascorbic acid and acetaminophen up to 1000 μmol l^{-1} make no significant contribution to the original whole blood or serum lactate value. In addition, no significant interference by 1000 μmol l^{-1} cysteine and creatinine, 1500 μmol l^{-1} uric acid and 5000 μmol l^{-1} salicylic acid was observed.

Further, the accuracy of the modified lactate sensor is demonstrated by comparison with the

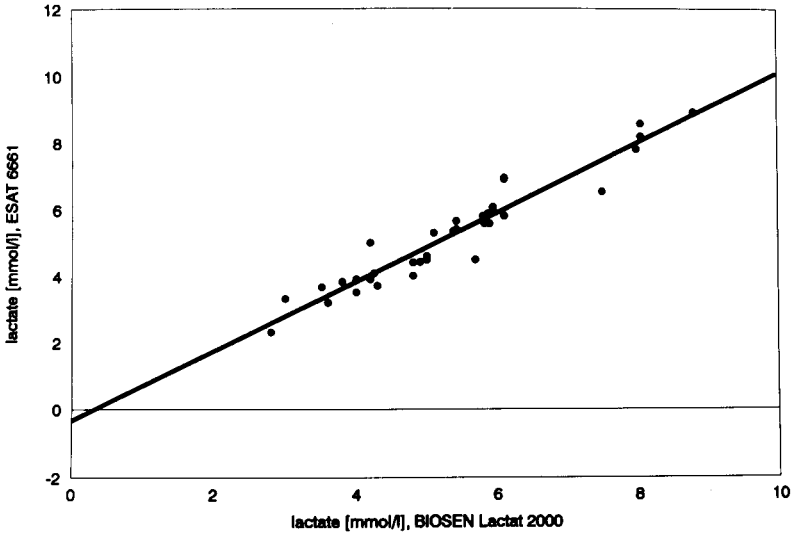

Fig. 5. Comparison of blood lactate measurement with the BIOSEN-Lactate 2000 using LOD-MOD and the ESAT 6661 method using LOD-NORM membrane: $y = (1.012 \pm 0.005)x - (0.212 \pm 0.05)$ mmol l^{-1} ($r = 0.987$; $n = 35$; $s_{y,x} = 0.65$ mmol l^{-1}).

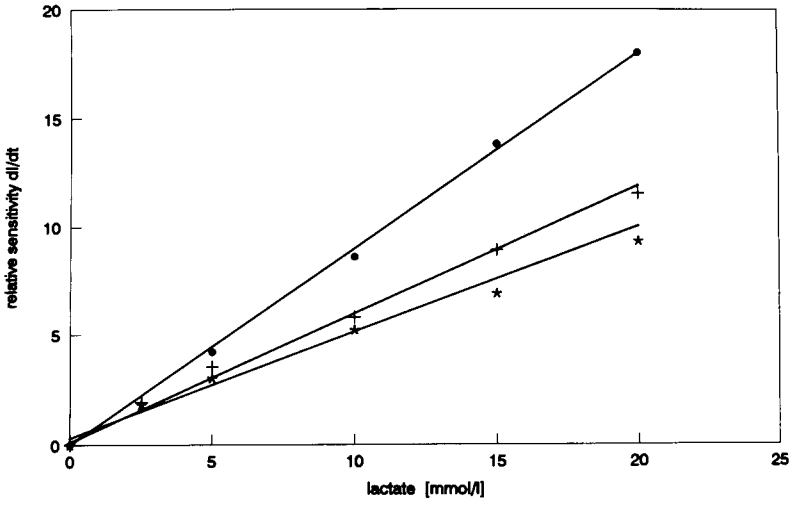

Fig. 6. Functional stability of the LOD-MOD membrane at an operational and storage temperature of 25°C. • = Day 1; + = day 10; * = day 29.

established ESAT 6661 analyser (Fig. 5).

The modified lactate oxidase membrane can be used for more than 2000 measurements. As shown in Fig. 6, the sensitivity is decreased by only 15% over a period of 15 days. After 29 days at room temperature the sensitivity is diminished to 60%, but the linear range remains unchanged.

Glucose. Parallel to the development of the modified lactate oxidase membrane, the optimum composition of the glucose oxidase membrane for application to undiluted media was investigated by screening perforated polycarbonate membranes with respect to porosity and thickness.

Because of the nature and the higher molecular weight of glucose compared with lactate, the requirements with respect to the porosity are different. Using polyurethane-immobilized glucose oxidase, the insertion of a polycarbonate membrane with a porosity below 0.030% ensures a linear glucose range up to 24 mmol l^{-1} which corresponds to 440 mg dl^{-1}. This membrane type is designated GOD-MOD. The insertion of the diffusion barrier in the glucose oxidase membrane results in the signal–time behaviour shown in Fig. 7. As compared with that of the unmodified glucose oxidase polyurethane membrane, the value of the stationary state current is reduced by a factor of ten and the response time is nearly ten times longer. However, exploiting the first derivative of the current–time curve, the response and measuring times were lowered to less than 15 s and 2 min, respectively.

Within the linear measuring range between 0.2 and 24.0 mmol l^{-1} glucose, the modified enzyme membrane is characterized by a serial precision below 5%.

The analysis of control serum samples shows an excellent aggreement of the data obtained with the GOD-MOD membrane (Moni-Trol I,

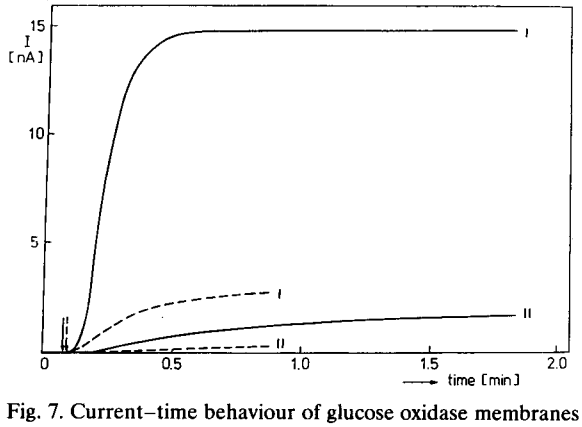

Fig. 7. Current–time behaviour of glucose oxidase membranes with respect to glucose and ascorbic acid sensitivity. I = GOD-NORM; II = GOD-MOD. Solid lines, 1 mmol l^{-1} glucose; dashed lines, 0.25 mmol l^{-1} ascorbic acid.

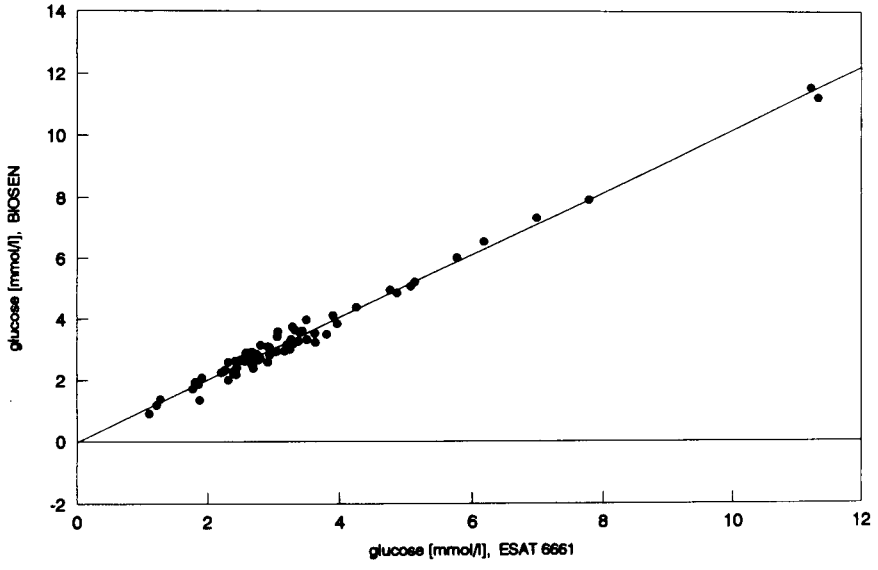

Fig. 8. Comparison of blood glucose analysis with the BIOSEN-Lactate 2000 using a GOD-MOD membrane and undiluted blood samples and the ESAT 6660 using a GOD-NORM membrane and 1 : 50 diluted whole blood: $y = (1.0133 \pm 0.008)x - (0.0229 \pm 0.01)$ mmol l^{-1} ($r = 0.9907$; $n = 70$; $s_{yx} = 0.28$ mmol l^{-1}).

3.94 mmol l^{-1}; Moni-Trol II, 13.20 mmol l^{-1}) and the declared values taken from the glucose dehydrogenase method (Moni-Trol I, 4.04 mmol l^{-1}; Moni-Trol II, 13.30 mmol l^{-1}).

The comparison with the established ESAT 6660 glucose analyser demonstrates the high accuracy of the newly developed glucose oxidase membrane (Fig. 8).

The modified glucose oxidase membrane can be used at room temperature for more than 10 days and more than 2000 analyses.

Conclusion

This study has shown that appropriate modification of the diffusion behaviour of enzyme membranes permits the measuring range of the enzyme sensor to be adjusted. Thus, based on the successful membrane design for application to dilute whole blood, modified glucose oxidase and lactate oxidase membranes have been developed for use with undiluted samples. The enzyme sensors described are incorporated in the Eppendorf ESAT and EBIO analyser and also in the BIOSEN-Lactate 2000 hand-held whole blood instrument providing a more rapid response and therefore a reduction in the time lag between sample withdrawal to the therapy ensuing from the test result.

Concerning the measuring time, the determination with undiluted whole blood or plasma generally results in a decrease in the measuring frequency. This is also observed with the newly developed glucose enzyme electrode module of the laboratory analyser Stat Profile 5 (Nova Biomedical, Waltham, MA) [25]. However, the membrane development for measurements in whole blood is one step forward to invasive metabolite analysis, one of the challenges of future enzyme sensors with respect to critical care and surgical monitoring.

The authors thank Mrs. I. Seyer and Mrs. I. Gall for valuable technical assistance and the laboratory staff of the Robert-Rössle-Hospital at Berlin-Buch for placing the blood samples at their disposal.

REFERENCES

1 A.P.F. Turner, I. Karube and G.S. Wilson (Eds.), Biosensors, Fundamentals and Application, Oxford University Press, Oxford, 1987.

2 A.P.F. Turner (Ed.), Advances in Biosensors 1, JAI Press, London, Greenwich, 1991.
3 F.W. Scheller and F. Schubert (Eds.), Biosensors, Elsevier, Amsterdam, 1992.
4 D.R. Matthews, E. Brown, A. Watson, R.R. Holman, J. Steemson, S. Hughes and D. Scott, Lancet, April (1987) 778.
5 D.P. Newman, US Pat., 3979274 (1976).
6 M. Lindh, K. Lindgren, A. Carlström and P. Masson, Clin. Chem., 28 (1982) 726.
7 G. Palleschi, M.A.N. Rahni, G. Lubrano, J.N. Ngwainbi and G.G. Guilbault, Anal. Biochem. 159 (1986) 114.
8 J. Nentwig, F. Scheller, H. Weise and D. Pfeiffer, DDR Pat., 2778884 (1986).
9 F. Scheller, F. Schubert, B. Olsson, L. Gorton and G. Johansson, Anal. Lett., 19 (1986) 1691.
10 P.W. Carr and L.D. Bowers, Immobilized Enzymes in Analytical and Clinical Chemistry, Wiley, New York, 1980, p. 245.
11 D. Pfeiffer and K. Bertermann, Thesis, Academy of Sciences of the GDR, Berlin, 1982, p. 106.
12 K. Kaiser, Thesis, Academy of Sciences of the GDR, Berlin, 1987, p. 55.
13 B. Olsson, H. Lundbäck, G. Johansson, F. Scheller and J. Nentwig, Anal. Chem., 58 (1986) 1046.
14 M. Römer, R. Haeckel, P. Bonini, G. Ceriotti, A. Vassault, P. Solere, and P. Morer, J. Clin. Chem. Clin. Biochem., 28 (1990) 435.
15 E. Lobel and J. Rishpon, Anal. Chem., 53 (1981) 51.
16 E. Raabo, Clin. Chem., 34 (1988) 173.
17 I.M. Barlow and S.P. Harrison, Clin. Chem., 34 (1988) 2371.
18 G. Hanke, J. Nentwig and F. Scheller, Z. Med. Lab. Diagn., 29 (1988) 390.
19 F. Scheller, I. Seyer, O. Scheller, A. Gesierich, K. Deutsch, A. Makower and M. Jänchen, DDR Pat., 131414 (1978).
20 D.R. Paul, Ber. Bunsenges. Phys. Chem., 83 (1979) 294.
21 T. Schulmeister and D. Pfeiffer, Biosensors Bioelectron., 8 (1993) in press.
22 P.W. Carr and L.D. Bowers, Immobilized Enzymes in Analytical and Clinical Chemistry, Wiley, New York, 1980, p. 217.
23 F. Schubert, Thesis Dr. Sci., Academy of Sciences of the GDR, Berlin, 1990, p. 17.
24 H.-L. Schmidt, W. Schuhmann, F.W. Scheller and F. Schubert, in W. Göpel, T.A. Jones, M. Kleitz, I. Lundström and T. Seiyama (Eds.), Chemical and Biochemical Sensors, VCH, Weinheim, 1991, p. 768.
25 G.J. Kost, D.A. Wiese and T.P. Bowen, J. Int. Fed. Clin. Chem., 3 (1991) 160.

Analytica Chimica Acta, 281 (1993) 503–511
Elsevier Science Publishers B.V., Amsterdam

A needle-type enzyme-based lactate sensor for in vivo monitoring

Yibai Hu, Yanan Zhang and George S. Wilson

Department of Chemistry, University of Kansas, Lawrence, KS 66045 (USA)

(Received 1st April 1992; revised manuscript received 24th August 1992)

Abstract

A miniature needle-type lactate sensor prepared by coupling the enzyme lactate oxidase (LOD) with an hydrogen peroxide probe has been developed which makes possible real-time in vivo lactate measurements. The sensor has a size of 0.35 mm o.d. with a cylindrical sensing cavity in which a multilayer detection element was placed. The linearity of sensor response was extended beyond the clinically relevant concentration range and the response time was about 30 seconds. Measurement of incubated plasma samples with lactate oxidase and catalase showed that the overall endogenous interferences caused a negligible error. In vitro characterization including effects of temperature, pH and P_{O_2} and stability was carried out as well. In vivo tests in rat subcutaneous tissue showed that the sensors functioned reliably. Good correlation was observed between the sensor output and plasma lactate measured simultaneously in situ with a flow injection system. Potential oxygen effects were also measured in vivo and the results showed that the sensor can tolerate reasonably low tissue oxygen levels even for hypoxic conditions in which P_{O_2} was as low as 10 mmHg.

Keywords: Biosensors; Hypoxia; Lactate sensor; Needle-type sensor; Microsensor; Subcutaneous tissue

There is a strong demand for lactate determination in clinical laboratories, especially in intensive care situations because of the association of lactate with several severe diseases. Such conditions as myocardial infarction, severe congestive heart failure, pulmonary edema, septicaemia and hemorrhage can cause shock which may produce lactic acidosis due to anaerobic metabolism [1,2]. This lactic acidosis is life threatening with a high mortality rate [3,4]. In these pathological conditions the information about metabolism may become immediately accessible for therapeutic interventions or for evaluation of optimal fluid therapy [5]. Blood lactate values exceeding 7–8 mM usually are associated with a fatal outcome [6]. The pattern of change or the trend towards an increase of blood lactate is a sensitive indicator of survival [7,8]. Thus in vivo real time lactate determination would be particularly advantageous in this context. In addition, in vivo real time lactate determination would be useful in sports medicine in leading to better evaluation of sport performance.

Enzyme electrodes for the determination of L-lactate have been developed by using immobilized enzymes such as lactate dehydrogenase (cytochrome b_2) (EC 1.1.2.3) [9,10], lactate dehydrogenase (EC 1.1.1.27) [11–13], lactate-2-monooxygenase (EC 1.13.12.4) [14,15] or lactate oxidase EC 1.1.3.2) [16–18]. Some of them have been successfully applied to clinical analysis, but a miniaturized implantable lactate sensor for continuous monitoring is still not yet available.

Shichiri et al. reported the first needle-type enzyme electrode for in vivo glucose measure-

Correspondence to: G.S. Wilson, Department of Chemistry, University of Kansas, Lawrence, KS 66045 (USA).

ment [19,20] in 1982. The development of needle-type glucose sensors suitable for subcutaneous monitoring has been focussed [21–28]. A needle-type implantable enzyme based glucose sensor has been developed in our laboratory recently and was successfully applied in animal experiments [29,30]. Here we report the development of a needle-type implantable lactate sensor in which a hydrogen peroxide probe is coupled with L-(+)-lactate oxidase (LOD). The enzyme catalyzes the following reaction:

$$\text{L-lactate} + O_2 \xrightarrow{\text{L-(+)-lactate oxidase}} \text{pyruvate} + H_2O_2$$

The hydrogen peroxide generated is detected amperometrically.

The in vitro performance of this sensor including the sensitivity, selectivity, stability and influence of oxygen on response has been evaluated. Finally its performance in vivo will be initially evaluated as well.

EXPERIMENTAL

Materials and equipment

L-(+)-lactate oxidase from *Pediococcus* sp. (EC 1.1.3.2) (38 units/mg), lithium L-lactate and bovine serum albumin were obtained from Sigma. Polyurethane (SG 85A) was obtained from Thermedics (Woburn, MA). Cellulose acetate (39.8% acetyl content) was purchased from Aldrich as was the glutaraldehyde (25% aqueous solution) used for enzyme immobilization. All solvents used for polymer solutions were of analytical grade.

Phosphate buffer, pH 7.4, was prepared from phosphate salts (0.1 M) and sodium chloride (0.15 M) with sodium azide (0.1 g/l) as preservative. An L-lactic acid stock solution (0.5 M) was prepared in phosphate buffer and stored at 4°C. All solutions were prepared with water from a Barnstead Nanopure II system.

Amperometry was performed by using a Bioanalytical Systems (W. Lafayette, IN) Model LC4A amperometric detector. Current–time curves were recorded on a Kipp and Zonen Model BD 40 strip-chart recorder.

Sensor fabrication

A Teflon coated Pt–Ir wire (0.25 mm o.d.; Medwire, New York) was stripped to create a cylindrical cavity of 1.5 mm in length at one end with a 3 mm Teflon coated tip at the distal end which served to protect the sensing element. A silver wire of 0.05 mm diameter was wrapped around the Teflon coated sensor body and subsequently anodized in chloride containing buffer to create a Ag/AgCl reference electrode. A cellulose acetate (CA) membrane was prepared by dip-coating the cavity in a 6% CA solution (in acetone–ethanol (1:1)) followed by air-drying. Three dips were found to be necessary for the film to be effectively ascorbate exclusive. A drop (0.6 μl) of freshly prepared enzyme solution, 1.5% lactate oxidase containing 2% bovine serum albumin (BSA) and 0.3% glutaraldehyde, was delivered to the sensing cavity with a microsyringe while the sensor was held in a horizontal position. The enzyme mixture was allowed to reticulate in a moistened environment for two hours and was dried in the air for one hour. The sensor was then

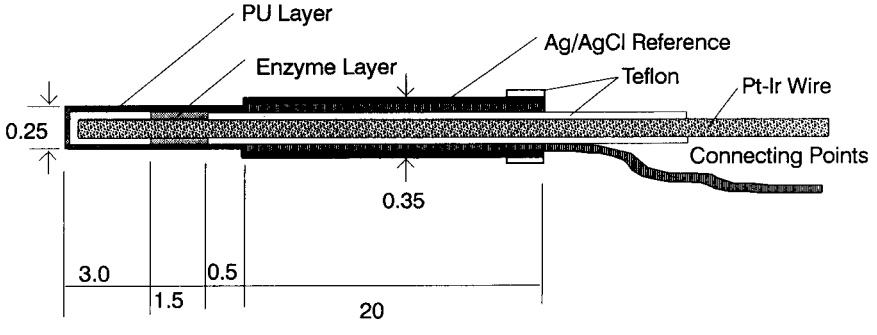

Fig. 1. Schematic diagram of the lactate sensor. Dimensions given in millimeters.

soaked in distilled water to wet the gel-like enzyme layer. This step served two purposes, one was to get rid of excess reagents that were not crosslinked and the other was to extend the enzyme layer along the axial direction to obtain a more uniform enzyme distribution in the cavity. The sensor was again dried in the air for one hour and coated with 5% polyurethane solution. The polyurethane coating was made with a wire loop as described elsewhere [29]. The sensor was then dried for ten minutes in the air and immersed in pH 7.4 phosphate buffer for sensitivity stabilization. Figure 1 shows a complete sensor which is equivalent in shape and size to a 26 Gauge needle (0.35 mm o.d.). The sensing part consists of the multilayer structure including a cellulose acetate (CA) inner layer to discriminate against interferences, an enzyme layer of lactate oxidase crosslinked with BSA and glutaraldehyde and an outer layer of polyurethane (PU) which serves to screen out macromolecules such as proteins and also to control the diffusion of lactate in order to increase the upper limit of linear range.

The response of the sensor to lactate was checked regularly until the sensitivity reached a stable value. This process usually took about 10–20 days.

In vitro calibration of the sensor

The sensor was dipped into a temperature and oxygen tension-controllable cell containing 5 ml of stirred phosphate buffer, pH 7.4, and a potential of +600 mV was applied between the working and the reference/counter electrodes. The background current was allowed to stabilize for at least 30 min. The calibration of the sensor was carried out by adding increasing amounts of L-lactic acid to the stirred buffer. The current was measured at the steady-state response and was related to the concentration of the analyte.

The sensors were stored in 0.1 M phosphate buffer, pH 7.4, or stored dry at 4°C.

In vivo studies

A overnight-fasted male rat (Sprague Dawley, body weight 400 gram) was anaesthetized with halothane anaesthetic (Halocarbon Laboratory, North Augusta, SC) through a mask. The sensors were polarized overnight before implantation. A 20 Gauge catheter was inserted into the subcutaneous tissue on the back of the neck parallel to the spine and the sensor was fed into the catheter in the opposite direction with the sensing tip first. The catheter was then pulled out of the tissue, leaving the sensor inside. The sensor was connected to an amperometric detector (LC4A Bioanalytical Systems, West Lafayette, IN) poised at 600 mV vs. Ag/AgCl and the current was recorded with a Kipp and Zonen BD 40 chart recorder. After the sensor output stabilized, a lactate injection was administered by delivering i.p. 1 to 2 ml of 20% sterile lactate in sodium salt. The plasma lactate was simultaneously monitored with an FIA system.

Blood lactate determination

An FIA system was used to determine the plasma and whole blood lactate. It consisted of a high pressure syringe pump (Model 314, ISCO), an injection valve (Model 7125, Gaertner Scientific) and a micro-flow-cell including a working electrode, an Ag/AgCl reference electrode and a Pt wire counter electrode (Fig. 2). The working electrode was an enzyme lactate sensor that had a similar configuration to the one used for in vivo experiments except that the sensitivity was higher. An electrochemical detector (Model 400, Prince-

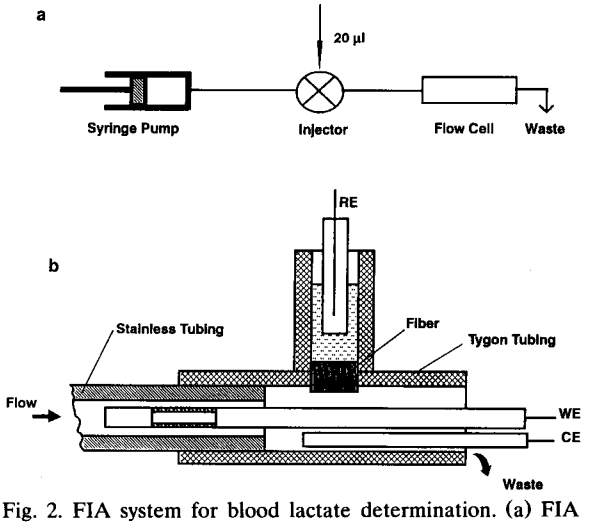

Fig. 2. FIA system for blood lactate determination. (a) FIA system. (b) Flow cell.

ton Applied Research) was employed. The flow-rate was 8 ml/h. The time for a single measurement was 3 min. The detection limit of the system was 0.05 mM and the calibration curve was linear up to 12 mM. The average recovery of spiked rat plasma was 95.8% (S.D. = 0.056, $n = 10$). In the determination of lactic acid in rat plasma for comparison with the in vivo sensor output, 30 μl of blood sample was collected from the end of the rat tail in a fluoride–oxalate tube [31] and centrifuged and measured immediately.

Oxygen effect on lactate sensor

The oxygen sensor was prepared which had the same configuration as the lactate sensor except that the enzyme layer was eliminate. It had a typical sensitivity of 2–7 nA/mmHg when calibrated in pH 7.4 buffer. Lactate and oxygen sensors were implanted through a 20 Gauge catheter into the subcutaneous tissue on the back of the neck. The output of the lactate sensor was monitored at 600 mV vs. Ag/AgCl constant potential and the oxygen sensor output was monitored at −600 mV. The outputs of the sensors were recorded simultaneously with chart recorders.

RESULTS AND DISCUSSION

In vitro characteristics

One of the functions of the outer polyurethane membrane is to reduce the flux of lactate to the enzyme layer and extend the linear dynamic range. The sensors with an upper limit of linear range between 12 and 20 mM showed sensitivities between 1.1 and 2.8 nA/mM. Figure 3 shows the typical response curves of a needle-type lactate sensor to L-(+)-lactic acid. Addition of lithium L-(+)-lactate standard solution produced a rapid increase in current, which reached a steady state within 30 s. Solution stirring produced essentially no effect on the output current. This indicated that the PU membrane served as a rate-limiting barrier for diffusion and made the output current independent of external mass transfer.

The lactate sensor output was dependent on pH in acidic solutions but became relatively constant over the range pH 7–8 (Fig. 4). Fig. 5 shows the effect of temperature on sensor output. Over the range 30–40°C, the mean temperature dependence was 2.3% per °C.

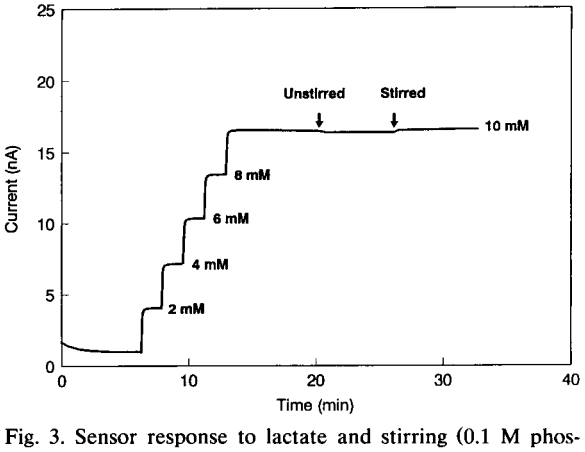

Fig. 3. Sensor response to lactate and stirring (0.1 M phosphate buffer, pH 7.40 at 37°C).

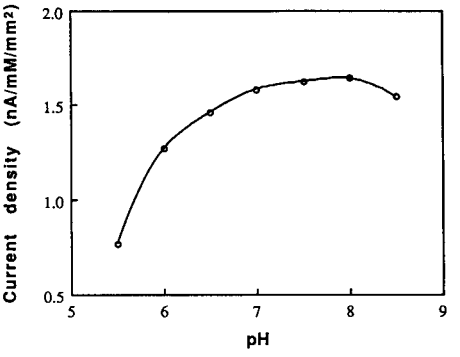

Fig. 4. pH dependence of lactate sensor (0.1 M phosphate buffer, 37°C, 5 mM lactate).

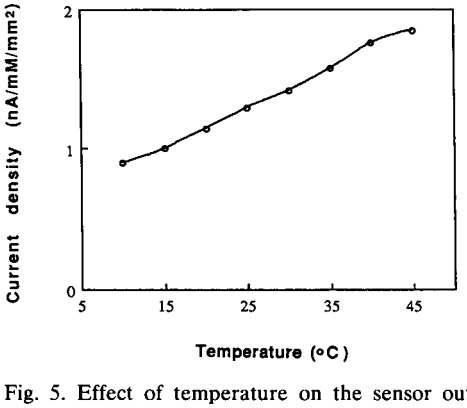

Fig. 5. Effect of temperature on the sensor output (0.1 M phosphate buffer, pH 7.40, 5 mM lactate).

Sensor selectivity

The specificity of the sensor was tested by the following procedure. The sensor was installed into the micro-flow-cell of the FIA system. Lactate oxidase and catalase were added to a freshly prepared rat plasma sample whose lactate content had been previously determined and the mixture was incubated at 37°C for 15 min. Thus lactate was eliminated from the plasma sample during the incubation due to the following reactions:

$$\text{L-lactate} + O_2 \xrightarrow{\text{LOD}} \text{pyruvate} + H_2O_2$$

$$H_2O_2 \xrightarrow{\text{Catalase}} H_2O + O_2$$

The sample was then injected and results are shown in Fig. 6. The plasma contained 1.78 mM lactate (peaks c) as calibrated by standard addition. The same plasma sample gave near negligible response (peaks d) when lactate was eliminated. The residual signal was about 3.1% of the lactate containing sample, which means that the endogenous interfering species in the plasma may cause an error approximately equivalent to 3.1% of the signal in this lactate concentration range.

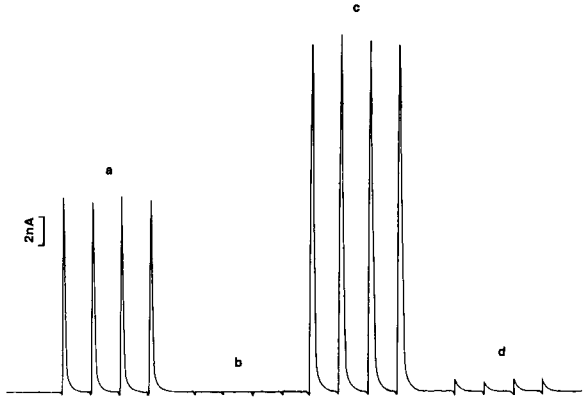

Fig. 6. Sensor response before and after elimination of lactate in plasma. (a) 3 μl of 0.1 M phosphate buffer was added into 30 μl of 1 mM lactate standard solution. (b) 1.5 μl of 2.7% lactate oxidase and 1.5 μl of 5% catalase were added into 30 μl of 1 mM lactate standard solution. (c) 3 μl of 0.1 M phosphate buffer was added into 30 μl of rat plasma. (d) 1.5 μl of 2.7% lactate oxidase and 1.5 μl of 5% catalase were added into 30 μl of rat plasma. All mixtures were incubated at 37°C for 15 min and then detected with the FIA system.

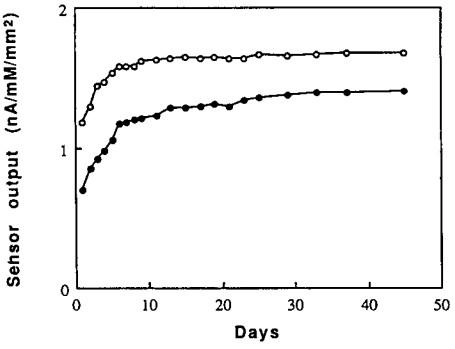

Fig. 7. Storage stability curves for two sensors. Sensors were stored in 0.1 M phosphate buffer, pH 7.40, 4°C.

One of the functions of the negatively charged inner CA membrane is to improve electrochemical selectivity of the sensor by discriminating against interferences. Our prior work showed that the multilayer structure of the implantable sensor was effective in minimizing the errors resulting from the presence of most of the endogenous interferences such as ascorbic acid, uric acid, L-cysteine, urea and fructose [29].

Stability

The sensors showed very good operational and storage stability. After 5 days of continuous use in the FIA system for 4 tested sensors, the response to a 2 mM lactate solution was found to be unchanged. Figure 7 shows the typical storage stability curves for two lactate sensors. A 1–2 week period was required for stabilization. The sensors could maintain stable sensitivity to lactate more than one month when stored in pH 7.4 buffer at 4°C. After 6 months dry storage in the refrigerator, the sensors returned to their full original sensitivity when immersed in 0.1 M phosphate buffer and polarized for about 60 minutes.

In vitro effect of oxygen on sensor

Since the lactate oxidase based sensor requires oxygen as the co-substrate to carry out the lactate oxidation, the effect of oxygen tension on the sensor output was tested in the buffer under different oxygen partial pressures. Sensor dependence on oxygen was decreased by the application of a polyurethane membrane. Figure 8 shows

TABLE 1

In vitro characteristics of lactate sensors [a]

	Sensor number					
	1	2	3	4	5	6
Sensitivity (nA/mM)	0.60	0.85	1.2	2.5	3.3	5.7
Linearity (mM)	28	25	20	12	10	8
Critical P_{O_2} (mmHg)	3	5	8	10	21	42

[a] Measurements made in 10 mM lactate solution pH 7.40, 37°C.

the P_{O_2} dependence for a sensor with low sensitivity 1.2 nA/mM (Fig. 8a) and a sensor with high sensitivity 5.7 nA/mM (Fig. 8b). The high sensitivity sensor showed a strong dependence on oxygen tension due to high demand for oxygen. When the oxygen partial pressure was decreased from 40 mmHg to 10 mmHg at 10 mM lactate, a nearly 25% decrease in output was observed. For the low sensitivity sensor, on the other hand, the response was found to be essentially independent of the oxygen partial pressure. No oxygen dependency was observed when the oxygen partial pressure dropped to as low as 8 mmHg at 10 mM lactate. Table 1 gives the characteristics of 6 lactate sensors and the corresponding P_{O_2} at which the sensor output starts to be affected by oxygen deficiency. A general rule can be drawn to ensure the proper functioning of the lactate sensors. The sensor sensitivity should not be higher than 2.5 nA/mM, the sensor linearity should be higher than 12 mM and the sensors can be used at $P_{O_2} > 10$ mmHg.

In vivo studies

In this study the subcutaneous tissue was chosen as the implantation site for an in vivo test. Our sensor design is compatible with subcutaneous implantation and it may also lead to potential future application as a subcutaneous sensor. Totally 13 sensors were tested in rats. Usually more than one sensor was implanted in each rat in order to obtain comparable results. Figure 9 illustrates the typical result of one experiment in which two lactate sensors and one blank sensor (without lactate oxidase but otherwise identical in configuration to the lactate sensor) were implanted in one rat. Two lactate injections were made during the experiment. The corresponding increase in both plasma lactate level (Fig. 9a) and sensor output (Fig. 9b and c) was observed almost immediately after the injection (less than two minutes). The blank sensor indicates the background signal (Fig. 9d) and the residual current (background) assumes a stable value and does not change due to the lactate administration. There seems to be a very short time lag between plasma and subcutaneous tissue lactate response in contrast to the observation for i.p. glucose injection where a lagtime of about 5 minutes between plasma and subcutaneous tissue glucose concentration is observed [30]. It is assumed that lactate transport in the body is faster than glucose.

Although the absolute correlation between plasma and subcutaneous tissue remains to be further clarified, it is reasonable to calculate an apparent "in vivo sensitivity" based on the plasma concentration [21] so that the sensor output can

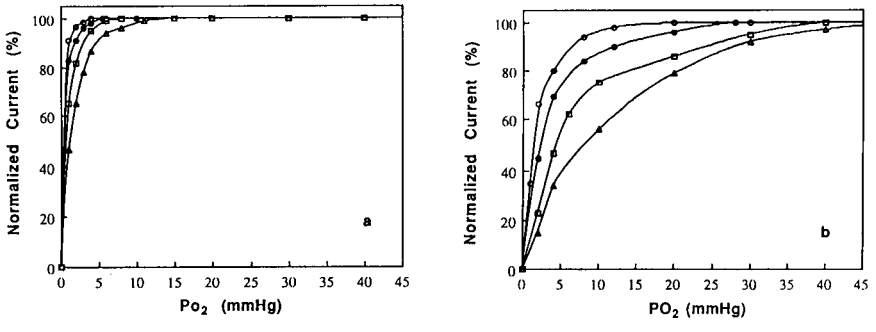

Fig. 8. In vitro effect of oxygen on lactate sensors. (a) Sensor with 1.2 nA/mM sensitivity, (b) 5.7 nA/mM sensitivity. Lactate concentrations: (○) 2 mM, (●) 5 mM, (□) 10 mM, (△) 15 mM.

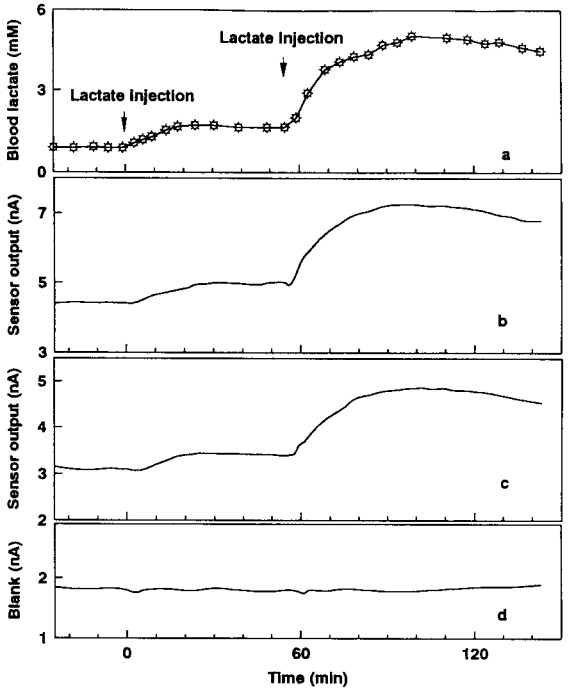

Fig. 9. In vivo response of lactate sensor. (a) Blood lactate concentration. (b) Lactate sensor (3) output. (c) Lactate sensor (8) output. (d) Blank sensor output.

be converted into corresponding concentration. Table 2 shows the in vivo sensitivities of 8 sensors. It is noted that there is a decrease in the apparent in vivo sensitivity as compared to the corresponding in vitro sensitivity. This phenomenon has been typically observed for other in vivo sensors. By using the values of the apparent in vivo sensitivity it was possible to transform the sensor output at any given time into an apparent subcutaneous lactate concentration. Figure 10 shows that the variations of apparent lactate concentration detected by the above two sensors closely follow those of plasma lactate.

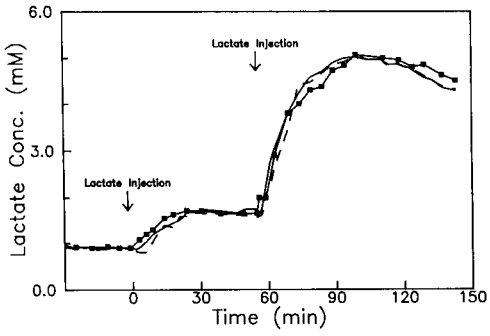

Fig. 10. Correlation between apparent subcutaneous tissue lactate concentrations calculated from the sensor output and plasma lactate concentration. Square: plasma lactate concentration. Solid curve: apparent tissue lactate concentration (from sensor 3). Dash curve: apparent tissue lactate concentration (from sensor 8).

Blood vessel, muscle and subcutaneous tissue may all be potential sites for sensor implantation. The site of implantation will also be dependent on the purpose of measurement, i.e. local or systemic metabolism. The subcutaneous tissue has been a favorite site [19,21–23] because it is easily accessible. The monitoring of peripheral lactate would be helpful in the early detection of anaerobic metabolism, but the possible kinetic relationship between the subcutaneous lactate level and that of blood must be investigated, especially under pathological conditions.

In vivo oxygen effect

As has been indicated in the in vitro experiment, the lactate sensor is essentially oxygen independent as long as the sensor sensitivity is controlled within a certain range. In vivo evaluation of the oxygen effect was carried out in rats. An oxygen sensor and two lactate sensors were implanted in each rat. Lactate administration was also performed in each experiment and the tissue

TABLE 2

Comparison of in vitro and apparent in vivo sensitivities of lactate sensors

	Sensor number							
	1	2	3	4	5	6	7	8
In vitro sensitivity (nA/mM)	6.1	3.2	4.0	0.6	2.0	1.4	2.7	2.4
In vivo sensitivity (nA/mM) [a]	0.23	0.38	0.69	0.25	0.33	0.10	0.70	0.42

[a] Apparent sensitivity.

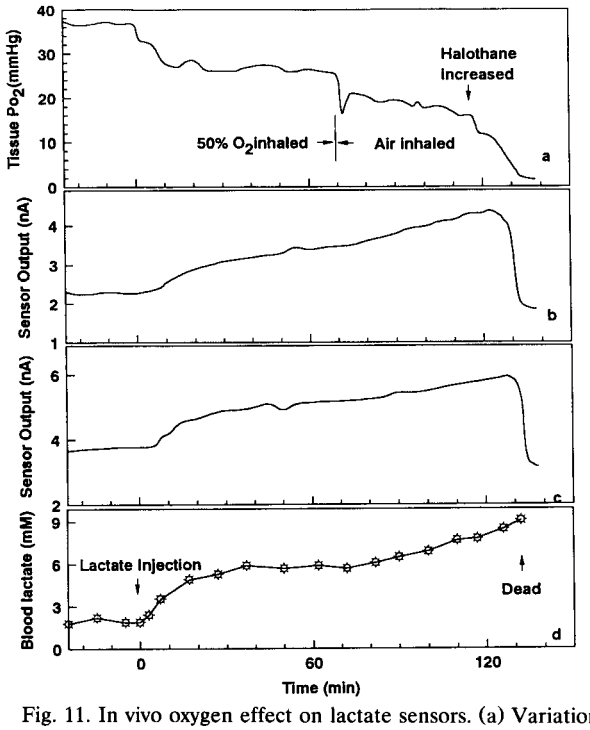

Fig. 11. In vivo oxygen effect on lactate sensors. (a) Variation of tissue oxygen tension. (b, c) Output current of two lactate sensors. (d) Plasma lactate concentration.

oxygen level was altered by changing the ratio of oxygen to air which was inhaled by the animal. No oxygen effect was observed except under extreme hypoxic conditions. Figure 11 shows a typical example of such experiments. Figure 11a indicates that the tissue oxygen level changes as the rat inhales different oxygen–air ratios. The tissue oxygen level also further decreases as the result of increased anesthesia. Figure 11b and c are the output of two lactate sensors that respond readily to the change of blood lactate (Figure 11d) without being affected by the tissue oxygen fluctuation. The lactate sensor output was affected only when the rat was dying of severe hypoxia which corresponds to an oxygen partial pressure lower than 8 mmHg in the subcutaneous tissue. These results suggest that in practical applications the sensor can function reliably in in vivo measurements. It can tolerate reasonably low tissue oxygen levels even for certain hypoxic conditions.

In summary, developing new implantable sensors for metabolic monitoring has great significance. There is a definite need for in vivo real time measurement of lactate in clinical medicine. The needle-type lactate sensor described here shows promise for implantation and the preliminary animal tests showed reliable performance in subcutaneous tissue. Other possible implantable sites, e.g. the circulatory system, are being tested.

We thank the staff of the Animal Care Unit at the University of Kansas for their assistance. This work was supported in part by the National Institutes of Health, Grant No. DK 30718 (GSW) and by Tongji Medical University, Wuhan, China (YH).

REFERENCES

1 N.E. Madias, Kidney Int., 29 (1986) 752.
2 Z. Mavric, L. Zaputovic, D. Zagar, A. Matana and D. Smokvina, Am. J. Cardiol., 67 (1991) 565.
3 D.S. Sheps, C. Conde, B. Cameron, W.C. Lo, R. Appel, A. Castellanos, D.R. Harkness and R.J. Myerburg, Am. J. Cardiol., 44 (1979) 1276.
4 K.M. Kessler, P. Kozlovskis, R.G. Trohman and R.J. Myerburg, Am. Heart J., 113 (1987) 1540.
5 M.T. Haupt, E.M. Gilbert and R.W. Carlson, Am. Rev. Resp. Dis., 131 (1985) 912.
6 P.B. Oliver, Am. J. Med., 48 (1970) 209.
7 J.L.Vincent, P. Dufaye, J. Berre, M. Leeman, P.J. Degaute and R. Kahn, Crit. Care Med., 11 (1983) 449.
8 B.N. Cowan, H.J.G. Burns, P. Boyle and I. McA. Ledingham, Anaesthesia, 39(1984) 750.
9 D.L. Williams, A.R. Doig and A. Korosi, Anal. Chem., 42 (1970) 118.
10 J.J. Kulys and G.J.S. Svirmickas, Anal. Chim. Acta, 117 (1980) 115.
11 W.J. Blaedel and R.A. Jenkins, Anal. Chem., 48 (1976) 1240.
12 T. Yao, Y. Kobayashi and S. Musha, Anal. Chim. Acta, 138 (1982) 81.
13 H. Durliat and M. Comtat, Anal. Chem., 52 (1980) 2109.
14 M. Mascini, D. Moscone and P. Palleschi, Anal. Chim. Acta, 157 (1984) 45.
15 E.B. Makovos and C.C. Lin, Biotechnol. Bioeng., 27 (1985) 167.
16 I. Karube, T. Matsunaga, N. Teraoka and S. Suzuki, Anal. Chim. Acta, 119 (1980) 271.
17 F. Mizutani, K. Sasaki and Y. Shimura, Anal. Chem., 55 (1983) 35.

18 L.C. Clark, L.K. Noyes, T.A. Grooms and M.S. Moore, Crit. Care Med., 12 (1984) 461.
19 M. Shichiri, Y. Yamasaki, R. Kawamori, N. Hakui and H. Abe, Lancet, (1982) 1129.
20 M. Shichiri, N. Hakui, Y. Yamasaki and H. Abe, Diabetes, 33 (1984) 1200.
21 G. Velho, P. Froguel and G. Reach, Diabetes Nutr. Metab., 1 (1988) 227.
22 U. Fischer, R. Ertle, P. Abel, K. Rebrin, E. Brunstein, H. Hahn von Dorsche and E.J. Freyse, Diabetologia, 30 (1987) 940.
23 J.C. Pickup, G.W. Shaw and D.J. Claremont, Diabetologia, 32 (1989) 213.
24 D.R. Matthews, E. Bown, T.W. Beck, E. Plotkin, L. Lock, E. Gosden and M. Wickham, Diabetic Med., 5 (1988) 248.
25 H. Ege, Artif. Organs, 13 (1989) 171.
26 M. Koudelka, F. Rohner-Jeanrenaud, J. Terretaz, E. Bobbioni-Harsch, N.F. de Rooij and B. Jeanrenaud, Biomed. Biochim. Acta, 48 (1989) 953.
27 W. Kerner, H. Zier, G. Steinbach, J. Brueckel, E.F. Pfeiffer and T. Weiss, Horm. Metab. Res., Suppl. Ser., 20 (1988) 8.
28 M. Mascini, D. Moscone and G. Palleschi, Artif. Organs, 13 (1989) 173.
29 D.S. Bindra, Y. Zhang, G.S. Wilson, R. Sternberg, D.R. Thévenot, D. Moatti and G. Reach, Anal. Chem., 63 (1991) 1692.
30 D. Moatti, F. Capron, V. Poitout, G. Reach, D.S. Bindra, Y. Zhang, G.S. Wilson and D.R. Thévenot, Diabetologia, 35 (1992) 224.
31 J.V. Westgard, B.L. Lahmeyer and M.L. Birnbaum, Clin. Chem., 18 (1972) 1334.

Analytica Chimica Acta, 281 (1993) 513–520
Elsevier Science Publishers B.V., Amsterdam

In vitro and in vivo evaluation of oxygen effects on a glucose oxidase based implantable glucose sensor

Yanan Zhang and George S. Wilson

Department of Chemistry, University of Kansas, Lawrence, KS 66045 (USA)

(Received 1st April 1992; revised manuscript received 24th August 1992)

Abstract

The oxygen effect on a glucose oxidase based implantable glucose sensor was investigated based on studies of tissue oxygen availability and demand for oxygen by the glucose sensor. In vitro measurements showed that the oxygen effect is directly related to the glucose sensor sensitivity and linearity. Results of in vivo measurements in rat subcutaneous tissue with simultaneously implanted oxygen sensor and glucose sensor also suggested similar influence. A practically useful glucose sensor that is essentially free of oxygen fluctuation can be constructed by controlling its sensitivity and linearity.

Keywords: Biosensors; Glucose sensor; Implantable sensor; Subcutaneous tissue

An implantable needle-type glucose sensor has been developed in our laboratories and its performance has been characterized extensively both in vitro [1] and in vivo [2,3]. Brief reviews of previous studies using implantable glucose sensors are also included in those reports. Studies concerning the in vivo environment in the subcutaneous tissue have been also undertaken to further understand the physiological activity around the implanted sensor and the interactions between the tissue and the sensor.

It is generally understood that the process of tissue response to an implanted foreign object (depending on the degree of tissue damage) includes inflammation, immune response and wound healing [4]. Changes in local pH, P_{O_2}, electrolyte concentration and rate of metabolism are also expected. Since the glucose oxidase based sensor requires oxygen as the co-substrate to carry out the glucose oxidation, oxygen supply can influence sensor output. It is therefore important to examine the tissue oxygenation and its effect upon the in vivo performance of the sensor. This approach necessitates studies of two aspects: the absolute demand of oxygen by the sensor and the relative availability of oxygen in the physiological environment. Fischer et al. [5] reported a study on oxygen tension measurement in anesthetized and conscious dogs. No oxygen effect was observed for the glucose sensor.

It is well documented that the tissue oxygen distribution is uneven because of the difference in tissue capillary density and therefore the measured oxygen tension is sensor size dependent because of the averaging effect [6]. A special oxygen sensor is needed to simulate the glucose sensor in both size and geometry to effectively assess the potential oxygen effect on a glucose sensor of certain geometry and configuration. The method of in vitro calibration of the in vivo oxygen sensors, on the other hand, is also subject to some serious limitations. Since the oxygen solubility in the solution is affected by many factors

Correspondence to: G.S. Wilson, Department of Chemistry, University of Kansas, Lawrence, KS 66045 (USA).

such as solution composition, types of electrolytes, temperature and pH, etc. [7], it is not practical to simulate the physiological fluid by mixing known species together and assuming that a measurement in such a medium is valid. This approach can raise more problems than it solves because organic species, especially proteins, alter the solution viscosity which causes changes in oxygen diffusion coefficient. For example, addition of 2.5% serum proteins to the buffer caused a 15% decrease in sensor response, which was verified to be due to the increase in viscosity instead of decrease in oxygen solubility [8].

Our primary goal in this study was to evaluate the oxygen demand by the glucose sensor and the availability of oxygen in the subcutaneous tissue. An oxygen sensor that was identical in size and geometry to the glucose sensor has been constructed and the oxygen effect on the glucose sensor was measured for both in vitro and in vivo situations.

EXPERIMENTAL

Glucose sensor and oxygen sensor

Glucose sensor fabrication has been reported elsewhere [1]. Figure 1 shows the schematic diagram of the glucose sensor. The sensing element is located 3 mm from the tip end and has a cylindrical cavity of 1–2 mm in length. The electrode is a Pt–Ir (10% Ir) wire of 0.17 mm diameter. The sensing layer consists of a cellulose acetate inner membrane, an enzyme layer of glucose oxidase crosslinked with glutaraldehyde and an outer membrane of polyurethane. The sensor sensitivity is essentially controlled by the thickness of the outer membrane. The overall diameter is 0.25 mm for the sensing element and 0.45 mm for the reference and sensing elements. The oxygen sensor has the same configuration as the glucose sensor except that the enzyme-glutaraldehyde layer is eliminated. The oxygen sensor had typical sensitivity of 2–7 nA/mmHg when calibrated in pH 7.4 phosphate buffer [9].

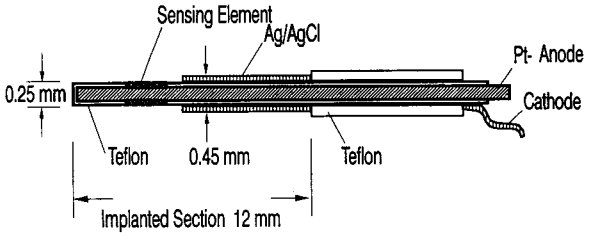

Fig. 1. Schematic of the glucose sensor.

In vitro study

A closed single-compartment cell with a capacity of 20 ml solution and a similar volume for the gas phase was used. Experiments were performed in 0.10 M phosphate buffer of pH 7.4 containing 0.15 M NaCl with 0.1% NaN_3 as preservative. Oxygen equilibrium in the cell was achieved by bubbling the buffer with an air–N_2 mixture whose ratio was regulated by two separate flow meters (Cole Parmer, Chicago, IL) while the solution was stirred constantly. The whole unit was submerged in a 37°C water bath (Fisher, Isotemp, Refrigerated circulator, Model 900). Both glucose and oxygen sensors were installed in the cell each with its own Ag/AgCl reference electrode and Pt wire counter electrode. The output was monitored with (BioAnalytical Systems, West Lafayette, IN) LC-4A amperometric detectors and recorded with Kipp & Zonen BD-40 chart recorders.

To reduce the volume error caused by buffer vaporization, the gas mixture was bubbled through two separate mixing bottles containing phosphate buffer at 37°C before being introduced into the cell chamber. Calibration of the oxygen sensor was also performed similarly in the absence of the glucose sensor.

In vivo study

A Sprague Dawley rat (body weight 350–450 g) was anaesthetized with halothane through inhalation and placed on a thermostated plastic cushion which had constant circulation of 37°C water. The rat was warmed with a 100-W lamp to maintain body temperature which tends to decrease with prolonged administration of anesthesia. Anesthesia from 4 to 10 hours was maintained by regulating a gas mixture of air and O_2 bubbling through halothane and body oxygen level was also controlled by feeding the rat with different air–O_2 ratios. The experimental set-up is shown in Fig. 2.

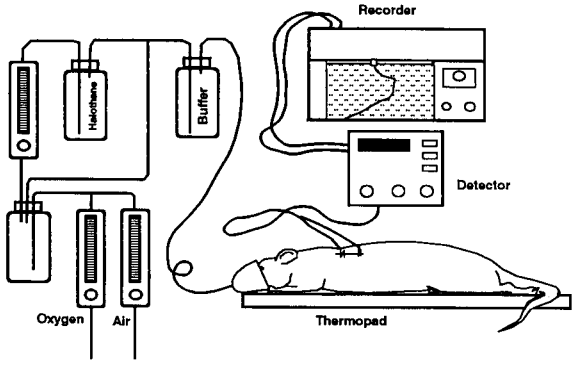

Fig. 2. Experimental setup for in vivo measurements.

Glucose and oxygen sensors were implanted through a 20 Gauge catheter into the subcutaneous tissue on the back of the neck and the output of glucose sensor was monitored at 600 mV vs. Ag/AgCl constant potential. The oxygen sensor output was monitored at −550 mV. The outputs of the two sensors were recorded simultaneously with chart recorders. Both sensors were calibrated before and after the in vivo experiments as stated above in the Experimental section.

The plasma glucose was independently measured with a YSI 2300 Stat Glucose Analyzer (Yellow Springs Instruments, Yellow Springs, OH). Blood was sampled from the tail vein, heparinized, and centrifuged. The glucose concentration in the plasma was then measured.

The in vivo experimental procedure was adapted from a protocol developed in the laboratory of G.Reach (INSERM U341, Hôtel-Dieu Hospital, Paris) [2].

RESULTS AND DISCUSSION

In vitro experiment

Eighteen sensors were fabricated with different sensitivities and linearities in order to test the influence of oxygen on the response. Generally, high sensitivity (in vitro) denotes > 3.0 nA/mM and low sensitivity defines the range of 0.5–1.5 nA/mM. In vitro measurements were performed in the closed electrochemical cell with three sensors (two glucose and one oxygen sensor) and each sensor had its own amperometric detector and chart recorder. The environment for all the sensors was thus identical and the two glucose sensors experienced the same P_{O_2} in the same buffer solution. Comparison between different sensors could therefore be made with confidence.

Figure 3 shows the calibration curves of two sensors measured under different oxygen tensions. Sensor A had a sensitivity of ~5 nA/mM and a linear dynamic range of ~8 mM in air saturated buffer. Sensor B was linear up to 30 mM in air saturated buffer and sensitivity of 0.58 nA/mM. It is clearly shown that sensor A was quite oxygen dependent while sensor B was affected little by oxygen. At a glucose concentration of 15 mM, for example, the change in sensor B output was only 5% when P_{O_2} changed from 150 mmHg to 7.6 mmHg. On the contrary, sensor A had a 30% decrease in current due to the same P_{O_2} change.

To further clarify the relationship between sensor sensitivity and oxygen effect, the system was first equilibrated with air and the baselines of the glucose sensors were stabilized. Two consecutive injections of glucose were made, with each injection giving a 5 mM increase in concentration in the cell, to create a total glucose concentration of 10 mM which was 3–5 mM higher than the normal blood glucose level. When the glucose sensors assumed stable current, N_2 was bubbled through the solution to reduce the oxygen tension. This process was carried out slowly and the

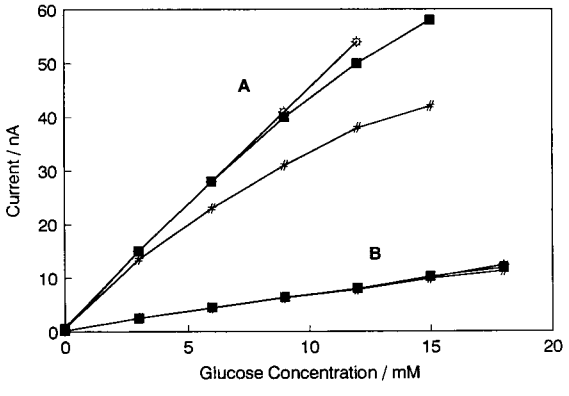

Fig. 3. In vitro oxygen effect on high (A) and low (B) sensitivity sensors. (○) P_{O_2} = 150 mmHg; (■) P_{O_2} = 40 mmHg; (#) P_{O_2} = 7.6 mmHg.

solution was constantly stirred to ensure the oxygen equilibrium throughout the cell. The oxygen partial pressure was monitored with the oxygen sensor. After the P_{O_2} reached a low level where the sensor response was affected by oxygen deficiency, the N_2 flow was partly shut down to allow a gradual build-up of oxygen in the system, as shown in Fig. 4A. The responses of two glucose sensors to a 10 mM glucose solution are shown in Figs. 4B and C. Figure 4B is characteristic of a low sensitivity glucose sensor (0.94 nA/mM; linearity, 25 mM) while Fig. 4C shows a high sensitivity sensor response (3.2 nA/mM; linearity, 12 mM). It is interesting to note that in Fig. 4B the sensor did not exhibit any oxygen dependence until the oxygen tension dropped to 5 mmHg as indicated by a decrease in signal at constant glucose concentration. When the oxygen tension is again increased a spike is observed which is due to oxidation of glucose accumulated inside the enzyme layer due to the lack of O_2 supply. The high sensitivity sensor of Fig. 4C showed similar behavior except that the current began to decrease at much higher oxygen tension (12 mmHg).

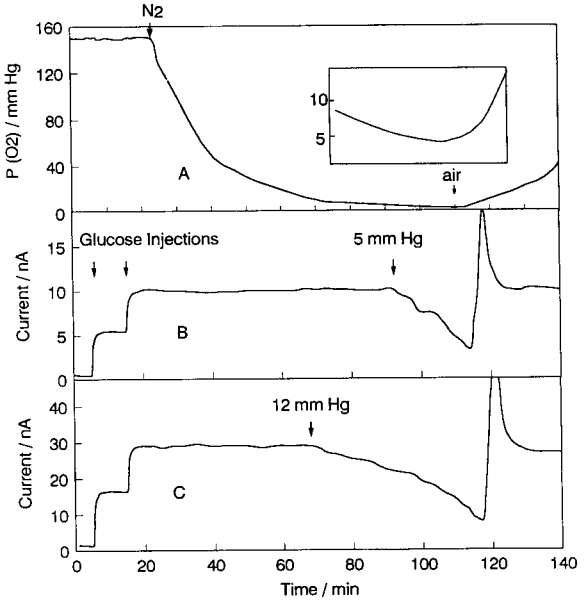

Fig. 4. Critical P_{O_2} value measurement for high and low sensitivity sensors. (A) Oxygen partial pressure; (B) glucose sensor 3 (see Table 1) and (C) sensor 7.

TABLE 1

Critical values of performance parameters of glucose sensors

	Sensor								
	1	2	3	4	5	6	7	8	9
Sensitivity (nA/mM)	0.54	0.90	0.94	1.1	2.5	2.6	3.2	4.0	5.4
Linearity (mM)	30	25	25	20	12	13	12	7	8
Critical P_{O_2} (mmHg)	3	6	5	8	16	17	12	30	40

Table 1 gives the characteristics of 9 glucose sensors and their corresponding critical P_{O_2} values, from which a general rule can be drawn to ensure the proper functioning of the glucose sensors. Based on the in vitro observation, the sensor sensitivity should not be higher than 2 nA/mM; the sensor linearity should be higher than 12 mM and under no circumstances should the sensors be used at $P_{O_2} < 7$ mmHg.

In vivo experiment

For the measurement of tissue P_{O_2}, two important factors, the oxygen sensor size and sensitivity, have to be considered. Since there is an uneven tissue oxygen profile which features higher oxygen tension at capillary sites and lower values around the midpoints between two capillaries, an oxygen sensor whose size is much smaller (e.g. 1–5 μm) than the distance between tissue capillaries will give different oxygen tensions at different sites of implantation [6]. The sensors used in this study, however, are not subject to this problem because the sensor has a cylindrical cavity of 1 mm in length and 0.25 mm in diameter which are well above the distances of tissue capillaries. This means that the P_{O_2} measured with this sensor is an averaged value which reflects the tissue oxygen availability instead of the actual tissue P_{O_2} at the site. Another important role that the sensor size imposes is that the measured tissue P_{O_2} is also sensor size dependent. Larger sensors introduce more capillary damage and increase the availability of local oxygen. They will, therefore, result in higher apparent P_{O_2}.

The sensor sensitivity, on the other hand, represents the oxygen consumption by the sensor. It

is essential that the sensitivity be suppressed to such a degree that the oxygen consumed by the sensor is negligible compared to the rate of tissue oxygen supply. Such a sensor will not create an oxygen gradient at the sensor surface and therefore will avoid lowered results.

The oxygen sensor used in this study has been carefully characterized both in vitro and in vivo [9]. It is linear up to 150 mmHg (air saturated buffer) and shows little stirring effect when calibrated in phosphate buffer containing 3% serum. Statistical measurements of rat subcutaneous P_{O_2} gave a range of 20–30 mmHg which is in agreement with the documented value [10].

Glucose sensors of different sensitivities and linearities were implanted in rat subcutaneous tissue and oxygen sensors were implanted parallel to the glucose sensors about 2 cm apart. One glucose sensor and one oxygen sensor were implanted in each rat. A total of 12 glucose sensors was tested in rats. Glucose sensors having high sensitivity were observed to have oxygen dependence. Figure 5 shows a sensor which is totally dependent on the tissue oxygen fluctuation. This sensor had an in vitro sensitivity of 4.0 nA/mM and dynamic range of 0–7 mM. Its in vivo sensitivity was estimated to be near 1.5–2.0 nA/mM glucose (usually subcutaneous sensors exhibit significant sensitivity decrease after implantation [2,11]). Other linear sensors with linearity higher than 12 mM and sensitivities less than 2 nA/mM were not observed to have oxygen dependency. Figure 6 illustrates a typical example in which three sensors (two glucose and one oxygen sensor) were simultaneously monitored in order to compare the difference between linear and non-linear sensors under identical oxygen conditions. Figure 6A shows the response of the oxygen sensor. The fluctuation in P_{O_2} level was manipulated by changing the composition of the air–O_2 mixture inhaled by the rat through the mask. The oxygen level of inhalating air corresponded to ~ 20 mmHg in the subcutaneous tissue. The oxygen level was equivalent to 26–30 mmHg when the rat was inhaling 50% oxygen. It should be pointed out, though, that the tissue oxygen level can be affected by the amount of anesthetic administered. The tissue oxygen level can be altered

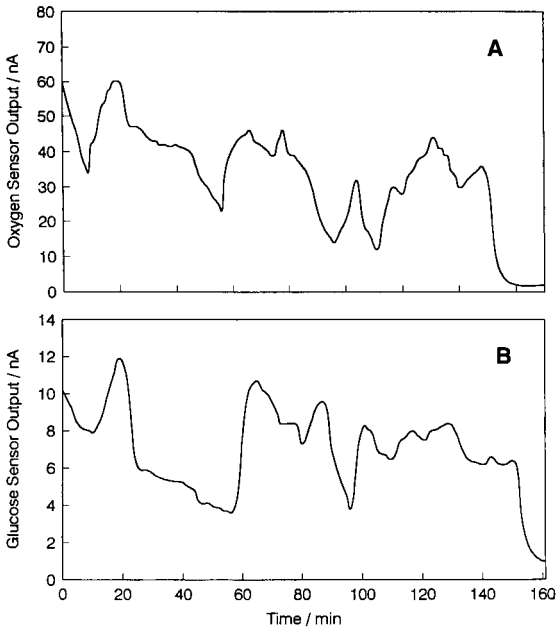

Fig. 5. In vivo oxygen effect on a high sensitivity non-linear glucose sensor. Irregular decrease in tissue oxygen was induced by temporarily increasing halothane to the air breathing rat. Normal tissue P_{O_2} was around 18 mmHg in this subject.

by merely changing the flow of halothane while keeping the air–O_2 ratio constant. Figure 6B shows the output of a non-linear sensor (3.2 nA/mM; linearity, 6 mM) and Fig. 6C is that of a linear sensor (1.1 nA/mM; linearity 12 mM). Figure 6D shows the corresponding plasma glucose change measured in situ.

The in vivo oxygen effect on the sensor was also demonstrated by an experiment shown in Fig. 7. Figure 7A shows the tissue oxygen level, Fig. 7B the glucose sensor output and Fig. 7C the plasma glucose level. Two injections of 30% *d*-glucose were administered i.p. during the experiment and the proper glucose level was obtained by the sensor while no oxygen effect was observed. In order to obtain the critical P_{O_2} value the rat was sacrificed by increasing the dose of halothane, which was followed by a sharp decrease in tissue oxygen. As soon as the oxygen effect was observed at the glucose sensor, oxygen was quickly supplied to the rat through the mask and the tissue oxygen returned instantly to its

original level, a condition which lasted for a few more minutes. This manipulation left a small defect in the glucose sensor curve (Fig. 7B) and a critical point of P_{O_2} for this sensor was determined to be ~ 8 mmHg.

An important observation that has been persistent in all the experiments is that the oxygen influence on the glucose sensor is dependent on the sensor in vivo sensitivity which decreases dramatically during the first few hours of implantation. The decrease in sensitivity is always accompanied by a decrease in the oxygen influence to the sensor. For most of the high sensitivity sensors, the oxygen effect was observed obviously in the initial period of implantation. It then diminishes gradually and, sometimes, becomes oxygen

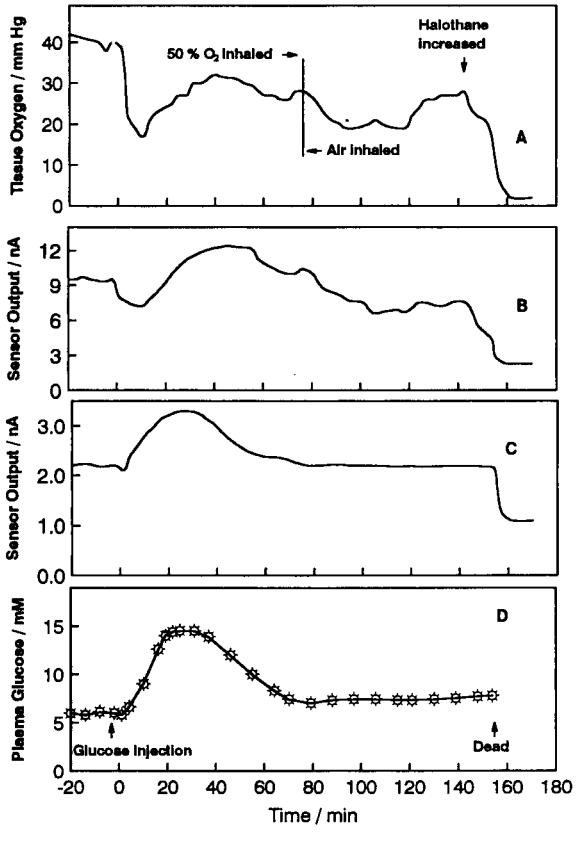

Fig. 6. In vivo oxygen effect on linear and non-linear sensors. (A) Tissue P_{O_2}; (B) non-linear sensor; (C) linear sensor; (D) blood glucose.

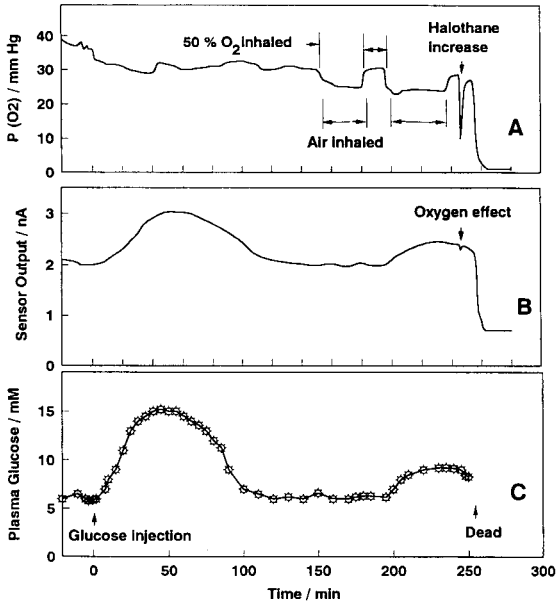

Fig. 7. In vivo critical P_{O_2} value measurement. (A) Tissue P_{O_2}; (B) glucose sensor output; (C) blood glucose.

independent when the in vivo sensitivity is substantially decreased (e.g. 20% of the in vitro sensitivity). In Figs. 5B and 6B, for example, stronger oxygen dependence is observed in the early stage of implantation and it gradually decreases to a lesser extent. The in vivo decrease in sensitivity is a commonly observed phenomenon for implantable biosensors for both oxygen dependent and oxygen independent types. This indicates that oxygen supply is probably not the cause of the decrease. This question is under further investigation in our laboratory.

All the in vivo tests were conducted with anesthetized rats. The subcutaneous P_{O_2} was constantly monitored while the air–O_2 ratio and the dosage of anesthetic were adjusted. In deep anesthesia, air breathing rats had typical oxygen levels of 17–25 mmHg. Rats breathing high content oxygen (60% O_2) usually showed values above 30 mmHg. Lightly anesthetized rats, however, showed larger fluctuations and higher levels of oxygen in the range of 30–50 mmHg when fed with high oxygen content gas. From these experiments and other reports [5] it is expected that

conscious animals will have slightly higher oxygen levels which is more favorable for the oxygen dependent glucose sensor.

Conclusion

The oxygen dependence of the glucose sensors, as has been demonstrated in this study, can be designed to fit the requirements for in vivo implantation. The demand for oxygen by the sensor is primarily determined by its sensitivity because the absolute current output is a direct measure of the rate of the catalytic reaction and therefore oxygen consumption. The oxygen effect can also be less significant when the intrinsic enzymatic reaction rate is much faster than glucose mass transfer through the outer membrane and where the oxygen flux is relatively higher. This is the case for linear sensors. A slight fluctuation in oxygen partial pressure will not affect the glucose diffusion controlled process and a linear response is maintained. The non-linear sensors, on the other hand, exhibit strong oxygen dependence (Figs. 5B and 6B) due to the fact that the overall process depends both on oxygen and glucose fluxes. The outer polyurethane membrane on the glucose sensor has been demonstrated to function only as a diffusional barrier to glucose while imposing little or no effect on oxygen diffusion [9]. The adjustment of glucose sensitivity by applying polyurethane membrane [1], in essence, serves to increase the relative oxygen supply because decrease in glucose flux increases the relative oxygen availability. This is, in fact, the ultimate strategy in the development of the GOx based glucose sensor.

Sensors with in vitro sensitivity of over 3 nA/mM have been observed to exhibit oxygen dependence in the 10–13 mmHg oxygen range during the intial period of in vivo monitoring. Although this oxygen tension is not expected in normal subcutaneous tissue (common observation for rat subcutaneous tissue is 23 ± 3 mmHg [10] and in this report (Fig. 6A and 7A) P_{O_2} between 20 and 30 mmHg), heterogeneity of tissue environment must be considered because local P_{O_2} level can be perturbed by trauma and inflammation. The oxygen effect, however, becomes much less significant when the sensors stabilize with time. Sensors with in vitro sensitivities of 3.5 nA/mM can turn into totally oxygen independent in rat subcutaneous tissue when sufficient time is allowed for sensor stabilization (for example, six to seven hours).

The criteria for an in vivo glucose sensor with a given geometry and surface area can be generally summarized as follows: (a) The in vitro sensitivity should be controlled within a range which could yield reasonable in vivo sensitivity while maintaining minimum potential oxygen influence. If the in vivo sensitivities stabilize at about 10–20% of the in vitro values, the optimal sensitivity for sensor preparation should rest in the range of 1.5–3.5 nA/mM. (b) Linearity is important to the sensors in terms of oxygen effect. Sensors with linear ranges higher than 12 mM in air saturated buffer are less likely to be affected by tissue oxygen fluctuation. (c) The sensors should not be used in the situation where the oxygen tension is below 7 mmHg. The exact values of these parameters will depend on the specific sensor design, but the interplay between glucose and oxygen fluxes will, in any case, define sensor performance.

This work was supported in part by the National Institutes of Health Grant No. DK 30718.

REFERENCES

1 D.S. Bindra, Y. Zhang, G.S. Wilson, R. Sternberg, D.R. Thévenot, D. Moatti and G. Reach, Anal. Chem., 63 (1991) 1692.
2 D. Moatti, F. Capron, V. Poitout, G. Reach, D.S. Bindra, Y. Zhang, G.S. Wilson and D.R. Thévenot, Diabetologia, 35 (1992) 224.
3 V. Poitout, D. Moatti, G. Velho, G. Reach, R. Sternberg, D.R. Thévenot, D.S. Bindra, Y. Zhang and G.S. Wilson, Trans. Am. Soc. Artif. Int. Org., 37 (1991) M298.
4 J. Black, Biological Performance of Materials, Marcel Dekker, New York, 1981.
5 U. Fischer, A. Hidde, S. Herrman, T. von Woedtke, K. Rebrin and P. Abel, Biomed. Biochim. Acta, 48, 11/12 (1989) 965.
6 I.A. Silver, in J.P. Payne and D.W. Hill (Eds.), A Symponium on Oxygen Measurement in Blood and Tissue and Their Significance, J&A Churchill Ltd., London, 1966, pp. 135–153.

7 M.L. Hitchman, in E. Gnaiger and H. Forstner (Eds.), Polarographic Oxygen Sensors, Springer-Verlag, New York, 1983, pp. 18–30.
8 D.B. Cater, I.A. Silver and G.M. Wilson, Proc. Roy. Soc. B, 151 (1960) 256.
9 Y. Zhang, D.S. Bindra and G.S. Wilson, unpublished results.
10 D.B. Cater, in J.P. Payne and D.W. Hill (Eds.), A Symposium on Oxygen Measurements in Blood and Tissues and Their Significance, J&A Churchill Ltd., 1966, pp. 155–172.
11 G. Velho, G. Reach and D.R. Thévenot, Biomed. Biochim. Acta., 48, 11/12 (1989) 957.

Analytica Chimica Acta, 281 (1993) 521–526
Elsevier Science Publishers B.V., Amsterdam

Industrial on-line monitoring of penicillin V, glucose and ethanol using a split-flow modified thermal biosensor

M. Rank

Pure and Applied Biochemistry, Chemical Centre, University of Lund, P.O. Box 124, S-221 00 Lund (Sweden)

J. Gram

Fermentation Pilot Plant, BIG, Novo Nordisk A / S, Novo Allé, DK-2880 Bagsvaerd (Denmark)

B. Danielsson

Pure and Applied Biochemistry, Chemical Centre, University of Lund, P.O. Box 124, S-221 00 Lund (Sweden)

(Received 1st April 1992; revised manuscript received 25th August 1992)

Abstract

Penicillin V, glucose and ethanol were monitored in 0.5 and 2.5 m^3 bioreactors using an enzyme thermistor, modified for split-flow analysis. Penicillin V was also monitored in a 160 m^3 bioreactor. The samples were split immediately before simultaneously entering the enzyme column and an identical reference column, (without enzyme). By using a reference column the non-specific heat arising from mixing and solvation effects caused by high salt and metabolite concentrations in the fermentation broth can be eliminated. Immobilized β-lactamase in the enzyme column was used to monitor three consecutive fermentations, but the penicillin V values were 10% higher than the values obtained by off-line liquid chromatographic (LC) analysis of the same samples. Another enzyme was therefore used with the same set-up. After purification from a broth supernatant, penicillin V acylase was used for on-line monitoring of penicillin production in a 160 m^3 bioreactor. The concentrations of penicilloic acid, *p*-hydroxypenicillin V and penicillin V were determined by off-line LC. The sum of these concentrations matched the on-line biosensor values very well. Glucose was monitored from the start in a *Saccharomyces* fermentation but after 5 h the analysis was switched to ethanol monitoring. It took 60 min to switch from a glucose oxidase column to a column with alcohol oxidase and obtain the first on-line ethanol value.

Keywords: Biosensors; Enzymatic methods; Flow injection; Liquid chromatography; Enzyme reactor; Ethanol; Fermentation; Glucose; Penicillin

The importance of the industrial production of fine chemicals and pharmaceuticals by fermentation has increased with the introduction of recombinant microorganisms. The cultivation of such microorganisms often has to be carefully controlled, which puts special demands on the instrumentation for on-line monitoring. Knowledge of the concentrations of substrates, products, inhibitors and other metabolites is of vital importance for carefully controlled fermentation but is seldom available on-line.

Highly specific biosensors combined with flow-injection analysis (FIA) are a suitable system for on-line monitoring of fermentations [1–5]. The enzyme thermistor is a calorimetric biosensor of the FIA type which measures the enthalpic

Correspondence to: M. Rank, Pure and Applied Biochemistry, Chemical Centre, University of Lund, P.O. Box 124, S-221 00 Lund (Sweden).

change when enzyme substrates in the samples are converted inside a column by an immobilized enzyme [6,7]. The split-flow technique is a convenient way of eliminating the non-specific heat that may be associated with complex samples such as fermentation broths [8]. The buffer and sample solutions are split into two equal flow streams just before entering the enzyme column and the reference column.

Physical problems using laboratory instruments in the fermentation process environment that have to be solved include up to 100% humidity, vibrations and temperature variations between 10 and 35°C.

EXPERIMENTAL

Instrumentation

The enzyme thermistor was developed and built at the University of Lund [9]. On-line sampling of the fermentation broth was performed with a hydrophilized polypropylene filtration probe (Advanced Biotechnology, Puchheim, Germany). The filtration part of the probe was inserted through the bioreactor wall using a fitting normally employed with pH electrodes. A flow of 1–3 ml min^{-1} of a 0.2-μm filtered sample stream was aspirated to the outside of the bioreactor using a peristaltic pump (see Fig. 1). The sample stream then entered the steel cabinet containing the analytical FIA system.

Another peristaltic pump was used to aspirate 0.5 ml min^{-1} of filtered broth sample into a six-position pneumatic sample selector (VICI, Houston, TX). This multi-channel peristaltic pump also aspirated the carrier buffer through the sample valve (Model 7000, Rheodyne, Cotati, CA) and further into the thermostated calorimeter with the two columns. A split-flow bottom plate was constructed and installed in the calorimeter in order to split the sample immediately before entering the two columns.

The enzyme thermistor with the automatic FIA system was assembled inside a steel cabinet flushed with cool dry air [10]. The first results from the pilot plant were recorded with an integrator (HP-3354, Hewlett–Packard, Avondale, PA). Subsequently, the signals from the amplifier were transferred to a Datalogger (Datataker 50, Data Electronics, Boronia, Australia). All information was then transferred via a local modem connection (MA-12, Westermo, Eskilstuna, Sweden) to a software program (Labtech Notebook, Wilmington, DE) installed in an IBM PS/2 computer located 60 m away in a control room inside the production building.

Analysis

The eluting buffer, 0.1 M phosphate buffer (pH 7.0) containing 4 mM sodium azide (Sigma, St. Louis, MO), was pumped through both columns at 0.9 ml min^{-1}. The sodium azide was exchanged with 5 g l^{-1} of benzoic acid (Sigma) when columns with catalase was used.

In order to prevent nucleophilic breakdown of penicillin V in phosphate buffer, all standards were prepared in dilute 0.01 M phosphate buffer

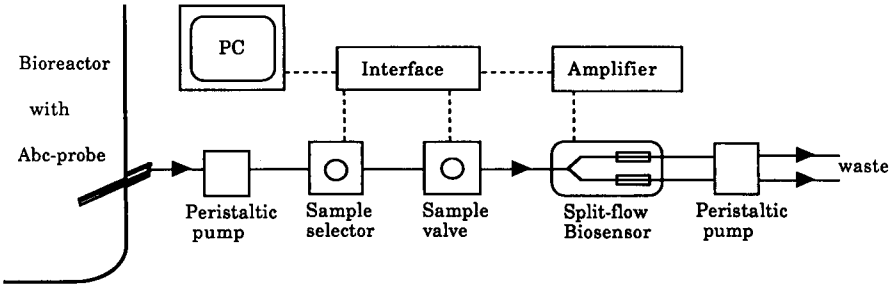

Fig. 1. Schematic diagram of the set-up. A continuous sample stream was aspirated from the bioreactor using a filtration probe and a peristaltic pump. The filtered sample was then transported into the FIA system with the split-flow biosensor. The signals were recorded with an amplifier and an interface permitted computer monitoring. The valves were also controlled by the PC.

(pH 7.0) and kept cold in an insulated box filled with ice [11]. Potassium penicillin V from Novo Nordisk (Bagsvaerd, Denmark) (1515 IU mg^{-1}) was used in all standards.

Samples were injected every 10 min in the order low-concentration standard, broth sample, high-concentration standard. The broth concentrations were calculated by linear regression from an average of the three latest values for each standard. Fresh standards were made every 24 h.

Enzyme columns

All immobilizations were according to Weetall [12] with 80–120-mesh controlled-pore glass (Fluka), γ-aminopropyltriethoxysilane and glutaraldehyde (Sigma). All enzymes were dialysed three times against 1 l of 0.1 M phosphate buffer (pH 7.0) using Spectra/Por membrane tubing, molecular weight cut-off 12000–14000 (Spectrum, Los Angeles, CA), before immobilization. The 0.1 M phosphate buffer was used throughout

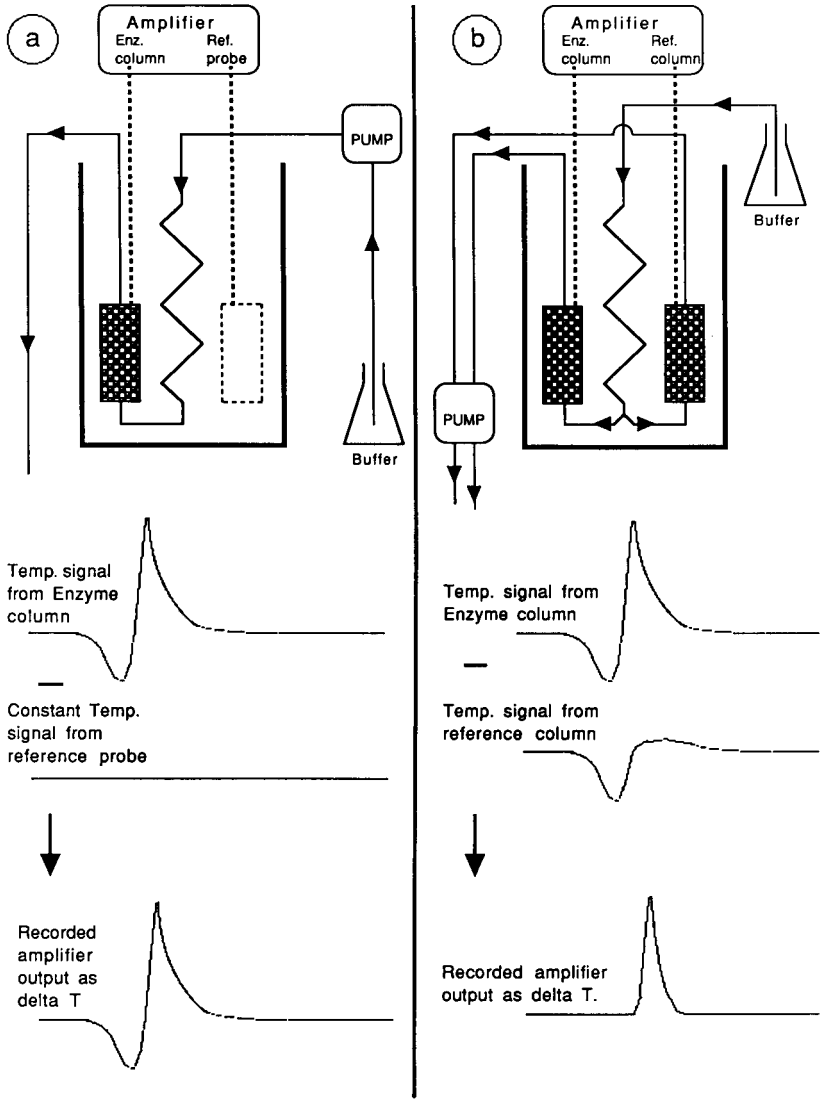

Fig. 2. (a) Standard one-column analysis compared with (b) the split-flow technique. In the latter the non-specific heat from fermentation broth samples is registered using a reference column without enzyme. This signal is subtracted from the signal recorded at the enzyme column. The amplifier signal resulting as ΔT represents the heat generated only by the enzymatic reaction.

all steps in the preparation of the enzyme columns.

Approximately 300 IU of β-lactamase (EC 3.5.2.6) from *Bacillus cereus* (Sigma) immobilized on CPG were packed in a 0.26-ml column. The remaining non-bound glutaraldehyde sites were saturated with 0.1% bovine serum albumin (BSA) (sigma) followed by 0.1% L-lysine (Sigma) dissolved in phosphate buffer. The reference columns were made in an identical way but instead of enzyme only BSA was bound.

Penicillin V acylase from a broth supernatant supplied by Novo Nordisk was purified by adding 8 g of active carbon to 100 ml of fermentation broth. This solution was stirred for 1 h at room temperature before it was precipitated by adding 70 ml of 96% ethanol. The precipitate was filtered through 16 g of Hiflo diatomaceous earth filter aid layered on top of a glass filter using a water aspirator. The permeate was precipitated using 0.35 vol. of 96% ethanol and after decantation the precipitate was washed with water–ethanol (1 + 1). The precipitated enzyme was dissolved in 0.1 M phosphate buffer (pH 7) and dialysed three times against 1 l of phosphate buffer.

The enzyme activity was determined spectrophotometrically by measuring the amount of 6-aminopenicillanic acid (6-APA) formed using *p*-dimethylaminobenzaldehyde as the colour reagent. This assay was modified from the procedure originally described by Balasingham et al. [13].

Approximately 400 IU of glucose oxidase (EC 1.1.3.4) from *Aspergillus niger*, type X-S (Sigma) were co-immobilized with 40000 IU of catalase (EC 1.11.1.6) from bovine liver (Sigma) in one 0.26-ml column and used to monitor glucose.

Standards were made with D-(+)-glucose (Merck) in dilute phosphate buffer. Approxi-

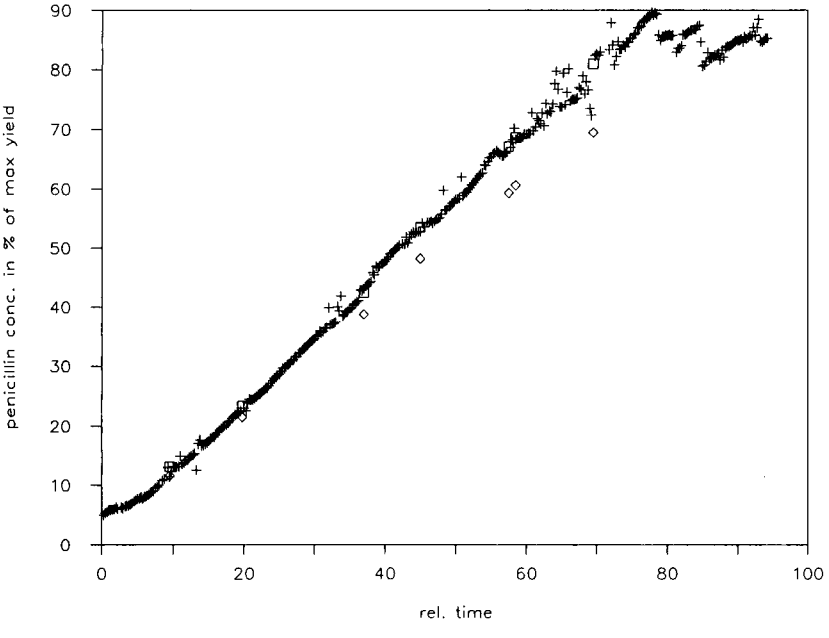

Fig. 3. The production of penicillin V in a 160-m^3 bioreactor was monitored on-line using an enzyme column with penicillin V acylase. Values from fermentation broth samples were plotted every 30 min. In addition seven samples were collected and analysed off-line by LC. The combined concentrations of penicillin V, penicilloic acid and *p*-hydroxypenicillin V obtained by LC analysis correlated very well with the on-line biosensor values. At the end of the fermentation the on-line values become dispersed, presumably due to the high viscosity of the broth. To compensate for this the broth was diluted four times which resulted in the rapid decrease in penicillin concentration. This information is only visible by on-line analysis. + = On-line biosensor values; □ = penicillin V, penicilloic acid and *p*-hydroxypenicillin V by LC; ◇ = penicillin V only by LC.

mately 250 IU of alcohol oxidase (EC 1.1.3.13) from *Pichia pastoris* (Sigma) was co-immobilized with 40000 IU of catalase in another 0.26-ml column used to monitor alcohols. Standards were made from 96% ethanol and for comparison broth samples were analysed by gas chromatography.

LC analysis

LC was used to perform off-line determination of penicillin V, penicilloic acid, *p*-hydroxypenicillin V and 6-APA. The assay was performed following a modified method derived from Hussey et al. [14].

RESULTS AND DISCUSSION

The instruments comprising the enzyme thermistor FIA system were well isolated inside the steel cabinet and circulating cool dry air compensated for temperature elevations in the bioreactor hall. The chemical problems of analysing complex fermentation broths were overcome by the use of the split-flow technique (see Fig. 2).

The linear range for on-line monitoring of penicillin V with β-lactamase was 0.1–500 mM when sample volumes from 20 to 500 μl were used. The concentration of the two β-lactam substrates penicillin and *p*-hydroxypenicillin V were determined by LC. When the two values were added and plotted against the on-line biosensor values, a deviation of 10% was observed.

Penicillin V acylase, on the other hand, hydrolyses the side-chain of penicillin which is a four times less exothermic reaction than that of β-lactamase, but with an improved substrate specificity. Penicillin V acylase was purified and immobilized before use for on-line monitoring of penicillin production in a 160-m^3 bioreactor. The linear range was 0.5–150 mM using sample volumes between 20 and 500 μl.

The ABC filtration probe was inserted into the bioreactor and a clear 0.2-μm permeate was obtained throughout the fermentation. The delay

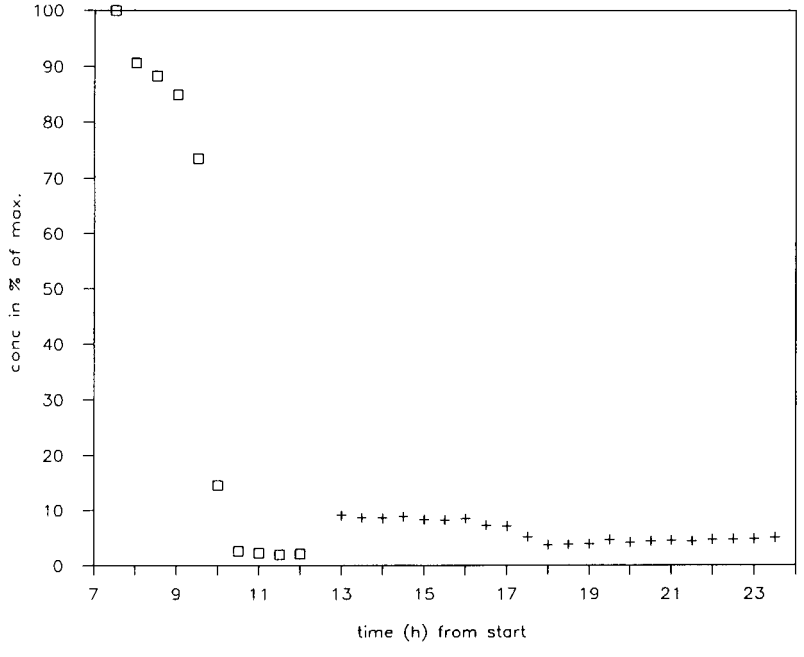

Fig. 4. On-line monitoring of glucose at the start of a *Saccharomyces* fermentation. After 5 h the glucose was depleted and the glucose oxidase column was exchanged with a column containing alcohol oxidase. The switch from glucose (□) to ethanol (+) monitoring took only 60 min. No fermentation monitoring was possible during the first 7 h, but the start up phase was included in the time scale.

from sample withdrawal to the registered peak was 5 min. The sum of the concentrations of the three side-chain substrates penicillin V, penicilloic acid and *p*-hydroxypenicillin V were determined by LC and plotted against the on-line biosensor values (see Fig. 3). The values obtained using a penicillin V acylase column correlated very well.

Glucose was monitored from start in a *Saccharomyces cerevisae* fermentation. After 5 h the column was exchanged and ethanol was monitored instead (see Fig. 4). The time from the exchange of columns and standards to the first on-line ethanol value was 60 min. Early experiments with alcohol oxidase (*Pichia pastoris*) revealed a slightly higher exothermic response for methanol and a reduced affinity for butan-1-ol. The values from on-line monitoring of ethanol correlated with two values obtained by GC analysis.

The hydrolysis of substrate analogues such as 6-APA might explain the 10% higher enzymatic biosensor response of β-lactamase. Future on-line monitoring of penicillin production will be performed with penicillin V acylase owing to the superior substrate selectivity.

The sudden minor changes in penicillin concentration observed in Fig. 3 were caused by variations in the carbohydrate feed. This underlines the importance of information that can be acquired by on-line monitoring, in this instance the direct impact of carbohydrate concentration on the product formation.

Dual substrate specificity is also experienced with alcohol oxidase and this has to be considered when interpreting on-line data.

Results using an alcohol oxidase from *Candida boidinii* (Boehringer, Mannheim) showed that ethanol instead of methanol is the best substrate for this enzyme [15]. The on-line system can therefore by improved by the correct choice of enzyme. The system is now being adapted for on-line monitoring of other broth molecules such as lactate.

This project was supported by a grant from the Nordic programme on bioprocess engineering under the auspices of NI (Nordic Fund for Technology and Industrial Development). The authors thank colleagues at Novo Nordisk for assistance.

REFERENCES

1 C.R. Lowe, Biosensors, Trends Biotechnol., 2 (1984) 59.
2 F. Valero, J. Lafuente, M. Poch, C. Sola, A.N. Araujo and J.L.F.C. Lima, Biotechnol. Bioeng. 36 (1990) 647.
3 B. Danielsson, Current Opinions in Biotechnology, 2 (1991) 17.
4 B. Mattiasson, B. Danielson, F. Winquist, H. Nilsson and K. Mosbach, Appl. Environ. Microbiol., 41 (1981) 903.
5 G. Decristoforo and B. Danielsson, Anal. Chem., 56 (1984) 263.
6 K. Mosbach and B. Danielsson, Anal. Chem., 53 (1981) 83A.
7 B. Danielsson and K. Mosbach, in A.P.F. Turner, I. Karube and G.S. Wilson (Eds.), Biosensors: Fundamentals and Applications, Oxford University Press, Oxford, 1986, p. 575.
8 B. Mattiasson, B. Danielsson and K. Mosbach, Anal. Lett., 9 (1976) 867.
9 B. Danielsson, B. Mattiasson and K. Mosbach, Appl. Biochem. Bioeng., 3 (1981) 97.
10 J. Gram, K. Nikolajsen, K. Holm and M. de Bang, Abstracts, ECB-5, Copenhagen, 1990, No. 311.
11 H. Bundgaard and J. Hansen, Int. J. Pharm., 9 (1981) 273.
12 H.H. Weetall, Methods Enzymol., 44 (1976) 134.
13 K. Balasingham, D. Warburton, P. Dunnill and D.M. Lilly, Biochim. Biophys. Acta, 276 (1972) 250.
14 R.L. Hussey, W.G. Mascher and A.L. Lagu, J. Chromatogr., 268 (1983) 120.
15 G.G. Guilbault, B. Danielsson, C.-F. Mandenius and K. Mosbach, Anal. Chem., 55 (1983) 1582.

Analytica Chimica Acta, 281 (1993) 527–533
Elsevier Science Publishers B.V., Amsterdam

Amperometric biosensor with PQQ enzyme immobilized in a mediator-containing polypyrrole matrix

Golam F. Khan, Eiry Kobatake, Yoshihito Ikariyama and Masuo Aizawa

Department of Bioengineering, Tokyo Institute of Technology, Nagatsuta, Midori-ku, Yokohama 227 (Japan)

(Received 1st June 1992; revised manuscript received 12th October 1992)

Abstract

An amperometric biosensor for fructose was fabricated by co-immobilizing a pyrrolo quinoline quinone (PQQ) enzyme (fructose dehydrogenase, FDH) with mediator in a thin polypyrrole (PP) membrane. Electron transfer between the prosthetic PQQ of FDH and the transducer electrode was promoted through a mediator-containing PP interface. Two methods of sensor preparation are described. In one, FDH was potentiostatically adsorbed as a monolayer on a transducer electrode, and a very thin (equivalent to a monolayer of FDH) PP membrane containing a mediator was electrodeposited on the adsorbed FDH. In the other, FDH and mediator [hexacyanoferrate(III) or ferrocene] were co-immobilized on an electrode by electrochemical polymerization of pyrrole. In the former instance, a highly sensitive and selective response for fructose was obtained with a wide detection range of up to 30 mM with a linear range from 10 μM to 10 mM. However, the stability of the sensor was poor owing to the easy leakage of mediator. The stability of the sensor was significantly improved in the latter instance, with a dynamic range for fructose detection from 50 μM to 5 mM.

Keywords: Amperometry; Biosensors; Enzymatic methods; Enzyme electrodes; Fructose; Membrane electrodes; PQQ

Recently, much attention has been paid to bioelectrocatalysis for the fabrication of biosensors composed of FAD enzyme, NAD(P) enzyme and PQQ enzyme. Various systems have been developed for the determination of glucose with glucose oxidase (GOD) using a redox coupler for shuttling electrons between the active prosthetic moiety and the electrode. Various sensors based on modified electrodes with ferrocene derivatives [1–3] and quinone derivatives [4–6] and electrodes composed of organic conducting materials [7–10] have been reported. However, these mediator-based biosensors suffer from the inherent drawback of leakage of mediating species from the enzyme layer into bulk solution and also from inefficient electron shuttling. Considering these points, several workers have developed new matrices in which mediators can be stably retained and efficient electron transfer can be assisted [11,12]. In previous papers [13–16], an electrochemically polymerized conductive polymer interface to promote electron transfer was introduced.

In a previous paper [16], the necessity for a new molecular interface where electron transfer between the prosthetic group of the enzyme and the transducer electrode proceeds smoothly was explained. It was also clarified that a conductive polymer-interfaced enzyme matrix is effective for the detection of fructose by using fructose dehydrogenase (FDH). It was also observed that the response current for fructose was very low compared with the current estimated from the activity

Correspondence to: M. Aizawa, Department of Bioengineering, Tokyo Institute of Technology, Nagatsuta, Midori-ku, Yokohama 227 (Japan).

of the enzyme electrode measured by an optical method [17,18]. It seems likely that a conductive wiring polymer, polypyrrole (PP) molecules, cannot reach as close to the enzyme active centre as low-molecular-weight electron mediators can. It is easily understood that the greater the distance between the central PQQ moiety and the transducer electrode is, the more difficult is electron transfer, although the distance is Å level. Without electron shuttling molecules the regeneration of the redox enzyme remains very slow. Therefore, a mediator was entrapped in the polypyrrole interface to promote electron transfer between the prosthetic group of FDH and the conductive macromolucule.

In this paper, mediators [hexacyanoferrate(III) and ferrocene] were incorporated in the enzyme-containing molecular interface for promoting the effective and sensitive determination of fructose in two different ways. The first is the two-step method, in which FDH is electrostatically adsorbed in the monolayer, followed by mediator entrapment and simultaneous electropolymerization of pyrrole. The other is the one-step method, in which electropolymerization of pyrrole is performed in the presence of both mediator and FDH. These two methods are illustrated schematically in Fig. 1. The role of the electron-transferring system, PQQ enzyme–mediator–polypyrrole–transducing electrode, is clarified from the viewpoint of designing effective transduction.

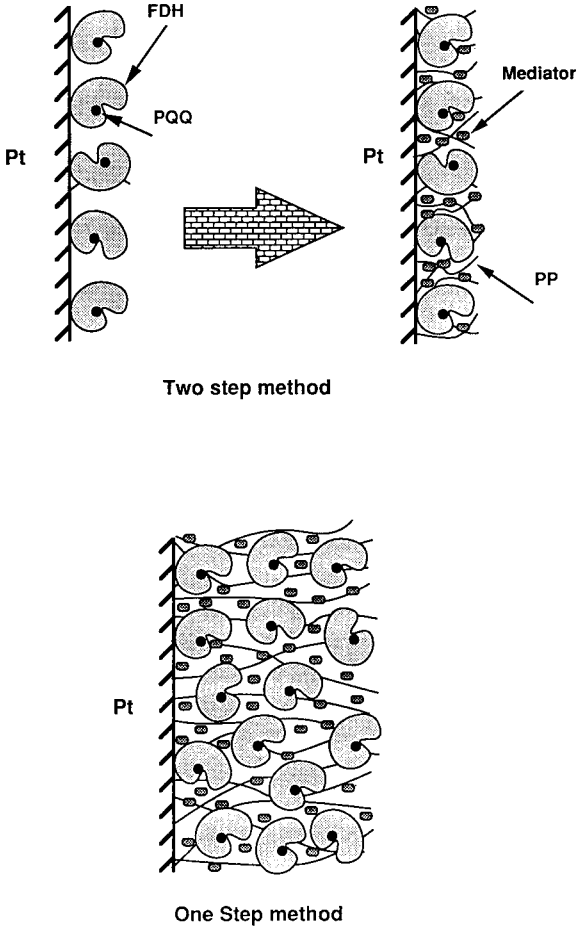

Fig. 1. Schematic illustration of the preparation of mediator co-immobilized enzyme electrodes. In the two-step method, electrochemical adsorption of FDH was performed at 0.5 mV, following which pyrrole was electropolymerized at 0.7 V in a mediator- and pyrrole-containing solution. In the one-step method, immobilization of FDH and mediator was performed by electropolymerization of pyrrole at 0.6 V in a pyrrole solution containing FDH and mediator.

EXPERIMENTAL

Chemicals

Fructose dehydrogenase (EC 1.1.99.11, grade III, 29.7 U mg^{-1}, MW 141 000) from *Gluconobacter* sp. was purchased from Toyobo (Osaka) and used as received. Pyrrole was purchased from Tokyo Kasei (Tokyo) and was distilled before use. Mediators [potassium hexacyanoferrate(III) (FCN) and ferrocenylmethyltrimethylammonium iodide (FTAI)] and other chemicals were of guaranteed-reagent grade. The supporting electrolyte was McIlvaine buffer of pH 4.5 prepared by mixing 0.1 M citric acid and 0.2 M disodium phosphate.

Fabrication of enzyme electrodes

In the two-step method, FDH was adsorbed on a platinum electrode (1 cm^2) in the monolayer by applying a potential of 0.5 V vs. Ag/AgCl for 10 min in phosphate buffer solution of pH 6.0 containing 5 mg ml^{-1} of FDH. All the electrode potentials are referred to Ag/AgCl. The details of the enzyme adsorption have been reported previously [19]. After thorough washing with dis-

tilled water, the FDH-adsorbed electrode was transferred into another solution containing 10 mM mediator, 0.1 M pyrrole and 0.1 M KCl. Mediator immobilization was performed in the course of polymerization of pyrrole by applying 0.7 V. The polymerization was terminated when 4 mC cm^{-2} charge had been passed.

In the one-step method, FDH and mediator were immobilized simultaneously during the polymerization of pyrrole in a solution containing 10 mg ml^{-1} of FDH, 10 mM mediator, 0.1 M pyrrole and 0.1 M sodium *p*-toluenesulphonate (electrolyte) by applying a potential of 0.6 V. Polymerization was terminated when 200 mC cm^{-2} had been passed. It took 3–5 min for the polymerization. The enzyme-entrapped electrode was thoroughly washed with McIlvaine buffer of pH 4.5 and was stored in the same buffer solution at 4°C until used.

Apparatus

Differential-pulse voltammetry was carried out with a Yanaco P-1100 polarographic analyser (Yanagimoto, Kyoto) and the results were recorded on a Graphtec (Tokyo) WX 4421 *X–Y* recorder. FDH adsorption and D-fructose detection were performed with an HA-301 potentiostat–galvanostat (Hokuto Denko, Tokyo) and a YEW Type 3086 *X–Y* recorder (Graphtec). All experiments were done in a conventional electrochemical cell consisting of a working electrode, a platinum plate auxiliary electrode and an Ag/AgCl reference electrode. Fructose determination was performed at 37°C and all the other electrochemical experiments at room temperature (25 ± 2°C). When fructose was determined each sample was injected into a magnetically stirred solution after the residual current had become constant. The steady-state background current became constant after ca. 5–30 min, depending on the applied potential.

RESULTS AND DISCUSSION

Electron transfer through mediator and conducting polymer interface

An enzyme electrode was fabricated by the one-step method and characterized electrochemically. The electrochemical properties of FDH-immobilized, PP-interfaced platinum (PP–FDH–Pt) electrode have been partly reported [16]. Here the effect of an electron mediator (FCN) on the electron transfer was further studied by differential-pulse voltammetry. Figure 2 shows the electrochemical behaviour of the electrode. A pair of reversible redox peaks were observed in both the presence and absence of FCN. The mid-wave potential of FDH with the polypyrrole-interfaced Pt electrode was 0.07 V, which coincided with the redox potential of prosthetic PQQ (0.06 V) [20]. Hence the redox peaks were attributed to the oxidation and reduction of the PQQ moiety of FDH. The mid-wave potential of the mediator-immobilized electrode was slightly more positive than that of the mediator, probably owing to the presence of FCN. The peak height of the mediator-immobilized electrode was 1.7–2.0 times higher than that of the mediator-free electrode. These results suggest that the electrochemical response of entrapped FDH was enhanced owing to the co-immobilization of FDH and FCN.

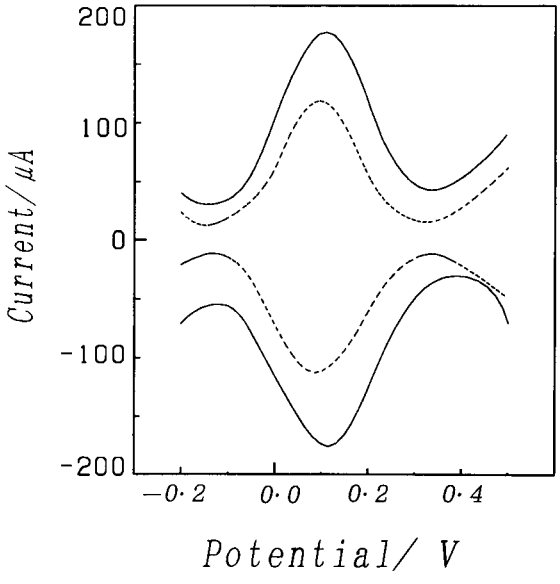

Fig. 2. Differential-pulse voltammograms of PP–FDH–Pt (- - - - -) and PP–FCN–FDH–Pt (———) electrodes in McIlvaine buffer solution of pH 4.5. Both electrodes were prepared by the two-step method. Pulse amplitude, 50 mV; pulse interval, 1 s, scan rate, 10 mV s^{-1}.

Current response of polypyrrole-interfaced FDH electrode

If the enzyme electrode is controlled at a potential more positive than the redox potential of PQQ (0.06 V), the reduced FDH (FDH–$PQQH_2$) will be regenerated to the oxidized state (FDH–PQQ), as the two electrons of the reduced PQQ moiety are transferred to the electrode with the generation of a continuous flow of anodic current addition of fructose. At a low potential such as 0.1 V, the background current was cathodic and the residual current was very high as the rest potential of the electrode was ca. 0.35 V. To make the residual current as small as possible, and to observe an anodic current, the determination of fructose was performed at 0.4 V. The response curves on addition of 5 mM fructose are presented in Fig. 3.

To ascertain the selectivity of the enzyme electrode, a series of saccharides were injected. Satisfactory selectivity towards fructose was obtained with both the FCN-mediated and non-mediated enzyme electrode. In other words, the mediator does not affect the specificity of the enzyme electrode. In both instances the responses were very fast, i.e., 3–5 s. It is highly probable that substrate diffusion was overcome by reducing the membrane thickness. The most noticeable difference between the mediator-containing enzyme electrode (PP–FCN–FDH–Pt) and the mediator-free electrode was the current generated, i.e., the former electrode exhibited a 5–6 times larger response current than the latter. This clearly shows the effectiveness of FCN for the smooth electrochemical regeneration of FDH by rapidly liberating electrons from the reduced FDH and by transferring the electrons through the PP interface to the transducer electrode.

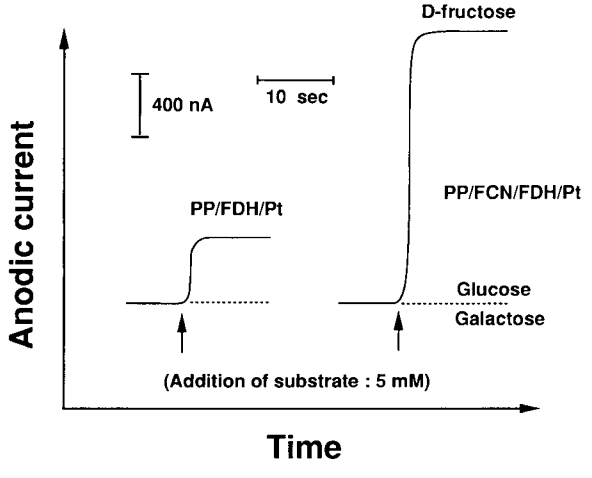

Fig. 3. Response curves for fructose with PP–FDH–Pt and PP–FCN–FDH–Pt electrodes. Both electrodes were prepared by the two step-method. The electrode potential was kept at 0.4 V.

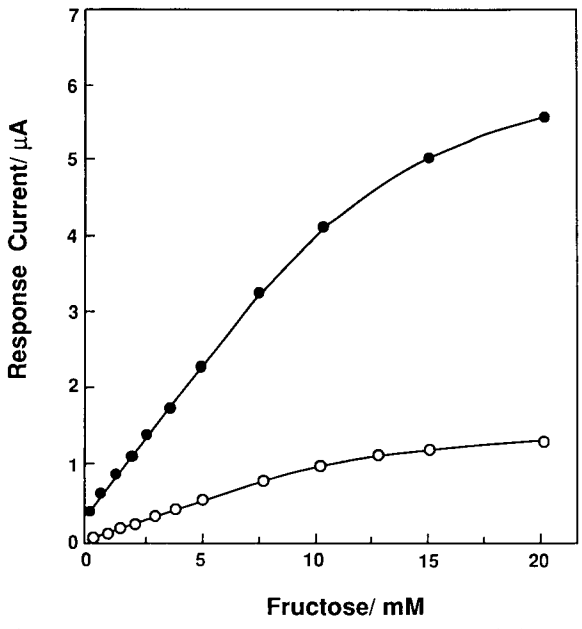

Fig. 4. Calibration graphs for fructose using the (○) PP–FDH–Pt and (●) PP–FCN–FDH–Pt electrodes. Both electrodes were prepared by the two-step method and used at 0.4 V.

The calibration graphs obtained with the PP–FDH–Pt and PP–FCN–FDH–Pt electrodes are shown in Fig. 4. In both instances the response current was directly proportional to fructose concentration up to 10 mM, with an upper detection limit of 30 mM fructose. The lower detection limits were 10 and 5 μM with the PP–FDH–Pt and PP–FCN–FDH–Pt electrodes, respectively. The slopes of the lines were about 80 and 450 nA, respectively.

Stability of enzyme electrodes fabricated by the two-step method

The stability of the mediator-containing electrode with time is shown in Fig. 5, together with that of the non-mediator-containing electrode. The PP–FDH–Pt electrode was used once a day and stored in buffer solution of pH 4.5 at 4°C. The enzyme electrode generated a constant response current for nearly 1 week with a slightly higher response on the third and fourth days. After 1 week the response gradually decreased by ca. 25% at the end of the second week. Possible reasons for the decrease in response are that the enzyme was gradually denatured owing to the long incubation in solution and repeated potential application, the electroconductivity of the conductive interface decreased with time and deterioration of polypyrrole caused by dissolved oxygen.

On the other hand, the PP–FCN–FDH–Pt electrode gave a gradually decaying response. In particular, the response decreased drastically in the first 2 days and the response current decayed gradually over 1 week. The main reason for the instability is probably leakage of the mediator from polymer matrix as the membrane was too thin (5–8 nm) to retain the low-molecular weight mediator inside the matrix. To improve the sensor stability it is necessary to keep the mediator in the matrix as long as possible. Several techniques were considered to prevent the leakage of the mediator, e.g., by covering the sensor with semipermeable membrane such as Nafion or by increasing the membrane thickness to retain a sufficient amount of mediator in the membrane matrix. With this in mind, we then proceeded to fabricate a more stable fructose sensor by the one-step method, because loading of large amounts of enzyme and mediator can be easily performed.

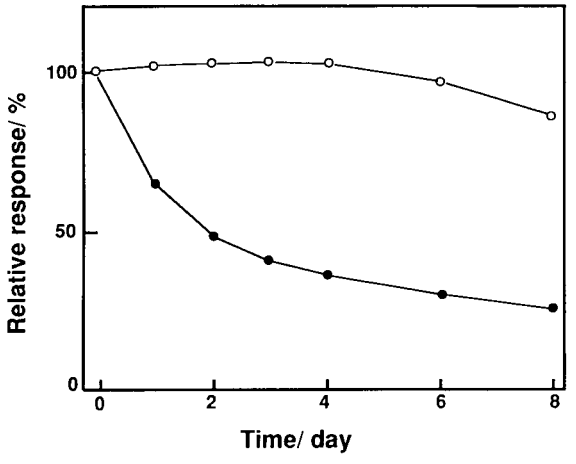

Fig. 5. Stability of (○) PP–FDH–Pt and (●) PP–FCN–FDH–Pt electrodes. The electrodes were stored at 4°C in buffer solution of pH 4.5. The same electrodes as used in Fig. 4 were taken. The electrode potential was controlled at 0.4 V.

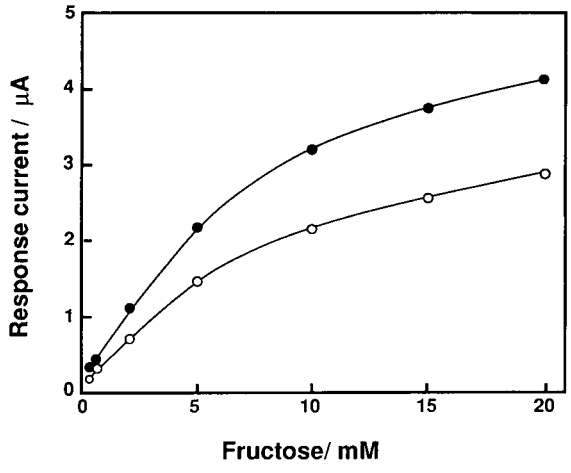

Fig. 6. Calibration graphs for fructose using (○) FCN and (●) ferrocene co-immobilized enzyme electrodes. Both electrodes were prepared by the one-step method and operated at 0.4 V.

Response of sensor prepared by the one-step method

The FCN and FTAI were employed as mediators. Calibration graphs for fructose were obtained using the two types of sensors. The two electrodes were prepared by the one-step method by passing a polymerization charge of 200 mC cm^{-2}. Figure 6 shows the calibration graphs obtained with the two electrodes. In each instance a highly sensitive determination was attained. The detection range was up to 30 mM with a lower detection limit of 50 μM. The linear calibration range was from 50 μM to 5 mM with slopes of ca. 300 and 400 nA 1 $mmol^{-1}$ for the FCN- and ferrocene-containing electrodes, respectively. The

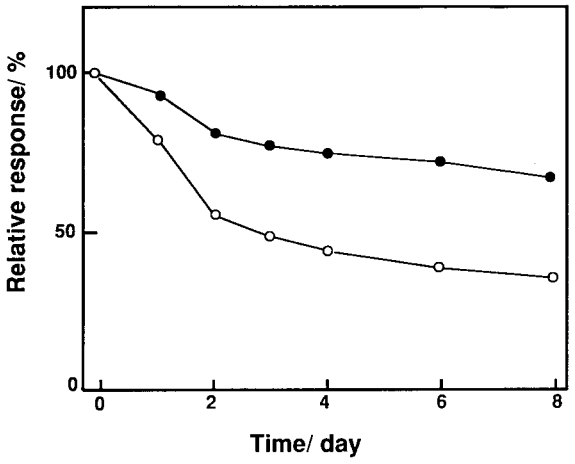

Fig. 7. Stability of the (○) FCN and (●) ferrocene co-immobilized enzyme electrodes at 0.4 V (the same electrodes as employed in Fig. 6). The electrodes were stored at 4°C in buffer solution of pH 4.5.

response of the latter sensor was 1.2–1.5 times greater than that of the former.

Stability of sensor prepared by the one-step method

The stability of sensors with time is shown in Fig. 7. The response current of the electrodes to 10 mM fructose decreased with time. On the second day ca. 60% and 80% of the electrode activity remained for the FCN- and ferrocene-entrapped electrodes, respectively. Approximately 40% and 70% the activity was exhibited on the eighth day. The initial sharp decrease of activity was due mainly to the leakage of the mediator loosely entrapped in the polymer matrix. The stability of the ferrocene-entrapped sensor was superior to that of the FCN-entrapped sensor, because the molecular size and structure of the ferrocene derivative (FTAI) are more favourable for the stable immobilization of the mediator in the hydrophobic PP matrix than those of FCN. FTAI is bulky and has two hydrophobic heads, whereas FCN is hydrophilic and less bulky. Therefore, FCN leaks out of the matrix more easily. The stability of the mediator co-immobilized electrode seems to depend predominantly on the chemical structure of the mediator, so that a macromolecular mediator such as a ferrocene-pendant polymer is likely to be preferable to a low-molecular-weight mediator in a thicker PP membrane.

In conclusion, the further functionalization of a conductive molecular interface has been demonstrated by incorporating an electron mediator having reversible electrochemical properties in the enzyme PP molecular interface. With the enzyme sensor prepared by the two-step method, very rapid (3–5 s) and highly sensitive (lower detection limit 5 μM) determinations were possible, but the output signal decayed rapidly owing to the leakage of the mediator from the membrane because the membrane was too thin to retain the mediator. On the other hand, with the enzyme electrode fabricated by the one-step method, a slower (8–10 s) and less sensitive sensor (lower detection limit 50 μM) was obtained. The antinomic relation of the fast response and the stability of these sensors may be overcome by incorporating macromolecular mediators such as ferrocene-pendant polymers or by covering the enzyme layer with semipermeable membranes. The stability of the enzyme electrode was superior to that of an enzyme electrode fabricated by the one-step method, as a thicker PP film was obtained in the latter instance. Of the two mediators investigated, the ferrocene derivative (FTAI) was found to be more stably retained in the polymer matrix, which resulted in improved stability.

REFERENCES

1 A.E.G. Cass, G. Davis, D. Francis, H.A.O. Hill, W.J. Aston, I.J. Higgins, E.V. Plotkin, L.D.L. Scott and A.P.F. Turner, Anal. Chem., 56 (1984) 667.
2 M.A. Lange and J.Q. Chambers, Anal. Chim. Acta, 175 (1985) 89.
3 C. Iwakura, Y. Kajiya and H. Yoneyama, J. Chem. Soc., Chem. Commun., (1988) 1019.
4 T. Ikeda, H. Hamada and M. Senda, Agric. Biol. Chem., 50 (1986) 883.
5 T. Ikeda, T. Shibata and S. Senda, J. Electroanal. Chem., 261 (1989) 351.
6 J.J. Kulys and N.K. Cenas, Biochim. Biophys. Acta, 744 (1983) 57.
7 Y. Degani and A. Heller, J. Phys. Chem., 91 (1987) 1285.
8 J.J. Kulys, Biosensors, 2 (1986) 3.

9 W.J. Albery, P.N. Bartlett and D.H. Gaston, J. Electranal. Chem., 194 (1985) 223.
10 K. McKenra and A. Brajter, Anal. Chem., 59 (1987) 954.
11 P.D. Hale, T. Inagaki, H.I. Karan, Y. Okamoto and T.A. Skotheim, J. Am. Chem. Soc., 111 (1989) 3482.
12 P.D. Hale, L.I. Boguslavsky, T. Inagaki, H.I. Karan, H.S. Lee and T.A. Skotheim, Anal. Chem., 63 (1991) 677.
14 M. Aizawa, S. Yabuki and H. Shinohara, in F.T. Hong (Ed.), Molecular Electronics, 1989, p. 269.
15 S. Yabuki, H. Shinohara and M. Aizawa, J. Chem. Soc., Chem. Commun., (1989) 945.
16 G.F. Khan, E. Kobatake, H. Shinohara, Y. Ikariyama and M. Aizawa, Anal. Chem., 64 (1992) 1254.
17 A. Ameyama, E. Shinagawa, K. Matsushita and O. Adachi, J. Bacteriol., 145 (1981) 814.
18 A. Ameyama, Methods Enzymol., 89 (1982) 20.
19 G.F. Khan, H. Shinohara, Y. Ikariyama and M. Aizawa, J. Electroanal. Chem., 315 (1991) 263.
20 H. Shinohara, G.F. Khan, Y. Ikariyama and M. Aizawa, J. Electroanal. Chem., 304 (191) 75.

Analytica Chimica Acta, 281 (1993) 535–542
Elsevier Science Publishers B.V., Amsterdam

Effect of enzyme ratio and enzyme loading on the performance of a bienzymatic electrochemical phosphate biosensor

E.M. D'Urso and P.R. Coulet

Laboratoire de Génie Enzymatique, EP 19 CNRS, Université Claude Bernard Lyon 1, ESCIL Bât. 308, 43 Boulevard du 11 Novembre 1918, 69622 Villeurbanne Cedex (France)

(Received 19th March 1992; revised manuscript received 16th September 1992)

Abstract

A membrane-bound bienzyme system involving purine nucleoside phosphorylase and xanthine oxidase for the design of an electrochemical biosensor for phosphate detection was studied. The effects on the performance of the biosensor of both the ratio of enzyme activities and the absolute activities in the enzyme loading solution were determined. Optimization of these parameters enabled the linear dynamic range and sensitivity to be improved. The relationship between sensitivity and immobilized activity was also investigated with the sensor equipped with xanthine oxidase alone. The resulting characteristics of the biosensor were compared with those obtained with either glucose oxidase or choline oxidase bound to the membrane.

Keywords: Amperometry; Biosensors; Enzymatic methods; Enzyme electrodes; Membrane electrodes; Phosphate

The work of Goldman and Katchalski in 1971 [1] and Bouin and co-workers in 1976 [2,3] demonstrated that the efficiency of immobilized dual enzyme systems was markedly dependent on both the absolute activities and the activity ratio in the coupling solution. Despite this discovery, when considering the numerous bienzyme membrane biosensors described in the last 20 years, little attention has been paid to these parameters for optimizing the performance of biosensors. In most instances, there is no obvious rationale in the choice of the enzyme immobilization parameters.

In the work presented here, the effect of the ratios of activities on the characteristics of the phosphate biosensor described previously [4] was studied. The two enzymes involved, purine nucleoside phosphorylase (PNP) and xanthine oxidase (XOD), were co-immobilized on a preactivated nylon membrane associated with a platinum electrode. PNP detects the phosphate ions present in the reaction medium, producing hypoxanthine as an intermediary metabolite in the microenvironment. XOD plays the role of an auxiliary enzyme, transforming the enzymatically generated hypoxanthine into substances that can be detected by the electrochemical transducer (Fig. 1). It should be noted that hypoxanthine can also be added directly to the reaction medium to determine the response of XOD working alone. In this instance, this enzyme plays the role of a biological amplifier because, according to the stoichiometry of the reaction, it generates 3 mol of electroactive species: 2 mol of H_2O_2 and 1 mol of uric acid for 1 mol of phosphate.

Correspondence to: P.R. Coulet, Laboratoire de Genie Enzymatique, EP 19 CNRS, Université Claude Bernard Lyon 1, E.S.C.I.L. Bât. 308, 43 Boulevard du 11 Novembre 1918, 69622 Villeurbanne Cedex (France).

Generally, in conventional enzymology, when coupled enzymatic reactions are used in solution for determining the concentration of a target analyte, it is recommended that a higher auxiliary enzyme activity be maintained compared with the detecting one, thus preventing the response of the first enzyme from being limited [5]. Heterogeneous systems with diffusional constraints such as membrane-bound enzymes are characterized by concentrations of the intermediate metabolites higher in the microenvironment than in the bulk phase and higher than it would be if the enzymes were free in solution [6]. Accordingly, the activity of the auxiliary enzyme, in order not to be limiting, should be increased in comparison with the requirements for soluble systems.

In fact, the problem is even more complex in two respects: the commercially available enzymes generally have different specific activities that are difficult to modify, and the yield of immobilization (depending on several parameters such as the nature of the support, the enzyme composition and the immobilization procedure), could be completely different for the two enzymes involved. In addition, if the immobilization of the biocatalysts is carried out in one step, a competition may occur between the enzymes for the binding sites of the activated membrane and it is very difficult to deal with these different phenomena.

In this study, PNP and XOD were co-immobilized at different ratios of activities and at different absolute activity values in order to optimize the performance of the phosphate sensor. Further, this may help to understand better the relationships between the initial activities in the coupling solution, and both the immobilized activities and the biosensor sensitivities with regard to phosphate and hypoxanthine.

EXPERIMENTAL

Reagents

Purine nucleoside phosphorylase (EC 2.4.2.1), of bacterial origin, lyophilized powder, xanthine

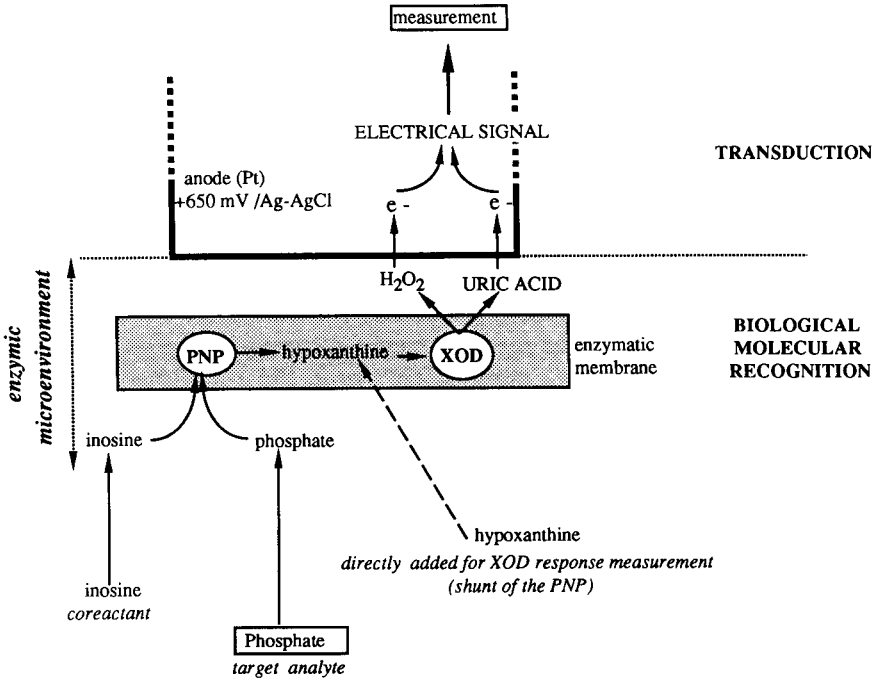

Fig. 1. Reactions occurring at the bioactive membrane-electrochemichal sensor interface.

oxidase (EC 1.2.3.2) from buttermilk, grade III, suspension in 2.3 M ammonium sulphate, inosine and hypoxanthine were purchased from Sigma (Paris) and bovine serum albumin (BSA) fraction V from Boehringer (Mannheim). Other reagents, of analytical-reagent grade, were supplied by Prolabo (Paris).

Immobilization procedure

Immobilization was achieved on preactivated polyamide membranes (Immunodyne type, 0.45 μm and 1.2 μm size cut-off) provided by Pall Industrie (St. Germain-en-Laye). The method recommended by the supplier for antibody immobilization was previously adapted to enzyme immobilization in this laboratory [7].

A 10-μl volume of the bienzymatic solution in 0.02 M veronal buffer–0.1 M KCl (pH 7.5) was deposited on each side of a disc membrane 8 mm in diameter (the XOD suspension was previously concentrated by centrifugation to avoid dilution of the PNP and also to compensate for the difference in specific activity between the two enzymes). The wetted membrane was allowed to dry for ca. 15 min at ambient temperature after enzyme deposition. The membranes were then washed twice with 1 M KCl–1% BSA and once with veronal buffer to eliminate the unbound molecules. The enzymatic membranes can be stored before use at −20°C in 0.02 M veronal buffer–0.1 M KCl (pH 7.5)–10% glycerol.

The loading activity will be defined as the activity theoretically deposited on the membrane during immobilization. These values are calculated from the initial suspension (XOD) or powder (PNP) activities stated by the supplier.

Instrumentation and procedure

The electroactive species (H_2O_2 and uric acid) are detected by a platinum electrode at +650 mV vs. an Ag/AgCl reference electrode, connected to a PRGE polarograph (Solea-Tacussel, Villeurbanne). The enzymatic membrane is maintained in close contact with the platinum anode by a screw-cap. Under working conditions, the electrode is immersed in 10 ml of 0.02 M veronal buffer–0.1 M KCl (pH 7.5). The temperature is maintained at 28°C by a thermostated circulating water-bath. Contact of the membrane with the bulk solution is achieved through a 4 mm diameter hole in the electrode cap. The anodic current resulting from the oxidation at the platinum electrode of the enzymatically generated electroactive species, is proportional in a definite range to the analyte to be determined. In fact, even if electroactive species measurements can be performed at high concentrations, a saturation response for the substrate is generally observed for enzymatic electrodes at much lower concentrations.

On addition of a substrate-containing sample, the current rapidly increases and a plateau corresponding to the steady-state response is reached within 2 and 3 min for hypoxanthine and phosphate, respectively.

Determination of sensitivity

The sensitivity to an analyte is given by the slope of the calibration graph obtained for increasing concentrations of standards in the reaction medium; it is expressed in mA l mol^{-1}. This can be done for electroactive species such as hydrogen peroxide and uric acid or for hypoxanthine and phosphate through the enzymic system.

Electrochemical determination of the enzyme activity retained on the support

The enzymatic membranes were tested in the reaction medium with their respective substrates at the optimum concentration, i.e., 0.85 mM hypoxanthine to determine the activity of XOD or 0.2 mM inosine and 2 mM phosphate for PNP. The electrochemical response was calibrated with a mixture of H_2O_2 and uric acid (2 + 1) to simulate the stoichiometry of the enzymatically generated electroactive species. The activities are expressed in nmol min^{-1} of electroactive species produced; in contrast, the activities given by the supplier are expressed in μmol min^{-1} of converted substrate. Hence, the stoichiometry of the overall reaction can be taken into account for calculations.

It should be noted that, as usual in heterogeneous enzymology, the apparent determined activities depend on diffusional processes. Further, when measuring the immobilized PNP activity, as no excess of soluble XOD is added, the deter-

mined activity depends on the co-immobilized XOD activity on the membrane.

RESULTS AND DISCUSSION

Determination of the optimum ratio of activities in the enzyme loading solution

Different mixtures were prepared with one enzyme maintained at a fixed activity value while the other varied: PNP was maintained at 447 mU while the XOD activity varied from 9 to 466 mU; XOD was then maintained at 466 mU while PNP varied from 8.9 to 447 mU. Thus, the ratio A_{PNP}/A_{XOD} varied from 0.02 to 50 and the sensitivities for both phosphate and hypoxanthine were measured. Under these conditions, an optimum for phosphate sensitivity was reached at a ratio of ca. 5 (Fig. 2, line a).

In contrast, the sensitivity to hypoxanthine directly added to the medium, corresponding to the shunt of PNP activity (see Fig. 1), is not modified by the variation of the activity ratio (line b). The relative standard deviation for the seven measured values is below 2%, which is not significant. Even a 50-fold dilution of XOD (ratio = 50) has no influence on the sensor sensitivity. Nevertheless, in such a case, the XOD activity may be limiting for the overall biosensor response as the sensitivity to phosphate levels off at ratio values higher than 5 (line a).

Relationship between sensitivities and immobilized activities

The main purpose was then to understand the relationship between the activity retained after immobilization and the sensitivity exhibited by the membrane. For each previous ratio, the immobilized activities of both PNP and XOD were measured. The results obtained are illustrated in Fig. 3. As shown in Fig. 3a, whereas the sensitivity for hypoxanthine remains constant, the XOD activity retained on the membrane is markedly dependent on the loading activity. In contrast (Fig. 3b), the immobilized PNP activity varies like the sensitivity to phosphate, as would be expected.

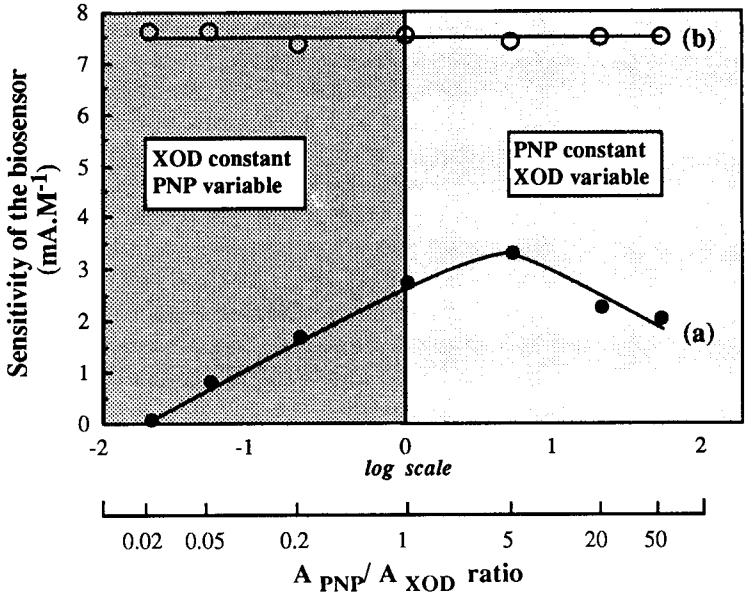

Fig. 2. Effect of the ratio of enzyme activities on the sensitivity of the biosensor for (a) phosphate and (b) hypoxanthine. Left, XOD activity was maintained at 447 mU while PNP activity varied from 9 to 466 mU; right, PNP activity was kept at 466 mU while XOD activity varied from 8.9 to 447 mU. The ratio A_{PNP}/A_{XOD} was then between 0.02 and 50. The measurements were performed at 28°C in 10 ml of 0.02 M veronal buffer–0.1 M KCl–0.2 mM inosine (pH 7.5).

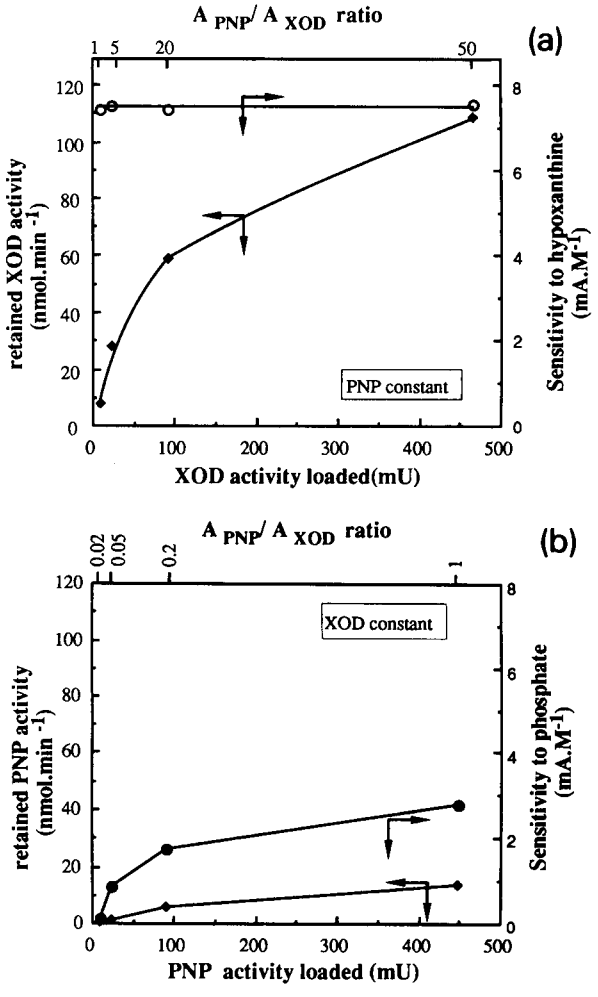

Fig. 3. (a) Correlation between sensitivity for hypoxanthine and immobilized XOD activity at different A_{PNP}/A_{XOD} ratios. PNP activity was kept at 466 mU while XOD activity varied from 8.9 to 447 mU. The ratio A_{PNP}/A_{XOD} was then between 1 and 50. Immobilized XOD activity was measured at 0.85 mM hypoxanthine with other conditions identical with those for sensitivity measurements. ○ = Sensitivity for hypoxanthine; ♦ = XOD activity retained on the 8 mm diameter membrane. (b) Correlation between sensitivity for phosphate and immobilized PNP activity at different A_{PNP}/A_{XOD} ratios. XOD activity was maintened at 447 mU while PNP activity varied from 9 to 466 mU. The ratio A_{PNP}/A_{XOD} was then between 0.02 and 1. Immobilized PNP activity was measured at 2 mM phosphate with other conditions identical with those for sensitivity measurements. ● = Sensitivity for phosphate; ♦ = PNP activity retained on the 8 mm diameter membrane.

TABLE 1
Effect of the ratios of the loading activities on the linear dynamic range for phosphate

A_{PNP}/A_{XOD} ratio	0.1	0.2	5	10
PNP loading (U)	0.1	0.2	5.0	10
XOD loading (U)	←	1.0	→	
Higher limit of linear dynamic range (μm)	25	45	90	90

When considering the values of the membrane activities, it should be noted that the retained activities are always superior for XOD compared to PNP even if the activity of PNP is higher than that of XOD in the enzyme loading solution. This is still true if an excess of soluble XOD is added for the PNP activity test (data not shown). This could be explained by a higher immobilization yield for XOD than for PNP. Such a result is in accord with the theory previously mentioned because in coupled reactions, the auxiliary activity should be higher than the detecting activity to avoid limiting conditions.

Effect of the enzyme activity ratio on the linear dynamic range for the biosensor response

The ratio range 0.1–10 was applied and the absolute loading activities were increased. The XOD activity was kept constant at 1 U while the PNP activity varied from 0.1 to 10 U. As can be seen in Table 1, the linear dynamic range for the phosphate response is broadened when the ratio increases.

It must be stressed that the performance of the phosphate biosensor is improved in terms of sensitivity and linear dynamic range compared with the results presented previously [4].

Effect of absolute loading activities on the linear dynamic range of the biosensor

Further experiments showed that the values of the absolute loading activities also play an important role when considering improvements in sensitivity and linearity. Different activities were co-immobilized at the same ratio ($A_{PNP}/A_{XOD} \approx 5$); the PNP activity loading varied from 34 to 2800 mU while the XOD activity loading varied from 8

to 665 mU. In each instance the sensitivities obtained for both phosphate and hypoxanthine were measured. As can be observed in Fig. 4 (line a), the sensitivity to phosphate increases with increasing absolute loading activity and then levels off with saturation of the membrane binding sites. Beyond a certain value, it appears useless to load higher activity on the membrane as no improvement is obtained. In addition, the cost should be as low as possible if an analytical use of the device is intended.

With biosensors, the measured sensitivity can be considered to provide a picture of the immobilized activity. As in classical catalysis, the rate of substrate conversion is dependent on the activity. This is the case with coupled reactions if the second enzyme does not become limiting on increasing the activity of the first (detecting) enzyme. The result obtained is in agreement with those of other workers for monoenzymatic systems [8–10]. This means that among the different activity values tested, XOD is not limiting for the overall reaction, i.e., the chosen ratio was the optimal value.

In contrast, and as observed before, the sensitivity to hypoxathine remains almost constant with increasing loading activity (Fig. 4, line b).

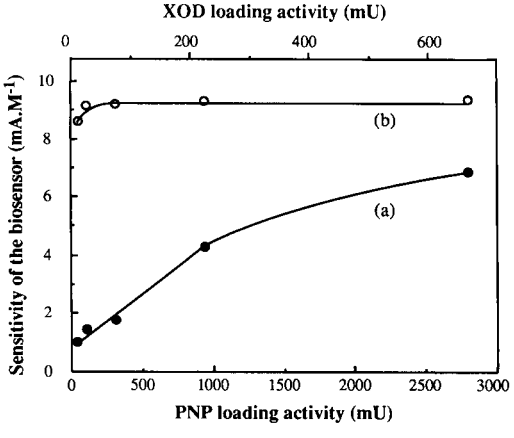

Fig. 4. Effect of the enzyme loading on the sensitivity of the biosensor for (a) phosphate and (b) hypoxanthine. The ratio A_{PNP}/A_{XOD} was fixed close to 5. PNP varied from 34 to 2800 mU and XOD from 8 to 665 mU. The measurements were performed at 28°C in 10 ml of 0.02 M veronal buffer–0.1 M KCl–0.2 mM inosine (pH 7.5).

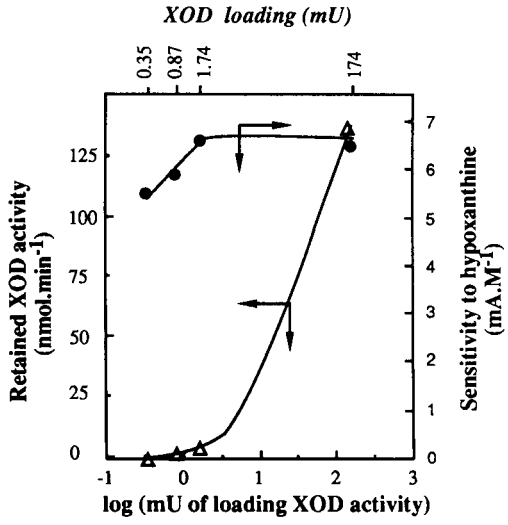

Fig. 5. Correlation between sensitivity for hypoxanthine and immobilized XOD activity at different activity loadings without PNP. XOD activity loading varied from 0.35 to 174 mU. Immobilized XOD activity was measured at 0.85 mM hypoxanthine with other conditions identical with those for sensitivity measurements. ● = Sensitivity for hypoxanthine; △ = XOD activity retained on the 8 mm diameter membrane.

Behaviour of XOD immobilized alone

XOD was immobilized without PNP using identical loading activities. No change occurred in the sensitivity of the biosensor to hypoxanthine (data not shown). Therefore, new loadings with lower activities were performed in order to determine whether the corresponding sensitivities to hypoxanthine would decrease. When the loading activity varied from 174 down to 0.87 mU (200-fold dilution), the retained activity decreased from 138.2 to 2.4 nmol min^{-1}, whereas the maximum variation of sensitivity was less than 18% (Fig. 5). For the lower loading value (0.35 mU), the retained activity is close to zero. Nevertheless, when the loading activity increased from 0.35 to 174 mU, the upper value of the linear dynamic range for hypoxanthine increased from 18 to 87 μM.

This experiment shows that the XOD electrode can be considered to have very good performance as a sensitivity can be measured when no enzymic membrane activity can be detected any longer! This phenomenon is due to the close vicinity in the biosensor tip between the enzyme and the transducer, which limits the diffusional

transport, back to the bulk phase, of the enzymatically generated electroactive species. In the relationship with heterogeneous catalysis, it could be said that at a very low enzyme loading, the enzymatic reaction is under kinetic control. On the other hand, it is under diffusional control at a high enzyme loading, when no more variations in sensitivities are observed.

Behaviour of other oxidases immobilized alone

The relationship between the sensitivity and the retained activity was studied for two other oxidases, glucose oxidase (GOD) and choline oxidase (ChOD). The immobilization procedure followed previous work [7,11]. First, different GOD activities varying from 0.0625 to 12.5 U and second, different ChOD activities varying from 0.05 to 10.7 U were loaded on the membrane. The retained GOD or ChOD activity and sensitivity to β-D-glucose or choline were determined with respect to the loading activities. As can be seen in Fig. 6, when no ChOD activity can be determined, the sensitivity to choline is zero; for GOD

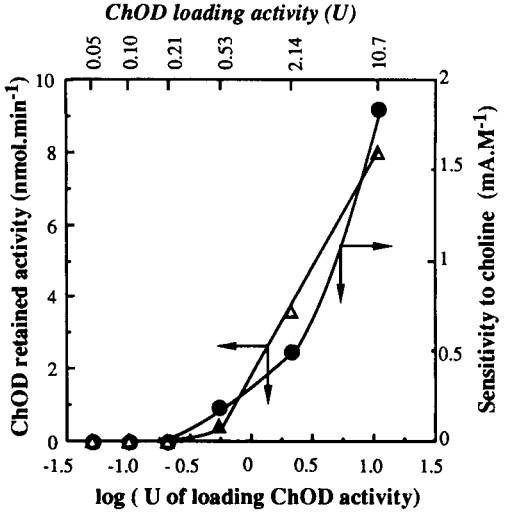

Fig. 6. Correlation between sensitivity for choline and immobilized ChOD activity at different loadings. ChOD activity loading varied from 0.05 to 10.7 U. Immobilized ChOD activity was measured at 28°C in 10 ml of 20 mM choline–0.1 M phosphate buffer–0.1 M KCl (pH 8.0). Sensitivity to choline was measured under the same conditions but without choline. ● = Sensitivity to choline; △ = ChOD activity retained on the 8 mm diameter membrane.

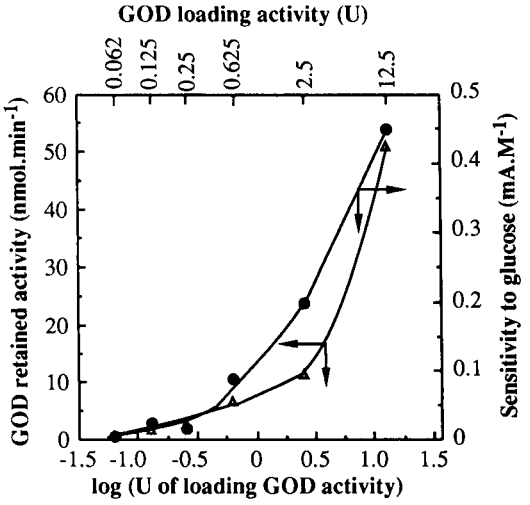

Fig. 7. Correlation between sensitivity for glucose and immobilized GOD activity at different loadings. GOD activity loading varied from 0.062 to 12.5 U. Immobilized GOD activity was measured at 28°C in 10 ml of 200 mM glucose–0.1 M acetate buffer–0.1 M KCl (pH 5.5). Sensitivity to glucose was measured under the same conditions but without glucose. ● = Sensitivity for glucose; △ = GOD activity retained on the 8 mm diameter membrane.

(Fig. 7), the lowest loading value leads to a detectable immobilized activity but the corresponding sensitivity to glucose is very low. Obviously, and in contrast to XOD, the curves for activity and sensitivity vary in a similar manner in both instances. This demonstrates that the behaviour of XOD cannot be explained only by microenvironmental vicinity effects.

Comparison between the three oxidases

The ratio of sensitivity to immobilized activity (R_{sa}), calculated for the lowest measurable activity, was determined in each instance. If the K_m values of the three enzymes are considered (Table 2), it can be seen that the higher the affinity of the enzyme for its substrate (lower K_m), the higher is R_{sa}. From these results, it can be expected that the sensitivity of a biosensor can be approximately predicted from the respective affinities exhibited by the enzymes for their substrates. When several possibilities are offered for target detection, it would be preferable to choose the enzyme or the enzyme system with the lower K_m. Nevertheless, the immobilization yield also

TABLE 2

Correlation between immobilized activity, sensitivity and affinity of three oxidases

Oxidase	Retained activity (mU)	Sensitivity (mA l mol^{-1})	R_{sa} [a] (arbitrary units)	K_m (M)
Xanthine oxidase	0.98	5.95	6.1	1.3×10^{-6}
Choline oxidase	0.22	0.19	0.86	1.2×10^{-3}
Glucose oxidase	0.82	0.006	0.007	33×10^{-3}

[a] The R_{sa} value was calculated for the lowest loading activity that allows an immobilized activity to be detected.

plays an important part in the performance of a biosensor and it can be very different from one enzyme to another.

Conclusions

It has been shown that the performance of a bienzymatic sensor is strongly dependent on two parameters: the enzyme activity ratio and the enzyme loading. A thorough study was conducted using as a model a phosphate sensor involving co-immobilized PNP and XOD associated with hydrogen peroxide detection. After optimization, the sensitivity of the bienzymatic sensor was improved and its linear dynamic range broadened.

The intimate vicinity of the surface of the enzymatic membrane and of the transducer creates a microcompartment in which the electroactive species are confined at higher concentrations than in the bulk phase. For XOD, this leads to a bioamplification effect enabling the biosensor to provide a signal, whereas no enzymatic activity can be detected on the same membrane tested under batch conditions.

An attempt was made to elucidate the behaviour of XOD through comparison with two other oxidases, GOD and ChOD, immobilized alone. It could be demonstrated that the relationship existing between the biosensor sensitivity and the immobilized activity on the enzymatic membrane depended on the affinity of the oxidases for their substrates. It is hoped that this approach could be applied to other enzymes, thus being of some help in predicting the performances of novel biosensors.

REFERENCES

1 R. Goldman and E. Katchalski, J. Theor. Biol., 32 (1971) 243.
2 J.C. Bouin, M.T. Atallah and H. O. Hultin, Biochim. Biophys. Acta, 438 (1976) 23.
3 J. C. Bouin, P.H. Dudgeon and H.O. Hultin, J. Food Sci., 41 (1976) 886.
4 E.M. D'Urso and P.R. Coulet, Anal. Chim. Acta, 239 (1990) 1.
5 H.U. Bergmeyer, in H.U. Bergmeyer (Ed.), Methods of Enzymatic Analysis, Vol. 1, Verlag Chemie, Deerfield Beach, FL, 2nd edn., 1974, p. 109.
6 K. Mosbach and B. Mattiasson, Acta Chem. Scand., 24 (1970) 2093.
7 C.H. Assolant-Vinet and P.R. Coulet, Anal. Lett., 19 (1986) 875.
8 F.W. Scheller, R. Renneberg and F. Schubert, Methods Enzymol., 137 (1988) 29.
9 K. Male and J.H.T. Luong, Biosensors Bioelectron., 6 (1991) 581.
10 T. Kimura, M. Yoshida, K. Oishi, M. Ogata and T. Nakakuki, Agric. Biol. Chem., 53 (1989) 1848.
11 R.M. Morelis and P.R. Coulet, Anal. Chim. Acta, 231 (1990) 27.

Analytica Chimica Acta, 281 (1993) 543–548
Elsevier Science Publishers B.V., Amsterdam

Protein sensors based on the potentiometric photoresponse of polymer membranes doped with photochromic spiropyran

Jun-ichi Anzai, Kenji Sakamura, Yasushi Hasebe and Tetsuo Osa

Pharmaceutical Institute, Tohoku University, Aobayama, Sendai 980 (Japan)

(Received 26th March 1992; revised manuscript received 26th September 1992)

Abstract

The potentiometric photoresponse of plasticized polymer [carboxylated poly(vinyl chloride)] membranes doped with a spirobenzopyran derivative was modulated significantly by specific adsorption of proteins on the membrane surface. The magnitude of the photoinduced potential of the membranes was decreased in the presence of 1–15 μg ml^{-1} of anti-DNP or 0.1–1.5 μg ml^{-1} of avidin in solution. The possible use of the membranes as protein sensor materials is discussed in terms of response time, selectivity and re-usability.

Keywords: Biosensors; Potentiometry; Membrane electrodes; Proteins; Spirobenzopyran

The development of reliable sensors for antigen and antibody determination has been a focal subject in biosensor technology. It has been demonstrated that potentiometric immunosensors can be constructed by immobilizing antigen or antibody on the electrode surface [1–3]. The potentiometric immunosensors detect the potential changes arising from the formation of immunocomplexes on the electrode surface. However, the response of such sensors is often too small to be used as an output signal for a reliable sensor [4,5].

A novel type of potentiometric membrane sensor for the measurement of antibodies and proteins has been devised by incorporating antigen–ionophore conjugates in a poly(vinyl chloride) (PVC) membrane [6–10]. The response mechanism of the sensors is that the complex formation between the conjugate and proteins modulates the background potential that is established by selective binding of marker ions to the ionophore in the membrane.

An alternative strategy for constructing potentiometric immunosensors has recently been developed based on the measurement of photoinduced potential changes of polymer [11] and semiconductor [12] devices. Using this method, Katsube et al. [12] constructed an immunogloblin G (IgG) sensor that can detect IgG at the nanomolar level. In previous work, photosensitive polymer membranes modified with a photochromic spiropyran were used to prepare protein sensors and preliminary results were reported [11]. So far PVC has been used as a matrix polymer for the membranes. PVC shows satisfactory chemical and physical characteristics for the preparation of self-standing membranes. However, the PVC-based polymer membranes sometimes suffer from poor adhesion to the surface of electrodes such as glass, carbon and semiconductors [13]. For this

Correspondence to: T. Osa, Pharmaceutical Institute, Tohoku University, Aobayama, Sendai 980 (Japan).

reason, in this work a carboxylated PVC (PVC-COOH) was used as a membrane material. The low impedance of the PVC-COOH-based membranes is an advantage [14]. This paper describes potentiometric protein sensors constructed with the use of PVC-COOH-based photosensitive membranes doped with a photochromic spirobenzopyran (**1**).

EXPERIMENTAL

Materials

Carboxyl-substituted poly(vinyl chloride) (PVC-COOH) was purchased from Aldrich [nominally 1.8% (w/w) carboxy residues] and used after purification by reprecipitation in methanol. Di-*n*-butyl sebacate (DBS) was obtained from Wako and used as received. Anti-dinitrophenyl (DNP)–BSA (Seikagaku Kogyo) and avidin (Funakoshi) were used as received. Procedures for the synthesis of 2,4-dinitrophenyldecylamine (2,4-DNP) (**2**) and 1′-*p*-nitrobenzyl-3′,3′-dimethyl-6-nitrospiro(2*H*-1-benzopyran-2,2′-indoline) (**1**) were reported previously [11]. *N*-Octadecylbiotinamide (C_{18}-biotin) (**3**) was prepared from the succinimidyl ester of biotin and octadecylamine in chloroform–2-propanol mixture. Elemental analysis: calculated for $C_{28}H_{53}N_3O_2S$, C 67.83, H 10.78, N 8.48; found, C 67.58, H 10.64, N 8.34%. All other reagents were of extra-pure reagent grade.

Preparation of sensor

The top of a glassy carbon (GC) rod (3 mm diameter) (Tokai Carbon) mounted in a PTFE tube was coated with a photosensitive membrane composed of PVC-COOH (32%), DBS (64%), **1** (2.5%), sodium tetraphenylborate (0.3%) and 2,4-DNP or C_{18}-biotin (1.2%). The polymer membranes were prepared by pouring a small amount of a tetrahydrofuran solution of the materials on the surface of the GC electrode and allowing the solvent to evaporate. The thickness of the membrane thus prepared was ca. 0.1 mm.

Measurements

Potentiometric measurements with the sensors were performed vs. an Ag/AgCl reference electrode with a 0.1 M tetramethylammonium chloride liquid junction, using a glass cell illustrated in Fig. 1. The light source was a 500-W xenon lamp and cut-off filters (Toshiba UV-D35 and O-55) were used to isolate UV (320 nm $< \lambda <$ 400 nm) and visible ($\lambda >$ 550 nm) light, respectively. After the steady-state potential had been obtained under dark conditions, UV or visible light was radiated on the membrane surface to induce the membrane potential. Anti-DNP–BSA, BSA or avidin was added to the sample solution from

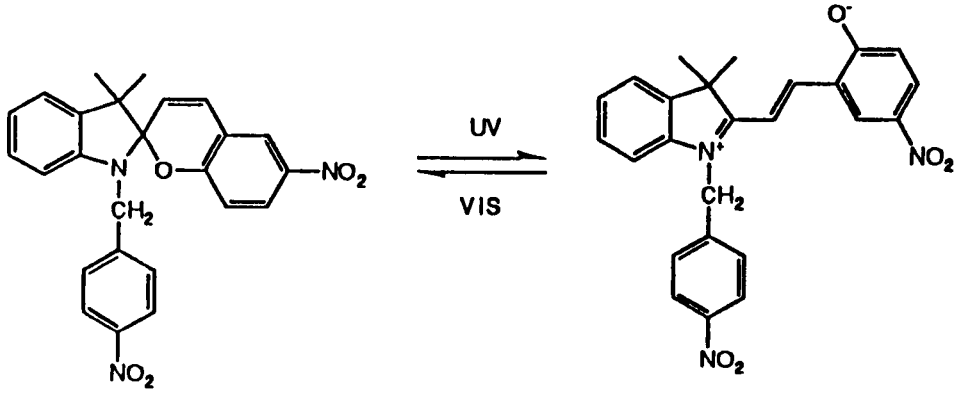

Scheme 1.

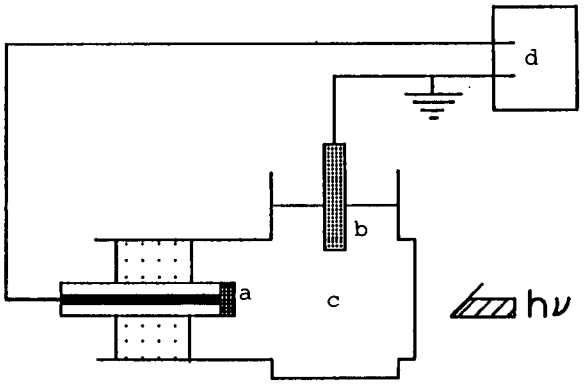

Fig. 1. Experimental set-up for the measurement of the potentiometric photoresponse of the membrane sensor. (a) Membrane-coated electrode; (b) reference electrode; (c) sample solution; (d) electrometer.

a concentrated stock solution. All measurements were made with a high-impedance electrometer at ca. 23°C. The noise level was within 1 mV. UV–visible absorption spectra were obtained by preparing the membrane on a quartz plate.

RESULTS AND DISCUSSION

It has already been reported that the membrane potential can be induced by photoirradiation of plasticized PVC membranes doped with spirobenzopyran derivatives as a result of the photoisomerization of the spirobenzopyran in the membrane [15–20].

In order to check the photoreactivity of **1** in the PVC-COOH membrane, absorption spectra of **1** were recorded before and after irradiation (Fig. 2). The membrane exhibited no absorption maximum at $\lambda > 500$ nm before irradiation. On exposing the membrane to UV radiation, the membrane turned purple within 2–3 min and a peak appeared around 575 nm, suggesting the formation of open-**1** in the membrane. The original spectrum was recovered by irradiation with visible light or thermally. The half-life of open-**1** in the membrane was ca. 4 min at 23°C in the dark. These results show that the photochemistry of **1** in the PVC-COOH membrane is almost the same as that in the parent PVC membrane.

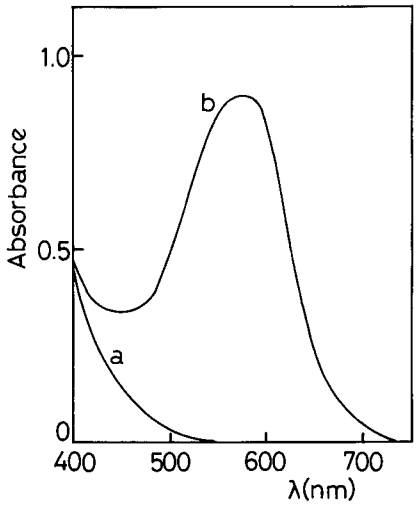

Fig. 2. Absorption spectra of PVC-COOH membrane (a) before and (b) after UV irradiation.

Figure 3 illustrates the potentiometric photoresponse of the GC electrode coated with te PVC-COOH–**1**–**2** membrane. After a steady-state potential had been obtained in the dark, the electrode potential shifted in the positive direction on UV irradiation and reached a steady-state value within ca. 5 min. The original potential was recovered by irradiation with visible light for 2–3 min or thermally. The half-life of the decay of the photoinduced potential was ca. 4 min. A similar

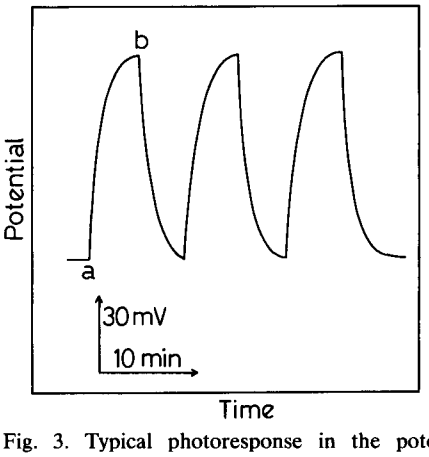

Fig. 3. Typical photoresponse in the potential of PVC-COOH–**1**–**2** membrane-coated GC electrode. The membrane was exposed to UV [at (a)] and visible [at (b)] light in 20 mM phosphate buffer (pH 7.0).

photoresponse was observed for a PVC-COOH–**1**–**3** membrane. The surface potential changes, which originate from the positive charge of the protonated open-**1**, should be responsible for the potentiometric response [15–20]. The initial potential of the electrode varied to some extent from membrane to membrane. However, this is not a drawback for the present purpose, because the system does not rely on the electrode potential itself but on the magnitude of the photoinduced potential.

The potentiometric response of the PVC-COOH–**1**–**2** membrane electrode to anti-DNP–BSA without irradiation was examined. The electrode potential was monitored with successively additions of anti-DNP–BSA to the sample solution. The electrode potential shifted slightly (2–3 mV) in the positive direction on addition of 10 μg ml^{-1} of antibody. This potential shift may be ascribed to the selective binding of antibody to the membrane surface, considering that no response was observed for antibody-free BSA in the same concentration region. Keating and Rechnitz [6,7] also reported the selective binding of anti-DNP–BSA on the surface of a PVC membrane doped with a DNP–ionophore conjugate. The potential response, however, was too small to be used as an immunosensor signal.

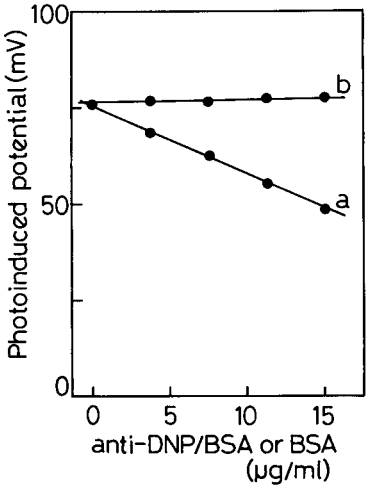

Fig. 4. Photoinduced potential of PVC-COOH–**1**–**2** membrane electrode in the presence of (a) anti-DNP–BSA and (b) BSA. Phosphate buffer (20 mM, pH 7.0) was used.

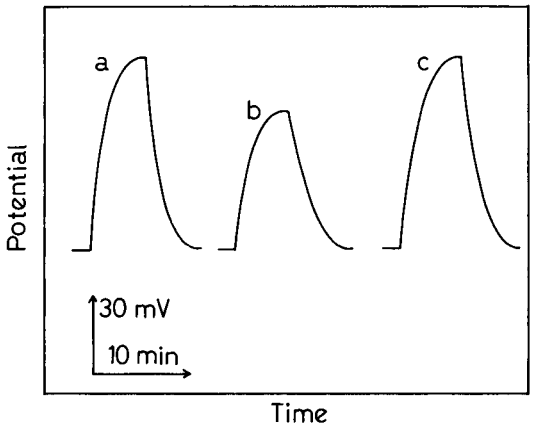

Fig. 5. Re-usability of PVC-COOH–**1**–**2** membrane electrode. Photoresponse (a) in the absence of antibody, (b) in the presence of 5 μg ml^{-1} of anti-DNP–BSA and (c) after rinsing with buffer for 5 min.

Figure 4 plots the magnitude of the photoinduced potential of the PVC-COOH–**1**–**2** membrane-coated electrode in the presence of anti-DNP–BSA and BSA. In the absence of antibody, the electrode exhibited a ca. 75 mV photoinduced potential. The photoresponse was suppressed by the addition of antibody to the solution, the photoinduced potential typically being ca. 50 mV for 15 μg ml^{-1} of antibody. Thus, a useful calibration was obtained for 1–15 μg ml^{-1} of anti-DNP–BSA by the use of the photoinduced potential rather than the electrode potential itself as an output signal. It is clear that the antibody-dependent photoresponse is associated with the immunoreaction between **2** and anti-DNP–BSA on the membrane surface, because antibody-free BSA has no significant effect on the photoresponse in the same concentration range. It was also checked that the PVC-COOH–**1** membrane (without hapten **2**) electrode exhibited no response to anti-DNP–BSA.

Figure 5 illustrates the re-usability of the antibody sensor. After the electrode had been exposed to antibody solution, the membrane surface of the electrode was rinsed with the working buffer for 5 min. With this treatment, a full response with regard to photoinduced potential was recovered and this renewed electrode could

be used repeatedly several times to measure the antibody.

Another protein, avidin, was used to assess the effect of protein binding on the photoresponse of the membrane-coated electrode. It is well known that avidin binds biotin very strongly in solution or immobilized form [21]. Figure 6 shows a calibration graph for the PVC-COOH–**1**–**3** membrane-coated electrode with avidin. The photoinduced potential was decreased in the presence of 0.1–1.5 μg ml^{-1} of avidin, which could be ascribed to the adsorption of avidin on the membrane surface by forming a complex with C_{18}-biotin (**3**). On the other hand, with the PVC-COOH–**1** membrane (without **3**), the photoresponse was not affected by avidin, confirming the essential role of biotin–avidin complexation.

Figure 7 shows re-usability of the PVC-COOH–**1**–**3** membrane. In contrast to the reversible binding of antibody with the PVC-COOH–**1**–**2** membrane, avidin could not be washed out from the membrane surface. Even after 24 h of rinsing with the buffer, the original magnitude of the photoresponse was not restored. This may arise from the strong binding between avidin and biotin (i.e., $K_a = 10^{15}$ l mol^{-1} in solution [21]).

The mechanism by which photoinduced potentials are suppressed by protein binding is not clear. The idea that the photochemical reaction of **1** in the membrane is disturbed by protein binding can be excluded because of the same intensity of the absorption peak at ca. 575 nm for UV-irradiated membranes before and after protein binding. The adsorbed proteins may affect the potential profiles at the membrane/solution interface.

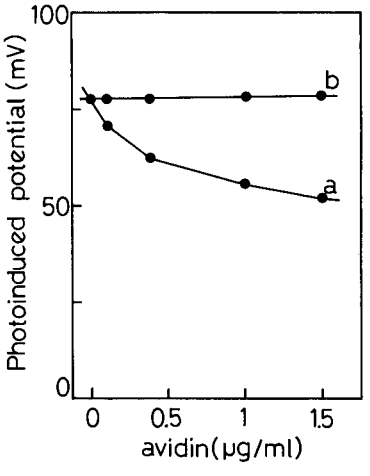

Fig. 6. Photoinduced potentials of (a) PVC-COOH–**1**–**3** and (b) PVC-COOH–**1** membrane electrodes in the presence of avidin. Phosphate buffer (20 mM, pH 7.0) was used.

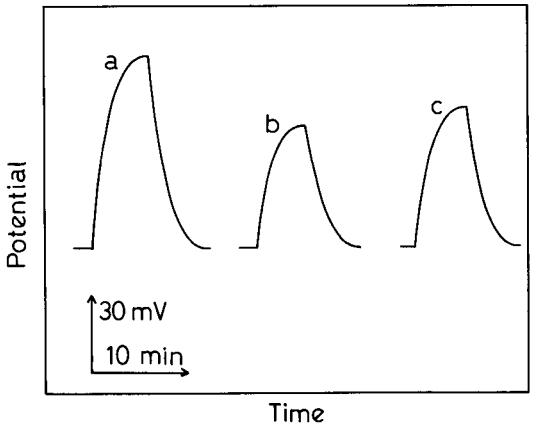

Fig. 7. Re-usability of PVC-COOH–**1**–**3** membrane electrode. Photoresponse (a) in the absence of avidin, (b) in the presence of 1.0 μg ml^{-1} of avidin and (c) after rinsing with buffer for 24 h.

This work was supported in part by a grant from Kowa Life Science Foundation.

REFERENCES

1 N. Yamamoto, Clin. Chem., 26 (1980) 1569.
2 M. Gotoh, E. Tamiya and I. Karube, J. Membr. Sci., 41 (1989) 291.
3 C.S. Lee, P.Y. Huang and D.M. Ayres, Anal. Chem., 63 (1991) 464.
4 S. Collins and J. Janata, Anal. Chim. Acta, 136 (1982) 93.
5 R.B.M. Schasfoort, P. Bergveld, R.P.H. Kooyman and J. Greve, Anal. Chim. Acta, 238 (1990) 323.
6 M.Y. Keating and G.A. Rechnitz, Analyst, 108 (1983) 766.
7 M.Y. Keating and G.A. Rechnitz, Anal. Chem., 56 (1984) 801.
8 R.L. Solsky and G.A. Rechnitz, Anal. Chim. Acta, 123 (1981) 135.
9 D.L. Bush and G.A. Rechnitz, J. Membr. Sci., 30 (1987) 313.
10 C.M. Merritt and J.W. Wiakelman, Anal. Chem., 61 (1989) 2362.

11 J. Anzai, Y. Hasebe, Y. Tobiki and T. Osa, Anal. Sci. (Suppl.), 7 (1991) 883.
12 T. Katsube, H. Uchida, H. Mackawa and T. Yagi, Jpn. Sensors Newslett., 5, No. 4 (1991) 30.
13 T. Satchwill and D.J. Harrison, J. Electroanal. Chem., 202 (1986) 75.
14 E. Lindner, E. Graf, Z. Niegreisz, K. Toth, E. Pungor and R.P. Buck, Anal. Chem., 60 (1986) 683.
15 J. Anzai, Y. Hasebe, A. Ueno and T. Osa, Kobunshi Ronbunshu, 43 (1986) 683.
16 J. Anzai, H. Sasaki, A. Ueno and T. Osa, Makromol. Chem., Rapid Commun., 7 (1986) 133.
17 J. Anzai, Y. Hasebe, A. Ueno and T. Osa, Bull. Chem. Soc. Jpn., 60 (1987) 1515.
18 Y. Hasebe, J. Anzai, A. Ueno, T. Osa and C.W. Chen, J. Phys. Org. Chem., 1 (1988) 309.
19 Y. Hasebe, J. Anzai, A. Ueno and T. Osa, Chem. Pharm. Bull., 37 (1989) 1307.
20 Y. Hasebe, N. Sumiya, J. Anzai and T. Osa, Kobunshi Ronbunshu, 47 (1990) 927.
21 M. Wilchek and E.A. Bayer, Anal. Biochem., 171 (1988) 1.

Analytica Chimica Acta, 281 (1993) 549–555
Elsevier Science Publishers B.V., Amsterdam

Transient data to predict steady-state responses for enzyme-based reactor–sensor systems

Christopher E. Uhegbu, Harry L. Pardue, Michael D. Love and Shahrzad Toosi

Department of Chemistry, Purdue University, West Lafayette, IN 47907 (USA)

(Received 10th April 1992; revised manuscript received 7th September 1992)

Abstract

An evaluation of the transient response of a glucose-selective device for the quantification of glucose is described. Data collected during the early parts of the responses were used to compute the signals that would be measured if the responses were monitored to steady state. The time-dependent responses were fitted to diffusion-limited, Michaelis–Menten and parallel-first-order models. The parallel-first-order and Michaelis–Menten models fit the data reasonably well; only the former gave reliable estimates of the steady-state signals. For the three models, plots of computed currents vs. concentration were linear for several fitting ranges. The measurement times were 5- to 10-fold shorter than the time required to reach steady state.

Keywords: Amperometry; Voltammetry; Biosensors; Data processing; Glucose

There is continuing widespread interest in devices commonly called biosensors [1–4]. These devices are not true sensors in the strictest sense of the word [5,6]. Rather, they consist of selective chemical reagents immobilized at or near the surfaces of true sensors such as electrodes [7–9] or on components such as optical fibers [10,11] that are parts of true sensor systems. Thus, the primary sensor responds to chemical changes that are forced to take place in a confined space rather than in the bulk of the solution as is the case with more conventional measurement approaches. Because these devices have the chemical reaction and measurement functions [12] combined into single units, they are more properly identified as reactor–sensor devices than as sensors alone.

Correspondence to: H.L. Pardue, Department of Chemistry, Purdue University, 1393 BRWN Building, West Lafayette, IN 47907-1393 (USA).

These observations have more than semantic significance. There are consequences of confining the chemical reaction and measurement functions into small spaces that impose performance characteristics on these devices that are very different than the characteristics of true sensors [5,6] used in the more conventional mode. This paper describes the first step of a longer-range study intended to use alternative measurement and data-processing approaches to improve a variety of performance characteristic of these so-called biosensor devices.

One consequence of confining the chemical reaction function into a small space is that the response times of the devices are frequently controlled by mass transfer and/or slow chemical reactions and consequently the response times of these devices are frequently much longer than for true sensors. Although some investigators have attempted to overcome this problem by measuring rates of approach to steady state [13], most

applications of these devices have involved measurements of steady-state responses [1–3,7–11]. Accordingly, measurement times are often much longer than those of the primary sensors used in the more conventional mode.

This paper describes results for an alternative measurement and data-processing approach that combines some of the attractive features of both the rate and steady-state approaches. In this alternative approach, transient data measured early in the response times are used with suitable models and curve-fitting methods to predict the signals that would be measured if the responses were monitored to steady state. This approach combines the higher speed of rate methods [13] with the higher sensitivity of steady-state methods. The new approach was evaluated for a glucose-selective reactor–sensor device consisting of glucose oxidase and an electron mediator immobilized on the surface of a glassy-carbon electrode with amperometric detection [8,9].

Results obtained with this predictive method are compared with measured values of steady-state signal.

EXPERIMENTAL

All solutions were prepared in deionized water that had been previously distilled and all reagents were used as received.

Reagents

Reagents used were glucose oxidase (EC 1.1.34, Type II, 25 000 units g^{-1}, Sigma, St. Louis, MO), sodium 4-(2-hydroxyethyl)-1-piperazineethanesulfonate (HEPES, Aldrich, Milwaukee, WI), polyethylene glycol (PEG, MW 400 diglycidyl ether, Polysciences, Harrington, PA). The oxidation/reduction polymer {poly[(vinylpyridine)Os $(bpy)_2$ $Cl^{2+/3+}$]/polyamine} was synthesized as described earlier [8,14]. Glucose (cat. no. G-5250, Sigma) solutions were prepared and diluted in an aqueous phosphate (20 mmol l^{-1}) buffer (pH 7.1) containing sodium chloride (100 mmol l^{-1}). These solutions were stored at 4°C for at least 24 h before being used.

Reactor–sensor device

The reactor–sensor device consisted of the glucose oxidase and electron mediator [Os-(II/III)] immobilized on the surface of a glassy-carbon electrode (3 mm diameter, Bioanalytical Systems, West Lafayette, IN). Solutions of glucose oxidase (2 g l^{-1}) and oxidation/reduction polymer (4 g l^{-1}) were prepared in HEPES buffer (10 mmol l^{-1}, pH 8.2) and a solution of PEG (2.3 g l^{-1}) was prepared in water. These solutions were mixed to give a final solution containing 18.3% glucose oxidase, 8.4% PEG and 73.3% polymer. This solution was coated onto the surface of the electrode and permitted to react as described earlier [8,9].

Instrumentation

The reactor–sensor device was characterized by using scanning voltammetry (100 B Electrochemical analyzer, Bioanalytical Systems). Time-dependent responses of the device in the presence of glucose were made with custom-designed circuitry consisting of a low-impedance, variable-voltage source, current offset control, current-to-voltage conversion and a variable-gain voltage amplifier with gain settings ranging from 0.01 to 10 V μA^{-1}.

The output voltage was digitized (LAB Master, Scientific Products, Cleveland, OH) and stored on-line with a microprocessor (AT&T PC 6300, Iselin, NJ) equipped with 640 kilobytes of random access memory, a math coprocessor, and a 40-megabyte hard disk. Data were transferred from the microprocessor to a supermicro computer data station (MC 5500, Massachusetts Computer, Westford, MA) for long-term storage, processing and display. The computer system has been described elsewhere [15].

Mathematical models

Three models were evaluated in this study. One model [16] based on diffusion-limited rate processes was used in the form

$$S_t = S_0 + (S_\infty - S_0) \times \left\{ 1 + 2 \sum_{i=1}^{n} (-1)^i \exp\left[-i^2 \Pi^2 (t - t_0)/\tau \right] \right\} \quad (1)$$

where S_t, S_0, and S_∞ are the signals at times t, 0, and ∞, and i is a dummy variable, τ is the characteristic diffusion time, and n is an arbitrary number representing the number of exponential terms included in the series. We included eight terms in this study.

A second model assumes Michaelis–Menten behavior and has been described in detail elsewhere [17]. The third model assumes two parallel-first-order processes and has also been described elsewhere [18,19].

All these models were implemented on the supermicro computer as described previously [15].

Procedures

All measurements were made on solutions controlled at 25°C in a water-jacketed, single-compartment electrochemical cell. Test solutions were covered at all times by a stream of nitrogen that had passed through a saturated solution of sodium sulfite to remove oxygen. An Ag/AgCl reference electrode was used and the gain setting on the detection circuitry was 2 V μA^{-1} for all studies. Solutions were stirred rapidly with a water-powered magnetic stirrer during all measurements of transient responses.

Prior to each run, the reactor–sensor device was immersed in a well-stirred blank buffer solution (20 ml) and as a precautionary measure, a potential was applied until anodic current decreased to a constant low value (ca. 0.05 μA). Then the polarizing voltage was changed to 0.38 V, data acquisition was started and the signal was monitored until it again decreased to a steady-state baseline (ca. 60 s) after which a glucose sample (5 ml) was added rapidly and data acquisition was continued until the response reached steady state (ca. 300 s) so that predicted values of steady-state responses could be compared to measured values.

RESULTS AND DISCUSSION

All uncertainties are quoted at the level of one standard deviation unit (± 1 S.D.). Glucose concentrations are quoted as those in the reaction mixture; concentrations in the sample were 5-fold higher than quoted values.

Response curves

Figure 1 includes a typical set of response curves for glucose concentrations between 0 and 30 mmol l^{-1} in the reaction mixtures. Zero time corresponds to the time at which glucose was introduced into the solution. All responses approach steady state monotonically but none, with the possible exception of that for the highest glucose concentration, reaches a true steady state during the 220-s observation period.

Estimates of measured values of steady-state current were obtained by averaging 30 data points between 190 and 220 s after sample introduction. Predicted values of steady-state current were obtained by fitting the models mentioned earlier to the data during the early part of each response.

Model selection

To evaluate the three models included in this study, we first fit each model to the full range of data collected (0–220 s). Figure 2A and B illustrates fits for two of the models. As shown in Fig. 2A, the diffusion-based model [16], with eight terms included does not fit the data very well. On the other hand, as shown in Fig. 2B, the two-component, parallel-first-order model [18,19], fits the data quite well. Similar fits were obtained for the Michaelis–Menten model [17].

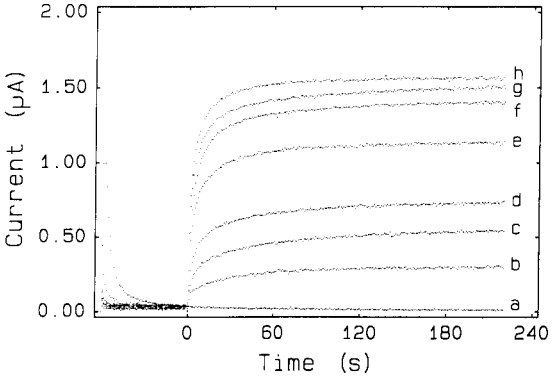

Fig. 1. Time-dependent response curves for different glucose concentrations. Concentrations: (a) 0; (b) 1; (c) 3; (d) 5; (e) 10; (f) 15; (g) 20; (h) 30 mmol l^{-1}.

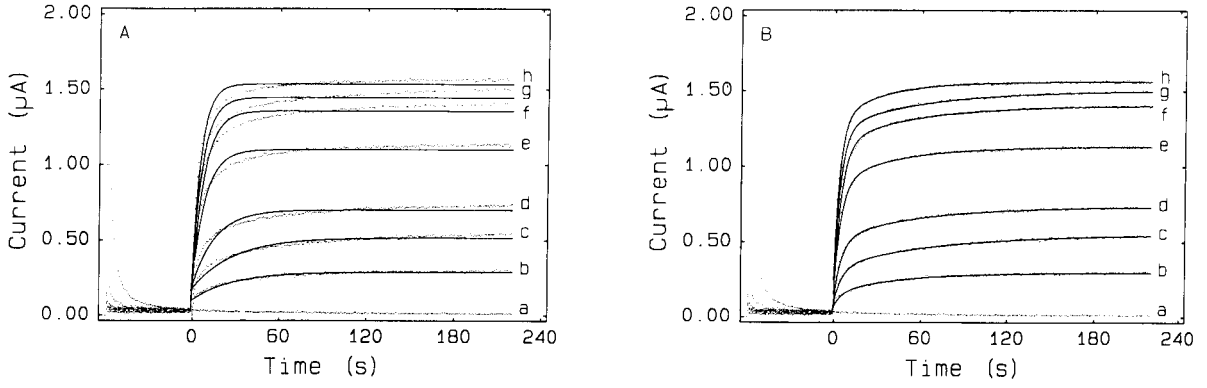

Fig. 2. Experimental and fitted responses for different glucose concentrations. Concentrations as in Fig. 1. (·····) Experimental; (———) fitted. (A) Diffusion-limited model; (B) Parallel-first-order model.

As a further test of the Michaelis–Menten model, initial rates were obtained from the data and Lineweaver–Burke plots were done. These plots (1/rate vs. $1/C$) were linear and yielded an apparent Michaelis constant of $K_m = 10$ mmol l^{-1}.

Although these results tend to favor the parallel-first-order and Michaelis–Menten models, the diffusion-based model was included in subsequent studies designed to compare predicted and measured values of steady-state current.

Predictive results

Goals here were to compare predicted and measured values of steady-state currents and relationships among glucose concentrations and predicted and measured values of steady-state current.

Predicted vs. measured currents. Figure 3 includes results from the diffusion-based (bottom plot) and parallel-first-order (top plot) models. Least-squares statistics for these plots are included in Table 1 for the 0–80-s fitting ranges for the two models. Analogous results for the Michaelis–Menten model and other fitting ranges are also given in the table. Of the three models tested here, the parallel-first-order model gives more ideal values of slopes (near unity), intercepts (near zero) and standard errors of the estimates than the other two models. Correlation coefficients are all close to unity.

These results tend to favor use of the parallel-first-order model.

Concentration dependencies. Figure 4 gives a comparison of plots of predicted and measured values of steady-state currents vs. concentration. As expected from discussions above, there are some differences. However, there is generally good agreement between the two data-processing approaches. Similar results were obtained for other fitting ranges.

In both cases, plots curve toward the concentration axis and the sensitivities approach zero at higher concentrations. However, measured and predicted currents for glucose concentrations between 1 and 10 mmol l^{-1} were approximately linear with concentration. To permit a more complete comparison of the different models, we

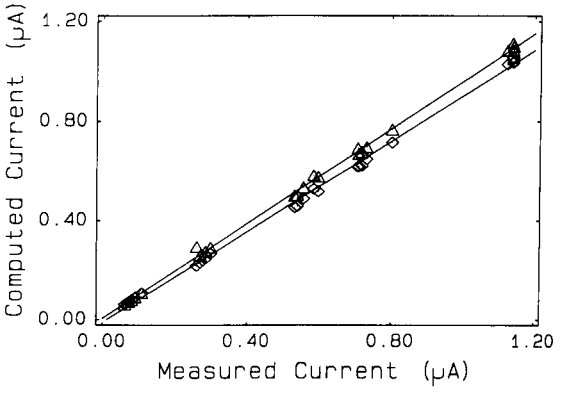

Fig. 3. Comparison of computed and measured steady-state currents. Measured currents are the average of 30 data points between 190 and 220 s. Models: (△) parallel-first-order and (◇) diffusion-limited fit over 0–80 s.

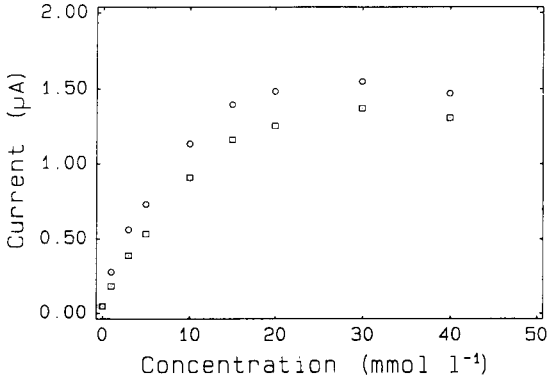

Fig. 4. Plots of predicted and measured currents vs. concentration. (○) Measured and (□) predicted (Michaelis–Menten model, 0–20 s fitting range).

performed linear least-squares fits of current vs. concentration (1–10 mmol l^{-1}) and have included the results in Table 2. The first row gives results for measured currents vs. concentration for comparison purposes.

Except for the fact that the parallel-first-order and the diffusion-based models did not give useful results for the 0–20 and 0–40 s fitting ranges respectively, there is little difference among the three models. Although the average slope for the parallel-first-order model is closer to that for measured data, there is more variation of the slopes for different fitting ranges than for the other models. Also, the standard errors of the estimates and correlation coefficients are slightly worse for this model than for the others. Actually, these statistics were expected to be degraded for all models because we are fitting a linear model to non-linear data.

Reproducibility

The last column in Table 2 includes pooled standard deviations for five replicates at each of eight concentrations. Except for the shortest fitting range with the parallel-first-order model, there is little difference in the reproducibilities among the different results. The standard deviations were somewhat smaller at lower concentrations than at higher concentrations. For example, at 1 mmol l^{-1}, standard deviations were only about 15 nA for both measured and predicted results. The most significant point here is not the magnitude of uncertainty but the fact that it is essentially the same for the predicted results as for measured results.

TABLE 1

Linear least-squares statistics for comparison of computed steady-state and measured [a] currents for several fitting ranges

Fitting range	Slope		Intercept (μA)		Standard error of estimate (nA)	Correlation coefficient (r^2)
	Value	S.D.	Value	S.D.		
Parallel-first-order model						
0–40	1.01	0.03	−0.008	0.02	51	0.984
0–80	0.956	0.008	0.006	0.005	14	0.999
0–120	0.980	0.003	0.004	0.002	5.3	> 0.999
0–140	0.991	0.003	0.004	0.002	4.5	> 0.999
Michaelis–Menten model						
0–40	0.864	0.02	−0.02	0.01	27	0.993
0–80	0.915	0.01	−0.01	0.007	18	0.997
0–120	0.938	0.007	−0.006	0.004	12	0.999
0–140	0.953	0.005	−0.003	0.003	8.2	> 0.999
Diffusion-limited model						
0–80	0.914	0.009	−0.01	0.006	17	0.998
0–120	0.938	0.006	−0.003	0.004	10	> 0.999
0–140	0.953	0.003	0.0007	0.002	6.1	> 0.999

[a] Average of 30 data points between 190 and 220 s.

Conclusions

The model for parallel-first-order processes gives the best fits of the full data range examined. Also the parallel-first-order model gives agreement between predicted and measured currents provided the fitting range is wide enough, but the Michaelis–Menten model gives satisfactory results for narrower fitting ranges. These differences notwithstanding, it appears that any of the three models can give results similar to those obtained by measuring steady-state currents directly. Moreover, this is achieved with a significant saving of time. For example, the minimum time used with the Michaelis–Menten model was 20 s whereas the time required to reach steady state is at least 220 s. This corresponds to a 10-fold reduction in measurement time with little or no loss of reliability. Although these conclusions are based on only one system, it is reasonable to expect that the general approach will apply equally well to other analogous systems if appropriate mathematical models are used. Moreover, if the data-processing algorithms were incorporated into an instrument system, they would be as transparent to the user as the direct-measurement mode in current use.

This study has demonstrated that transient responses from these types of detection devices can be modeled successfully. That is a critical first step in using these curve-fitting methods to solve some of the more serious problems associated with these devices such as the loss of sensitivity at high concentration (see Fig. 4) and large dependencies on experimental conditions such as en-

TABLE 2

Linear least-squares statistics for current vs. glucose concentration [a] for predicted and measured currents

Range	Slope (μA mmol^{-1} l)		Intercept (μA)		Standard error of estimate (nA)	Correlation coefficient (r^2)	Pooled S.D. [b] (nA)
	Value	S.D.	Value	S.D.			
Measured currents [c]							
0–220	0.0908	0.003	0.25	0.02	49	0.977	36
Parallel-first-order model							
0–40	0.0926	0.006	0.23	0.04	84	0.939	74
0–80	0.0866	0.003	0.25	0.02	45	0.978	37
0–120	0.0885	0.003	0.25	0.02	49	0.976	36
0–140	0.0894	0.003	0.26	0.02	49	0.976	36
0–220	0.0976	0.005	0.25	0.02	50	0.976	36
Average	0.0909	0.004					
Michaelis–Menten model							
0–20	0.0867	0.001	0.13	0.01	29	0.989	35
0–40	0.0838	0.002	0.16	0.01	35	0.986	35
0–80	0.0862	0.003	0.20	0.02	41	0.982	36
0–120	0.0871	0.003	0.22	0.02	43	0.980	36
0–140	0.0877	0.003	0.23	0.02	45	0.978	36
0–220	0.0882	0.003	0.23	0.02	46	0.978	36
Average	0.0866	0.0016					
Diffusion-limited model							
0–80	0.0859	0.003	0.20	0.02	41	0.981	36
0–120	0.0865	0.003	0.22	0.02	44	0.979	36
0–140	0.0871	0.003	0.24	0.02	46	0.966	36
0–220	0.0876	0.003	0.24	0.02	47	0.977	36
Average	0.0868	0.0007					

[a] Five replicate runs at each of four concentrations of glucose, from 1 to 10 mmol l^{-1}. [b] Five replicate runs at each of eight concentrations of glucose, from 1 to 40 mmol l^{-1}. [c] Average of 30 data points between 190 and 220 s.

zyme activity, inhibitors, activators and temperature. We are currently extending these studies to address and hopefully solve some of these problems.

This work was supported by Grant No. GM 13326-24 from the National Institutes of Health.

REFERENCES

1 J.E. Frew and H.A.O. Hill, Anal. Chem., 59 (1987) 933A.
2 F. Scheller, F. Schubert, D. Pfeiffer, R. Hintsche, I. Dransfeld, R. Renneberg, U. Wollenberger, K. Riedel, M. Pavlova, M. Kühn, H. Müller, P.M. Tan, W. Hoffmann and W. Moritz, Analyst, 114 (1989) 653.
3 J. Janata, Anal. Chem., 62 (1990) 33R.
4 M. Thompson and U.J. Krull, Anal. Chem., 63 (1991) 393A.
5 J.M. Hawkins and R. Allen (Eds.), The Oxford Encyclopedic English Dictionary, Clarendon Press, Oxford, 1991, p. 1321.
6 D.B. Guralink (Ed.), Webster's New World Dictionary of the American Language, Simon and Schuster, New York, 2nd College Edition, 1980, p. 1297.
7 P.N. Bartlett and R.G. Whitaker, Biosensors, 3 (1987/88) 359.
8 B.A. Gregg and A. Heller, J. Phys. Chem., 95 (1991) 5970.
9 B.A. Gregg and A. Heller, J. Phys. Chem., 95 (1991) 5976.
10 F.V. Bright, T.A. Betts and K.S. Litwiler, Anal. Chem., 62 (1990) 1065.
11 B.P.H. Schaffar and O.S. Wolfbeis, Biosens. Bioelectron., 5 (1990) 137.
12 H.L. Pardue and J. Woo, J. Chem. Ed., 6 (1984) 409.
13 T. Schulmeister and F. Scheller, Anal. Chim. Acta, 170 (1985) 279.
14 P.A. Lay, A.M. Sargeson and H. Taube, Inorg. Synth., 24 (1986) 291.
15 J.W. Skoug, W.E. Weiser, I. Cyliax and H.L. Pardue, Trends Anal. Chem., 5 (1986) 32.
16 B. Olsson, H. Lundback, G. Johansson, F. Scheller and J. Nentwig, Anal. Chem., 58 (1986) 1046.
17 S.D. Hamilton and H.L. Pardue, Clin. Chem., 28 (1982) 2359.
18 J.B. Landis and H.L. Pardue, Clin. Chem., 24 (1978) 1700.
19 B.G. Willis, W.H. Woodruff, J.R. Frysinger, D.W. Margerum and H.L. Pardue, Anal. Chem., 42 (1970) 1350.

Analytica Chimica Acta, 281 (1993) 557–568
Elsevier Science Publishers B.V., Amsterdam

Integrated enzyme reactor/detector for the determination of multiple substrates by image analysis

Glenn B. Martin and Garry A. Rechnitz

Hawaii Biosensor Laboratory, Department of Chemistry, University of Hawaii, Honolulu, HI 96822 (USA)

(Received 26th February 1992; revised manuscript received 8th September 1992)

Abstract

An image analyzer system was used to develop a multicomponent analysis method for enzyme substrates. Image analysis provides a technique which can spatially resolve closely spaced responses, thus allowing for the detection of multiple substrates with a single reactor/detector. For successful implementation of this method a procedure for immobilizing large amounts of enzyme activity onto a highly crosslinked polydextran support (> 300 U/ml gel) was devised. A microsized integrated reactor/detector (< 4.5 μl) was constructed by packing the insoluble enzymes into a small capillary. Using this new technique, the concentrations of mixtures containing glucose and glucose-6-phosphate (0–8 mM) were predicted using immobilized glucose oxidase and glucose-6-phosphate dehydrogenase.

Keywords: Image analysis; Spectrophotometry; Multicomponent analysis; Spatial resolution

Enzymatic methods are widely used in environmental, food and, especially, clinical analysis [1–4]. Commonly, immobilized or insolubilized enzymes are used in some type of flow system, such as flow-injection analysis (FIA), for analytical substrate determinations [5,6]. This analysis system relies on a two-step process; first the enzyme reactor converts the substrate to product and second the signal response is acquired in a separate detector. Simultaneous reaction and detection is of great interest and utility in analytical applications [1,7,8]. Several reports have been published which describe the use of various immobilized reagents and catalysts (like chromogenic reagents, luciferase, aminofluoranthrene and luminol) for utilization in systems which have integrated reaction and detection into a single step [9–17]. The predominant reasons for interest in this topic are the possibility of performing kinetic-based measurements and simultaneous multianalyte determinations.

Kinetic measurements achieve a faster analysis time and greater sensitivity, in many instances, in comparison to determinations made with an equilibrium method [1]. This is usually accomplished by discriminating against side reactions as well as extraneous signals of the blank or sample matrix [7]. The use of a stopped-flow technique, in conjunction with a reactor/detector, allows for the determination of the complete system time–response profile, with the rate being controlled by enzyme kinetics and associated diffusion processes.

The second important advantage of an integrated reactor/detector is the possibility for parallel, multiple analyte detection on a single sample. Many properties of the system response including temporal, spectral, chemical and spatial

Correspondence to: G.A. Rechnitz, Hawaii Biosensor Laboratory, Department of Chemistry, University of Hawaii, Honolulu, HI 96822 (USA).

can be the basis for signal discrimination between multiple analytes. Probably the most commonly applied methods of discrimination are the first three, which do not rely a priori upon the geometry of the reactor/detector. However, these three methods suffer from a lack of generality and separatory power [18]. Recently much interest has been expressed in the use of spatial resolution, by use of a charged coupled device (CCD), as a powerful method for component signal isolation [18,19]. The analyst is presented with the challenge of constructing the "reaction chamber" so that an array is amenable to CCD detection. The usual approach employs the use of photochemistry to control the reaction area on a solid substrate [18,19]. An alternative procedure for producing spatially separated reaction sites is to create each separately and then combine them in a suitable way for the desired analytical purpose.

The goal of our research, therefore, is to integrate the powerful analytical technique of enzymatic analysis with the spatial discrimination properties of the CCD to perform muticomponent analysis on a single sample aliquot. As a model system, two enzymes, glucose oxidase and glucose-6-phosphate dehydrogenase, were selected for use. By first separately immobilizing these enzymes onto polyamine-modified polydextran beads and then packing the beads together into a glass capillary, it is possible to construct a reactor/detector with spatially resolvable enzyme activities. This reactor/detector is then incorporated into a simple flow system and mounted under a microscope objective. With the aid of a CCD camera, a monitor and a video cassette recorder (VCR) the complete time–response profile of the system can be observed and recorded. The recorded data are then quantified with an image analyzer.

MATERIALS AND METHODS

Reagents

Sephadex G-25–300, nominal molecular weight (NMW) exclusion limit 5000 and G-150-120, NMW exclusion limit 150 000, were obtained from Sigma. Insoluble preparations of glucose-6-phosphate dehydrogenase, alcohol dehydrogenase, malate dehydrogenase, and lactate dehydrogenase, attached to polyacrylamide were purchased from Sigma. Glutaraldehyde (grade I), sodium borohydride, D-glucose-6-phosphate, β-D-(+)-glucose, malate, lactate, phenazine methosulphate (PMS), Leuconostoc glucose-6-phosphate dehydrogenase (G6PDH), poly-L-ornithine (average MW 154 000), nicotinamide-adenine dinucleotide (NAD), nicotinamide-adenine dinucleotide phosphate (NADP), and tris(hydroxymethyl)aminomethane were also purchased from Sigma. Dichloroindophenol (DCPIP) was obtained from Aldrich. Potassium periodate and hydrazine dihydrochloride came from Baker. Sodium dihydrogen phosphate dibasic, hydrogen chloride, sodium hydroxide, ethylene diamine (EDA), and borosilicate glass capillaries (0.7 mm i.d.) were from Fisher Scientific. Ethanol, 95%, came from Quantum. Glucose oxidase 6500 U/ml (GOx) was purchased from Biozyme Laboratories. Deionized water (> 16 Mohm cm) was used throughout all experiments.

Instruments and equipment

A Narishige, Model PP-83, pipet puller was used for that purpose. The injection valve used for the flow system was a Rheodyne 7000. A Reichart-Jung BioStar Series 1820 inverted microscope was used for magnification purposes. The camera, monitor and video cassette recorder (VCR) were a Model MTI-CCD72 from Dage, a PVM-1380 from Sony and a Model HR-D66OU from JVC, respectively. The image analyzer was the IBAS-II Image Analysis System (version 2.0) from Kontron (Munich).

Solutions

A 10 mM phosphate buffer of pH 8.0 and 100 mM in sodium chloride was used during activation, derivatization and immobilization procedures performed on the Sephadex gels. For the flow system experiments, the carrier stream consisted of a 50 mM Tris–HCl buffer of pH 8.0 and 100 mM in sodium chloride. This same buffer was used for making up substrate samples for injection into the reactor.

Oxidation and amine derivatization of polydextran

A 250 mg quantity of Sephadax was weighed out and hydrated in 10 ml of deionized water for at least 2 h. The gel was washed 2 times with deionized water and 2 times with buffer. The gel typically was suspended in 2–5 ml of pH 8 phosphate buffer and cooled for at least 20 min in an ice bath.

For the addition of potassium periodate, the quantity to be added was dissolved in the buffer by sonication. The periodate solution was added to the gel solution in 500-μl aliquots over several minutes while the gel was kept well agitated by bubbling argon gas into the vial. The mixture was allowed to react for 1 h. The gel was washed 3 times with 10 ml of deionized water aspirating off the excess solution each time.

The beads were derivatized with either hydrazine or an amine. For hydrazine derivatization, 90 mg of hydrazine dihydrochloride were dissolved in 2 ml of buffer. The pH of the solution was then adjusted to approximately 6.0 with 1 M sodium hydroxide. This solution was immediately added to the oxidized gel with continued agitation. After 2 h, the resulting imine bond was stabilized by reduction with approximately 5 mg of sodium borohydride. After reacting for 2 h at room temperature, the gel was washed 4 times with 5–10 ml of buffer and stored for future use.

For ethylene diamine derivatization, 300 μl of EDA were added to 5.0 ml of buffer and the pH was adjusted to 7 with 2 M HCl. Then 500 μl of the oxidized gel were pipetted into the solution. The rest of the procedure was the same as for hydrazine derivatization.

For polyornithine derivatization, about 15 mg of polyornithine were added directly to the oxidized gel. The rest of the procedure was the same as for hydrazine derivatization.

Attachment of enzyme via its carbohydrate moiety

Because glucose oxidase (GOx) is a glycoprotein, it can be immobilized through the carbohydrate moiety following oxidation by periodate [20]. Typically, 200 μl of 2 mg/ml of enzyme were oxidized with 0.5 mg of potassium periodate. This was accomplished by making up a GOx solution of 4 mg/ml in 100 μl of buffer. The enzyme solution is then cooled to 4°C. Potassium periodate is dissolved in buffer at a concentration of 5 mg/ml and 100 μl are added to the enzyme solution while stirring. Oxidation of the enzyme is allowed to continue for an hour or more.

A 250-μl aliquot of the washed derivatized polydextran beads was added to the enzyme solution and allowed to react for 3–4 h, without stirring. After this time, the imine bond was reduced by addition of about 2 mg of sodium borohydride. Typically, after 2 h the gel was washed and tested for enzymatic activity.

Attachment of enzyme via its amine groups

For attachment of enzyme through its primary amines the immobilization was carried out by cross-linking the derivatized beads and enzyme with glutaraldehyde. Buffer-washed derivatized beads (250 μl) were reacted with 100 μl of 25% glutaraldehyde. After 2 h, the beads were washed 4 times with buffer, and 150 μl of either a 0.8 mg/ml G6PDH solution or a 2 mg/ml GOx solution were added to the derivatized beads. This reaction is allowed to proceed for 2 additional hours, and then 2 mg of sodium borohydride is added to reduce the resulting imine bonds to stabilize the attachment.

Evaluation of biocatalytic beads

Biocatalytic beads prepared in this manner were then examined for the desired characteristics. First, the beads were examined for structural integrity by visual examination under a microscope. The degree to which the bead structure remained intact was readily observed. Second, a test for enzyme activity was undertaken. The beads were thoroughly washed with buffer and their immobilized enzyme activity was determined by pipetting a 10-μl sample of the gel into 200 μl of substrate cocktail, containing 200 μM PMS, 1.0 mM NAD or NADP and 400 μM DCPIP, and the disappearance of color was monitored. The insoluble enzymes obtained from Sigma were tested for activity in a similar manner. If the beads showed satisfactory catalytic activity, their flow characteristics were examined.

A syringe was used to suck the enzyme beads into a capillary tube. The DCPIP dye solution was injected into the capillary tube. It was easily apparent from the flow of the dye whether the interior of the bead was readily accessible or if the pores had been blocked by attachment of the enzyme.

Reactor / detector and flow system

The reactor/detector was fabricated by taking a capillary tube and narrowing one end by pulling a fine tip with the pipet puller. The tip was then filed to approximately a 0.5 mm i.d. opening. A small amount of polypropylene fiber was then inserted into the capillary from the end with the larger opening and compacted into the constricted end. Beads were then sucked into the capillary sequentially to form several different layers (both enzyme and non-enzyme) in the reactor. Finally, another small amount of fiber was inserted and forced against the beads to hold them in place. Care must be exercised in packing the capillary as it is critical that the beads be tightly packed so that no shifting or movement occurs during use in the flow system. The total volume of the reactor/detector was no more than 5 μl; see Fig. 1a.

The capillary reactor was next incorporated into the flow system. The flow system consisted of an injection valve, with a 100-μl sample loop, and a syringe to force the carrier stream through the system. The capillary was placed onto the microscope stage and secured into position with masking tape. The position of the stage could then be adjusted to bring the capillary into alignment with the microscope objective. The objective and camera together gave a magnification factor of 170 ×. A polypropylene sheet (4 × 4 cm) of 0.067 mm thickness was placed over the capillary to diffuse the light allowing for more even illumination thereby reducing shadowing occurring within the capillary. The image was brought into focus and the light intensity was adjusted so that the image analyzer gave a reading of ca. 240 greyscale

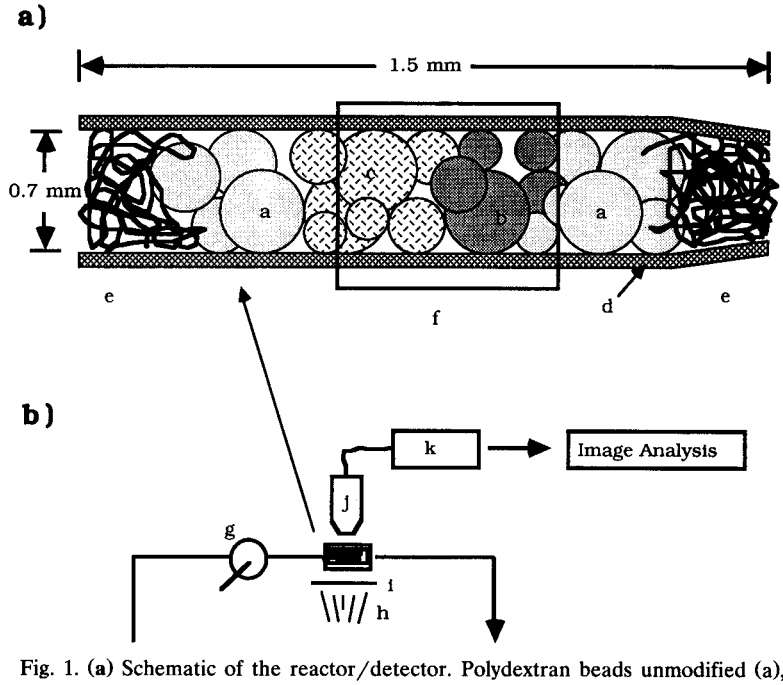

Fig. 1. (a) Schematic of the reactor/detector. Polydextran beads unmodified (a), and with GOx (b) or G6PDH (c) attached are closely packed into a capillary tube (d). The beads are held in place with polypropylene fibers (e). Only a section of the capillary (f) is captured for image analysis. (b) Schematic of the flow system and image recording equipment. The set-up consists of a sample injector (g), light source (h), diffuser (i), CCD camera (j) and VCR (k).

units at its brightest part. With the CCD camera mounted onto the microscope the image could simultaneously be displayed on the monitor and recorded on video cassette tape; see Fig. 1b.

Sample preparation and injection

A 50 mM Tris–HCl buffer of pH 8.0 and 100 mM in sodium chloride was used throughout for preparation of samples and as the carrier stream. Samples were prepared by first making stock solutions of the two substrates, glucose and glucose-6-phosphate as well as the reaction/detection cocktail containing PMS, DCPIP, and NAD. The stock solutions were then combined and diluted with buffer so that samples had a substrate concentration ranging from 0 to 8 mM with each containing 200 μM PMS, 825 μM DCPIP and 1020 μM NAD.

Initially, separate injections of each substrate (8 mM) were made to determine the location of the G6PDH and GOx beads. The reactor/detector was then aligned so that both types of enzyme beads were observable at the same time. Sampling was done sequentially in 3 steps, i.e. injection, reaction and flush. The injection step took approximately 30 s with about 170 μl being pushed through the capillary. With a 100-μl volume between the injector and the capillary, approximately three quarters of the sample passed through the reactor/detector by the completion of the injection step. The injection was halted to allow enzyme catalysis under quiescent conditions. Upon completion of the injection step, recording of the system–response profile was begun. After 210 s, recording was stopped and the system was flushed with about 1.5 ml of carrier buffer. The system was then ready for injection of the next sample. This 3-step sequence could be carried out in about 5 min.

Image analysis

Once all the samples had been injected, the video taped images were analyzed to determine the system–response profile for each sample. For image processing the video tape was replayed, and at the appropriate time an image was imported and digitized by the image analyzer. Objects (small areas of the image) are then located

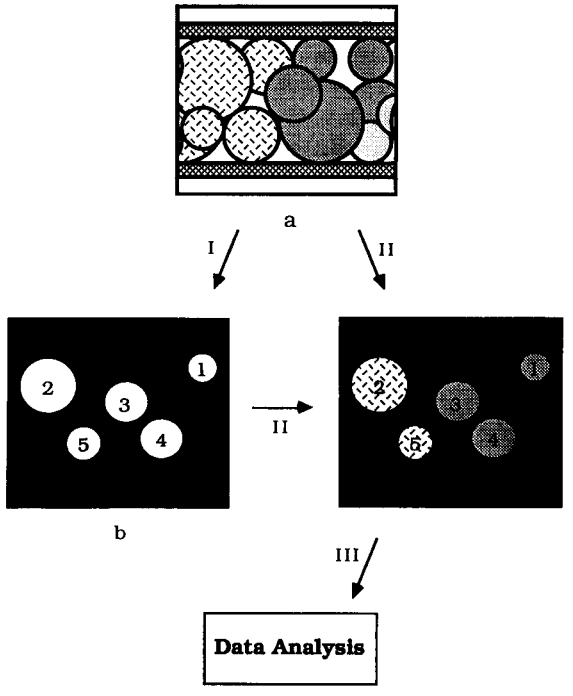

Fig. 2. Illustration of the image analysis procedure. A selected video image (a) is imported into the analyzer and digitized. In the first step (I) a mask (b) is created by defining the areas, i.e. objects (1–5), for which the greymean and associated standard deviation is to be calculated. The mask is layed over each new imported image to be analyzed (II). The instrument then calculates the greymean and standard deviation for each object of the image (III).

either automatically or with a user-interactive subroutine. For analysis of the reactor/detector images a mask was created; the mask consisted of circular objects which were positioned over regions where shadowing was minimal. This usually meant that an object was located completely within an individual bead or in an area where there was substantial overlap between two beads. Once all the objects have been defined, the instrument creates a mask which is layed over each imported image. The instrument can then calculate the greymean (proportional to the inverse of the absorbance on a scale of 0–256) and standard deviation for each object of every image; see Fig. 2. Further information on image analysis can be found in Ref. 21.

Following creation of the mask, it was necessary to determine the appropriate time to quan-

tify the system response for the various samples. This was done by following the system profile when 8 mM glucose was injected into the reactor/detector; see Fig. 3. Because the supply of $DCPIP_{ox}$ began to be depleted at times longer than 105 s, this was the optimal time for determining the response profile for all samples. An initial "blank" reading was also obtained for each sample 5 s after completion of the sample injection step.

RESULTS AND DISCUSSION

Insoluble enzyme properties

In our work, the solid support that was selected had to fulfill a number of criteria, the most important property being good optical transparency. This requirement disqualified all opaque supports. Other considerations included a well defined shape, particle size, mechanical strength, and ease of derivatization. The defined shape and particle size requirements are important because of the multicomponent detection scheme, which relies upon the utilization of an image analyzer. Little compression or expansion of the support should occur during operation of the FIA system because this interferes with the reproducibility of repeated image analyses on the capillary reactor. Either a polysaccharide or polyacrylamide support, therefore, is a natural choice because these types of materials meet all of the requirements stated above and in addition have some other advantages. Polyacrylamide has a large number of carboxamide groups available for attachment while polysaccharides are efficiently and safely activated by oxidation with periodate which introduces aldehyde functional groups [22]. Also, these two types of support have low non-specific adsorption, good stability, and freedom from microbial attack. Finally, the remaining carboxamide groups on polyacrylamide and the residual hydroxyl groups of derivatized polysaccharide impart a non-ionic hydrophilic environment which protects the attached protein [23].

The enzyme immobilization procedure also must meet a number of specific needs. These include maintaining the good optical properties

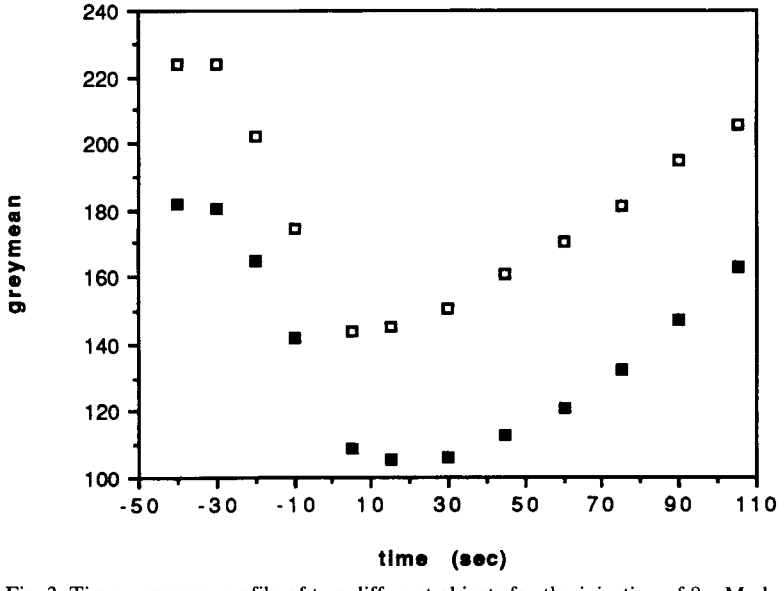

Fig. 3. Time–response profile of two different objects for the injection of 8 mM glucose. The sample injection step begins at −30 s and is completed at 0 s by stopping the flow. Enzyme catalysis then takes place under quiescent conditions. Linear response is observed until at least the 105 s mark, the time at which response data was collected for all samples.

and flow characteristics of the support and yet, at the same time, loading the support with a large amount of enzyme activity. To accomplish these goals it is important that any method selected for the attachment of the enzyme does not severely alter the spherical structure or the flow characteristics of the polydextran. Even though these characteristics seem to be easily obtainable in theory, in practice close attention to detail is necessary to achieve superior performance. Initial immobilization attempts were made with larger pore, lightly cross-linked, polydextran. However, this material proved to have a structure that is quite sensitive to the amount of amine derivatization. With smaller pore, highly cross-linked polydextran, the amount of amine attachment is much less critical, but due to the lack of access of the interior of the beads by large macromolecules (> 5000 MW), problems of low enzyme loading had to be overcome by utilization of a macromolecular spacer arm [24].

Large-pore polydextran

With oxidation of more than 1 μmol of periodate per 25 mg of G-150–120 Sephadex, the gel structure is destroyed by attachment of ethylene diamine. This is probably due to the introduction of large numbers of closely packed positively charged groups. Interestingly, this effect is not observed upon derivatization with hydrazine even at oxidation with up to 52 μmol periodate per 100 mg gel. Glucose oxidase coupled to hydrazine derivatized gel, either through the carbohydrate moiety or available amines, showed a high amount of enzyme activity (300–600 U/ml of gel). With the molecular weight of GOx being greater than the 150000 nominal molecular weight exclusion limit of this polydextran, low enzyme loading might be expected; nevertheless, a large amount of GOx is immobilized perhaps due to the opening of the pores by periodate oxidation. This allows GOx to penetrate into the gel interior and gain access to many more anchoring sites than are available on the surface of the beads. Because large-pore polydextran GOx beads exhibited significant back pressure due to the flaccidity of this enzyme gel, they proved to be unsuitable for use in the packed-capillary reactor/detector.

Insoluble enzymes from Sigma

Although immobilized enzymes are commercially available, our experience has been that they do not necessarily have the characteristics desirable for this particular application. In this case, the insoluble enzymes purchased from Sigma had much the same flow characteristics as the large-pore biocatalytic beads synthesized in our laboratory but with much lower enzyme activity than our polyornithine derivatized small-pore beads. In addition, the polyacrylamide support used for these insoluble enzymes proved to be opaque.

Small pore polydextran

The Sephadex preparation G-25-300 behaved much differently than the large pore polydextran. First, because this gel is highly cross-linked, it can withstand oxidation on the order of 400 μmol periodate per 100 mg of gel. Second, its structural integrity was maintained upon derivatization with ethylene diamine, polyornithine as well as hydrazine. In initial experiments, hydrazine and ethylene diamine were used to derivatize the gel. Because the pore size is significantly smaller than the size of the enzyme, it was expected that a lower amount of enzyme loading would be effected. It was hoped that perhaps enough enzyme would be immobilized for use in the reactor/detector. Unfortunately, both direct attachment of oxidized GOx and glutaraldehyde cross-linking failed to bind enough enzyme for our purpose; immobilized activity was only about 1 U/ml gel.

We reasoned that a long spacer, with multiple functional groups, would be superior for coupling a protein to these small pore beads. The approach, then, was to hyperaminate the bead, especially the exterior, by reacting the periodate-oxidized beads with a solution of polyornithine. This produced a sort of "fuzzy" bead, with a polydextran core, impenetrable to large macromolecules, but with an exterior coating which can bind copious amounts of protein. Multipoint attachment of the spacer and the protein, more likely with polyfunctional spacers, substantially increases the stability of the immobilization [22]. A further advantage of this method is that the attached protein is not firmly affixed to the bead and probably tends to dangle away from the bead

surface. This is ideal for our purposes because solution can easily flow around the enzyme and into the interior of the gel. Thus, it is predicted that even though the enzyme is tethered to a macroscopic particle, its properties probably closely resemble those of the free enzyme. An additional bonus with the small-pore polydextran was the unexpected uptake of DCPIP by the beads due to a weak interaction of the dye with the dextran matrix. This allowed for use of much lower dye concentrations than were anticipated and significantly increased the color changes observed. These beads were ideal in fulfilling our criteria of high biocatalytic activity while maintaining the structure and flow properties of the original underivatized polydextran support.

Colorimetric detection of enzyme activity

Both flavoenzymes (many oxidases) and dehydrogenases can be detected colorimetrically by linking the enzyme to a suitable redox dye. Phenazine methosulfate (PMS) is commonly used as an electron shuttle between either reduced $FADH_2$, NADH or NADPH and DCPIP as illustrated below.

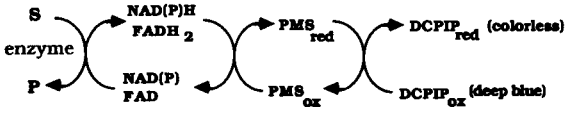

Although reduced glucose oxidase and PMS readily transfer electrons to molecular oxygen, reduced DCPIP does not, and it therefore is not necessary to exclude oxygen from the system. Because of the generality of this colorimetric scheme, it is ideal for this application as it would be nearly impossible to use more than one or possibly two detection methods for the determination of all the different enzymes incorporated into a reactor/detector.

Reactor / detector

As mentioned earlier, it is important that the beads within the capillary are tightly packed; if they are not, the beads can shift in two different ways. In the first, beads can shift en masse but still maintain their relative positions. If this occurs and the shift is not too large, it is still possible to use the system response obtained for new samples; however, a new mask must be created to assure that the objects overlay the same beads as in previously analyzed images. The second type of shift is one where the beads move relative to one another. If this occurs it is impossible to continue, the data already obtained can only be discarded, and the system response must be recalibrated with a new mask.

Another important consideration in constructing the reactor/detector is in the relative and absolute activities of the various immobilized enzyme beads. Because the various enzyme responses are to be spatially resolved it is important that the rate of substrate conversion be fast enough so that the reaction time is short compared to the time needed for diffusion of reduced DCPIP to adjacent beads. This way "crosstalk", i.e. smearing of the individual bead responses, is kept to a minimum. In addition, it was determined that the forced convection during the well defined sample injection mode makes only a small contribution to the overall time–response profile in this stopped flow system. It has been our experience that when the system response is measured within 4 min from the time of injection smearing of the response is not a major concern.

Calibration and validation of the system response

To demonstrate how well the reactor/detector could estimate the concentration of the substrates for various sample mixtures, a system response profile was obtained for both a "training" set and a "validation" set of substrate samples. The "training" set was used to calibrate the system response for the two substrates, glucose and glucose-6-phosphate, as well as for an interferent, ethanol. Once this was accomplished, the "validation" set samples were analyzed, and the estimated concentration is compared to the known concentration.

Data analysis

To analyze the data, the difference between the blank and response reading was recorded for each object. This net response was then standardized by adjusting all responses of each object by

the same amount, which gave the lowest response a value of zero. Objects 1, 7 and 8 showed responses that were linearly dependent on glucose concentration throughout the concentration range used, whereas objects 2, 5, 6 and 9 showed responses that approached saturation values for the G6P concentrations used. Figure 4a depicts the net glucose (objects 1 and 8) and G6P (objects 5

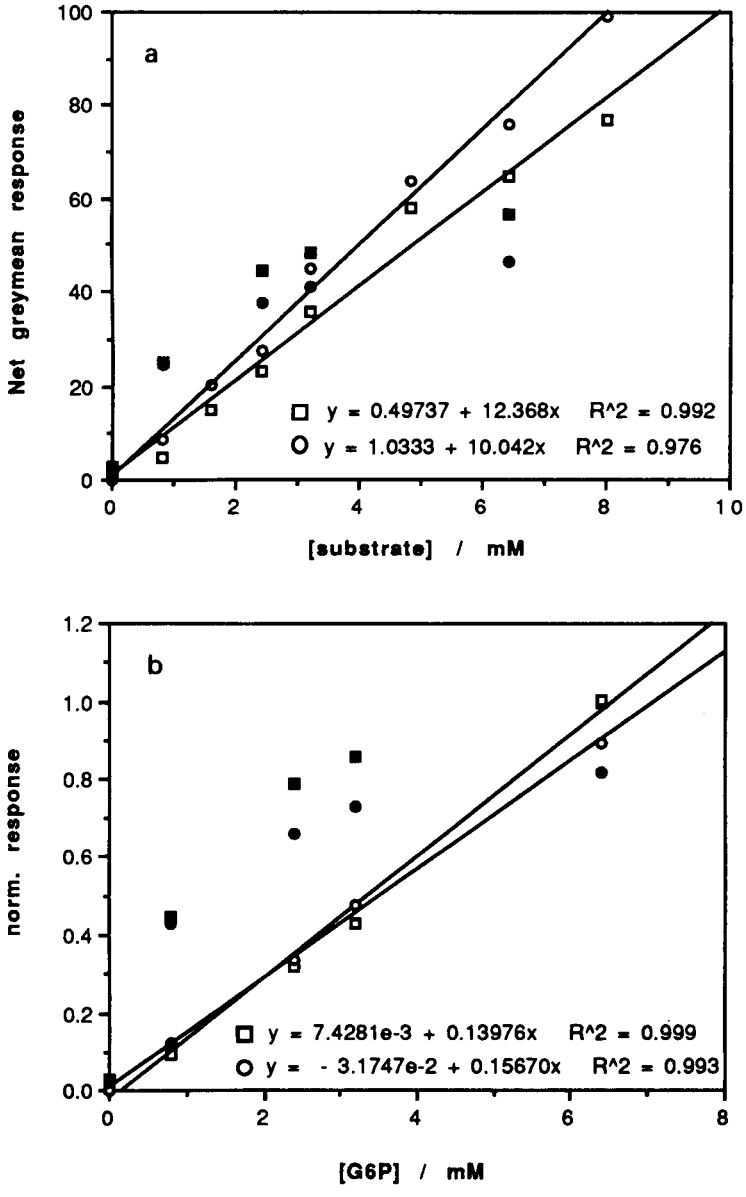

Fig. 4. (a) Net response for glucose and G6P after blank correction and zeroing each object. The glucose objects (□, ○) exhibited linear response for the whole concentration range and, therefore, could be used directly for determining the glucose concentrations for the "validation" sample mixtures. The G6P response (■, ●), however, was not linear, but instead it exhibited saturation behavior. (b) Linear transformation (□, ○) of the G6P response (■, ●). The transformed response showed good linear behavior and was used to predict the G6P concentrations for the "validation" sample mixtures.

and 9) responses obtained for the training set samples and Fig. 4b shows the normalized linear transforms of the normalized net G6P responses. Therefore, although linear regression could be performed directly on the glucose data without further manipulation, this was impossible to do with the G6P data. It was possible to first linearize the G6P data by performing a Reiner transformation [1]:

$$r_{lin} = (r/R_{max})/(1 - r/R_{max})$$

r = measured response and R_{max} = maximum response.

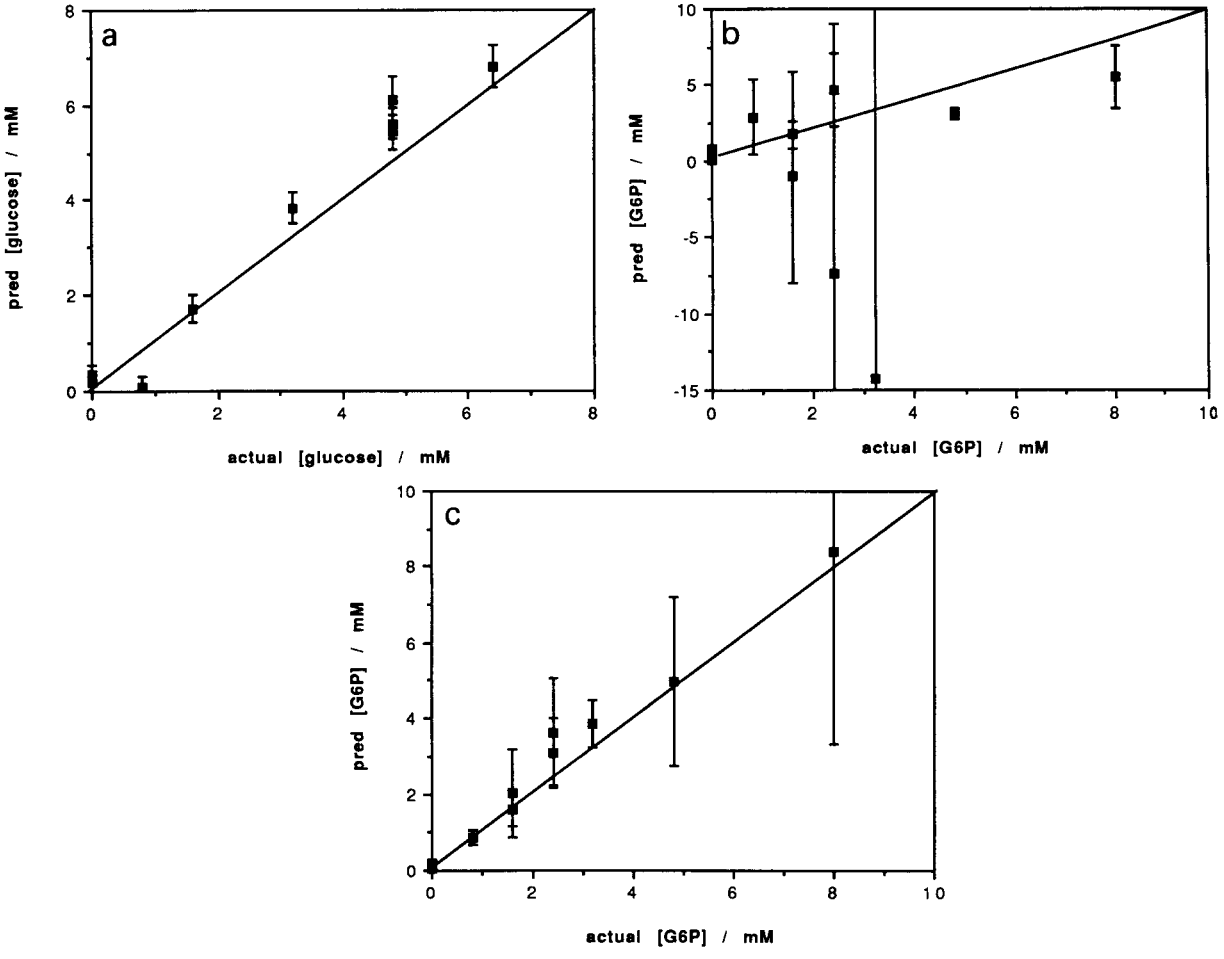

Fig. 5. (a) Predicted glucose concentrations compared to the actual glucose concentration for the "validation set" of samples. The predicted values are the average of 4 objects and the error bars represent 1 S.D. (b) Predicted G6P concentrations, not corrected for glucose interference, compared to the actual G6P concentrations for the "validation" samples. The predicted values are the average of 3 objects and the error bars are for 1 S.D. The negative predicted values are due to a large glucose interference which causes the response to be greater than the maximum response attributable to G6P (R_{max}). (c) Predicted G6P concentrations, corrected for glucose interference, compared to the actual G6P concentrations for the "validation" samples. The predicted values are the average of 3 objects and the error bars are for 1 S.D. The large imprecision seen at the higher G6P concentrations is due to responses near the maximum response for G6P (R_{max}) where small changes in the response correspond to large changes in concentration.

The R_{max} value was chosen so that the transformed data are as linear as possible over the G6P concentration range used and is indicative of the maximum G6P response obtainable for this system.

A particular object's response reflected one of four different possibilities. These are: either only a glucose or a G6P response, a combination of glucose and G6P responses, or no response to either substrate. Analysis of the training set data suggested that the responses that occurred were of the glucose only and the G6P/glucose combination types. That is to say that when a mixture of glucose and G6P was injected, some objects (1, 7 and 8) showed a response which was dependent upon only the sample's glucose concentration, while other objects (2, 5, 6 and 9) exhibited a response which was dependent upon both the concentration of glucose and G6P in the sample. Pure ethanol samples gave no response and thus caused no direct interference.

Figure 5a shows the predicted versus actual concentrations for the validation set when the training set was used to determine the linear regression response for objects 1, 7 and 8. The correlation between the predicted and actual glucose values is reasonable for most validation samples. Figure 5b shows the predicted versus actual concentration of glucose-6-phosphate for the validation set when the training set was used to determine the linear regression for objects 2, 5, 6, and 9. Obviously, the prediction is not very good as can be seen by the large standard deviations and the prediction of negative G6P concentrations. The negative values arise from a sample response, where the measured response was greater than that of the maximum response (R_{max}) used to linearize the response. Therefore, a negative value for the G6P prediction indicates that a large component of the response can be attributed to glucose.

To improve prediction of the G6P concentration, it was necessary to first adjust the response of a sample by subtracting the glucose response associated with that sample. This is done by first taking the predicted glucose concentration for that sample and calculating the response that can be attributed to it for objects 2, 5, 6 and 9. This calculated response was then subtracted from the objects' total response to produce a net response which was attributed to only the G6P present in the sample. These net responses can then be linearized and used to predict the G6P concentration. As can be seen in Fig. 5c, the G6P prediction is markedly improved, the correlation with the actual value being quite good. These results are comparable to the glucose prediction in both precision and accuracy except at the highest G6P concentration. This value has a large uncertainty due to the response being quite close to the maximum response for G6P. Decreased precision is observed at high substrate concentrations because only a small change in the response is associated with a large change in the concentration.

Conclusion

The concept of performing muticomponent enzyme analysis with a combination reactor/detector is demonstrated. By immobilizing the enzymes in an appropriate manner, suitable for spatial resolution by image analysis, it is possible to determine a number of substrates (analytes) simultaneously. The versatility of this approach may be limited by the usual constraints found with other multienzyme methods, such as pH dependence, buffer compatibility, comparable K_ms, etc. These constraints can usually be overcome by adjustment of the immobilized enzyme activity. Other constraints involving the use of simultaneous analysis are the compatibility of the reagents required to report enzyme activity, although separate parallel reactors/detectors could be used for analysis with incompatible detection schemes. In addition, high enzyme activities are required i.e. > 100 U/ml. These last two limitations could be significantly reduced if a diffusion barrier could be erected between the various enzyme sites to limit "crosstalk" between the individual responses. Additionally, because a sample injection cycle could be typically only completed in 5 min, improvement in sample throughput should be considered. Improvement in reactor/detector design to decrease signal smearing and allow for greater sample throughput should be feasible. The "pearls-on-a-string"

type reactor appears quite suitable for this purpose [5].

Although it was possible to predict G6P concentrations, data analysis was somewhat less than straightforward due to non-linearity of the response, which results from the fact that G6P responses were above $R_{max}/2$. Data analysis could be significantly simplified if all responses were within the linear response range so that standard chemometric analysis, such as partial least squares, would be applicable to the data.

Glenn Martin would like to express appreciation to Todd Q. Barker, Alan K. Hauser and Mark H. Smit for fruitful discussions and comments. Also, the assistance of Marilyn Dunlap is greatly appreciated for the many patient hours of assistance with the image analysis. The authors would like to acknowledge the National Science Foundation (Grant CHE-8921156) for financial support.

REFERENCES

1 G.G. Guilbault, Analytical Uses of Immobilized Enzymes, Marcel Dekker, New York, 1984.
2 J. F. Lawrence (Ed.), Trace Analysis, Vol. 3, Academic Press, Orlando, 1984, p. 31.
3 P.W. Carr and L.D. Bowers, Immobilized Enzymes in Analytical and Clinical Chemistry, Wiley, New York, 1980.
4 H.H. Weetall, Anal. Chem., 46 (1974) 602A.
5 M. Valcarcel and M.D. Luque de Castro, Flow Injection Analysis. Principles and Applications, Wiley, New York, 1987.
6 J. Ruzicka and E.H. Hansen, Flow Injection Analysis, Wiley, New York, 2nd. edn., 1988.
7 P. Linares, M.D. Luque de Castro and M. Valcarcel, Anal. Chim. Acta, 230 (1990) 199.
8 R.Q. Thompson and S.R. Crouch, Anal. Chim. Acta, 144 (1982) 155.
9 F. Lazaro, M.D. Luque de Castro and M. Valcarcel, Anal. Chim. Acta, 214 (1988) 217.
10 K. Yosimura, Analyst, 133 (1988) 471.
11 K. Yosimura, Bunseki Kagaku, 36 (1987) 656.
12 F. Lazaro, M.D. Luque de Castro and M. Valcarcel, Anal. Chim. Acta, 219 (1989) 231.
13 P.J. Worsfold and A. Nabi, Anal. Chim. Acta, 179 (1986) 307.
14 A. Nabi and P.J. Worsfold, Analyst, 111 (1986) 1321.
15 A. Nabi and P.J. Worsfold, Anal. Proc., 23 (1986) 415.
16 G. Gubitz, P. Van Zoonen, C. Gooijer, N.H. Velthorst and R.W. Frei, Anal. Chem., 57 (1985) 2071.
17 K. Hool and T.A. Nieman, Anal. Chem., 59 (1987) 869.
18 S.M. Barnard and D.R. Walt, Nature, 353 (1991) 338.
19 S.P.A. Fudor, J.L. Read, M.C. Pirrung, L. Stryer, A.T. Lu and D. Solas, Science, 251 (1991) 767.
20 H. Hsiao and G.P. Royer, Arch. Biochem. Biophys., 198 (1979) 379.
21 L.A. Lavia, Biotechniques, 7 (1989) 9.
22 R. Axen and J. Porath, Nature, 210 (1966) 367.
23 R.F. Taylor (Ed.), Protein Immobilization. Fundamentals and Applications, Marcel Dekker, New York, 1991.
24 I. Parikh, S. March and P. Cuatrecasas, in S.P. Colowick and N.K. Kaplan (Eds.), Methods Enzymol., 34 (1974) 77.

Analytica Chimica Acta, 281 (1993) 569–576
Elsevier Science Publishers B.V., Amsterdam

Electrochemical transduction of the acetylcholine–acetylcholinesterase reaction by bilayer lipid membranes

Dimitrios P. Nikolelis and Manolis G. Tzanelis

Laboratory of Analytical Chemistry, Department of Chemistry, University of Athens, Panepistimiopolis, Kouponia, GR 157 71 Athens (Greece)

Ulrich J. Krull

Chemical Sensors Group, Department of Chemistry, Erindale Campus, University of Toronto, 3359 Mississauga Road North, Mississauga, Ontario L5L 1C6 (Canada)

(Received 31st July 1992; revised manuscript received 14th October 1992)

Abstract

This work reports the transduction of the reaction of the enzyme acetylcholinesterase (AChE) with acetylcholine (ACh) as a model to demonstrate how transient electrochemical signals from bilayer lipid membranes can be obtained by appropriate selection of the lipid composition of membranes. Membranes were prepared from mixtures of egg phosphatidyl choline (PC) and dipalmitoyl phosphatidic acid (DPPA) for this purpose. Hydronium ions generated by the enzymatic reaction at the surface of BLMs caused a transient current due to a dynamic alteration of the electrostatic fields at the surface of such membranes. The results were consistent with an electrostatic mechanism of perturbation of the surface structure of the BLMs, where changes of local hydronium ion activity which were associated with the enzymatic reaction altered the extent of ionization of the headgroups of the DPPA, thereby providing a transient charging current which lasted for a period on the order of seconds. The delay time for observation of the transient was directly and reproducibly related to the concentration of the substrate, which could be determined over a range of μM to mM levels. Investigation of the effects of solution pH, the presence of Ca^{2+} and the use of the enzyme inhibitor Neostigmine confirmed that the response was due to a genuine selective chemical transduction process.

Keywords: Biosensors; Enzymatic methods; Acetylcholine; Acetylcholinesterase; Bilayer lipid membranes

Considerable progress has been made in the construction of enzyme electrodes, but the response times of these biosensors is often reported to be in the 1 to 5 min region owing to the thickness of the layers which contain the enzymes [1]. Highly porous gels that minimize diffusional limitations have been used to prepare thin membranes (50 μm) for enzyme support [2], and very thin layers (1–2 μm) of enzymes have been immobilized on glass electrodes to prepare devices capable of response times of 5 to 10 s [3]. However, sensitivity was compromised in both of these systems, and the short response times were obtained for substrate concentrations in the mM range. Bilayer lipid membranes (BLMs) can be excellent host matrices for maintenance and transduction of the activity of many biochemically

Correspondence to: U.J. Krull, Chemical Sensors Group, Department of Chemistry, Erindale Campus, University of Toronto, 3359 Mississauga Road North, Mississauga, Ontario L5L 1C6 (Canada).

selective species such as enzymes, antibodies and receptors [4]. Such a matrix would have a thickness in the order of 10 nm, and a reaction zone of considerably less thickness indicating that response times could be relatively fast. The BLM is suited for transduction of chemical reactions by virtue of increases in ion conductivity which can be observed when the physical or electrostatic structure is perturbed by such reactions. A particular process which could provide rapid response involves the storage of electrical energy across the membrane by virtue of charging of the electrical double layer. A critical phenomenon associated with a rapid change of the extent of ionization of functional groups located at the surface of a membrane may provide a rapid and large signal based on a transient ion current which would have an appearance similar to that observed during ion-channel gating [5]. The object of this work was to prepare BLMs which could rapidly transduce the reaction of an enzyme to provide an electrochemical signal as result of a surface charging process which was generated by alteration of the structure of the electrochemical double layer.

The interactions of hydronium and calcium ions with BLMs composed of egg phosphatidyl choline (PC) and dipalmitoyl phosphatidic acid (DPPA) have previously been examined by an electrochemical method [6,7]. The results indicate that the surface charge density of such membranes can be manipulated by modification of the pH of bulk solution and the presence of Ca^{2+} to produce structural alterations within membranes. Furthermore it has been shown that the physical and electrostatic structure of a lipid membrane can be modulated by a selective chemical reaction. The transduction of the reaction of acetylcholinesterase (AChE) with acetylcholine (ACh) by lipid monolayer membranes and vesicles formed from PC/DPPA mixtures has already been studied by spectrofluorometric methods and fluorescence microscopy [8,9]. The hydrolysis of acetylcholine by the enzyme results in alteration of the pH at the surface of a membrane, and the resulting phase redistribution becomes evident as indicated by a transient alteration of the fluorescence signal.

It has previously been suggested that the reaction of ACh with AChE at planar BLMs can lead to the formation of ion channels in membranes formed from soybean lecithin [10,11], however the control of such conductivity and subsequent use for analytical determinations has not been developed. This paper describes the design,implementation and criteria for optimization of BLMs based on PC/DPPA mixtures as transducers for the reaction of AChE with ACh. The membranes provide transduction by alterations of charging of the double layer based on the extent of ionization of DPPA, which can be activated by the enzymatic reaction to provide a result which phenomenologically appears as a gated ion conduction process (i.e. an electrochemical switch).

EXPERIMENTAL

Materials and equipment

The apparatus and materials used throughout this study were essentially identical to those described previously [6,7]. Solventless BLMs were formed in an orifice of 0.32 mm diameter, which was located in a Saran Wrap™ partition (10 μm thickness) that was used to separate two identical solution cell compartments. Each plexiglass solution chamber had a volume of 10 ml and an air/electrolyte interface area of 3 cm^2. An external 25 mV d.c. voltage was applied across the membrane between two Ag/AgCl reference electrodes. A digital electrometer (Model 614, Keithley Instruments, Cleveland, OH) was used as a current-to-voltage converter. The electrochemical cell and the electronic equipment were isolated in a grounded Faraday cage.

The lipids that were used in this work were egg phosphatidyl choline (PC; lyophilized, Avanti Biochemicals, Birmingham, AL) and dipalmitoyl phosphatidic acid (DPPA; Sigma, St. Louis, MO). Other chemicals supplied by Sigma included HEPES (*N*-2-hydroxyethyl-piperazine-*N'*-2-ethanosulfonic acid) which was used for the adjustment of pH, acetylcholinesterase (AChE; EC 3.1.1.7 type VI-S from electric eel, lyophilized powder with an activity of 275 U mg^{-1} protein [12]), and acetylcholine chloride. Neostigmine

methyl sulfate was kindly donated by Cooper, Athens. Water was purified by passage through a cartridge filtering system (Milli-Q, Millipore, El Paso, TX) and had a minimum specific resistivity of 18 Mohm cm. All other chemicals were of reagent grade.

Procedures

Stock solutions of PC (2.5 mg ml^{-1}) and DPPA (2.5 mg ml^{-1}) in 80% *n*-hexane and 20% absolute ethanol were protected from light and were stored at 0°C in a nitrogen atmosphere. Dilute solutions containing 0.20 mg ml^{-1} total lipid were prepared daily for formation of BLMs. The BLMs were supported in a 0.1 M KCl electrolyte solution which contained 10 mM HEPES as a buffer.

A stock solution of 1.0 mg ml^{-1} of AChE in 10 mM Tris–HCl buffer (pH 7.4) was stored in a freezer. Samples of 100 μl volume were removed on a daily basis and were used for deposition of the protein onto the air/water interface in the electrochemical cell. A stock solution of acetylcholine chloride in water (2.00 mg ml^{-1}) was prepared weekly and was stored in a freezer.

The process of membrane formation by a modified "monolayer folding" technique was described previously [6,7]. Lipid solution (10 μl) was added dropwise from a microliter syringe to the water surface in one cell compartment near the partition. A volume of 3 μl of the protein solution was applied to the same air/water interface subsequent to the deposition of lipid in the experiments which investigated the electrochemical activity of the AChE–ACh reaction. The level of the electrolyte was dropped below the orifice and was then raised again within a few seconds. The formation of a membrane was verified by the magnitude of the ion current, and by the electrical properties of the membranes. The ion current stabilized over a period of 5–10 min. All solutions were gently stirred and all experiments were done at 25 ± 1°C.

RESULTS AND DISCUSSION

Control of the ion current which can pass through BLMs formed from mixtures of egg PC and DPPA has previously been reported [6]. Above a pH of 5.0 the DPPA was entirely ionized, indicating that a substantial negative surface potential was responsible for selectively attracting K^+ permions to the membrane surface. Ion conduction predominantly occurred through zones that were enriched in charged lipid when the DPPA content was less than 25% (w/w) in the membrane, and was associated with phase separation of the two lipid components. The phase separation was absent above a DPPA content of 25% (w/w) and conduction was directly related to the net average surface charge of the membranes. The process of conduction was sensitive to the extent of ionization of the acidic groups, owing to surface charge effects and associated molecular packing and hydrogen bonding with water [13,14]. These results suggest that modulation of the ion conductivity of BLMs could be established by a selective biochemical reaction such as that of an enzyme with substrate which produces products that influence local hydronium ion activity.

An important limitation of transduction by egg PC/DPPA membranes is that a pH change of 2 units (e.g. in a pH range of 3.5 to 5.5) was required to obtain a signal of about 5 pA, which represents a relatively small analytical signal when considering that the background ion current is in the 1 to 10 pA range. The sensitivity of the response to pH can be adjusted by means of introduction of Ca^{2+} to the electrolyte solution which is used to support the egg PC/DPPA BLMs [7]. For membranes that contain more than 25% (w/w) DPPA, the interaction of Ca^{2+} with divalent negatively charged lipid (pH about 8) provides a phase separation of the two lipids components, which leads to the formation of conductive zones by the charged lipid. This results in an alteration of the range of pH sensitivity, and more importantly in an enhancement of sensitivity by up to 5–10 fold (dependent on pH range). Therefore it is possible to use Ca^{2+} to control and maximize the signal-to-noise ratio of a response of ion current to a pH change that is generated by an enzyme–substrate reaction.

Acetylcholinesterase is one of the most efficient enzymes known and can hydrolyze 3×10^5

ACh molecules per molecule of enzyme per minute to choline and acetic acid. AChE isolated from electrophorus electricus is tetrameric and is composed of equivalent subunits of 80000 Daltons, each of which contains an active center [15]. The material isolated from eel is readily available, shows the highest specific activity [16], and is of interest in the area of enzyme labelling of antibodies [17,18]. Transient or permanent alterations of ion permeability through BLMs which were caused by the reaction of AChE with ACh have been previously reported [10,11,16,19,20]. The structure of AChE is such that there are hydrophobic portions of the molecule which permit incorporation into BLMs, leaving the active site at the aqueous interface [21]. For these latter experiments the enzyme was added to the bulk solution after formation of BLMs, and ACh was subsequently injected. We have repeated similar experiments using BLMs containing 15% (w/w) DPPA. The change of pH of the bulk solution was measured using a glass electrode (Fig. 1), and could be correlated with the observed ion current. The calibration curve of ion current with pH, shown in Fig. 1, indicated that the signal induced by the enzyme reaction was directly and quantitatively due to the average pH in bulk

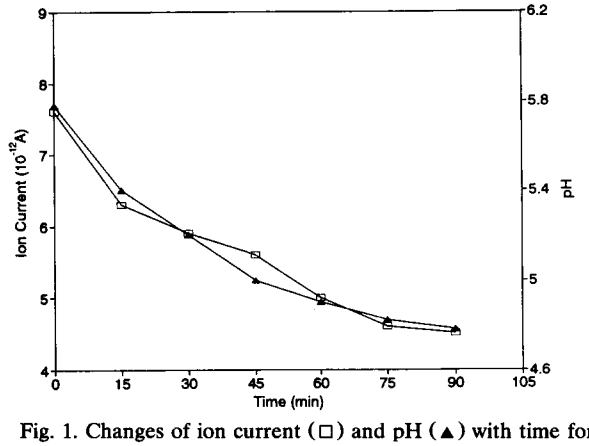

Fig. 1. Changes of ion current (□) and pH (▲) with time for membranes consisting of 15.0% DPPA; 200 μl of Ach (2 mg ml^{-1}) are injected into the cis cell compartment which contains 2.25 U of AchE in bulk solution. (Note that the time scale of this experiment was sufficient for the pH to decrease on both sides of the BLM, and this resulted in the change of ion current through the membrane.)

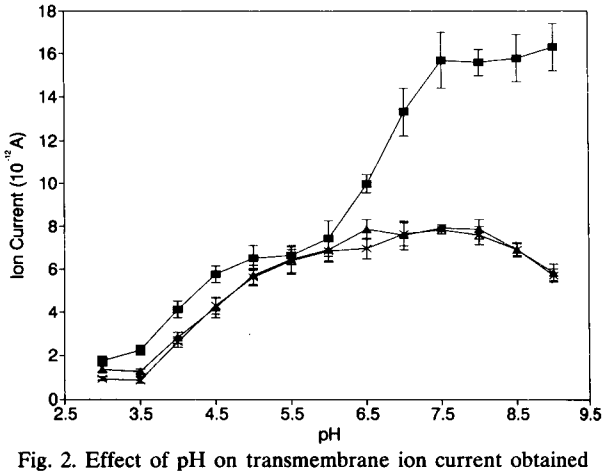

Fig. 2. Effect of pH on transmembrane ion current obtained with solventless BLMs with constant DPPA composition in the absence and presence of 2.25 U of AChE suspended in bulk electrolyte solution. (×) Membranes composed of 15% DPPA and without the enzyme; (▲) membranes composed of 15% DPPA and with the enzyme present; (■) membranes composed of 35% DPPA, without enzyme and in the presence of 1.0 mM Ca^{2+} in the electrolyte solution.

solution. Figure 2 indicates that the presence of the protein in the electrolyte solution does not significantly alter the structure or interfacial charge at the surface of BLMs. There were no indications of substantial ion current gating events and the response of the ion current was slow, as expected for the pH changes associated with a reaction of 2.25 U of AChE with ACh which occurred in a relatively large volume of solution.

AChE was deposited directly onto egg PC/DPPA mixtures at the air/water interface of the electrochemical cells to promote incorporation and maximize the loading of the protein when BLMs were formed. The volume of 3 μl of the AChE stock solution provided a total of about 1.8×10^{13} molecules of enzyme. This was spread over an area of 3 cm^2 after 10 μl of lipid solution (approximately 1.7×10^{15} lipid molecules) had been spread at the air/water interface. The monolayer folding technique transfered approximately 0.16 mm^2 of this material to the aperture for BLM formation. This provided a final lipid-to-protein ratio of about 100:1 and 4.8×10^9 enzyme molecules at either surface of a BLM if it is presumed that the protein was homogeneously

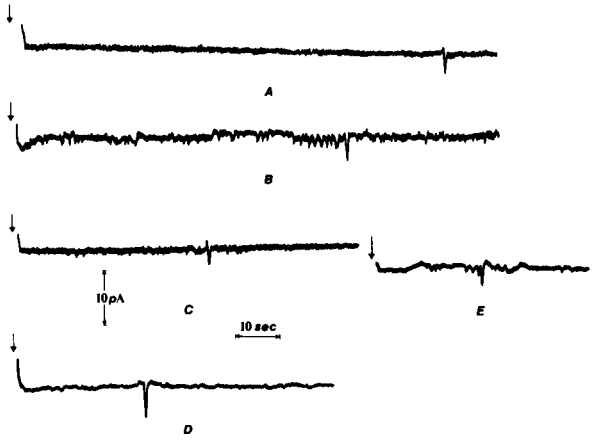

Fig. 3. Experimental results obtained at pH 5.5 (0.1 M KCl, HEPES 10 mM, without Ca^{2+}) with membranes consisting of 15.0% DPPA when 3 μl of AChE (1.0 mg ml^{-1}) was co-deposited at the air/water interface. ACh concentrations: (A) 5.50×10^{-6} M; (B) 1.10×10^{-5} M; (C) 3.30×10^{-5} M; (D) 6.60×10^{-5} M; (E) 1.10×10^{-4} M. Arrow (↓) indicates injection of substrate.

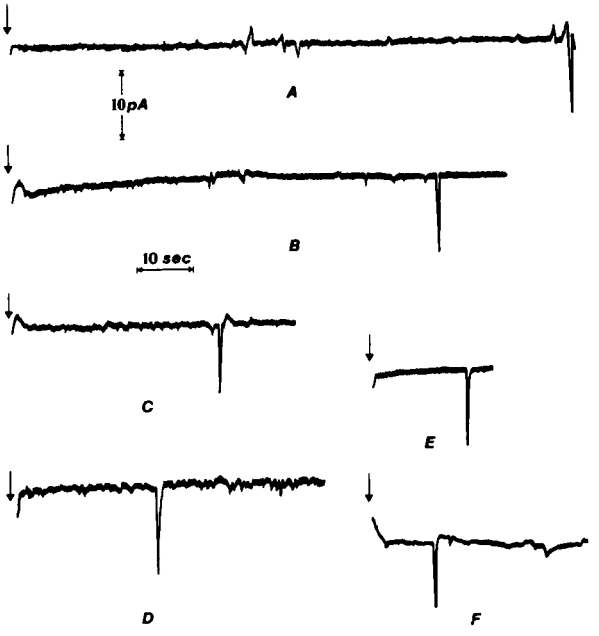

Fig. 4. Experimental results obtained at pH 8.0 (0.1 M KCl, HEPES 10 mM, Ca^{2+} 1 mM) with membranes consisting of 35.0% DPPA when 3 μl of AChE (1.0 mg ml^{-1}) was co-deposited at the air/water interface. ACh concentrations: (A) 2.20×10^{-6} M; (B) 5.50×10^{-6} M; (C) 1.10×10^{-5} M; (D) 2.20×10^{-5} M; (E) 3.85×10^{-5} M; (F) 5.50×10^{-5} M. Arrow (↓) indicates injection of substrate.

distributed [8], and that there was no loss of protein from the air/water interface. If the activity of the enzyme remained unchanged after incorporation of the protein into the BLMs, then the surface of the membrane should be occupied by 2×10^{-4} U of enzyme, which could produce approximately 0.2 nmoles of acetic acid per minute.

Figures 3 and 4 show recordings of the signals obtained at pH 5.5 and 8.0, respectively, for different concentrations of ACh. It can be seen that the transient responses appear as singular events (no further transients were observed over periods of 10 min) which occur in direct proportion to the reciprocal of time as shown in Fig. 5.

A number of control experiments using BLMs were completed to demonstrate that the transient signals were due to the ACh–AChE reaction. Signals were not evident in experiments that investigated the addition of substrate or choline to the electrolyte solution in the absence of AChE, or additions of ACh to denatured enzyme (AChE heated to 65°C for 30 min). Further studies involved the use of Neostigmine, a reversible inhibitor of the function of AChE [15,20,22]. Various amounts of Neostigmine were added to one solution compartment after the preparation of membranes which contained AChE. Subsequent addition of ACh to the same solution compart-

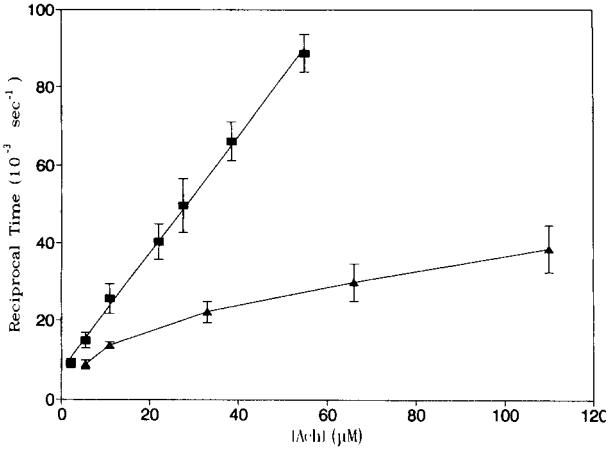

Fig. 5. Calibration of the analytical signal from experiments as shown in Figs. 3 and 4. Each point represents the mean of 5 determinations. (▲) pH 5.5; (■) pH 8.0.

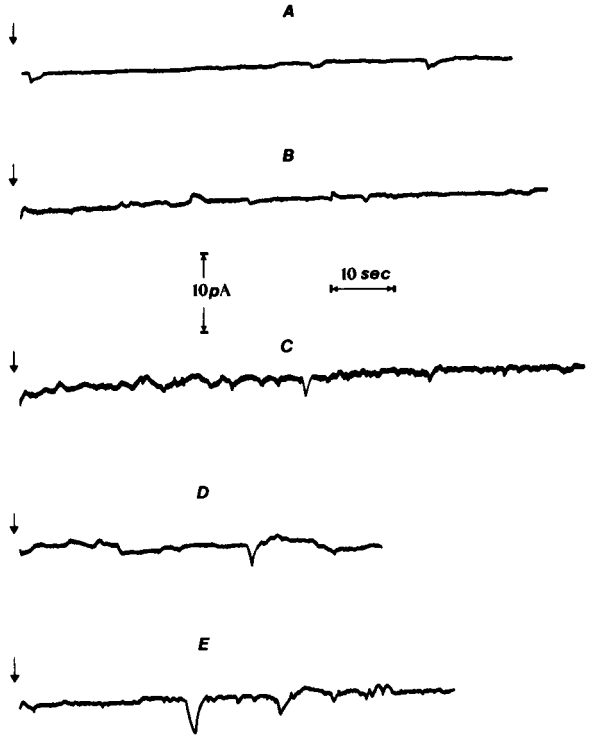

Fig. 6. Effect of Neostigmine on the time-dependence of the development of the transient signal obtained with 5.50×10^{-5} M Ach at pH 8.0 (0.1 M KCl, 10 mM HEPES, 1 mM Ca^{2+}) with membranes consisting of 35.0% DPPA. Neostigmine concentrations; (A) 7.50×10^{-5} M; (B) 1.50×10^{-5} M; (C) 3.75×10^{-6} M; (D) 1.50×10^{-6} M; (E) 7.50×10^{-7} M. Arrow (↓) indicates injection of substrate.

ment provided the results shown in Fig. 6. These results are consistent with a reduction of enzyme activity as controlled by the concentration of Neostigmine. A quantitative characterization of the ACh–AChE reaction was attempted by construction of a Lineweaver–Burk plot based on the delay time for appearance of the transient signal vs. the reciprocal of substrate concentration. The experimentally determined value of K_m was 5×10^{-5}, which agrees well with the published value of 9×10^{-5} for AChE from electric eel [12,18] (considering the impact of the negative surface potential of the BLM on the cationic substrate [23–25]).

The transient current signals have a duration of seconds or less and are indicative of a rapid reorganization of charge at the surface of membranes. Long term changes of ion current as observed for experiments which altered the bulk pH of the supporting electrolyte were not observed. Substantial changes of the pH of bulk solution were not expected from the relatively small amount of enzyme in the cell compartment, however the local pH at the surface of a BLM should have varied dynamically as the enzyme converted substrate to product. The diffusion of substrate and product should control the ultimate pH at the surface of the membrane, which would be expected to be at a value which was decreased from that of the original buffered solution. Higher buffer concentrations caused the transient to appear at longer times. For example, at pH 6 and using 5 to 10 μl of enzyme solution, the change from a 2 mM to a 10 mM HEPES buffer increased the time delay by approximately 60%. Previous results indicated that a lower pH at the surface of a membrane should have resulted in a permanent change of the ion permeability through the membrane, but this was not observed in these experiments and provided evidence against the development of conductive zones through the membrane.

The development of a transient current signal must be related to the dynamic acidification caused by the enzyme reaction at the surface of BLMs. This would indicate that a substantial change in the structure and/or electrostatic fields of the membrane must rapidly occur as the pH is altered. Previous reports have indicated that the ionizable head groups of DPPA in a membrane can be titrated to a distinct endpoint, and the transmembrane ion current has been shown to alter dramatically near such an endpoint [6]. These results confirm that for membranes which contain distinct ionizable groups it is possible to induce significant structural changes within a membrane by variation of pH over a small range.

The most significant difference between experiments that report long-term changes of transmembrane ion permeability [6,7] and those reported herein is that previous work has made adjustments of pH in bulk solution concurrently on both sides of BLMs, while this new work has provided pH changes only at the one membrane interface which is exposed to the substrate. The

fact that only a charging event is observed in experiments that use the enzyme indicates that it is possible to control the structure of one leaflet of a BLM without disturbing the structure of the opposing surface. It should be possible to test these suggestions by direct adjustment of the pH of the electrolyte solutions, given that the structural change, and associated charging or permeability phenomena, are dependent on the manipulation of surface charge density. Adjustment of the pH in one solution compartment by rapid addition and mixing of HCl (5 s) to change the pH from 8.0 to 5.5 resulted in immediate development of a transient current similar in profile and magnitude to that observed in experiments using the ACh–AChE reaction. A permanent change in ion current was not observed in these experiments. Subsequent addition of an identical quantity of HCl in the second solution compartment in the same manner resulted in the development of another transient current signal, which was immediately followed by a gradual decrease in the ion current through the membrane. The final steady-state ion current was attained in 10 to 15 s, and was of a magnitude similar to that found previously in experiments which had simultaneously adjusted the pH on both sides of a BLM (Fig. 2). Subsequent rapid addition of KOH in one solution compartment to change the pH from 5.5 to 8.0 resulted in the development of a further transient current signal similar to that observed on acidification but opposite in direction, and cycling between pH 8.0 and 5.5 reproducibly provided transient signals. Injections of electrolyte solution of volumes identical to the HCl or KOH provided no measurable response. These results indicate that the transient signal is the result of a pH change which controls surface charge. The ion current is not directly affected by hydronium ion as a carrier of charge since the transients are indistinguishable when moving in either direction between pH 5.5 and 8.0. These results further suggest that the signal is the result of an interfacial charging phenomenon, and that the signal generation mechanism is reversible and reproducible.

The BLMs serve as generic transducers of local pH changes, which can be provided by a variety of different reactions with one example being the selective reaction of ACh with AChE. Figures 3 to 5 indicate that the analytical information about the concentration of substrate is embodied in the time-dependence of a transient of relatively constant magnitude. The signal profile provides an interesting opportunity for development of a sensor which can act as a modulator or switching device. The signal magnitude is dependent on the pH of the bulk solution, and the quantity and extent of ionization of DPPA. The signal magnitude is increased when the degree of ionization of DPPA is large, as for example at pH 8.0, or in the presence of Ca^{2+}. Larger quantities of DPPA in a membrane tend to provide increased signal magnitudes as shown by the results of membranes composed of 15% and 35% DPPA. A clear continuation of this trend is not evident for membranes containing 60% DPPA. The magnitude of the electrical potential applied between the electrodes across a BLM can also be used to increase the magnitude of the transient, and the charging current increases linearly with applied potential over the tested range of 25 to 100 mV.

Competition between the production rate of hydronium ion from the reaction (presumably controlled by substrate diffusion as based on the high turnover number of AChE) with diffusion away from the membrane surface and reaction with buffer would indicate that at low substrate concentrations the reduction of pH may reach an equilibrium value that is insufficient to produce the transient current response. The detection limit measured in these experiments was about 1 μM ACh, which required about 3 min before observation of the transient current (the transient signal was of a similar magnitude to that observed at higher substrate concentrations). The pH of the bulk solution also sets the activity of an enzyme and a compromise between transient signal magnitude and activity may be necessary for other enzyme reactions, but was unnecessary for the case of AChE which has an optimum pH with respect to activity between pH 7 and 8 [18].

Even though the BLM system described in this work is unsuitable for practical biosensor implementation, the basic physical chemistry can be enabled in practical devices that make use of

ordered lipid membranes. Recent reports about the development of immobilized lipid films on metal electrodes, where immobilization has been by adsorption or covalent attachment, indicate that a practical configuration may be constructed [26,27].

We are grateful to the Natural Sciences and Engineering Research Council of Canada and the University of Athens for financial support of this work, and to Cooper Ltd. for provision of Neostigmine methylsulphate.

REFERENCES

1 J. Janata, in R.P. Buck, W.E. Hatfield, M. Umaña and E.F. Bowden (Eds.), Biosensor Technology, Fundamentals and Applications, Marcel Dekker, New York, 1990, p. 17.
2 R. Tor and A. Freeman, Anal. Chem., 58 (1986) 1042.
3 S. Kumaran, H. Meier, A.M. Danna and C. Tran-Minh, Anal. Chem., 63 (1991) 1914.
4 J. Janata, Anal. Chem., 62 (1990) 33R.
5 B. Hille, in Ionic Channels of Excitable Membranes, Sinauer, Sunderland, MA, 1984, Chap. 1.
6 D.P. Nikolelis, J.D. Brennan, R.S. Brown and U.J. Krull, Anal. Chim. Acta, 257 (1992) 49.
7 D.P. Nikolelis and U.J. Krull, Anal. Chim. Acta, 257 (1992) 239.
8 U.J. Krull, J.D. Brennan, R.S. Brown, S. Hosein, B.D. Hougham and E.T. Vanderberg, Analyst, 115 (1990) 147.
9 J.D. Brennan, R.S. Brown, C.P. McClintock and U.J. Krull, Anal. Chim. Acta, 237 (1990) 253.
10 K. Kaufmann and I. Silman, Naturwissenschaften, 67 (1980) 608.
11 K. Kaufmann, Funkt. Biol. Med., 4 (1985) 215.
12 G.G. Guilbault, in Handbook of Enzymatic Methods of Analysis, Marcel Dekker, New York, 1976, Chap. 2, p. 83.
13 J.M. Boggs, Biochim. Biophys. Acta, 906 (1987) 353.
14 T. Janas and H. Ti Tien, Biochim. Biophys. Acta, 939 (1988) 624.
15 P. Taylor, in L.S. Goodman and A. Gilman (Eds.), The Pharmacological Basis of Therapeutics, 6th edn., MacMillan, New York, 1980, Chap. 6, p. 100.
16 W. Leuzinger and M. Schneider, Experientia, 28 (1972) 256.
17 M. Mascini, F. Zolesi and G. Palleschi, Anal. Lett., 15 (1982) 101.
18 C. Blake and B.J. Gould, Analyst, 109 (1984) 533.
19 J. Del Castillo, A. Rodriguez, C.A. Romero and V. Sanchez, Science, 153 (1966) 185.
20 M.K. Jain, Arch. Biochem. Biophys., 164 (1974) 20.
21 T. Weidmer, U. Brodbeck, P. Zahler and B.W. Fulpius, Biochim. Biophys. Acta, 506 (1978) 161.
22 E. Shaw, in P.D. Boyer (Ed.), The Enzymes, Structure and Control, Vol. I, 3rd edn., Academic Press, New York, 1970, Chap. 2, p. 125.
23 L. Wojtczak and M.J. Nalęcz, Eur. J. Biochem., 94 (1979) 99.
24 K.S. Famulski, M.J. Nalęcz and L. Wojtczak, FEBS Lett., 103 (1979) 260.
25 K.S. Famulski, M.J. Nalęcz and L. Wojtczak, FEBS Lett., 157 (1983) 124.
26 M. Otto, M. Snejdarkova and M. Rehak, Anal. Lett., 25 (1992) 653.
27 J.D. Brennan, R.S. Brown, V. Ghaemagghami, K.M. Kallury, M. Thompson and U.J. Krull, in H. Mottola and G. Steinmetz (Eds.), Chemically-Modified Surfaces, Elsevier, Amsterdam, 1992, p. 275.

Analytica Chimica Acta, 281 (1993) 577–584
Elsevier Science Publishers B.V., Amsterdam

Na^+,K^+-ATPase-based bilayer lipid membrane sensor for adenosine 5′-triphosphate

Yoshikazu Adachi, Masao Sugawara, Kazuya Taniguchi and Yoshio Umezawa

Department of Chemistry, Faculty of Science, Hokkaido University, Sapporo 060 (Japan)

(Received 26th April 1992; revised manuscript received 10th September 1992)

Abstract

A potentiometric sensor for adenosine 5′-triphosphate (ATP) was constructed based on a planar bilayer lipid membrane (BLM) embedded with Na^+,K^+-ATPase (Na^+ pump). The planar bilayer lipid membranes were formed across a small circular aperture bored through a thin Teflon film by the folding of two monolayers spread on the air/water interface. The incorporation of Na^+,K^+-ATPase into the BLM was achieved by fusion methods. The sensor thus fabricated was found to respond potentiometrically toward ATP anions. The magnitude of the membrane potential increased with increase in the ATP concentration from 10^{-6} to 10^{-3} M. The detection limit was estimated to be 1.0×10^{-6} M. The response was reasonably selective to ATP ions with the selectivity order ATP > UTP, GTP > AcP, CTP ≫ ADP. The sensor output was found to require the added K^+ as expected, and was inhibited by a specific inhibitor, ouabain. The results were explained as being due to the active transport of Na^+ and K^+ using the hydrolysis energy of ATP, and are briefly discussed in terms of the potential use of Na^+,K^+-ATPase as a sensory element for ATP.

Keywords: Biosensors; Enzymatic methods; Potentiometry; Adenosine triphosphate; Lipid membrane

Electrochemical detection of adenosine 5′-triphosphate (ATP) has been reported based on different approaches. A potentiometric liquid membrane electrode was developed by exploiting host–guest interaction between a protonated macrocyclic polyamine and ATP polyanion at the membrane surface [1]. Also, an amperometric enzyme electrode was constructed based on a substrate recycling with glucose-6-phosphate dehydrogenase, pyruvate kinase and hexokinase, in which ATP is converted stoichiometrically into NADH and determined amperometrically [2]. Further, an enzyme thermistor permitted calorimetric determination of ATP based also on substrate recycles involving ATP with pyruvate kinase, hexokinase, L-lactate dehydrogenase, lactate oxidase and catalase [3].

In this paper a new type of electrochemical biosensor for ATP is described, which is based on a different principle from those described earlier [1–3]. A so-called Na^+ pump, Na^+,K^+-ATPase, was used as the sensory element, which undergoes active transport of Na^+ and K^+ across an artificial bilayer lipid membrane (BLM), utilizing the chemical energy arising from the hydrolysis of ATP in the presence of Mg^{2+} [4–6]. It appears that the use of biological pumps as sensory elements has not been reported previously, except for the work described by Thompson et al. [7], who demonstrated that auxin-receptor H^+,K^+-ATPase incorporated into a bilayer membrane generated a transmembrane current responding to auxin.

Correspondence to: Y. Umezawa, Department of Chemistry, Faculty of Science, University of Tokyo, Hongo, Tokyo 113 (Japan) (permanent address).

Na^+,K^+-ATPase is known to transport three Na^+ outward and two K^+ inward in a single turnover process under physiological conditions. This translocation of a net positive charge (one Na^+) generates a membrane potential with the outside positive relative to the inside [4–6] or transient and steady ion currents [8] across biological membranes. The work carried out so far on electrophysiological studies by means of transmembrane current [9–11], radiotracers [12,13] and voltage-sensitive dyes [14,15] has demonstrated that the rate of Na^+/K^+ exchange and consequently the translocation of the charge with Na^+,K^+-ATPase is dependent on the concentration of ATP [16,17]. On the other hand, few studies have been reported on the direct observation of membrane potentials generated by the pump action of Na^+,K^+-ATPase. Jain et al. [18] demonstrated that a black lipid membrane exposed to an aqueous solution containing crude membrane fragments of Na^+,K^+-ATPase exhibited a negative potential change toward ATP. As far as we know, no direct observation of membrane potentials using BLMs incorporated with purified Na^+,K^+-ATPase has been successful.

Recently, it proved possible to observe this membrane potential using an electrometer with a very high input impedance ($> 10^{15}$ Ω), which was not available earlier. In this paper, the membrane potential thus detected is shown to provide a useful analytical measure of ATP concentration in aqueous solution.

EXPERIMENTAL

Reagents

L-α-Phosphatidylcholine (PC) (purity > 99%, from frozen egg yolk) was purchased from Sigma (St. Louis, MO). Cholesterol (Chol) was obtained from Wako (Osaka, Japan) and recrystallized twice from methanol. Adenosine 5′-triphosphate disodium salt (Na-ATP), adenosine 5′-diphosphate disodium salt (Na-ADP), and adenosine 5′-monophosphate sodium salt (Na-AMP) (all from equine muscle), cytidine 5′-triphosphate sodium salt (Na-CTP) (synthetic), guanosine 5′-triphosphate sodium salt (Na-GTP) (by enzymatic phosphorylation of 5′-GMP) and uridine 5′-triphosphate sodium salt (Na-UTP) (from equine muscle) were purchased from Sigma. Acetylphosphate lithium potassium salt (Li,K-AcP) and ouabain were purchased from Kojin (Tokyo) and NBCo Biochemicals Division of ICN Biomedicals (Cleveland, OH), respectively. Tris(hydroxymethyl)aminomethane (Tris) was obtained from Wako. Other reagents were of analytical-reagent grade. The sample and buffer solutions were prepared with distilled water obtained using a batch-type water still (Autostill WB-21, Yamato Scientific, Tokyo).

Isolation and purification of Na^+,K^+-ATPase

Na^+,K^+-ATPase was prepared from pig kidney red outer medulla as described [19]; kidney microsome was prepared by centrifugation, then incubated with deoxycholate to solubilize and purify the protein [20]. To reduce a ouabain-insensitive fraction of ATPase, the above pretreated enzyme was further treated with sodium iodide [21]. The purified enzyme was then suspended with a homogenizer in 250 mM sucrose containing 1 mM Tris–EDTA to give a protein concentration of 7–9 mg ml^{-1} and stored at −80°C until use. The specific activity of these preparations was 10–30 μmol ATP (mg protein)$^{-1}$ min^{-1} at 37°C and pH 7.40. The hydrolysis of ATP was coupled to the oxidation of NADH using pyruvate kinase and lactate dehydrogenase [21].

Fabrication of the cell compartment

The cell compartment used for membrane potential measurements was the same as described [22,23] except that a Teflon film (12.5 μm thick) was used for the fabrication of a small aperture (200–300 μm diameter) on which BLMs were to be formed.

Formation of Na^+,K^+-ATPase incorporated BLMs

The folding method was used for the formation of BLMs, with a slight modification [24]. After inserting two Ag/AgCl reference electrodes in each compartment, 1.5 ml of buffer solution was placed in both compartments. The *cis*-side was 100 mM Tris–HCl solution (pH 7.40)

containing 250 mM sucrose, 50 mM K_2SO_4, 5 mM Na_2SO_4 and 5 mM $MgSO_4$, and the *trans*-side was 100 mM Tris–HCl solution (pH 7.40) containing 250 mM sucrose, 5 mM K_2SO_4, 50 mM Na_2SO_4 and 5 mM $MgSO_4$. The water level in each compartment was set below the aperture of the Teflon film by aspirating the buffer solutions with syringes connected to Teflon tubes. At this stage, the electric resistance between the two Ag/AgCl electrodes generally became > 1000 GΩ, which guaranteed that the two compartments were electrically open circuited by the Teflon film. A 5-μl volume of 2% (w/v) PC–Chol (molar ratio 4 : 1) solution in *n*-hexane was spread on buffer solutions in both compartments with a microsyringe. A 5–10-min standing period was allowed for hexane to evaporate, so that solvent-free lipid layers were formed at the air/water interface.

Incorporation of Na^+,K^+-ATPase into the BLMs was achieved by fusing the protein from either the *cis*-side (method A) or the *trans*-side (method B):

In method A, the water levels in both compartments were gradually and synchronously raised by operating two syringes until the water levels reached above the aperture of the Teflon film. After the formation of an impedance-matched bilayer membrane (vide infra), a standing period of 45–60 min was allowed for the membranes to stabilize. The fusion of Na^+,K^+-ATPase was then performed: 50 μg of Na^+,K^+-ATPase were injected into the *cis*-side solution with stirring. Thus, incorporation of Na^+,K^+-ATPase into the BLM was constrained to occur from the K^+-rich (*cis*) side. This experimental procedure was based on the fact that the ATP hydrolysis site of the protein tends to face the K^+-rich side if incorporated from a K^+-rich solution rather than an Na^+-rich solution [25]. Stirring of the solution was continued for more than 30 min to ensure the incorporation of the protein.

In method B, after spreading a lipid solution on buffer solutions in both compartments as described above, 10 μg of Na^+,K^+-ATPase were dropped on the *trans*-side lipid layer with a microsyringe. The water levels were raised in the same manner as described in method A. Folding of a pure lipid layer in the *cis*-side and an Na^+,K^+-ATPase-injected lipid layer in the *trans*-side was then performed to form an Na^+,K^+-ATPase-incorporated bilayer membrane. Method B was used for constructing the calibration graph shown in Fig. 3b.

During the formation of BLMs, the transmembrane current was monitored with a patch-clamp amplifier (Model CEZ-2200, Nihon Koden, Tokyo) connected to a synchroscope (Model SS-5702, Iwasaki Tsuushinki, Tokyo). When the formation of the BLMs was successfully achieved, the membrane resistance generally became around 30–50 GΩ. If no membrane was formed, the water levels were lowered below the aperture by operating the two syringes, and the above procedure was repeated. After the formation of a membrane, the Teflon tubes were removed from the chamber in order to exclude electrical noise from the outer source. The BLMs thus formed typically exhibited an electrical conductance of 10 nS–10 pS.

The durability of the present BLMs was fairly high provided that the membrane system was kept undisturbed from physical vibration. It was observed that the BLM exposed to the Tris–HCl buffer solution (described above) was stable and retained its resistance for over 30 h. However, the incorporation of Na^+,K^+-ATPase into the BLM was found to halve the lifetime of the BLM.

The formation of the BLM by the above procedure was confirmed by the gramicidin method [26,27]: a single channel conductance of ca. 170 pS with a rectangular shape was observed, revealing that the lipid bilayer membrane was successfully formed. This method was based on the characteristic property of gramicidin A, leading to the formation of a conducting channel only if present in a dimerized state in bilayer membranes. After the formation of a lipid membrane, 10 μl of a 100 μg ml^{-1} dimethyl sulphoxide (DMSO) solution of gramicidin D, a mixture of gramicidin A, B and C, was injected into both the *cis*- and *trans*-side solutions with stirring. After the stirring was stopped, the channel conductance due to gramicidin A under applied potentials of $+100$ and -100 mV was measured with a patch-clamp amplifier (Model EPC-7, List-Electronic, Darm-

stadt-Eberstadt). The data were filtered at 1 kHz using an eight-pole Bessel-type low-pass filter (Model FV664 dual-channel programmable filter, NF Electronic Instruments, Kanagawa) and digitized through an A/D conversion interface with a sampling interval of 200 μs (Model TL-1 DMA interface, Axon Instruments, Burlingame, CA). The data thus acquired were recorded on a hard disk of a personal computer (Model Deskpro 386S, Compaq Computer, Houston, TX) in which pCLAMP software (version 5.5.1, Axon Instruments) was installed.

The actual success of the formation of lipid membranes by the above folding procedure (method A) was 30% out of 20 trials, and half of them were usable for membrane potential measurements in terms of impedance matching between the membrane and measuring systems.

Measurement of membrane potentials

The change in the observed potentials was measured between two Ag/AgCl reference electrodes dipped in both sides of the membrane using an electrometer (vibrating-reed type, Model TR-8411, Advantest, Tokyo), the input impedance of which was $> 10^{15}$ Ω, and was recorded on a strip-chart recorder (Model R-01, Rikadenki, Tokyo). The *trans*-side was connected to ground, and therefore the *cis*-side has the sign and magnitude of the generated potentials. The measuring system was isolated from electrical noise and environmental vibration by performing all experiments in a Faraday cage placed on a vibration-free table (Fig. 1). All experiments were carried out in a room thermostated at 24 ± 1°C. The *cis*-side solution was stirred with a microstirrer tip, whereas the *trans*-side solution was not stirred. For the impedance matching between the membrane and electrometer, membranes with resistance < 100 GΩ were adopted for the following experiment. If the membrane resistance was $>$ 100 GΩ, the measurement system behaved more like a complete open circuit.

After ensuring a steady potential (within 1 mV per 2 min), addition of the analyte (ATP) solution to the *cis*-side solution for both methods A and B was made in order to give the lowest concentration to be examined. The major ionic species of

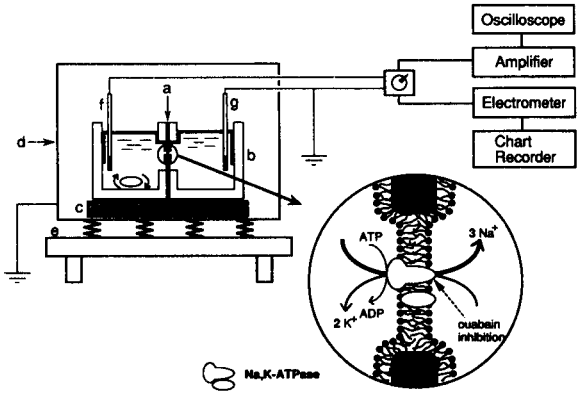

Fig. 1. Experimental set-up for the measurement of membrane potentials for the present Na^+,K^+-ATPase-incorporated bilayer lipid membrane sensor. (a) Teflon film 12.5 μm thick with a small aperture 200 μm diameter; (b) Teflon chamber; (c) magnetic stirrer; (d) Faraday cage; (e) vibration-free table; (f) Ag/AgCl electrodes. The electrode in the *trans*-side solution was connected to ground. Inset: schematic view of a possible orientation of Na^+,K^+-ATPase in the sensor membrane and direction of ouabain binding.

ATP under the present experimental condition of pH 7.40 are 88% of ATP^{4-} and 12% of $HATP^{3-}$, based on one of its acid dissociation constants ($pK_5 = 6.5$) [28]. The reason why ATP was added to the *cis* (K^+-rich)-side is simply that this matches the physiological condition that ATP is hydrolysed in the K^+-rich side of the biological membrane. Although this is a physiologically matched condition, there is an obvious analytical difficulty with method A in that the analyte (ATP) is added to the solution in which an unknown excess amount of Na^+,K^+-ATPase might be retained without being incorporated into the BLM. As a result, ATP might be consumed in excess by this "Na^+,K^+-ATPase in solution" without contributing to the generation of membrane potentials. On the other hand, in method B, where Na^+,K^+-ATPase was fused from the *trans*-side solution, this difficulty was avoided.

When the shift in the membrane potential became within 1 mV per 2 min after the injection of the analyte, it was regarded as being a steady potential; at least 10 min were needed to attaining this steady potential. Further addition of analyte solution to the *cis*-side solution was made after obtaining each steady potential. All interfer-

ing substances (ions) were added as sodium salts except for AcP. The electrochemical cell assembly for potential measurement was as follows: Ag,AgCl/100 mM Tris–HCl (pH 7.40), 5 mM Na_2SO_4, 50 mM K_2SO_4, 5 mM $MgSO_4$, analyte (*cis*-side)/PC–Chol (molar ratio 4:1), Na^+,K^+-ATPase (BLM)/100 mM Tris–HCl (pH 7.40), 50 mM Na_2SO_4, 5 mM K_2SO_4, 5 mM $MgSO_4$ (*trans*-side)/Ag,AgCl.

RESULTS AND DISCUSSION

Potential vs. time profile

Figure 2 shows a typical time course of the membrane potential for the present ATP sensor with change in ATP concentration. After a steady potential (2 mV min^{-1}) had been attained in a buffer solution without ATP, 10 μl of 150 mM ATP solution were added to the *cis*-side solution to bring its ATP concentration to 1 mM (arrow A). The membrane potential shifted toward a negative value and reached a steady potential after 10 min. A further increase (arrow B) in ATP concentration to 5 mM enhanced both the rate and magnitude of the potential increase. The slow response time of the present sensor may be due to the large time constant of the measuring system: the membrane resistance of the present bilayer lipid membrane was 10–100 GΩ, which was 1000–10000 times higher than those of the conventional solvent polymeric membranes [29].

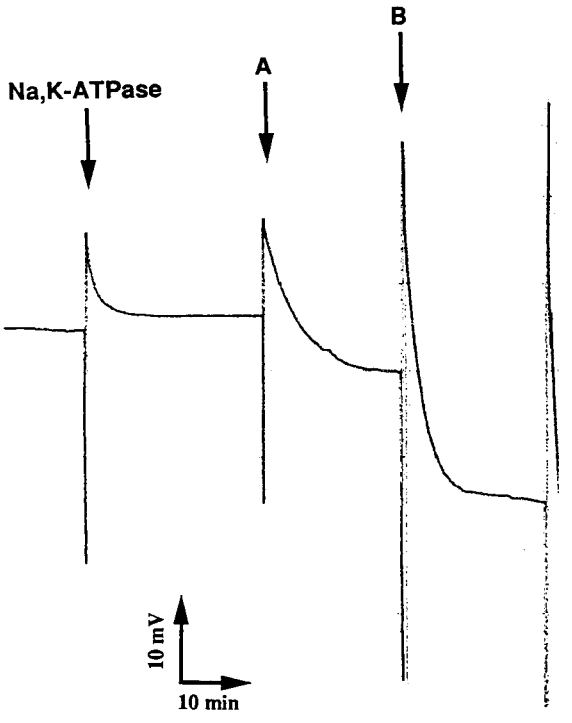

Fig. 2. Typical time course of the observed membrane potential with the present sensor with stepwise increase in ATP concentrations. The BLM was formed by method A (see text). The initial composition of the *cis*-side solution was 100 mM Tris–HCl (pH 7.40), 250 mM sucrose, 50 mM K_2SO_4, 5 mM Na_2SO_4 and 5 mM $MgSO_4$, and that of the *trans*-side solution was 100 mM Tris–HCl (pH 7.40), 250 mM sucrose, 50 mM Na_2SO_4, 5 mM K_2SO_4 and 5 mM $MgSO_4$. At the times indicated by arrows, a small volume of ATP stock solution was added stepwise to the *cis*-side solution to increase its ATP ion concentration from 0 to 1 mM (arrow A), and from 1 to 5 mM (arrow B). Only the *cis*-side solution was stirred.

Concentration dependence

The relationship between the concentration of ATP in the *cis*-side solution and the potentiometric response of the present ATP sensor was examined. Figure 3a shows a typical plot of the observed membrane potential with a single membrane vs. ATP concentration. The absolute magnitude of the potential change increased with increasing concentration of ATP from 10^{-3} M to 10^{-2} M and the detection limit (signal-to-noise ratio $\geqslant 3$) was 1.7×10^{-4} M.

Improvement of the detection limit of the present ATP sensor was achieved with the BLM formed by method B in which ATP was added to the opposite side of the membrane exposed to the excess Na^+,K^+-ATPase. As shown in Fig. 3b, the membrane potential showed a sharp concentration dependence in the range 10^{-6}–10^{-3} M ATP in the *cis*-side solution with a detection limit (signal-to-noise ratio $\geqslant 3$) of 6.3×10^{-6} M. This improvement is simply due to the absence of excess Na^+,K^+-ATPase in the *cis*-side solution, which hydrolyses added ATP. The relative standard deviation of the measurement in 1×10^{-4} M ATP solution was 23% with four different sets of membrane preparations.

The average value of the steady potentials in the absence of the analyte (ATP) for method B

TABLE 1

Potentiometric selectivities of Na^+,K^+-ATPase-based BLM sensor for various nucleotides and acetyl phosphate

Analyte [a]	Selectivity [b]
Na-ADP	0.004
Na-CTP	0.091
Li,K-AcP	0.130
Na-GTP	0.681
Na-UTP	0.882
Na-ATP	1.000

[a] Measurements for each analyte were made with different membrane preparations. [b] The selectivity was defined and obtained as the ratio of the increase in potential induced by successive addition of 5 mM interfering ion and 5 mM ATP, respectively, in the *cis*-side buffer solution.

was -16 mV ($n = 4$) and the relative standard deviation in this instance was 64% ($n = 4$).

Selectivity

The potentiometric selectivity of the present ATP sensor against several nucleotides and acetyl phosphate was investigated. The results are summarized in Table 1, in which the selectivity was obtained as the ratio of the increase in potential induced by 5 mM possible interfering substances to that of 5 mM ATP. In the present approach for estimating selectivities, therefore, we did not rely on the Nicolsky–Eisenman formalism [1,30]. The selectivity against ADP was found to be 0.004, and the overall selectivity order for method A was ATP > UTP, GTP > AcP, CTP ≫ ADP. Hence it is concluded that the present sensor was reasonably selective to ATP ions, although the number of interfering substances examined was limited. The observed selectivity order with the present Na^+,K^+-ATPase embedded membrane sensor was found to be parallel to that in the hydrolysis of substances with corresponding biological membranes; no evidence has been reported that ADP is a substrate for Na^+/K^+ exchange, whereas acetyl phosphate is a substrate for Na^+ transport in the absence of K^+ [31,32]. Other nucleotides (UTP, GTP and CTP) are also substrates for Na^+,K^+-ATPase but their affinity is less than that of ATP [33–35].

Effect of K^+

The effect of K^+ on the induction by ATP of membrane potentials with the present BLM sensor was examined with the BLM formed in the 100 mM Tris–HCl buffer solution (pH 7.40) containing 250 mM sucrose, 50 mM Na_2SO_4 and 5 mM $MgSO_4$. In this experiment, the ionic compositions in both the *trans*- and *cis*-side solutions were made equal in order to minimize the effect of diffusion potential. The result is shown in Fig. 4. When K^+ was absent, no change in the mem-

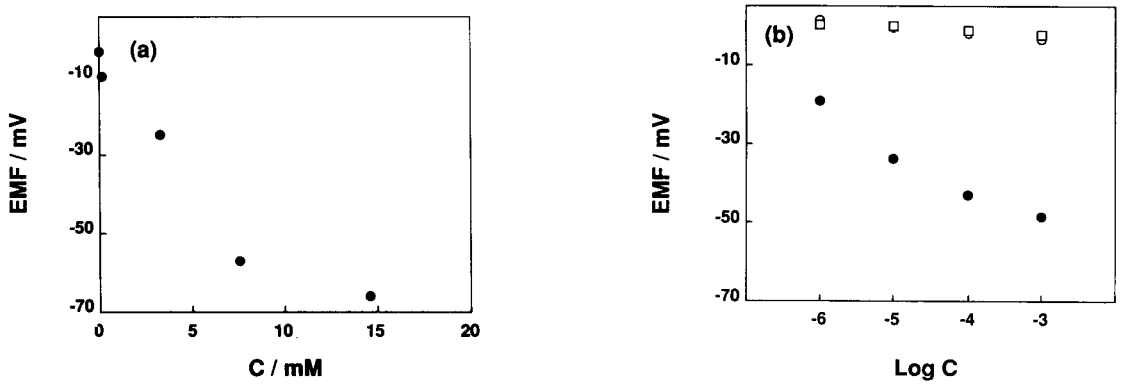

Fig. 3. (a) Relationship between the concentration of ATP and the observed membrane potentials with the present sensor. The potential values obtained with a single membrane preparation were plotted. The BLM was formed by method A (see text). (b) Relationship between the concentration of (●) ATP, (○) ADP and (□) AMP and the observed membrane potentials with the present sensor. The average values of the observed membrane potentials with four different membrane preparations were plotted. The BLM was formed by method B (see text). The compositions of the *cis* and *trans*-side solutions were identical with those in Fig. 2.

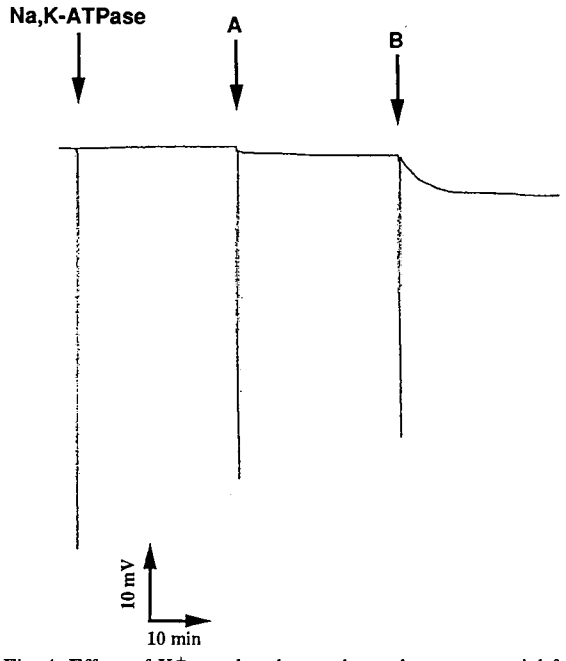

Fig. 4. Effect of K^+ on the observed membrane potential for the present sensor. The BLM was formed by method A (see text). The compositions of the *cis*- and *trans*-side solutions were identical: 100 mM Tris–HCl (pH 7.40), 250 mM sucrose, 50 mM Na_2SO_4 and 5 mM $MgSO_4$. Left-hand arrow, injection of Na^+,K^+-ATPase into the *cis*-side solution; arrow A, injection of ATP solution into the *cis*-side solution (final concentration 10 mM); arrow B, injection of K_2SO_4 solution into both solutions (final concentration 10 mM).

brane potential was induced on addition of ATP (arrow A). This is due to the fact that under K^+-free conditions, the so-called "Na^+/Na^+ exchange mode" takes place, in which the protein pumps Na^+ both inward and outward with a coupling stoichiometry of 1:1. This particular case is known as the electroneutral process [4–6], and accordingly no generation of a membrane potential is expected. When 10 mM K_2SO_4 solution was added to the both the *cis*- and *trans*-side solutions (arrow B), the membrane potential shifted to a negative value, as expected. This results confirm that the added K^+ is necessary for the present sensor to respond potentiometrically to ATP, exploiting the electrogenic Na^+–K^+ exchange of the Na^+ pump.

Effect of ouabain

Ouabain is a specific inhibitor for Na^+,K^+-ATPase, which binds from the extracellular side of the protein, and stabilizes the low-energy state of Na^+,K^+-ATPase to inhibit the transport of K^+ [4,5]. To confirm that the observed membrane potential originated from the pump action of Na^+,K^+-ATPase in the BLM, this particular reaction involving ouabain was used. After full development of the ATP-dependent membrane potential (Fig. 5, arrow A), 10 μl of 150 mM ouabain solution in DMSO were added to the *trans*-side solution to make its final concentration 1 mM (Fig. 5, arrow B). The membrane potential decreased and had completely disappeared after 10 min. The delay of the response after the addition of ouabain appeared to come from the experimental requirement that the *trans*-side solution should not be stirred in order to avoid occasional breaks of the bilayer membrane. Addition of DMSO without ouabain caused no change in the membrane potential. Also, addition of ouabain to the *cis*-side solution caused no inhibition. These results are schematically explained as shown in the inset in Fig. 1, and the ouabain-sensitive decrease in membrane potential was found to be

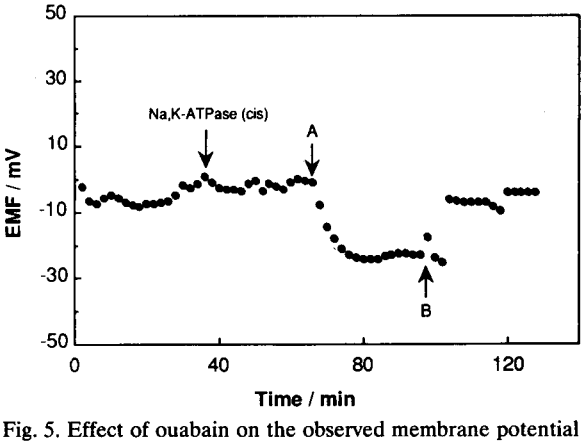

Fig. 5. Effect of ouabain on the observed membrane potential for the present sensor. The BLM was formed by method A (see text). Left-hand arrow, injection of Na^+,K^+-ATPase into the *cis*-side solution; arrow A, injection of ATP solution into the *cis*-side solution (final concentration; 10 mM); arrow B, injection of ouabain–DMSO solution into the *trans*-side solution (final concentration 1 mM).

due to the inhibition by ouabain of the pump action of Na^+,K^+-ATPase incorporated in the BLM. As described earlier, ATP was added only to the *cis*-side solution. As a result, Na^+,K^+-ATPase whose ATP-binding site faces the *cis*-side hydrolyses ATP and causes generation of membrane potentials. On the other hand, ouabain is known to function at a site 180° opposite from the ATP binding site of the protein.

In conclusion, although improvement of the stability of the bilayer membranes is a prerequisite for practical analytical use of the present sensor, the results obtained here demonstrate the potential use of Na^+,K^+-ATPase as a sensory element for a new type of sensing system.

The authors thank Drs. S. Kaya and H. Minami for technical advice. This research was supported by Grant Nos. 03640481 and 03205001 from the Ministry of Education, Science and Culture, Japan.

REFERENCES

1 Y. Umezawa, M. Kataoka, W. Takami, E. Kimura, T. Koike and H. Nada, Anal. Chem., 60 (1988) 2392.
2 X. Yang, G. Johansson, D. Pfeiffer and F. Scheller, Electroanalysis, 3 (1991) 659.
3 D. Kirstein, B. Danielsson, F. Scheller and K. Mosbach, Biosensors, 4 (1989) 231.
4 J.C. Skou, FEBS Lett., 268 (1990) 314.
5 J.-D. Horisberger, V. Lemas, J.-P. Kraehenbühl and B.C. Rossier, Annu. Rev. Physiol., 53 (1991) 565.
6 H.-J. Apell, J. Membr. Biol., 110 (1989) 103.
7 M. Thompson, U.J. Krull and M.A. Venis, Biochem. Biophys. Res. Commun., 110 (1983) 300.
8 A. Eisenrauch, E. Grell and E. Bamberg, in J.H. Kaplan and P. De Weer (Eds.), The Sodium Pump: Structure, Mechanism, and Regulation, Rockfeller University Press, New York, 1991, p. 317.
9 R.F. Rakowski, L.A. Vasilets, J. LaTona and W. Schwarz, J. Membr. Biol., 121 (1991) 177.
10 R.F. Rakowski and C.L. Paxon, J. Membr. Biol., 106 (1988) 173.
11 R. Borlingaus, H.-J. Apell and P. Läuger, J. Membr. Biol., 97 (1987) 161.
12 W. Schwarz and Q. Gu, Biochim. Biophys. Acta, 945 (1988) 167.
13 R.F. Rakowski, Biophys. J., 55 (1989) 663.
14 R. Goldshleger, Y. Shahak and S.J.D. Karlish, J. Membr. Biol., 113 (1990) 139.
15 R. Goldshleger, S.J.D. Karlish, A. Rephaeli and W.D. Stein, J. Physiol., 387 (1987) 331.
16 S.J.D. Karlish, D.W. Yates and I.M. Glynn, Biochim. Biophys. Acta, 525 (1978) 230.
17 R.L. Post, C. Hegyvary and S. Kume, J. Biol. Chem., 247 (1972) 6530.
18 M.K. Jain, F.P. White, A. Strickholm, E. Williams and E.H. Cordes, J. Membr. Biol., 8 (1972) 363.
19 P.L. Jørgensen, Biochim. Biophys. Acta, 356 (1974) 36.
20 Y. Hayashi, M. Kimimura, H. Homareda and H. Matsui, Biochim. Biophys. Acta, 482 (1977) 185.
21 K. Taniguchi, K. Suzuki and S. Iida, J. Biol. Chem., 257 (1982) 10659.
22 H. Minami, N. Sato, M. Sugawara and Y. Umezawa, Anal. Sci., 7 (1991) 853.
23 H. Minami, M. Sugawara, K. Odashima, Y. Umezawa, M. Uto, E.K. Michaelis and T. Kuwana, Anal. Chem., 63 (1991) 2787.
24 M. Montal and P. Mueller, Proc. Natl. Acad. Sci. U.S.A., 69 (1972) 3561.
25 L.E. Hokin and J.F. Dixon, Methods Enzymol., 156 (1988) 141.
26 M.C. Goodall, Arch. Biochem. Biophys., 147 (1971) 129.
27 R. Coronado and R. Latorre, Biophys. J., 43 (1983) 231.
28 L.G. Sillen and A.E. Martell (Eds.), Stability Constants, Supplement No. 1, Chemical Society, London, 1971.
29 G. Horvai, E. Gráf, K. Tóth, E. Pungor and R.P. Buck, Anal. Chem., 58 (1986) 2735.
30 K. Umezawa and Y. Umezawa, in Y. Umezawa (Ed.), CRC Handbook of Ion-Selective Electrodes: Selectivity Coefficients, CRC Press, Boca Raton, FL, 1990, p. 3.
31 L. Beaugé and G. Berberián, Biochim. Biophys. Acta, 772 (1984) 411.
32 M. Campos, G. Berberián and L. Beaugé, Biochim. Biophys. Acta, 938 (1988) 7.
33 J.D. Robinson, Arch. Biochem. Biophys., 213 (1982) 650.
34 F.M.A.H.S. Stekhoven, H.G.P. Swarts, R.S. Zhao and J.J.H.H.M. de Pont, Biochim. Biophys. Acta, 861 (1986) 259.
35 M. Guerra, J.D. Robinson and M. Steinberg, Biochim. Biophys. Acta, 1023 (1990) 73.

Analytica Chimica Acta, 281 (1993) 585–589
Elsevier Science Publishers B.V., Amsterdam

Highly sensitive detection of allergen using bacterial magnetic particles

N. Nakamura and T. Matsunaga

Department of Biotechnology, Tokyo University of Agriculture and Technology, Koganei, Tokyo 184 (Japan)

(Received 30th March 1992; revised manuscript received 9th September 1992)

Abstract

A fluoroimmunoassay method using bacterial magnetic particles for the highly sensitive detection of allergen was developed. Fluorescein isothiocyanate (FITC)-conjugated IgE antibody was immobilized on bacterial magnetic particles using a heterobifunctional reagent, *N*-succinimidyl 3-(2-pyridyldithio)propionate. The decrease in fluorescence intensity on aggregation of FITC-labelled bacterial magnetic particle conjugates was determined by spectrofluorimetry. The relative fluorescence intensity decreased with increasing allergen concentration. A linear relationship was obtained between the relative fluorescence intensity and allergen concentration in the range of 0.5–100 pg ml^{-1}.

Keywords: Fluorimetry; Immunoassay; Allergens; Bacterial magnetic particles; Magnetic bacteria

The radioallergosorbent test (RAST) [1] has been used for the detection of allergens. However, RAST is time consuming and demands complicated procedures, giving results independent of clinical symptoms. A simple and safe method is still required for the detection of allergen.

Magnetic bacteria, which orient and swim along geomagnetic fields, have been found in fresh and marine sediments [2,3]. These bacteria contain magnetite particles with controlled size (50–100 nm). These bacterial magnetic particles form alignments of 10–30 particles and disperse very well because they are covered with a stable lipid membrane [4]. In previous work, the pure culture of magnetic bacteria capable of growing under aerobic conditions was successfully achieved [5]. Bacterial magnetic particles (BMPs) have been isolated from magnetic bacteria and applied in clinical studies [6,7]. BMPs have been employed for enzyme and antibody immobilization [8]. Enzymes and antibodies immobilized on BMPs showed higher activities than those on artificial magnetic particles.

Recently, a solid-phase fluoroimmunoassay using antibody immobilized on BMPs was developed for the rapid detection of mouse immunoglobulin G (IgG) [9]. The use of BMPs allows the separation of the bound and free antibody fractions by application of a magnetic field. This technique also overcomes the problem of mixing during the incubation period.

This paper reports the highly sensitive detection of allergen using BMP-immobilized fluorescein isothiocyanate (FITC)-conjugated antibody with a heterobifunctional reagent, *N*-succinimidyl 3-(2-pyridyldithio)propionate (SPDP).

Correspondence to: T. Matsunaga, Department of Biotechnology, Tokyo University of Agriculture and Technology, Koganei, Tokyo 184 (Japan).

EXPERIMENTAL

Materials

Sodium 2,4-dinitrobenzenesulphonate was purchased from Tokyo Chemical Industry (Tokyo). Bovine serum albumin (BSA) and FITC were obtained from Sigma (St. Louis, MO) and SPDP from Pierce (Rockford, IL). Monoclonal mouse IgE (anti-DNP) [10], purified from the ascitic fluid of BALB/c × C_{57} BL-F_1 mice bearing the SPE-7 hybridoma, was purchased from Seikagaku Kogyo (Osaka). Other reagents were of analytical-reagent or laboratory grade. Deionized, distilled water was used in all procedures.

Preparation of dinitrophenylated bovine serum albumin (DNP–BSA)

A DNP–BSA conjugate (13.8 mol of DNP per mole of BSA) was prepared by using sodium dinitrobenzenesulphonate and BSA as described by Little and Eisen [11]. DNP–BSA was employed as a model allergen.

Cultivation of magnetic bacteria

Magnetic bacteria were isolated from sludge obtained from ponds in Tokyo and were cultured in MSGM medium as described previously [12]. The pH of the medium was adjusted to 6.75 with NaOH solution before sterilization. The cells were cultured in 5 l of medium at 25°C for 7–10 days. Magnetic bacteria grown to the stationary phase (about 2×10^8 cells ml^{-1}) were centrifuged at 5000 *g* for 10 min. The collected cells were washed with 10 mM 1-(2-hydroxyethyl)piperazine-4,2-ethanesulphonic acid (HEPES) buffer (pH 7.4).

Preparation of BMPs and immobilization of antibody

BMPs were isolated from magnetic bacteria by the following method. Approximately 10^{12} cells suspended in 20 ml of HEPES buffer were disrupted by three passes through a French pressure cell at 1300 kgf cm^{-2}. The disrupted cells were treated in a UR-200P ultrasonic disrupter (Tomy Seiko, Tokyo) for 5 min at 0°C five times. BMPs were collected from the sonicated cell fraction by using a samarium–cobalt magnet (18 × 11 × 14 mm) that produced an inhomogeneous magnetic field (0.4 T on the surface of the magnet and an average gradient of 0.2 T cm^{-1}). BMPs collected at the bottom of the tube due to the presence of the magnet and the supernatant was removed. The collected BMPs were washed with HEPES buffer at least five times and kept at 4°C in phosphate-buffered saline (PBS) (pH 7.4) before use. The particle size of BMP was measured with an SA-CP3 particle size analyser (Shimadzu, Kyoto).

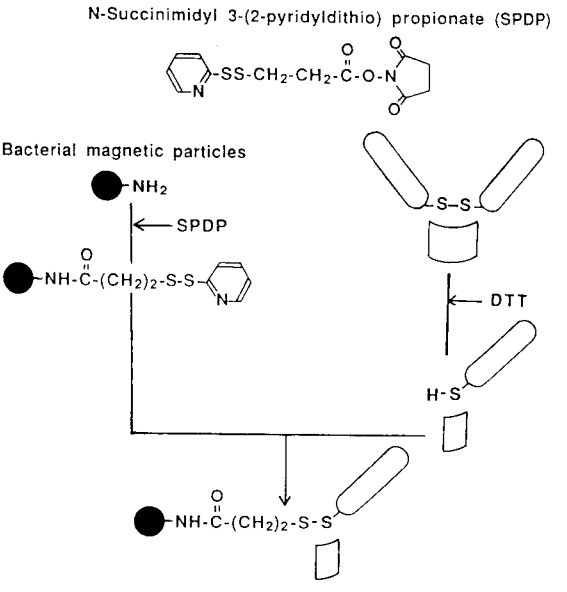

Fig. 1. Structure of SPDP and schematic diagram of immobilization of antibody on BMPs using SPDP.

Figure 1 shows the structure of SPDP and a schematic diagram of the immobilization of antibody on BMPs. For the reduction of antibody, 25 μl of dithiothreitol (DTT) solution (200 mM in PBS) were added to 500 μl of IgE solution (100 μg ml^{-1}). The mixture was incubated for 2 h at room temperature. After incubation, the sample was purified using an NAP-10 column, eluting with PBS according to the manufacturer's instructions (Pharmacia, Uppsala). The organic membrane of BMPs was modified by adding 500 μl of ethanol containing 0.6 mg of SPDP to 1 ml of BMPs suspension (5 mg ml^{-1}) [13]. The suspension was then dispersed by sonication and incubated for 2 h at room temperature. The

modified BMPs were washed with PBS and incubated with reduced IgE solution for 12 h at 4°C. Reduced IgE was directly immobilized on BMPs. Antibody-coupled BMPs were washed with PBS several times to remove excess antibodies. The concentration of antibody in the solution was determined by the Bio-Rad protein assay before and after immobilization and the amounts of antibody immobilized on BMPs were calculated. Conjugation of FITC was carried out by a modified method of The and Feltkamp [14]. Antibody-coupled BMPs (5 mg) were suspended in 2 ml of borate buffer (0.5 M, pH 9.2). FITC (500 μg) was added to the solution and incubated for 2 h with stirring. After the incubation, FITC-antibody conjugated BMPs were washed with PBS and collected using a samarium–cobalt magnet.

Fluoroimmunoassay of allergen by using FITC-conjugated IgE antibody immobilized on BMPs

DNP–BSA was diluted with gelatin veronal buffer (GVB) (pH 8.3, gelatin concentration 0.1%). 50 μl of antibody BMP conjugate (100 μg ml^{-1}) and 50 μl of sample were mixed and incubated in a test-tube (16.5 mm o.d.) for 15 min at 37°C. The agglutination reaction was enhanced by applying an inhomogeneous magnetic field (the test-tube was placed on a samarium–cobalt magnet) which increased the FITC–antibody–BMP aggregation when these conjugates reacted with allergen. The strength of the applied magnetic field was adjusted by changing the position of the magnet and measured by using a GK-3 flux meter (Shimadzu. The mixture was then added to 2 ml of GVB (gelatin concentration 1%) and mixed for a few seconds. The fluorescence intensity of FITC-labelled BMPs was measured with an RF-5000 spectrofluorimeter (Shimadzu) with the excitation wavelength set at 490 nm and the emission wavelength at 516 nm using a 10×10 mm quartz glass cuvette at 25°C.

RESULTS AND DISCUSSION

Preparation of BMPs

When BMPs were prepared by the French pressure and ultrasonication method, they were well dispersed in buffer. The median diameter of BMPs was 0.12 μm, and BMPs purified in this way retain their magnetosome membrane, which consists mainly of phospholipid as described [9]. On the other hand, BMPs that were treated with chloroform–methanol (2:1, v/v) after ultrasonication were not covered with a magnetosome membrane. Figure 2 shows the particle size distribution of BMPs with and without a magnetosome membrane. BMPs without a magnetosome membrane formed larger aggregates (the median diameter was 12.5 μm) than with this membrane (the median diameter was 0.12 μm). BMPs were covered with 98% lipids and 2% other compounds including proteins. Phospholipids comprised 58% of the total lipid and phosphatidylethanolamine, which has amino residues, accounted for 50% of the total phospholipids present. The magnetosome membrane contains amino residues and can be activated by SPDP. SPDP reacts with primary amines via an *N*-hydroxysuccinimide ester to instal a flexible spacer chain terminating with a maleimide for conjugation with thiol-containing proteins. Therefore, IgE can be immobilized on the membrane activated by SPDP.

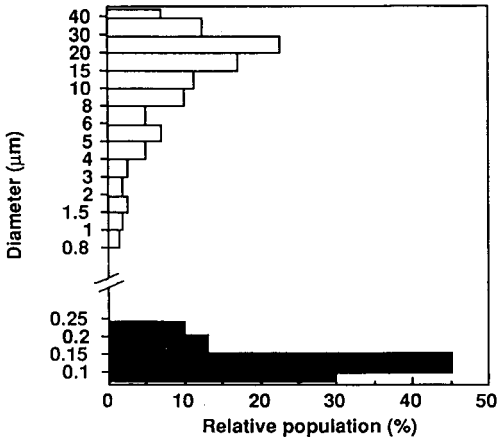

Fig. 2. Particle size distribution of BMPs (■) with and (□) without a magnetosome membrane.

Immobilization of FITC-conjugated IgE on BMPs

Reduced IgE antibody was immobilized on BMPs activated with SPDP. The extent of anti-

body coupling with BMPs without a magnetosome membrane was 72 μg per mg of particles, whereas the coupling with BMPs with a magnetosome membrane was 220 μg per mg of particles. BMPs were covered with a stable lipid membrane. There was slight aggregation in each particle as a result of its own magnetic properties. Therefore, BMPs with a magnetosome membrane were superior in dispersion to BMPs without a magnetosome membrane. Hence the extent of antibody coupling with BMPs with a magnetosome membrane was about three times higher than that achieved when BMPs without a magnetosome membrane were used. In this study, we have described the use of bacterial magnetic particles which consist of magnetite coated with a lipid membrane. These particles bind large amounts of capture antibody and show a low non-specific adsorption of antibody. The surface of the particles was modified to incorporate a cross-linker molecule terminating with a maleimide. This functionality was used to couple the antibody through thiols obtained by reduction with dithiothreitol. FITC was then coupled to antibody as described under Experimental.

Determination of allergen by FITC–IgE–BMP conjugates

A sample containing a model allergen (DNP–BSA) was mixed with FITC–IgE–BMP conjugates in a test-tube and incubated at 37°C with application of an inhomogeneous magnetic field (0.2 T cm^{-1}). FITC–IgE–BMP conjugates were collected with a samarium–cobalt magnet and the supernatant was removed after incubation for 15 min. FITC–IgE–BMP conjugates were resuspended in GVB containing 1% of gelatin. This suspension was poured into a quartz glass cuvette and the fluorescence intensity of FITC-labelled BMPs was monitored. Figure 3 shows the particle size distribution of FITC–IgE–BMP conjugates after reaction with and without allergen for 15 min. The mean particle size was 2 μm in the absence of allergen. When 10 pg ml^{-1} of allergen were added to the FITC–IgE–BMP suspension, the mean particle size was 7 μm.

In order to separate the aggregates resulting from a specific immunoreaction, gelatin was used.

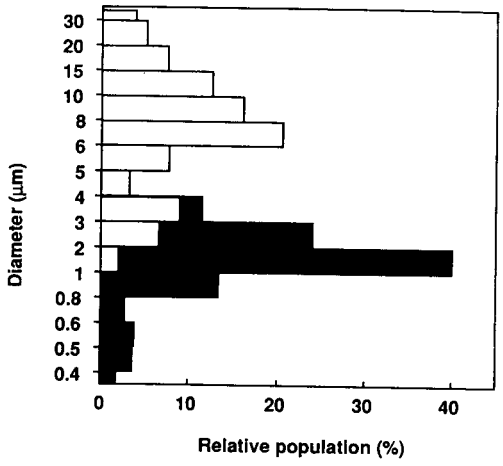

Fig. 3. Particle size distribution of BMP conjugates after the reaction with allergen. Allergen concentration: □ = 10 pg ml^{-1}; ■ = 0 pg ml^{-1}.

A low gelatin concentration (0.1%) in GVB and a high gelatin concentration (2%) did not clarify the difference due to rapid or slow sedimentation of the FITC–IgE–BMP conjugates as a result of the gelatin viscosity [9]. The difference between the relative fluorescence intensity decrease based on specific and non-specific aggregation was maximum when 1% gelatin was used. The fluorescence intensity of FITC–IgE–BMP conjugates decreased owing to their aggregation. The aggregation of FITC-labelled BMPs was enhanced and

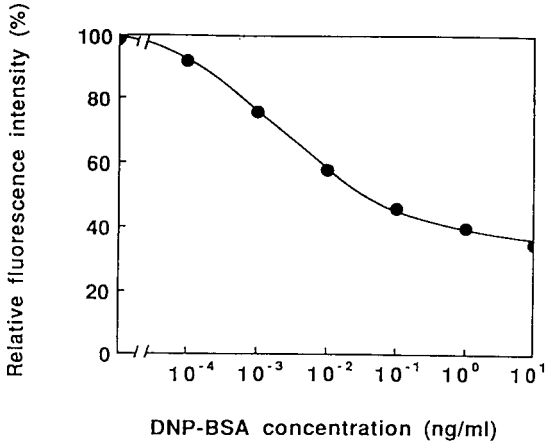

Fig. 4. Relationship between relative fluorescence intensity and allergen concentration. Reaction was carried out at 37°C for 15 min.

TABLE 1

Relative fluorescence intensity of BMP conjugates when allergens were added

Allergen	Relative fluorescence intensity (%)
None	100
DNP–BSA	56
IgG	98
BSA	97

the relative fluorescence intensity thus decreased by applying a magnetic field during incubation (data not shown). After 15 min of incubation, the fluorescence intensity became constant. The allergen concentration was measured by using FITC–IgE–BMP conjugates.

Figure 4 shows the relationship between the relative fluorescence intensity and DNP–BSA concentration. The relative fluorescence intensity decreased with increasing allergen concentration, with a linear relationship in the range 0.5–100 pg ml^{-1}. The minimum detectable concentration of allergen was 0.5 pg ml^{-1}. The fluorescence intensity was reproducible with an average relative error of 5% when a sample containing 10 pg ml^{-1} of allergen was measured for five times. The present method is more sensitive than the methods described previously.

The selectivity of this method was examined. The fluorescence intensity decreased slightly when other proteins such as BSA and mouse IgG were used (Table 1), because antibody was specifically immobilized on the BMPs, which were also dispersed. Therefore, the fluorescence intensity decrease from BMP conjugates depended on the specific antigen–antibody reaction, which resulted in a shortening of the incubation time required. Further, the high sensitivity of this method for allergen detection is achieved by combining an aggregation reaction with fluoroimmunoassay. This method is also non-radioactive and does not require a separation step. This method is preferable to previously reported magnetic particle-based assays because of the ca. 10–100 times higher sensitivity.

The results presented in this paper demonstrate that antigen–antibody reaction-based BMP conjugates can be developed to perform simple, rapid immunoassays.

This work was partially supported by a Grant-in-Aid for Special Project Research, No. 03205032, from the Ministry of Education, Science and Culture.

REFERENCES

1 K.A. Kelly, G.M. Lang, P.G. Bundeson, V. Holford-Strevens and A.H. Sehon, J. Immunol. Methods, 39 (1980) 317.
2 R.P. Blakemore, Science, 190 (1975) 377.
3 J.L. Kirschvink, J. Exp. Biol., 86 (1980) 345.
4 Y.A. Gorby, T.J. Beveridge and R.P. Blakemore, J. Bacteriol., 170 (1988) 834.
5 T. Matsunaga, T. Sakaguchi and F. Tadokoro, Appl. Microbiol. Biotechnol., 35 (1991) 651.
6 T. Matsunaga and S. Kamiya, in K. Atsumi, M. Kotani, S. Ueno, T. Katila and S.J. Williamson (Eds.), Biomagnetism '87, Tokyo Denki University Press, Tokyo, 1988, pp. 410–413.
7 T. Matsunaga, K. Hashimoto, N. Nakamura, K. Nakamura and S. Hashimoto, Appl. Microbiol. Biotechnol., 31 (1989) 401.
8 T. Matsunaga and S. Kamiya, Appl. Microbiol. Biotechnol., 26 (1987) 328.
9 N. Nakamura, K. Hashimoto and T. Matsunaga, Anal. Chem., 63 (1991) 268.
10 Z. Eshhar, M. Ofarim and T. Waks, J. Immunol., 34 (1980) 775.
11 J.R. Little and H.N. Eisen, in C.A. Williams and M.W. Chase (Eds.), Methods in Immunology and Immunochemistry, Academic, New York, 1967, pp. 128–133.
12 R.P. Blakemore, D. Maratea and R.S. Wolfe, J. Bacteriol., 140 (1979) 720.
13 J. Carlsson, H. Drevin and R. Axen, Biochem. J., 173 (1978) 723.
14 T.H. The and T.E.W. Feltkamp, Immunology, 18 (1970) 865

END OF SPECIAL ISSUE
PAPERS ON BIOSENSORS

Analytica Chimica Acta, 281 (1993) 593–600
Elsevier Science Publishers B.V., Amsterdam

Flow-injection spectrophotometric determination of lysine in feed samples [1]

J. Saurina and S. Hernández-Cassou

Departament de Química Analítica, Universitat de Barcelona, Diagonal 647, 08028 Barcelona (Spain)

(Received 8th February 1993; revised manuscript received 13th April 1993)

Abstract

A flow-injection spectrophotometric method is described for the determination of lysine, based on the product of the reaction between lysine and 1,2-naphthoquinone-4-sulphonate in basic medium. The influence of different physical, chemical and hydrodynamic parameters on absorbance were studied. At 480 nm, the response is linear up to 1.5×10^{-4} M, the detection limit is 1.9×10^{-6} M and the relative standard deviation is 0.8%. Sample throughput is 80 h^{-1}. The method was applied to the determination of free lysine in commercial feed samples, by means of multivariate calibration techniques, without the need of chromatographic separation. Good concordance is shown between this method and the standard procedure for amino acid analysis.

Keywords: Flow injection; Spectrophotometry; Lysine; Feed samples; 1,2-Naphthoquinone-4-sulphonate; Multivariate calibration

Lysine is an essential amino acid in human and animal nutrition that is not synthesized by the organism. In addition, lysine is scarcely present in vegetal proteins and for this reason, free lysine is frequently added to the diet of vegetarians or herbivorous animals in order to supply this deficiency.

The determination of lysine and other amino acids is usually carried out by liquid chromatography. Lysine, like most amino acids, is not readily detected by spectroscopy and chemical derivatization is required to increase the sensitivity [1]. Chromatographic separation provides selectivity but the process may be inadequate to analyze a great number of samples because it is time-consuming. Flow-injection analysis (FIA) is a faster technique and may thus contribute to the development of rapid, sensitive and inexpensive methods. The selectivity in these flow systems could be achieved by using selective reagents or by suppressing interferences in order to obtain a specific signal for the analyte. The recent literature reports batch [2,3] and FIA [4] methods for lysine determination in which the selectivity is based on enzymatic reagents.

An alternative possibility is to avoid the tedious chromatographic step by determining the individual components of complex mixtures simultaneously without their previous separation. Multivariate calibration techniques, especially those based on factor analysis (principal component regression (PCR) and partial least squares regression (PLS)) can overcome the lack of selectivity derived from the use of a general spectrophotometric reagent. PCR and PLS are based

Correspondence to: S. Hernández-Cassou, Departament de Química Analítica, Universitat de Barcelona, Diagonal 647, 08028 Barcelona (Spain).

1 Presented at the *4th Symposium on Kinetics in Analytical Chemistry*, held in Erlangen, Germany, 27–30 September 1992.

on the concentration of the information into the lowest number of principal components or factors able to describe the whole system. More detailed descriptions of multivariate calibration procedures are given elsewhere [5–7]. These methods require the treatment of multivariate data which can be generated more easily by means of the flow injection methodology in connection with microcomputers. The application of multivariate calibration techniques to flow systems has been reported in several papers [8–10].

In this work, a flow injection method for the determination of free lysine in feed samples is presented. It is based on the spectrophotometric reaction between lysine and 1,2-naphthoquinone-4-sulphonate (NQS) in basic medium which is a general reaction for primary and secondary amino groups. The use of this reagent in continuous flow systems as well as the advantages that it represents have recently been proposed [11]. Since the feed samples contained other amino acids apart from lysine, and in order to avoid a chromatographic process, the lysine concentration was determined by applying PCR and PLS to the spectrophotometric data generated by a flow injection–diode array system.

EXPERIMENTAL

Reagents

Lysine hydrochloride (analytical grade) was supplied by Merck. Working solutions were prepared from an aqueous solution of lysine 0.01 M.

Sodium 1,2-naphthoquinone-4-sulphonate (NQS) (analytical grade, Aldrich) was used as received. Stock solutions of NQS 10^{-3} M in 0.1 M hydrochloric acid are stable for at least two weeks.

Buffer stock solution (0.1 M sodium carbonate (analytical grade, Scharlau) + 0.075 M sodium hydroxide (analytical grade, Merck)) was used to neutralize the NQS solution and to adjust the pH to the required value.

Commercial feed samples were obtained from Cooperativa Agropecuaria de Guissona, (Lleida, Spain).

Apparatus

Two different detectors were used: a Beckman DU7 single beam spectrophotometer for developing the method and a Hewlett-Packard HP 8452A diode array spectrophotometer (DAS) for the analysis of feed samples. A Hellma flow cell (10 mm path length and 18 μl volume) was used with both detectors. The amino acid autoanalyzer was from Pharmacia LKB Biotechnology, Model Alpha Plus (Series Two). Other equipment has previously been indicated [11].

Flow injection system and measurement procedure

A three-channel manifold (Fig. 1) with a peristaltic pump P (Scharlau HP4) and a variable-volume electrical injection valve V (Sirtex MV-8) was used. Solutions were pumped through standard Tygon tubing while PTFE tubing and PTFE standard T-pieces were used for all connections. The sample solution S was injected through the valve into channel C which carried distilled water. The reagent solution of NQS in HCl 0.1 M flowed through channel R and merged with the buffer solution of channel B in the mixing chamber M with magnetic stirring. This neutralization was carried out on-line since the reagent quickly decomposes in alkaline media. The colorimetric reaction took place in a reaction coil (10 m × 0.35 mm) which was immersed in a water bath T, at 80°C. Data were collected at 303 and 480 nm with the Beckman DU7 spectrophotometer or by scanning spectra from 390 to 590 nm, in steps of 2 nm, with the DAS furnished with a floppy disk

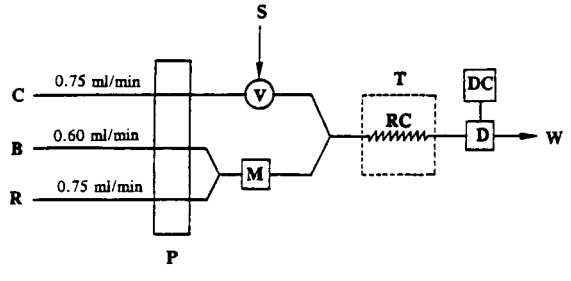

Fig. 1. Flow injection manifold. V = Injection valve, P = pump, M = mixing chamber, T = thermostatic bath, RC = reaction coil, D = detector, D = data acquisition unit, S = sample, C = carrier (water), R = reagent, B = buffer, W = waste.

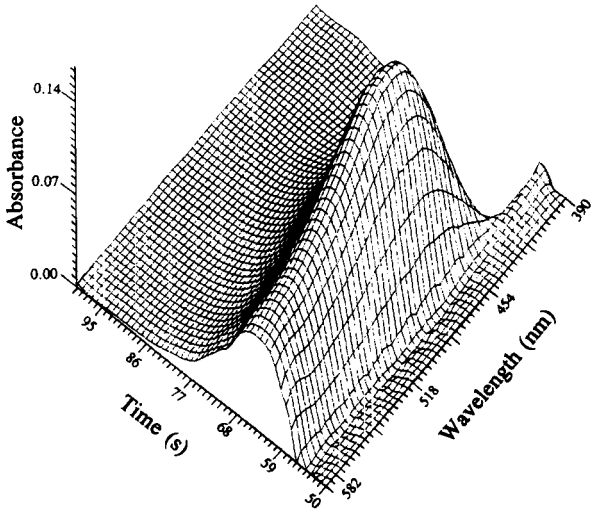

Fig. 2. Tridimensional flow injection profile for the NQS–Lys derivative obtained using the manifold of Fig. 1. $C_{Lys} = 5 \times 10^{-5}$ M, $C_{NQS} = 1 \times 10^{-3}$ M, buffer solution = sodium carbonate 0.1 M + sodium hydroxide 0.075 M, temperature = 80°C, total flow rate = 2.1 ml min^{-1}, reaction coil = 1000 cm × 0.5 mm, injection volume = 135 μl.

drive for bulk data storage (Hewlett-Packard ChemStation, Model 9153A).

Collection of data

Spectral data from the DAS were stored at an HP workstation running under the HP environment. The data files were transferred to an IBM-PC environment by means of an HP Vectra ES/12 computer. Additional translation of the original spectral data from binary to ASCII code was performed with a homemade program.

For each sample injection, 20 spectra were recorded along the FIA peak, at intervals of 3 s, starting 50 s after the injection. In order to improve the reproducibility, each spectrum collected was the average of 5 individual spectra with an integration time of 0.1 s. Figure 2 is an example of a tridimensional flow injection profile for a lysine solution. Spectra corresponding to the maximum of the peaks were chosen as multivariate data in the calibration procedure, but the number of working wavelengths was finally reduced to 50, each 4 nm.

Feed sample treatment

Samples were subjected to a solid–liquid extraction procedure in order to recover the free lysine: 3 g of feed sample was lixiviated with 50 ml of aqueous solution of 1% phenol for 30 min in a conical flask by means of magnetic stirring (phenol was added to prevent the development of microorganism colonies). The extract was filtered twice, first by using a paper Whatman 40 and then through a nylon membrane of 0.45 μm pore size. The filtered extract solutions were stored in a fridge. The whole lixiviation procedure was performed twice to give two independent solutions for each type of feed sample. Thus, twenty extract solutions were finally available from ten feed samples.

Solutions for injection into the flow system were prepared by diluting 5 ml of the filtered extract with distilled water up to a final volume of 25 ml. Eight spiked solutions were also prepared from the extracts of two different feed samples, providing additional concentrations of lysine of 40, 80, 100 and 200 μM.

Solutions for injection into the amino acid autoanalyzer were prepared by mixing 250 μl of the feed extract with 25 μl of 1 mM norleucine internal standard solution and filtered through a nylon membrane of 0.2 μm pore size.

RESULTS AND DISCUSSION

In preliminary studies, two- or three-channel manifolds were used to study the development of the reaction. The sample was injected into different carriers such as the final reagent solution, the buffer solution or an inert stream of distilled water. The highest and simplest peak shapes were obtained with the scheme shown in Fig. 1, and this arrangement was therefore adopted for subsequent experiments.

The influence of different chemical, physical and hydrodynamic parameters on the absorbance of the product of the reaction between NQS and lysine (NQS–LYS derivative) was studied. In all cases, the sample was injected in triplicate and the individual flow channel ratios were kept constant (1:0.8:1 for C, B, and R respectively). If

not specifically indicated, the concentrations of lysine and NQS were 10^{-4} M and 10^{-3} M, respectively, and the composition of the buffer solution was sodium carbonate 0.1 M + sodium hydroxide 0.075 M.

Effect of temperature and flow-injection variables

The rate of reaction between NQS and lysine is temperature dependent since it is a kinetic process. In this study, the total flow rate was 1.1 ml min^{-1} and the reaction coil dimensions were 10 m length × 0.35 mm inside diameter. The absorbance of NQS–LYS derivative increased continuously with an increase in temperature from room temperature to 80°C, and it remained constant in the range 80–90°C. Then a temperature of 80°C was chosen for subsequent experiments.

Using the same conditions as in the previous paragraph, the volume of the sample inserted was varied from 30 to 300 μl. Peak height increased up to a volume of 150 μl, while in the range 150–300 μl it was virtually constant. A good compromise between high sensitivity and sample throughput was achieved by selecting an injection volume of 135 μl.

The length (L) and inside diameter (i.d.) of the reaction coil and the total flow rate (Q) are interrelated to determine the residence time of the sample which depends on these variables and they were thus studied together. These parameters were varied in the ranges: L = 100–1000 cm, i.d. = 0.35–1.1 mm and Q = 0.8–3.6 ml min^{-1}. The results shown in Fig. 3 indicate that maxima of absorbance were obtained for a residence time of about 1 min. In addition, for any residence time, the values of absorbance were lower when a wider reactor was used, probably due to the less effective thermostatization of the sample bolus in the flow system. A reaction coil of 1000 cm length × 0.5 mm i.d. together with a total flow rate of 2.1 ml min^{-1} were chosen. In these conditions, the residence time was 1 min and the total dispersion was 5.5.

Influence of chemical variables

The effect of reagent concentration was studied in the range 5×10^{-4} to 0.01 M at four lysine concentrations. At working conditions where the lysine concentration was lower than 2×10^{-4} M, the absorbance of NQS–LYS derivative was not dependent on the reagent concentration. However, the background noise increased drastically with the reagent concentration and it is a limiting factor at NQS concentrations above 2×10^{-3} M. Thus a NQS concentration of 10^{-3} M was chosen as suitable compromise.

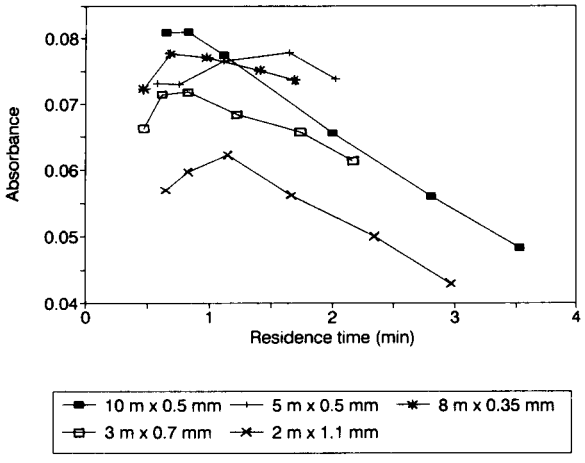

Fig. 3. Effect of residence time on the absorbance of the NQS–Lys derivative for different reaction coils. $C_{Lys} = 1 \times 10^{-4}$ M. See Fig. 2 for other conditions.

As has been mentioned, the reaction only took place in basic media, and in consequence, the NQS acid solution was neutralized on-line, with the buffer solution, to avoid decomposition of the reagent. The effect of pH on the reaction was studied with buffer solutions containing 0.1 M Na_2HPO_4 + 0.1 M H_3BO_3 + 0.1 M $NaHCO_3$ + different concentrations of NaOH. The pH values of the waste solutions issuing from the system were in the range 7.2 to 10.5. The concentration of the lysine solutions injected was 2×10^{-4} M. The maximum analytical signal was obtained in the range of pH 8.8–10.5. On the basis of this study a buffer solution of Na_2CO_3 0.1 M + NaOH 0.075 M was prepared, which provides a final pH value of 9.7.

Figures of merit

The figures of merit of the flow injection method, under the conditions described above, at

TABLE 1

Figures of merit of the flow injection method

	303 nm	480 nm
Linear range	up to 10^{-4} M	up to 1.5×10^{-4} M
Straight line equation	$A = 2370C + 0.005$	$A = 690C + 0.0016$
Coefficient of regression	0.9998	0.99990
R.S.D. (%)	1.3	0.8
Limit of detection	1.5×10^{-6} M	1.9×10^{-6} M

the two analytical wavelengths corresponding to the maxima of the absorption spectra of the NQS–LYS derivative (303 and 480 nm) are summarized in Table 1. The values of the relative standard deviation in this table correspond to the injection in triplicate of 10 solutions of lysine 10^{-4} M. The precision was also calculated on four non-consecutive days by injecting six solutions of lysine 10^{-4} M every day. Fresh solutions of reagent and buffer were prepared daily. The analysis of variance [12] shows that variations of the absorbance between days (relative standard deviation (R.S.D.) = 4.8%) are more important than between solutions (RSD = 1.1%). This fact can be attributed to the small day to day fluctuations in the individual flow rates of the channels. However, the variations between days are small enough to permit the use of the flow injection method, in any case, with a total RSD of 2.5% without the need of daily calibration. The method at 303 nm is about 3 times more sensitive than at 480 nm. The limit of detection is similar in both cases and the precision is better at 480 nm, because the background noise at 303 nm is higher. Thus, the detection at 480 nm is more useful for analytical determinations. The sample rate was 80 injections per hour.

The effect of foreign substances (glucose, phenol, salicylic acid, primary, secondary and tertiary aliphatic amines, quaternary ammonium salts, urea, ammonium ion) on the absorbance of NQS–LYS derivative was investigated. The lysine concentration was 10^{-4} M and the foreign substance presented a ten-fold excess. The criterion for interference was fixed at ±5%. At 480 nm only hydroxylamine and primary and secondary amino groups interfered.

Determination of lysine in feed samples

This flow injection method was applied to the determination of the free lysine content of ten commercial feed samples. The extracts of these samples were previously analyzed by the standard procedure with an amino acid autoanalyzer [13]. The results indicated that other amino acids apart from lysine were also present. Table 2 shows the composition in percentage of most characteristic amino acids in the feed samples. It can be seen that feed samples contain a wide range of different concentrations of lysine and the other amino acids, and the molar ratio $C_{Lys}/C_{amino\ acid}$ is not

TABLE 2

Percentage of some amino acids (grams of amino acid/100 grams of sample) in the feed samples, determined by the autoanalyzer standard procedure

Sample	Percentage of amino acid							
	Lys	Pro	Gly	Ala	Leu	Arg	Phe	Trp
Pig feed 1	0.036	0.021	0.0054	0.033	0.009	0.045	0.006	0.009
Pig feed 2	0.065	0.022	0.0055	0.039	0.018	0.073	0.009	0.011
Pig feed 3	0.038	0.015	0.0039	0.027	0.009	0.049	0.006	0.012
Pig feed 4	0.149	0.027	0.0057	0.045	0.019	0.043	0.010	0.010
Pig feed 5	0.039	0.018	0.0048	0.026	0.013	0.051	0.008	0.011
Pig feed 6	0.046	0.031	0.0066	0.042	0.026	0.062	0.013	0.010
Pig feed 7	0.039	0.021	0.0057	0.041	0.009	0.060	0.006	0.011
Horse feed	0.013	0.0117	0.0054	0.029	0.012	0.027	0.009	0.024
Sheep feed	0.012	0.041	0.0044	0.020	0.008	0.021	0.006	0.022
Chicken feed	0.063	0.016	0.0047	0.026	0.011	0.049	0.008	0.010

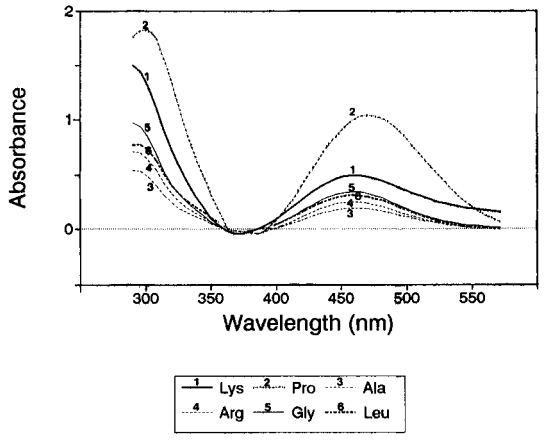

Fig. 4. Spectra of NQS–Lys, NQS–Pro, NQS–Arg, NQS–Ala, NQS–Leu and NQS–Gly derivatives. The concentration of amino acid in all cases was 1×10^{-3} M. See Fig. 2 for other conditions.

constant neither for each sample nor for each amino acid. These amino acids could interfere with the flow injection determination of lysine if univariate calibration would be used because NQS is a general spectrophotometric reagent for amino groups. In a univariate calibration it would be impossible to apply the standard addition method without removing interferences, since there is no exclusive spectral zone for lysine, as can be seen in Fig. 4.

In the present work, however, two multivariate calibration procedures (principal component regression (PCR) and partial least squares regression (PLS)) have been tested in order to avoid the lack of selectivity of the NQS–amino acid derivatives. The use of the whole spectrum as multivariate data will allow the determination of lysine in the feed samples by multivariate calibration since the shape of the spectrum of NQS–LYS derivative differs from the others sufficiently to obtain good estimations. PCR and PLS model the concentrations as function of spectral responses. An advantage of these inverse calibration methods consist in that only the analytes, lysine in this work, must be known. However unknown species or interferences have to be implicitly modelled. This can be achieved by using problem and calibration samples with the same nature, so it involves the use of extract solutions of feed samples for the calibration. Moreover, the composition and the nature of this calibration set allows to take into account the effect of the presence of variable amounts of other amino acids in the extract solutions belonging to the prediction set.

Each sample solution was injected in triplicate and two different types of data files were constructed for their multivariate calibration treatment. The first contained the spectrum of each individual injection (File 1 in Table 3), whereas in the second type the average spectrum of the three injections for each sample was stored (File 2 and File 3 in Table 3). When File 2 was used the calibration was carried out with the six calibration solutions indicated with a footnote c in Table 4 while in the calibration set of File 1 and File 3 the eight additional spiked solutions (prepared from the four solutions indicated with footnote a in Table 4) were also included. The problem solutions were the same in the three cases tested.

PCR and PLS require prior knowledge of the number of principal components (NF), which can be determined by cross validation techniques de-

TABLE 3

% Error defined as in Eqn. 1 for both PCR and PLS algorithms
(NC = number of calibration solutions, NP = number of problem solutions, NF = number of principal components. The data files are described in the text)

Data file	NC	NP	NF	% Error by PCR		% Error by PLS	
				Calibration	Prediction	Calibration	Prediction
File 1	14	13	5	10.6	23.2	6.5	17.6
File 2	6	13	5	0.1	23.2	0	23.3
File 3	14	13	5	10.6	23.0	4.8	14.9

TABLE 4

Concentration of lysine in the extracts of feed samples used in the calibration and prediction sets, determined by the autoanalyzer standard and the flow injection procedures (concentration in mol $l^{-1} \times 10^5$)

Sample solution	Standard method	Flow method
Pig feed 1 [a]	3.04	[b]
Pig feed 1 [a]	2.83	1.71
Pig feed 2 [c]	5.16	4.94
Pig feed 2	5.23	5.78
Pig feed 3 [c]	2.98	2.89
Pig feed 3	3.36	2.22
Pig feed 4 [c]	11.6	11.8
Pig feed 4	13.3	14.1
Pig feed 5	3.16	3.03
Pig feed 5	3.10	4.01
Pig feed 6	4.25	4.63
Pig feed 6	3.60	3.71
Horse feed [c]	1.01	1.08
Horse feed	1.15	1.05
Sheep feed [a,c]	0.96	1.52
Sheep feed [a]	0.97	0.0
Chicken feed [c]	4.72	4.72
Chicken feed	5.06	5.54
Pig feed 7	3.36	3.83
Pig feed 7	3.16	3.47

[a] Sample solutions used to prepare spiked solutions for the calibration set. [b] Do not tested. [c] Sample solutions used in the calibration set.

scribed by Wold [14] (standard error of residuals in the prediction: SEP function), and by the theory of error in factor analysis described by Malinowski [15] (indicator function, IND). The number of principal components in the calibration samples was estimated by plotting the SEP and IND functions. The NF was five for the three files analyzed. These principal components are related to the causes of variation required for the explanation and fitting of the model. Additional factors were rejected because they contained mostly noise and they did not contribute to the improvement of the predictions. In the same way, results became worse when the number of principal components chosen was less than five.

The calibration solutions employed for these multivariate methods were some of the filtered extracts, whose concentration of lysine had been previously determined. The percentage of error, %error, for both calibration and prediction steps is collected in Table 3 and calculated as follows:

$$\%\text{error} = \left[\sum (C_{\text{true}} - C_{\text{calc}})^2\right]^{1/2} / \left(\sum C_{\text{true}}^2\right)^{1/2} \quad (1)$$

where C_{true} is the concentration of lysine found with the autoanalyzer standard procedure and C_{calc} the concentration of lysine obtained by the proposed flow injection method. In this Table 3, results show that the best accuracy is achieved with the PLS algorithm. The calculated values improved both when the eight spiked samples are included in the calibration set and when the average spectrum of each sample injected was used. Table 4 shows the results from File 3 of the flow injection method using PLS, for both prediction and calibration sets, and those obtained by the autoanalyzer standard procedure. It can be seen that the two methods are in good agreement, so the presence of variable amounts of other amino acids in the samples does not have a significant effect in the multivariate determination of lysine. This concordance in addition to the high sample throughput indicate that the proposed method is adequate to perform the analysis of lysine in feed without the need of separating the other amino acids present in the samples.

The authors thank Drs. R. Tauler and A. Izquierdo-Ridorsa and Mr. T. Padró from Analytical Chemistry, and Dr. M. Martínez from Inorganic Chemistry for their help with parts of this work, and to Cooperativa Agropecuaria de Guissona for providing the feed samples. J.S. also thanks to Ministerio de Educación i Ciencia for a FPI grant. This work has been partially financed by DGICYT project PB90-0821.

REFERENCES

1 H. Lingeman and W.J.M. Underberg (Eds.), Detection-oriented Derivatization Techniques in Liquid Chromatography, Marcel Dekker, New York, 1990.
2 I. Molnár-Perl and M. Pintér-Szakács, Anal. Chim. Acta, 257 (1992) 209.
3 M. Hikuma, M. Kawarai, Y. Tonooka and K. Hashimoto, Anal. Lett., 24(12) (1991) 2225.

4 A. Pohlmann, W.W. Stamm, H. Kusakabe and M.-R. Kula, Anal. Chim. Acta, 235 (1990) 329.
5 P.J. Gemperline and A. Salt, J. Chemometr., 3 (1989) 343.
6 K.R. Beebe and B.R. Kowalski, Anal. Chem., 59(17) (1987) 1007A.
7 E.R. Malinowski and D.E. Howery, Factor Analysis in Chemistry, Wiley, New York, 1980.
8 M. Blanco, J. Coello, H. Iturriaga, S. Maspoch, M. Redón and J. Riba, Anal. Chim. Acta, 259 (1992) 219.
9 E.R. Malinowski, J. Chemometr., 6 (1992) 29.
10 M.J.P. Gerritsen, G. Kateman, M.A.J. van Opstal, W.P. Bennekom and B.G.M. Vandegiste, Anal. Chim. Acta, 241 (1990) 23.
11 J. Saurina and S. Hernández-Cassou, Anal. Chim. Acta, 283 (1993) in press.
12 J.C. Miller and J.N. Miller, Statistics for Analytical Chemistry, Ellis Horwood, Chichester, 1984.
13 D.H. Spackman, W.H. Stein and S. Moore, Anal. Chem., 30 (7) (1958) 1190.
14 S. Wold, Technometrics, 20 (1978) 397.
15 E.R. Malinowski, J. Chemometr., 1 (1987) 33.

Analytica Chimica Acta, 281 (1993) 601–605
Elsevier Science Publishers B.V., Amsterdam

Flow-injection spectrophotometric determination of amino acids based on an immobilised copper(II)–zincon system

L. Lahuerta Zamora

Departamento de Quimica, Colegio Universitario CEU, 46113 Moncada, Valencia (Spain)

J. Martínez Calatayud

Departament de Quimica Analitica, Universitat de Valencia, 46100 Burjasot, Valencia (Spain)

(Received 2nd February 1993; revised manuscript received 29th March 1993)

Abstract

The flow-injection spectrophotometric determination of different amino acids was carried out by reaction with copper(II) ions entrapped in a polymeric material and filling a packed-bed reactor; the released copper(II), complexed with the amino acid, reacted with zincon in a basic medium producing a blue colour that was monitored at 600 nm. The method was applied to determine the contents of different amino acids in pharmaceutical formulations. The calibration graph for glycine was linear over the range 0.5–20 μg ml^{-1} with a relative standard deviation of 0.8% ($n = 6$) at 10 μg ml^{-1} and a sample throughput of 108 h^{-1}.

Keywords: Flow-injection; UV–Visible spectrophotometry; Amino acids; Pharmaceuticals

Amino acids are considered to be the main indicators of the nutritional requirements in various pathological states [1]. Amino acids in biological samples are determined by classical ion-exchange chromatography and postcolumn reaction with ninhydrin. A certain number of alternative reagents (fluorescamine, *O*-phthalaldehyde, dansyl chloride, etc.) have been introduced. The titrimetic determination of amino acids in vitamin preparations has been officially recommended [2]. Flow-injection (FI) methods for the determination of glycine with the aid of an atomic absorption spectrometric detector have recently been published; one of them proposes a high-presure assembly due to the presence of finely powdered copper carbonate as a packed-bed reactor [3]; the immobilization by physical entrapment of this reagent served for a low-pressure FI assembly [4].

Packed-bed reactors feature interesting advantages in continuous-flow methodologies [5,6] over homogeneous systems [7–12]. The approaches to the preparation of a solid-bed reagent are usually dictated by its nature and by the analytical purpose of the immobilization. A broad category of reagent immobilization approaches involve the physical confinement of the reagent in a polymeric material [13].

This paper deals with the spectrophotometric determination of amino acids, a technique more usually associated with pharmaceutical analysis than the experimental work was carried out mostly with glycine and the analytical applications were empirically extended to proline, histidine, alanine, leucine and phenylalanine. The procedure

Correspondence to: J. Martínez Calatayud, Departament de Quimica Analitica, Universitat de Valencia, 46100 Burjasot, Valencia (Spain).

is based on the reaction of the amino acid with immobilized copper(II) ions and the released copper(II) is complexed by zincon and monitored spectrophotometrically.

EXPERIMENTAL

Reagents and apparatus

All reagents were of analytical-reagent grade unless indicated otherwise. Aqueous solutions were prepared in deionized water of glycine (Probus), proline (UCB, pure), histidine (UCB, pure), alanine (Scharlau, pure), leucine (UCB, pure), phenylalanine (Tanabe Seiyaki) caffeine (Fluka, pure), acetylsalicylic acid (Panreac, pure), ascorbic acid (Merck) sorbitol (Acofarma, pure), sodium carbonate (Probus), sodium hydroxide (Probus), sodium borate (Panreac), murexide (Panreac), zincon (Panreac, pure) and alizarin red (Scharlau).

The solid-bed reactor was prepared as described previously [4,14] with the aid of $CuCO_3 \cdot Cu(OH)_2 \cdot 2H_2O$ (Panreac). AL-100-A polyester resin solution (Reposa) containing low-molecular-weight polyester chains and a cobalt compound as activating agent of the reaction was used. Ethyl methyl ketone as a catalyst was obtained from Akzo.

Flow-injection assembly

A two-channel (for carrier and reagent) continuous-flow manifold was used with the column between the injection valve and the detector. A Rheodyne Model 5041 sample injector and Gilson Minipuls 2 pump were used. Cu(II)–zincon was determined using a Lambda 16 UV–visible spectrometer (Perkin-Elmer) at a wavelength of 600 nm and provided with an 18-μl flow cell. PTFE tube coils in the FI assembly were of 0.8 mm i.d.

RESULTS AND DISCUSSION

A survey of the literature, with regard to the optimum medium for the reaction of amino acids with the entrapped copper carbonate, led to the preselection of three reagents for the possible spectrophotometric determination of copper(II) ions: alizarin (with maximum absorbance for the formed complex at 500 nm), murexide (480 nm) and zincon (600 nm).

Further preliminary tests were carried with the aid of the flow assembly depicted in Fig. 1a, in which the buffered (borax–NaOH, pH 9.3) sample solution was continuously flowing through the packed-bed reactor (length 13.5 cm), particle size 150–200 μm and copper carbonate-to-resin weight ratio 1:1. The resulting solution then merged with the stream containing 10^{-3} mol l^{-1} of the reagent being tested (also at pH 9.3 buffer) and the spectra of the resulting solutions were recorded. The recorded absorbances (at the wavelength producing the maximum absorbance) were 0.291 for murexide, 0.547 for alizarin red and 0.825 for zincon. Zincon was selected as the spectrophotometric reagent producing the highest outputs.

The influence of pH on the formation of the copper(II)–zincon complex was studied by batch procedures in which the pH of the zincon–copper(II) mixture [25 ml of buffered borax–

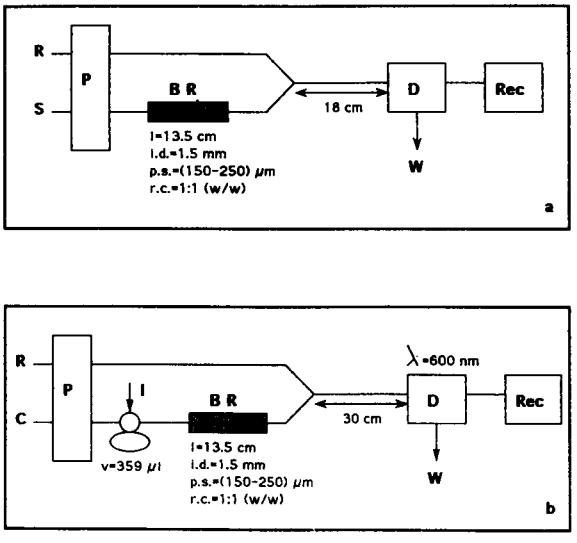

Fig. 1. Continuous-flow manifolds for the determination of amino acids; (a) for preliminary tests and (b) proposed manifold. R = reagent stream; S = sample stream; C = carrier; BR = immobilized copper(II) reactor; D = detector; W = waste; Rec = recorder; for l, i.d., p.s. al r.c., see text.

sodium hydroxide (pH 10.8) solution containing 4×10^{-5} mol l^{-1} of the ligand and 1 ml of distilled water containing 3×10^{-4} mol l^{-1} Cu^{2+}] was adjusted with drops of 1.0 mol l^{-1} HCl (pH meter). The spectra of the resulting solutions were recorded against distilled water. Absorbance values at the maximum, 600 nm (the absorbance of zincon at this wavelength is zero), at various pH values were as follows (pH, absorbance): 5.76, 0.718; 7.88, 0.731; 8.38, 0.738; 9.06, 0.742; 9.60, 0.746; and 10.40, 0.737. pH 9.60 (carrier, reagent and sample solutions) was selected for further work.

The finally proposed FI assembly is depicted in Fig. 1b. The sample volume was 350 μl and flow-rates were 2.7 and 3.4 ml min^{-1} for the carrier and reagent, respectively. For optimization of the zincon concentration, aqueous solutions of zincon were prepared in the range 2×10^{-6}–4×10^{-4} mol l^{-1} and aliquots containing 20 μg ml^{-1} of glycine were injected; transient signals were recorded at 600 nm. On plotting peak-height against zincon concentration a plateau was observed over the range (2.0–4.0) $\times$ 10^{-4} mol l^{-1}. A zincon concentration of 2.0×10^{-4} mol l^{-1} was selected for further work.

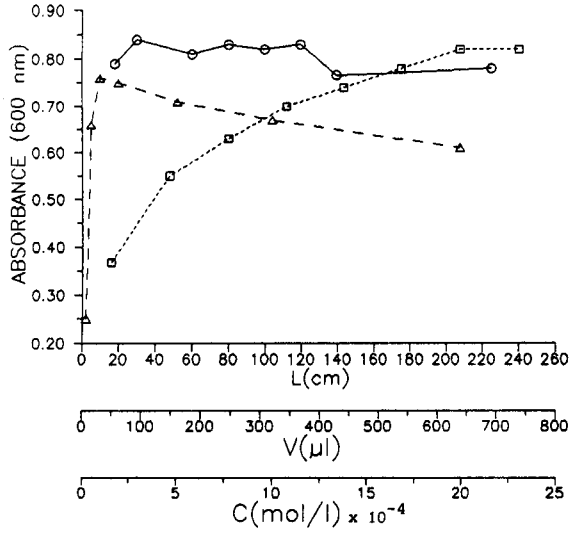

Fig. 2. Influence of chemical and FI parameters on the transient outputs. ○ = length of the reaction coil; □ = sample volume injected; △ = zincon concentration.

TABLE 1

Influence of flow-rates of reagent and carrier streams

Flow-rate (ml min^{-1})		Peak height absorbance at 600 nm
Reagent	Carrier	
0.7	2.1	0.568
1.6	2.1	0.896
3.3	2.1	0.807
5.0	2.1	0.701
6.7	2.1	0.585
3.4	0.8	0.387
3.4	1.9	0.612
3.4	3.2	0.726
0.7	0.8	0.871
1.6	1.8	0.792
3.4	2.7	0.797
5.0	2.7	0.712
6.7	2.7	0.624

The influence of the coil length for the reaction of copper(II) and zincon was studied from 18 to 225 cm, with flow-rates of 2.7 and 3.4 ml min^{-1} for the carrier and reagent, respectively. The results are shown in Fig. 2, from which 30 cm was selected as the most suitable reactor length.

The optimization of the flow-rates of the carrier and reagent was studied in three different sets by (a) varying the flow-rate of the carrier with the flow-rate of the reagent kept constant at 3.4 ml min^{-1}; (b) varying the flow-rate of the reagent with the flow-rate of the carrier kept constant at 2.7 ml min^{-1}; and (c) testing different carrier to reagent flow-rate ratios in the range 0.40–1.14. Table 1 gives the heights of the transient signals obtained. The selected peak corresponded to flow-rates of 2.7 and 3.4 ml min^{-1} for the carrier and reagent, respectively.

The influence of sample volume was studied from 51 to 769 μl, and it was found to be an influential parameter (see Fig. 2). The selected value was that which gave the best compromise between sensitivity (Peak height) and sample throughput (peak base width). A sample volume of 359 μl was selected for further work.

The influence of pH was refined by applying the selected values for the FI assembly in the pH

range 9.7–8.4. A pH of 9.0 (adjusted with sodium tetraborate–hydrochloric acid buffer) gave the highest outputs. The influence of the concentration of the buffer was also tested, from 0.8×10^{-2} mol l^{-1} sodium tetraborate plus 2.8×10^{-3} mol l^{-1} hydrochloric acid to 7.5×10^{-2} mol l^{-1} sodium tetraborate plus 2.0×10^{-2} mol l^{-1} hydrochloride. A solution of 1.25×10^{-2} mol l^{-1} sodium tetraborate and 4.6×10^{-3} mol l^{-1} hydrochloric acid was selected as the optimum.

The re-optimization of zincon concentration was studied from 0.2×10^{-4} to 20.8×10^{-4} mol l^{-1} (see Fig. 2) and resulted in the selection of 1×10^{-4} mol l^{-1} as the optimum concentration.

The study of the influence of temperature up to 75°C was carried out by different experiments: (a) with the carrier container inside the water-bath, (b) with the reagent container inside the water-bath (c) with the packed-bed reactor inside the water-bath. The experiments did not result in an increase in the transient outputs when the temperature was increased, so room temperature was selected for further work.

Analytical applications

A study of the analytical application of the continuous-flow procedures was carried out to establish the application range, reproducibility and sample throughput.

The calibration graph for glycine was linear over the range 0.5–20 μg ml^{-1} and could be described by the equation $A = -0.0231 + 0.0405$[glycine concentration (μg ml^{-1})], with a correlation coefficient 0.9996 ($n = 6$), where A = peak-height absorbance.

A set of 23 different samples containing 10 mg ml^{-1} of glycine were injected into the carrier stream in order to determine the reproducibility (R.S.D.) and sample throughput; the results obtained were 0.85% and 108 h^{-1}, respectively.

The tolerance of the method to other compounds that may be present in typical pharmaceutical samples containing amino acids was investigated by using solutions containing 10 mg ml^{-1} of the amino acid and various concentrations of the interferents up to 500 mg ml^{-1}. Table 2 gives the calculated relative errors; only ascorbic acid resulted in a serious interference.

TABLE 2

Influence of foreign compounds

Interference	Maximum conc. studied (μg ml^{-1})	Relative error (%)
Potassium iodide	500	0.3
Sodium fluoride	500	2.7
Caffeine	100	2.6
Sodium citrate	250	1.7
Sorbitol	500	2.5
Thiamine	100	1.9
Ascorbic acid	20	4.1
Acethylsalicylic acid	100	1.5

The glycine contents in Actilevol phials (from Boizot) and Okal tablets (from Puerto Galiano) were determined. At least five different preparations were analysed and the results compared with those supplied by the manufacturer: Actilevol, declared 500, found 495 mg per phial, relative error 1%, Okal, declared 100, found 97 mg per tablet, relative error 2.9%.

The method was also applied to the determination of the amino acids proline, histidine, alanine, leucine and phenylalanine. Calibration graphs were constructed and the linearity ranges, the regression equations and the corresponding correlation coefficients are given in Table 3.

Conclusions

A spectrophotometric procedure has been developed for the determination of amino acids with application to the analytical control of pharmaceutical formulations. The use of solid reagents enables a simple FIA manifold and the use of a spectrophotometric detector is more common

TABLE 3

Determination of different amino acids

Amino acid	Linear equation (C in μg ml^{-1})	Linearity range (μg ml^{-1})	Correlation coefficient ($n = 6$)
Proline	$0.003 + 0.013C$	0.5–30	0.9999
Histidine	$-0.002 + 0.028C$	0.5–15	0.9998
Alanine	$-0.012 + 0.054C$	0.5–15	0.9999
Leucine	$-0.002 + 0.034C$	0.5–20	0.9996
Phenylalanine	$-0.009 + 0.031C$	0.5–10	0.9999

than atomic absorption spectrometry in pharmaceutical analyses. The developed procedure allows determination of minor concentrations of amino acid: 0.5–20 vs. 10–90 by AAS [4] and a higher sample injection of 108 vs. 40.

REFERENCES

1 H. Galjarrd, Genetic Metabolic Disorders, Elsevier, Amsterdam, 1980.
2 S. Williams (Ed.), Official Methods of Analysis of the Association of Official Analytical Chemists, Association of Official Analytical Chemists, Arlington, VA, 14th edn., 1984.
3 J. Martínez Calatayud and J.V. Garcia Mateo, Analyst, 116 (1991) 327.
4 J.V. Garcia Mateo and J. Martínez Calatayud, Anal. Chim. Acta, in press.
5 J. Ruzicka and A. Aindal, Anal. Chim. Acta, 216 (1989) 243.
6 H.A. Mottola, Quim. Anal., 8 (1989) 119.
7 E.A. Novikov, L.K. Shipgun and Yu.A. Zolotov, Anal. Chim. Acta, 230 (1990) 157.
8 J. Martínez Calatayud, C. Gomez Benito and D. Gaspar Gimenez, J. Pharm. Biomed. Anal., 8 (1990) 667.
9 J. Martínez Calatayud and C. Gómez Benito, Anal. Chim Acta, 231 (1990) 259.
10 G.K. Low and R. Mathews, Anal. Chim. Acta, 231 (1990) 259.
11 M.A. Shakir and A.T. Faizullah, Analyst, 114 (1989) 951.
12 B.F. Band, F. Lázaro, M.D. Luque de Castro and M. Valcarcel, Anal. Chim. Acta, 229 (1990) 177.
13 V. Garcia Mateo and J. Martínez Calatayud, Chem. Anal. (Warsaw), 38 (1993) 1.
14 L. Lahuerta Zamora and J. Martínez Calatayud, Anal. Chim. Acta, 265 (1992) 81.

Analytica Chimica Acta, 281 (1993) 607–610
Elsevier Science Publishers B.V., Amsterdam

Flow-injection spectrophotometric determination of molybdenum(VI) by extraction with quinolin-8-ol

D. Thorburn Burns, M. Harriott and P. Pornsinlapatip

Department of Analytical Chemistry, The Queen's University of Belfast, Belfast BT9 5AG (UK)

(Received 6th April 1993)

Abstract

Molybdenum (0–2.5 μg) may be determined spectrophotometrically at 385 nm after flow-injection extraction into chloroform of the chelate of molybdenum(VI) with quinolin-8-ol. The carrier stream was dilute sulphuric acid, pH 0.85. The injection rate was 20 h^{-1}. The calibration graph is linear up to 10 μg ml^{-1} Mo and the detection limit is 0.11 μg ml^{-1} based on injection volumes of 250 μl. The system has been applied to the determination of molybdenum in low alloy and mild steels.

Keywords: Flow injection; Spectrophotometry; Molybdenum; Quinolin-8-ol

Several air-segmented [1–3] and continuous flow systems [4–10] have been described for the determination of molybdenum in various kinds of samples such as plants, rocks, soils, water and steels. The reaction utilised were those of molybdenum(V) with thiocyanate [4–6], molybdenum(VI) with Tiron [10] and the molybdenum(VI) catalysed oxidation of iodide by hydrogen peroxide [1–3,7–9]. None of the reported catalytic procedures nor that based on Tiron is suitable for the direct determination of molybdenum in steels due to residual interference from iron and common alloying elements. The manual molybdenum(V) thiocyanate liquid–liquid extraction method is satisfactory for steels except at high tungsten to molybdenum ratios [11] but has not been found to be amenable to flow-injection analysis (FIA) for kinetic reasons. Thus it was decided to examine the FIA–liquid–liquid extraction of molybdenum 8-quinolinolate (oxinate), the formation of which was reported by Eberle and Lerner [12] to be selective at low pH. The flow and the reaction conditions have been optimised and the developed system applied to the determination of molybdenum in low alloy steels.

Correspondence to: D.T. Burns, Department of Analytical Chemistry, The Queen's University of Belfast, Belfast BT9 5AG (UK).

EXPERIMENTAL

Apparatus

Absorbances were measured at 385 nm with a Pye-Unicam SP6-550 UV–visible spectrophotometer fitted with a 30-μl special optical glass cell (10 mm optical pathlength) (Hellma) and recorded with a Philips PM 8252A recorder. Solutions were pumped with a fixed speed proportioning pump (Technicon) fitted with Acidflex pump tubing for the organic phase and Tygon pump tubing for the aqueous phase. Samples (250 μl) were injected using an "Omnifit" 6-way injection valve fitted with a by-pass coil. Flow lines were PTFE tubing (0.8 mm i.d.). The flow system is shown diagrammatically in Fig. 1. An Omnifit "Hex" three-way connector was used for mixing

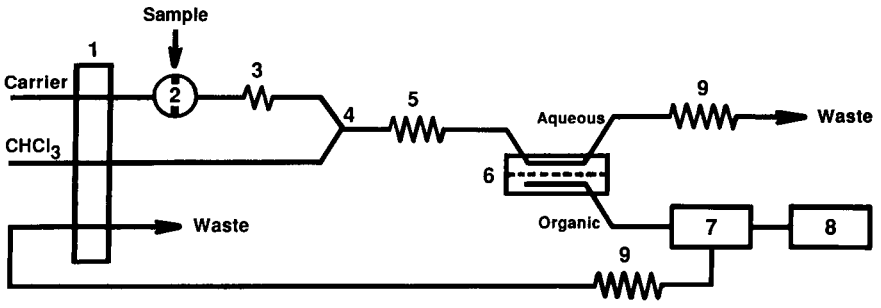

Fig. 1. Schematic diagram of flow injection system: 1 = proportioning pump; 2 = injection valve, 250 μl; 3 = mixing coil, 0.75 m × 0.8 mm i.d.; 4 = mixing point, 'Hex'; 5 = extraction coil, 1.5 m × 0.8 mm i.d.; 6 = phase separator; 7 = spectrophotometer; 8 = recorder; 9 = restrictor coil, 2.5 m × 0.8 mm i.d. Flow-rates at pump: carrier, dilute sulphuric acid, pH 0.85, 0.70 ml min^{-1}; chloroform, 0.82 ml min^{-1}; organic waste, 0.80 ml min^{-1}.

aqueous and organic phases. The two phases were separated using a membrane phase separator, based on the design of Al-Wehaid [13] and fitted with a 1-μm pore size PTFE membrane (Zefluor, Gelman Sciences).

Reagents

All reagents were of analytical-grade unless stated otherwise. Doubly distilled water was used throughout.

Molybdenum(VI) stock solution (1000 μg ml^{-1})

This was prepared by dissolving 2.1463 g of sodium molybdate, $Na_2MoO_4 \cdot 2H_2O$ (AnalaR, Hopkin and Williams, dried to constant weight at 120°C) in 1000 ml of water.

Quinolin-8-ol solution (6%, w/v)

This was prepared by dissolving 18.2 g of quinolin-8-ol (99%, Aldrich) in 8 ml of concentrated sulphuric acid diluted to 100 ml, then made up to 300 ml with water. The pH was adjusted to 0.85 by careful drop-wise addition of concentrated sulphuric acid.

Buffer solution, pH 0.85

This was prepared by mixing 500 ml of 2.4% (v/v) hydrochloric acid with 90 ml of 1.5% (w/v) potassium chloride, adjust if necessary to pH 0.85 by dropwise addition of concentrated hydrochloric acid, with thorough mixing after each addition.

Dilute sulphuric acid solution, pH 0.85

This was prepared by adding 10.0 ml of concentrated sulphuric acid (AnalaR, BDH) to 250 ml of water and then diluting to 1000 ml. The pH was adjusted to 0.85 by dropwise addition of concentrated sulphuric acid with thorough mixing after each addition.

General procedure

Samples and standards were examined using the flow system and conditions shown in Fig. 1. Peak heights were measured. At an injection rate of 20 h^{-1} the recorded peaks were sharp and the base-line quite stable.

Procedure for steel samples

Dissolve an accurately weighed sample (to contain 300–800 μg Mo) in 5 ml of 20% (v/v) sulphuric acid in a 100-ml Kjeldahl flask, warming gently until the dissolution is almost complete. Add 5–10 drops of concentrated nitric acid and boil to expel any nitrous fumes. Cool, add 7–8 ml of distilled water and digest till clear. Cool and partially neutralise, just to the point of formation of hydrated iron(III) oxide, by addition of 0.3–0.4 g of sodium hydroxide in pellet form. Cool. Transfer quantitatively to a 25-ml volumetric flask and make up to volume with distilled water.

Aliquots of samples (5 ml) and of standards (up to 5 ml) were prepared for analysis by addi-

tion of 7 ml of 0.85 pH buffer, 5.0 ml of 6% quinolin-8-ol solution and dilute sulphuric acid, pH 0.85, to make up the total volume to 20 ml. After mixing the pH should be checked to be within 0.85–1.0.

The solutions should be used within 1 h of preparation. The peak height absorbances were measured using the flow system and conditions given in Fig. 1. The amount of molybdenum present was evaluated from a calibration graph (0–10 μg Mo ml^{-1}).

Examination of the main experimental variables

The experimental variables were examined in a univariate manner using a fixed sample concentration and sample volume (5 μg Mo(VI) ml^{-1}; 250 μl).

TABLE 1

Effect of diverse ions on the determination of molybdenum (VI) (1.25 μg Mo)

Ion	Ion/Mo(VI) (w/w)	Peak-height change (%)
Mn(VII)	2500:1	0
Co(II)	50:1	0
Pb(II)	50:1	0
Zn(II)	10:1	0
	50:1	+20
Cu(II)	10:1	0
	50:1	+7
Al(III)	100:1	0
	500:1	+10
Sn(II)	1:1	0
	5:1	+100
Fe(II)	50:1	0
	100:1	0
	500:1	0
	1000:1	+10
Fe(III)	100:1	0
	350:1	0
	500:1	−10
Ni(II)	50:1	0
Cr(III)	50:1	0
	100:1	−4
V(V)	1:1	0
	2:1	+6
W(VI)	2.5:1	0
	5:1	+12

TABLE 2

Determination of molybdenum in steels

Type	B.C.S. Steel No.	Molybdenum content% (w/w)	
		Certified	Found [a]
Mild steel	323	0.100 (0.095–0.105)	0.093 ± 0.002
	325	0.16 (0.15–0.16)	0.155 ± 0.012
Ni–Cr–Mo steel	189	0.36 (0.34–0.373)	0.363 ± 0.005
	219/1	0.48 (0.47–0.50)	0.475 ± 0.008
	219/3	0.60 (0.59–0.61)	0.602 ± 0.049
Low alloy steel	251/1	1.57 (1.54–1.61)	1.506 ± 0.039
	254	1.29 (1.24–1.36)	1.292 ± 0.043
	256	0.535 (0.52–0.55)	0.519 ± 0.017
	258	0.425 (0.415–0.44)	0.425 ± 0.010

[a] Values of 5 replicates ± 95% confidence limits.

The quinolin-8-ol concentration was varied between 0.5 to 2.0% (w/v). The peak heights were constant for samples buffered to pH 0.85 in the range 1.0–2.0%. A concentration of 1.5% was used in subsequent work.

The pH was varied in the range 0.5–1.2 by addition of nitric, hydrochloric or sulphuric acid to the molybdenum(VI) solution in the presence of 1.5% quinolin-8-ol. The peak heights increased with pH; sulphuric acid gave the highest peaks at pH > 0.8. The absorbance for molybdenum increased with pH over the range 0.5–0.90 and was constant thereafter up to pH 1.2. Iron(III) oxinate extracts above pH 0.95 and hence it is necessary to work below this pH to avoid interference from iron(III). Careful control of pH to be 0.90 ± 0.05 was found to give satisfactory results.

The effect of variation of the length of the extraction coil on peak heights was examined using 5 μg ml^{-1} Mo(VI) samples containing 1.5% quinolin-8-ol buffered at pH 0.85. Peak heights increased with tube length up to 1 m and were then constant. An extraction tube length of 1.5 m was used thereafter.

The possible interference of various ions was checked for the determination of 5 μg Mo(VI) ml^{-1}. The results are summarised in Table 1. The only ions of interest in steel analysis were vanadium(V) and tungsten(VI).

RESULTS AND DISCUSSION

A linear calibration graph was obtained over the range 0–10 μg Mo(VI) ml^{-1}. For the determination of 5 μg ml^{-1} the relative standard deviation was 1.7% ($n = 10$) and the detection limit ($3 \times$ baseline noise) was 0.11 μg ml^{-1}. The results for the determination of molybdenum in British Chemical Standard (BCS) steels (Table 2) agree well with the certificate values.

Matrix iron at ratios of 1000:1 does not interfere if partially oxidised as in the sample preparation procedure herein. At moderate adverse ratios of tungsten or vanadium to molybdenum, prior separation of molybdenum is necessary using, for example, thiocyanate and extraction into isoamyl acetate [14]. The quinolin-8-ol was added to the samples and not to the carrier stream to avoid clogging at the connectors.

One of the authors (PP) wishes to thank Kasetsart University for leave of absence and the DuPont Science Grant made to DTB for financial support. The authors are grateful for the assistance given by the Bureau of Analysed Samples.

REFERENCES

1 R. Fuge, Analyst, 95 (1970) 171.
2 E.G. Bradfield and J.F. Stickland, Analyst, 100 (1975) 1.
3 B.F. Quin and P.H. Woods, Analyst, 104 (1979) 552.
4 H. Bergamin F°., J.X. Medeiros, B.F. Reis and E.A.G. Zagatto, Anal. Chim. Acta, 101 (1978) 9.
5 F.J. Krug, O. Bahia F°., and E.A.G. Zagatto, Anal. Chim. Acta, 161 (1984) 245.
6 H. Bergamin F°., F.J. Krug, B.F. Reis, J.A. Nobrega, M. Mesquita and I.G. Souza, Anal. Chim. Acta, 214 (1988) 397.
7 Fang Zhao-Lun and Xu Shu-Kun, Anal. Chim. Acta, 145 (1983) 143.
8 M. Trojanowicz, A. Hulanicki, W. Matuszewski, M. Pałys, A. Fuksiewicz, T. Hulanicka-Michalak, S. Raszewski, J. Szyller and W. Augustyniak, Anal. Chim. Acta, 188 (1986) 165.
9 L.C.R. Pessenda, A.O. Jacintho and E.A.G. Zagatto, Anal. Chim. Acta, 214 (1988) 239.
10 K. Yoshimura, S. Matsuoka and H. Waki, Anal. Chim. Acta, 225 (1989) 313.
11 A.G. Fogg, J.L. Kumar and D.T. Burns, Analyst, 100 (1975) 311.
12 A.R. Eberle and M.W. Lerner, Anal. Chem., 34 (1962) 627.
13 A. Al-Wehaid, Ph.D. Thesis, University of Hull, 1987.
14 G.F. Kirkbright, T.S. West and C. Woodward, Talanta, 13 (1966) 1645.

Analytica Chimica Acta, 281 (1993) 611–620
Elsevier Science Publishers B.V., Amsterdam

Polypyrrole-based potentiometric biosensor for urea

Part 1. Incorporation of urease

S.B. Adeloju and S.J. Shaw

Centre for Electrochemical Research and Analytical Technology, Department of Chemistry, University of Western Sydney, Nepean, P.O. Box 10, Kingswood NSW 2747 (Australia)

G.G. Wallace

Intelligent Polymer Research Laboratory, Department of Chemistry, University of Wollongong, P.O. Box 1144, Wollongong NSW 2500 (Australia)

(Received 22nd February 1993; revised manuscript received 26th April 1993)

Abstract

A method is described for the incorporation of urease into a polypyrrole film by galvanostatic polymerisation on gold-coated plastic films and solid gold electrodes. The presence of urease in the polypyrrole film was verified by x-ray photoelectron spectroscopy, amino acid analysis, scanning electron microscopy and cyclic voltammetry. The enzyme activity in the polypyrrole–urease film was confirmed by its catalytic conversion of urea to carbon dioxide and ammonia. The use of both spectrophotometric and potentiometric methods for the detection of the catalytic activity of the polypyrrole–urease film and their potential use for the determination of urea is discussed.

Keywords: Biosensors; Potentiometry; Enzymatic methods; Conducting polymer; Polypyrrole; Urea; Urease

Urease is an important enzyme in biological systems where it plays a catalytic role in the conversion of urea to carbon dioxide and ammonia, as illustrated below:

$$NH_2CONH_2 \xrightarrow[H_2O]{\text{Urease}} CO_2 + 2NH_3$$

The use of this catalytic reaction for the development of a sensor for urea is of significant interest. However, most of the approaches that have been adopted, so far, for the development of such a biosensor for urea have mainly focused on the incorporation of the enzyme into commercially available polymer membranes such as teflon [1], tetrafluoroethylene [2], and some polymer gels, where it induces the catalytic conversion of urea, as indicated above. Unfortunately, there are several disadvantages and difficulties associated with these methods of enzyme incorporation. One alternative approach for the incorporation of the enzyme into a polymer backbone which has become very popular in recent years is based on the electropolymerisation of pyrrole on various electrode materials [3–5]. Some of the distinct advantages that could be accomplished by the incorporation of urease into a polypyrrole polymer backbone include better electrical properties due to the conductivity of polypyrrole film, ease of polymerisation and incorporation of the enzyme, relatively fast and inexpensive polymerisation procedure and readily available fresh polymer film.

Correspondence to: S.B. Adeloju, Centre for Electrochemical Research and Analytical Technology, Department of Chemistry, University of Western Sydney, Nepean, P.O. Box 10, Kingswood, NSW 2747 (Australia).

While this approach is now widely used for the incorporation of glucose oxidase [6–9], its use for urease has been somewhat limited.

In this paper the incorporation of urease into a polypyrrole polymer backbone based on galvanostatic polymerisation on solid gold electrodes or gold coated plastic films will be investigated. Verification of the presence of the enzyme in the polypyrrole film will involve the use of scanning electron microscopy (SEM), amino acid assay (AAA), cyclic voltammetry (CV) and x-ray photoelectron spectroscopy (XPS). The catalytic role of the enzyme in the polypyrrole-urease film, based on the conversion of urea to carbon dioxide and ammonia, will be examined by a spectrophotometric method [10] and chronopotentiometry. The potential use of the catalytic activity of the polypyrrole–urease film for the detection of urea will also be demonstrated.

EXPERIMENTAL

Electrode preparation for electropolymerisation

The gold coated plastic film was pretreated with ethanol and then washed thoroughly with Milli-Q water. Gloves were worn at all times when handling the substrate and polymer films. Gold electrodes with a surface area of 0.28 cm^2 were used for cyclic voltammetric measurements.

Electropolymerisation of the conductive polypyrrole–urease film

The electrolyte (either water or sodium nitrate) and aqueous 0.49 M pyrrole were mixed together to give the desired concentration and then the solution was purged with nitrogen for 10 min, to remove any oxygen from the solution. A three electrode voltammetric cell was used for all electropolymerisation procedures. Gold coated plastic film or solid gold electrodes were used as the working electrode, while platinum or gold coated plastic film were employed as the auxiliary electrode, and either SCE or Ag/AgCl was used as the reference electrode.

The electropolymerisation was performed galvanostatically using a current density of 0.25 mA cm^2 and a polymerisation period of 20 min, unless otherwise stated. Samples for amino acid analysis and XPS were electropolymerised for 60 min. All polymers were produced without stirring.

Instrumentation

A potentiostat/galvanostat designed and built within the Faculty of Science and Technology at the University of Western Sydney, Nepean, was employed for the electropolymerisation. The galvanostat was connected to a computer controller (Kaga monitor and Micro Bee keyboard) and an Epson LX-400 printer. A Kyowa (Model RFB-8) light microscope with a camera attached for both coloured or black and white photographs was used. A Waters Picotag amino acid analyser was used for the determination of amino acids. The surface analysis equipment consists of a triple chamber multitechnique analysis instrument (manufactured by Kratos, Manchester). XPS (0.8 eV energy resolution) was employed. The cyclic voltammograms were performed on an AMEL polarographic analyzer (Model 433) attached to an IBM compatible computer (Microwaves *touch-1*) and an Epson printer (Super 5, EP-1201 A). A Shimadzu UV–visible recording spectrometer (UV-2100) was used to monitor the Nesslerization reaction. The spectrometer was connected to a Shimadzu X-Y plotter (FPG-302-003-SS).

Chemicals and standard solutions

The pyrrole purchased from Sigma was distilled under vacuum prior to use and was stored covered with aluminium foil in the refrigerator to prevent UV degradation. The urease and standard amino acids were also purchased from Sigma and kept in the refrigerator at 3°C.

The sodium and potassium nitrate were of analytical reagent (AR) grade purity and 2.0 M stock solutions were prepared and later diluted to give the required standard solutions. A 3.0 M KCl solution (AR grade) was used as a filling solution for the reference electrode (Ag/AgCl).

All chemicals such as urea, NH_4Cl, $HgCl_2$ and NaOH were of AR grade purity. Nessler's reagent was prepared based on the standard method for the examination of water and waste water [10]. A 5.0 M urea stock solution was prepared and di-

luted daily to give a 1.0 M standard urea solution and a 0.05 M EDTA solution (pH 6) was used to prevent calcium and magnesium precipitation. Milli-Q water was used for all sample preparation.

Procedure

The polymer film used for the amino acid analysis was grown on the gold-coated plastic film and was then removed from the substrate, weighed on a microbalance and finally transfered into a hydrolysis tube. The samples were then frozen at −3°C until analysed. Initially the amino acids were hydrolysed for one hour in 6.0 M HCl at 150°C. The amino acids were separated by ion exchange on a column consisting of 6-μm beads of polystyrene cross-linked with 8% divinylbenzene and derivatised to form a sulphonated cation exchanger in the ionic form. Elution was achieved via a stepped sequence of three sodium citrate based buffers which increase in pH from 3.29 to 4.52 and in a cation concentration from 0.20 to 1.40 M. Detection was achieved by post-column derivatisation with ninhydrin/dimethylsulfoxide followed by detection of absorption peaks at 570 and 440 nm.

The procedure for cyclic voltammetry involves rinsing the polymer several times with Milli-Q water to remove any weakly bound urease molecules, after electropolymerisation. The electrode was then placed in a nitrogen purged electrolyte (either sodium or potassium nitrate). The experimental parameters used for the cyclic voltammetric analysis are listed below: deoxygenation period: 300 s, number of cycles: 20, scan rate: 50 mV s^{-1}, initial potential: 400 mV and final potential: −700 mV.

The enzyme activity in the polypyrrole–urease film was determined by a modified Nesslerization procedure [10]. 1 ml of Nessler's reagent and 1 ml of EDTA solution was added to the standard ammonium chloride solution and this was allowed to develop colour for 10 min. The absorbance was measured at 480 nm against a blank solution containing 50 ml of water and 1 ml of both Nessler's reagent and EDTA solution. A calibration graph was produced from these known ammonium ion concentrations. After electropolymerisation of polypyrrole–urease, 0.045 g of the plastic film and polymer was weighed into a sample vial.

For the catalytic reaction, 2 ml urea (1.0 M) and 1 ml of EDTA solution was added to a sample vial, containing 0.045 g of polypyrrole–urease film and it was allowed to react for 10, 20, 35 or 60 min (with stirring). After the required reaction period, 1 ml of the Nessler's reagent was added and was left to develop for 10 min, before performing the spectrophotometric measurements. The blank solution contained 2 ml of urea and 1 ml of EDTA but no polypyrrole–urease film. Controls were monitored to ensure that the polypyrrole film did not cause an increase in the absorbance. Also, a control for urease only was performed to examine if the enzyme (containing amino groups) reacted with Nessler's reagent. From the calibration graph the concentration of ammonia produced from the catalytic reaction can be determined and this can be related to the concentration of urea in the solution.

RESULTS AND DISCUSSION

Galvanostatic film formation

The stability and ease of polymerisation of polypyrrole films can be investigated by chronopotentiometric studies. Figure 1 illustrates the chronopotentiograms for polypyrrole–nitrate and polypyrrole–urease film. The initial potential produced for polymerisation of a polypyrrole–nitrate film was 606 mV, but a much higher potential (2489 mV) was obtained for the deposition of polypyrrole–urease onto the gold substrate. This indicates that the polypyrrole–urease film was more difficult to polymerise than the polypyrrole–nitrate film. The higher potential resulting from polymerisation of the enzyme is also indicative of the high resistance and low conductivity of the enzyme solution. The enzyme, as a macromolecule, does not produce a conductive solution when dissolved in water without the addition of an electrolyte. Consequently, a very large cell potential (iR drop) is produced when this solution is used to form the polypyrrole film. The high cell potential (2489 mV) produced dur-

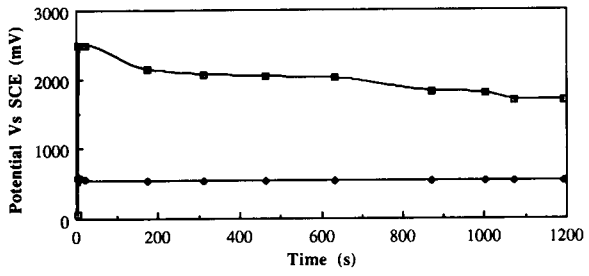

Fig. 1. Chronopotentiogram for (□) polypyrrole–nitrate; (♦) polypyrrole–urease. The pyrrole concentration was 0.49 M, 0.10 M sodium nitrate and 500 μg ml^{-1} urease. A current density of 0.25 mA cm^{-2} for 20 min on gold electrode was employed.

ing the electropolymerisation of the polypyrrole–urease film may be contributed by the rather complex matrix in which the enzyme is present. Nevertheless, the reduction of this potential is necessary to ensure that it does not have a deleterious effect on the activity of the enzyme.

Additionally, there was very little change in the potential as a function of time during the growth of the polypyrrole-nitrate film (as shown in Fig. 1). In contrast the polypyrrole–urease film showed a significant reduction in potential as the polymerisation period increased. This observation indicates that the polypyrrole–urease film became more conductive with the increase in the polymerisation period. Although the conductivity of the polypyrrole–urease film is comparatively lower than that of polypyrrole–nitrate film, nevertheless, evidence of conductivity in the former film is significant for the development of a biosensor for urea.

The pretreatment of the enzyme solution by filtration through a 541 Whatman filter paper reduced the cell potential during the galvanostatic growth to 1000 mV. The dramatic change in the cell potential when the enzyme solution is filtered prior to electropolymerisation suggests

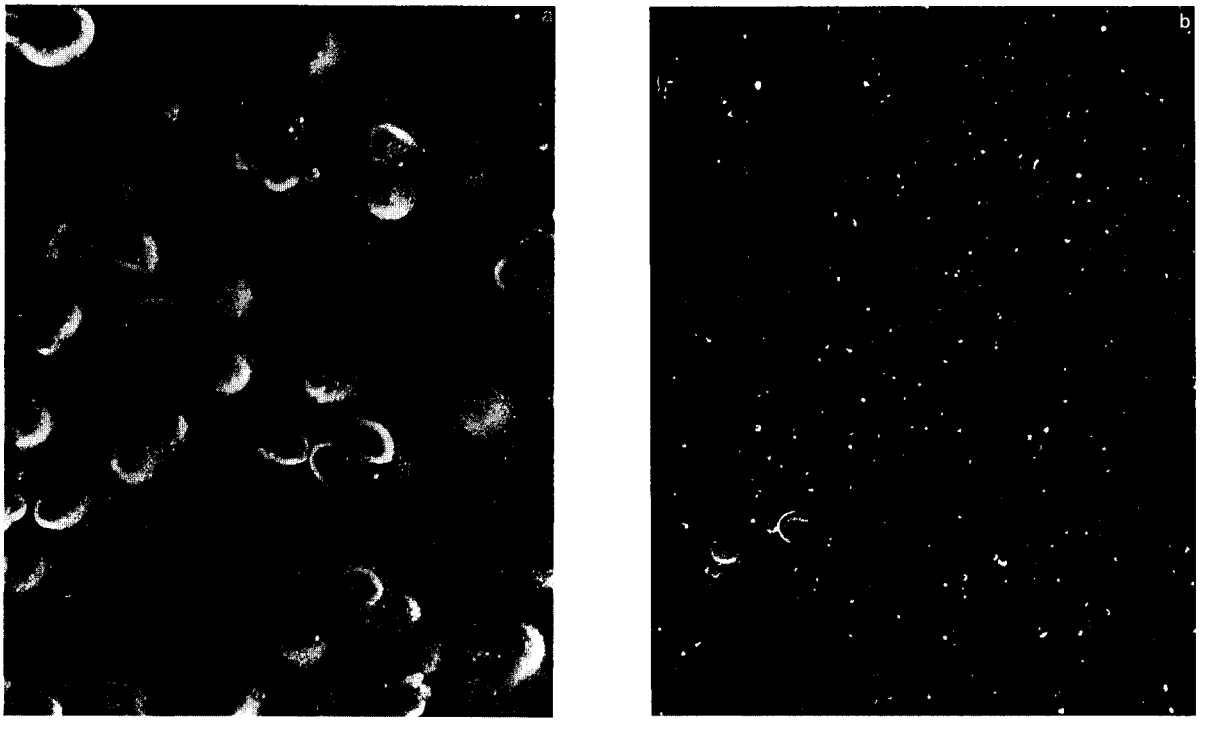

Fig. 2. (a) A scanning electron micrograph of a polypyrrole–nitrate film, prepared with 0.1 M $NaNO_3$ and 0.49 M pyrrole for 20 min with a 0.25 mA cm^{-2} current density on gold coated plastic. Magnification 400 ×. (b) Scanning electron micrograph of a polypyrrole–urease film, prepared from a 2000 μg ml^{-1} urease solution and 0.49 M pyrrole for 20 min with a 0.25 mA cm^{-2} current density on a gold coated plastic. Magnification 400 ×.

that other substances in the urease solution contributed to the high potential obtained in the unfiltered medium. The lower cell potential obtained in the filtered urease solution would ensure that the destruction of the catalytic activity of the enzyme does not occur.

Microscopic evidence of urease incorporation into polypyrrole

The examination of the gold-coated plastic surface after the galvanostatic polymerisation revealed that a vast morphological change occurred when the polypyrrole film was prepared in the presence of different counter ions. The polypyrrole–nitrate film gave, as shown in Fig. 2a, three distinct layers under the scanning electron microscope: a gold coated plastic film, a uniform thin polypyrrole–nitrate film with nuclei present and propagated polypyrrole–nitrate nuclei, which were spherical and sometimes clumped together.

Figure 2b illustrates the morphological change which occurred when nitrate was replaced by urease. The most obvious difference was the size of the propagated polypyrrole nuclei. The enzyme membrane had a uniform thin layer of polypyrrole film, but no large propagated polypyrrole–nitrate nuclei were visible in the polypyrrole film, compared to the nitrate film (Fig. 2a). These observations indicate that the nitrate ion is a much better counter ion than the urease and hence enabled the formation of a thicker and more uniform polymer. On this basis, it appeared that there were two reasons for difference in the polymer morphology for the polypyrrole–urease film and polypyrrole–nitrate film. Firstly, the urease solution was less conductive than the nitrate electrolyte and hence film formation was more difficult in this medium. Secondly, as the enzyme is a macromolecule and it can therefore interfere with the polymerisation reaction because of steric hinderance, the formation of polypyrrole–urease will be more difficult. The chronopotentiometric studies also indicate that the polypyrrole–urease film was not easily formed, as indicated by the much higher potential obtained during the galvanostatic formation of the polypyrrole–urease film.

Presence of amino acids in the polypyrrole–urease film

A major source of evidence for the incorporation of urease into the polypyrrole film during galvanostatic polymerisation can be obtained by monitoring the presence of typical amino acids associated with the enzyme. This can be accomplished by performing amino acid analysis on the polypyrrole–urease film. Table 1 illustrates that the polypyrrole–nitrate film contains on average, less than or equal quantities of amino acids than those present in the blank solution (acid only). The ratio of amino acids in the polypyrrole–nitrate films compared to the blank were generally less than or equal to 1.0. This, in effect, represents the typical background level found in amino acid analysis. In contrast, both polypyrrole–urease film formed with 2000 and 500 μg ml^{-1} urease had up to 10-fold and 4.5-fold the quantity of amino acids, respectively. Also, both polypyrrole–urease films contained similar ratios of amino acids. Hence, it would appear that the use of a 500 μg ml^{-1} urease solution was adequate for the incorporation of the enzyme into the polypyrrole film. However, as the effect of the

TABLE 1

Ratio of amino acid in polypyrrole–urease film (Asx, D/N = Asn + Asp; Glx, E/Q = Glu + Gln)

Amino acid	Ratio of amino acid compared to the blank		
	Polypyrrole–nitrate (0.1 M)	Polypyrrole–urease (2000 μg ml^{-1})	Polypyrrole–urease (500 μg ml^{-1})
Asx, D/N	0.8	9.3	9.9
Glx, E/Q	0.9	5.5	5.6
Ser, S	1.0	5.0	6.0
Gly, G	1.1	5.3	5.5
His, H	0.5	4.5	5.1
Arg, R	1.0	2.9	3.6
Thr, T	1.2	4.5	5.5
Ala, A	0.6	2.7	3.0
Pro, P	1.1	3.6	4.5
Tyr, Y	0.8	3.2	3.6
Val, V	0.9	4.4	5.6
Met, M	1.1	1.5	1.3
Cys, C	–	–	–
Ile, I	0.9	4.9	6.0
Leu, L	0.8	3.9	4.7
Phe, F	0.8	4.1	5.7
Lys	0.9	7.9	8.5

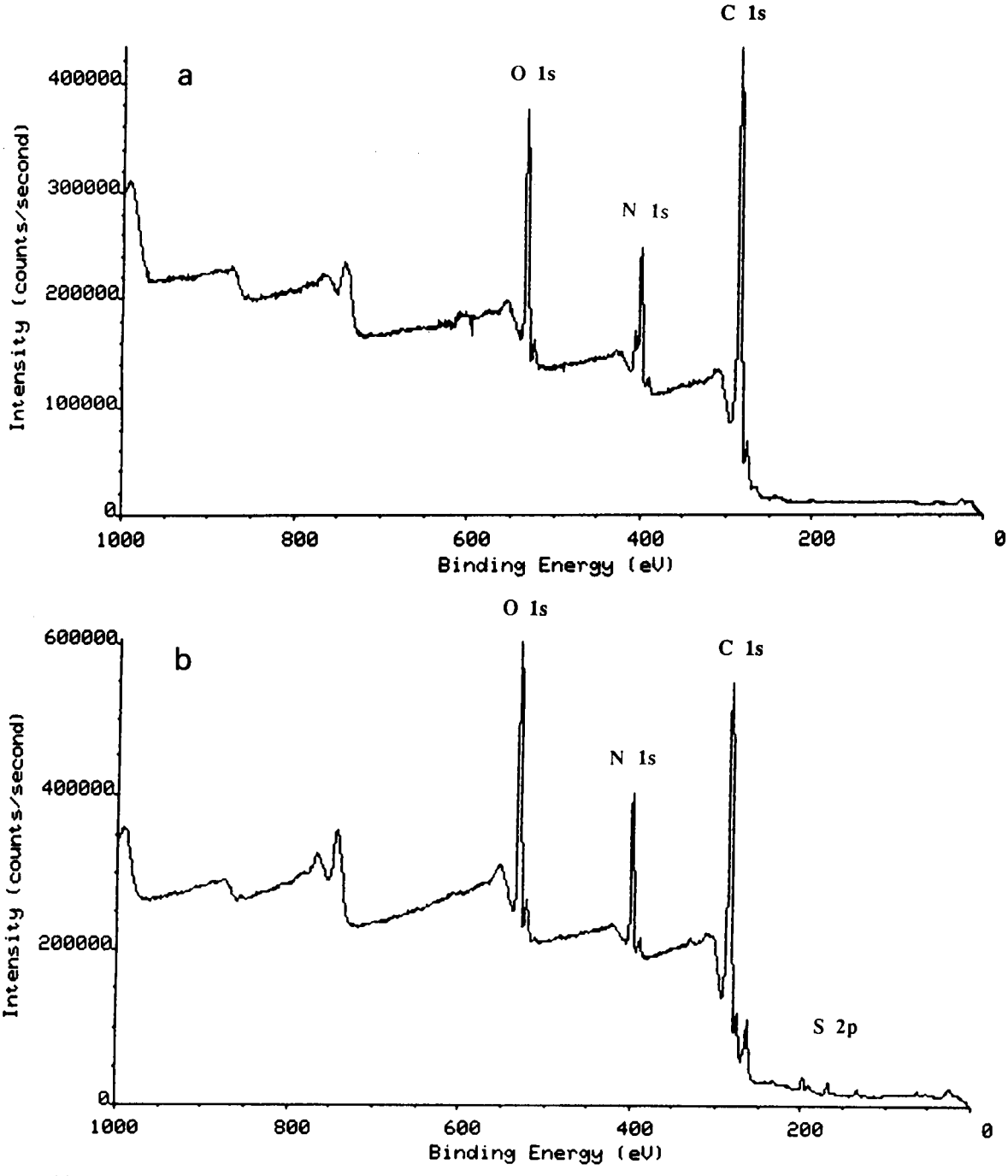

Fig. 3. (a) XPS wide-scan spectrum of a polypyrrole–nitrate film. Prepared from 0.1 M $NaNO_3$ and 0.49 M pyrrole with a current density of 0.25 mA cm^{-2} for 20 min, on gold coated plastic. (b) XPS wide-scan spectrum of polypyrrole–urease film. The film was prepared from 2000 $\mu g\ ml^{-1}$ urease and 0.49 M pyrrole for 60 min with a 0.25 mA cm^{-2} current density on gold coated plastic.

TABLE 2

Amino acid composition of polypyrrole–urease films prepared with filtered and unfiltered urease solutions

Amino acid (mg g^{-1})	Filtered solution	Unfiltered solution
Asx, D/N	3.01	0.77
Glx, E/Q	3.01	0.8
Ser, S	1.02	0.27
Gly, G	0.89	0.35
His, H	0.60	0.15
Arg, R	1.15	0.21
Thr, T	0.68	0.19
Ala, A	0.85	0.25
Pro, P	0.60	0.14
Tyr, Y	0.47	0.14
Val, V	0.76	0.17
Met, M	0.22	0.05
Ile, I	0.59	0.13
Leu, L	1.36	0.26
Phe, F	0.47	0.11
Lys, K	1.07	0.24
Total (mg g^{-1})	16.75	4.19

enzyme concentration on its activity in the polymer is not known, this requires further investigation with a suitable detection system. The other advantage of a less concentrated urease solution is a lower resistance which enables better electropolymerisation and hence may provide better enzyme activity. Until the latter is proven it is suffice to conclude that both polypyrrole–urease films contained the typical amino acids associated with the presence of the enzyme and this confirms its incorporation by the galvanostatic polymerisation method.

The pretreatment of the urease solution also increased the amount of enzyme incorporated into the polypyrrole matrix. The magnitude of protein incorporated into the polymer was monitored by the concentration of amino acids found in the polymer and therefore the total concentration of amino acids in the film. Table 2 shows a comparison between the concentration of amino acids present in polypyrrole films formed with and without filtration of the enzyme solution. The results indicate that the filtered urease solution contained approximately four times more amino acids than the polymer formed with an unfiltered solution. This may be due to the unfiltered solution containing other particulate matter that prevents polymerisation of the monomer, such as cellulose, other proteins or macromolecules. Therefore, the pretreatment of the urease solution has a double advantage, it increases the concentration of urease in the polymer and it decreases the chance of enzyme deactivation by dropping the cell potential to 1000 mV.

XPS of the polypyrrole–urease film

The use of a surface analytical technique such as XPS is significant for identifying the surface composition of the polypyrrole films. The ability to perform a diverse range of elemental analysis by this technique should enable the identification of typical elemental composition of both the polypyrrole backbone and that of the incorporated enzyme. Consequently, two samples (polypyrrole–nitrate and polypyrrole–urease) were analysed by XPS, in order to establish the presence of the enzyme in one of these films. The XPS analysis of the polypyrrole–nitrate film (no enzyme present) based on a wide scan of the polymer, as illustrated in Fig. 3a, indicates the presence of oxygen (533 eV), nitrogen (400 eV) and carbon (283 eV). These responses were expected since polypyrrole contains C–C bonds and N–C bonds, and the nitrate ion contains N–O bonds.

The wide scan XPS analysis for the polypyrrole–urease film, illustrated in Fig. 3b, shows the usual C 1s, N 1s and O 1s peaks, similar to those of the polypyrrole–nitrate film (film without enzyme) and therefore characteristic of the polypyrrole backbone. However, three additional peaks were identified between 100 to 200 eV, which are indicative of Cl, S and P. In the wide scan it was evident that these three peaks were extremely small, in comparison to the C, N and O intensities, and appeared initially to be due to background noise. However, further investigation with a narrower scan (220 to 120 eV) revealed that these were definite responses for Cl, S and P. The evidence of sulfur in the XPS analysis is of main interest because all enzymes contain amino acids that have sulfur bonds and this is clearly not present in the polypyrrole–nitrate film (without

enzyme), as evident in Fig. 3a, where no sulfur response was apparent around 169 eV. It appears that P and Cl are present as impurities from either the enzyme or the electropolymerisation solution.

Evidently, the S 2p response provides conclusive indication that sulfur is present, and it was more than nine times larger than the background noise. However, it appears that the S 2p peak was a combination of two unresolved peaks. These peaks may be due to different sulfur bonding in the enzyme. In conclusion, the identification of sulfur in the XPS analysis provides additional evidence that urease was incorporated into the polypyrrole backbone during the galvanostatic polymerisation of pyrrole in the presence of the enzyme.

Cyclic voltammetry on the polypyrrole–urease film

The cyclic voltammogram obtained for polypyrrole–nitrate film in a 0.1 M $NaNO_3$ electrolyte is illustrated in Fig. 4a. The characteristic oxidation and reduction couple of the polypyrrole appeared at 117 and 50 mV (Vs Ag/AgCl), respectively. However, when urease was substituted for the nitrate ion, the cyclic voltammetric behaviour of the film was altered (Fig. 4b), resulting in two reduction peaks at 2 mV and −530 mV, respectively. The first peak was characteristic of the reduction of polypyrrole (even though the potential has shifted by approximately 50 mV), while the second peak is associated with either the insertion of the enzyme or the insertion of a cation into the polypyrrole conductive film. Charge balance on the enzyme may be induced by a cation such as Na^+, while an anion such as NO_3^- may act as the negatively charged species. Hence, the exchange of NO_3^- with the urease will induce an unbalanced charge and consequently the cation (Na^+) may enter the polymer to balance the charge. In effect, if the second reduction peak (−530 mV) was due to a cation effect, the cyclic voltammetric measurement on this film in the presence of a different cation (K^+) and the same anion (NO_3^-) will alter the behaviour of the polypyrrole–urease film due to the differences in the cation size. The effect of the presence of two

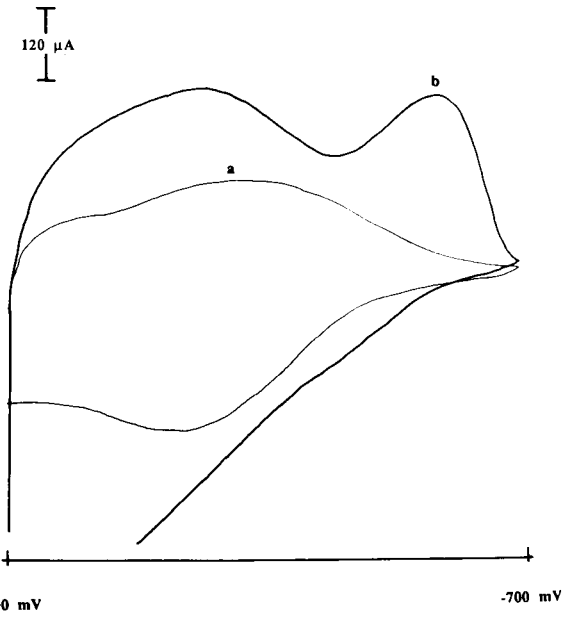

Fig. 4. Cyclic voltammogram of some polypyrrole films: (a) polypyrrole–nitrate film, 0.1 M $NaNO_3$ and 0.49 M pyrrole, polymerised for 20 min with a current density of 0.25 mA cm^{-2} on a solid gold substrate. (b) Polypyrrole–urease film, 2000 $\mu g\ ml^{-1}$ urease and 0.49 M pyrrole, polymerised for 20 min at a current density of 0.25 mA cm^{-2}.

different cations on the cyclic voltammogram of this film is clearly illustrated in Fig. 5. The shift of the potential of the polypyrrole backbone peak by about 100 mV and that of the second reduction peak by about 171 mV is indicative of the cation effect. This therefore suggests that the second reduction peak may be due to a cation effect and not associated with the direct response of urease. Also, as there were no oxidation peaks obtained for polypyrrole–urease film, it is clearly evident that the system was irreversible.

The cyclic voltammetric evidence of the charge balance effect induced by cations can nevertheless be related to the presence of the enzyme in the film. The cation insertion was only necessary to balance the charge within the polymer when the nitrate ion exchanges position with the enzyme. Hence, this second peak can be used as a screening test for the incorporation of urease into the polypyrrole film. The cyclic voltammetry performed on the film can be used to determine indirectly whether or not the urease has been

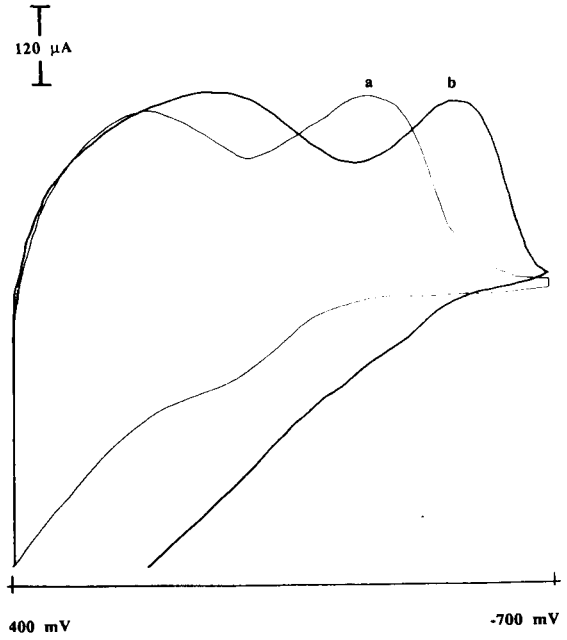

Fig. 5. Cyclic voltammogram of polypyrrole–urease in different electrolytes. Prepared as Fig. 4b: (a) 0.1 M $NaNO_3$ (b) 0.1 M KNO_3 for the cyclic voltammetric electrolyte.

incorporated into the polypyrrole conductive film, as evident by the presence of two distinct reduction peaks.

Enzyme activity of the polypyrrole–urease film

The evidence of enzyme activity on the polypyrrole–urease film can be obtained chemically by the investigation of its catalytic role in the conversion of urea to ammonia and carbon dioxide. The detection of such a process electrochemically is somewhat difficult as both carbon dioxide and ammonia are not directly electroactive. In an indirect way the accomplishment of this may be possible through derivatisation or electrochemical monitoring of other related effects such as a change in pH, conductivity or resistance. An immediate solution to this problem, however, is to detect the presence of ammonia spectrophotometrically, using a Nesslerization procedure. As expected, the blank solution made up of urea and EDTA did not develop any coloured interfering species at the wavelength of 480 nm used for this measurement. However, the control solution made up of EDTA, polypyrrole–urease film and buffer developed a constant yellow coloration, and on average it gave a positive interference which corresponds to about 3.28 $\times 10^{-5}$ M NH_3, but the concentration of ammonia in the solution did not increase with increasing time. This indicates that a catalytic process is not involved in the generation of the interference. On the other hand, the addition of the polypyrrole–urease film to the urea and EDTA solution resulted in an increase in the concentration of NH_3 with increasing time. Evidently, the catalytic role of the enzyme in the polypyrrole–urease film increased as expected with increasing time, resulting in an increase in the catalytic products as illustrated in Fig. 6. At the end of 60 min, about eight times the concentration of ammonia was produced in the reacting solution compared to the control solution. This confirms that the polypyrrole–urease film produced by galvanostatic polymerisation maintained enzyme activity. However, no response was evident when the polypyrrole–urease film was used as a potentiometric sensor. It appears therefore that the spectrophotometric technique was more sensitive than potentiometry. Evidently, in order to detect a potentiometric change for the catalytic decomposition of urea, a much higher concentration of urease would need to be entrapped into the polypyrrole film.

Potentiometric sensing of urea

The incorporation of a much higher concentration of urease into the polypyrrole film, based on

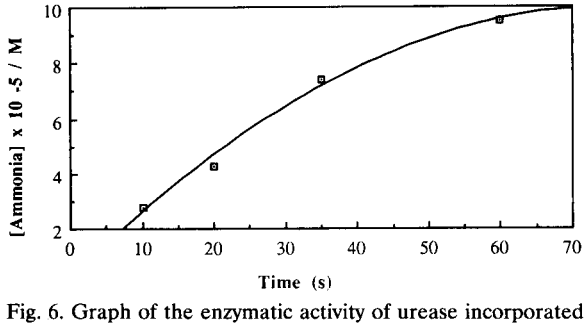

Fig. 6. Graph of the enzymatic activity of urease incorporated in a polypyrrole conducting film. The activity of the enzyme was monitored by the production of ammonia as a function of time.

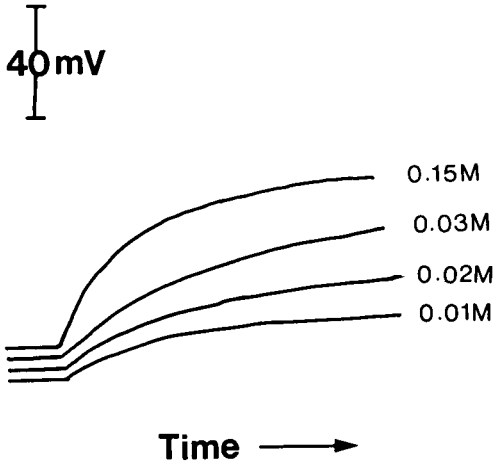

Fig. 7. Effect of urea concentration on the response of polypyrrole–urease biosensor, after pretreatment of the enzyme solution. Conditions were the same as Fig. 1, except 4000 μg ml^{-1} urease was employed and polymerisation was for only 3 min.

the pretreatment of the urease solution, enabled the sensing of urea with the polypyrrole–urease film. Figure 7 illustrates the effect of an increasing concentration of urea as a function of potential change. Clearly, an increase in the urea concentration caused a corresponding increase in the potential change. This potentiometric response was not obtained without the pretreatment of the urease solution. Further optimisation of the polypyrrole–urease film is necessary for the development of a potentiometric biosensor for urea. This is reported in Part 2 [11].

Conclusion

The results obtained in this study has demonstrated that urease has been successfully incorporated into the polypyrrole conductive polymer. The evidence obtained for the incorporation of the enzyme include a change in the polymer morphology as confirmed by SEM, the presence of amino acids in the polypyrrole–urease film, identification of sulfur atoms in the XPS spectrum and an additional cyclic voltammetric response due to the incorporation of cations into the film to maintain a charge balance as the nitrate ion replaces the urease in the polymer. Also spectrophotometric evidence clearly reveals that the enzyme was active in the conversion of urea to carbon dioxide and ammonia, thus enabling the determination of urea in solution. An increase in the concentration of enzyme loaded into the conductive polymer was achieved by pretreatment of the urease solution and consequently, the polypyrrole–urease film responded potentiometrically to an increasing concentration of urea.

The authors are grateful to the University of Western Sidney, Nepean, for the provision of research support and an Australian Postgraduate Research Award for this project. Many thanks to Don Barnett and Kim Yip for the amino acid analysis at CSIRO Division of Food Technology, Ryde and to Dr. Robert Lamb at the University of New South Wales for the XPS analysis.

REFERENCES

1 G. Palleschi and M. Mascini, Anal. Lett., 21 (1988) 1115.
2 M. Mascini and G. Guilbault, Anal. Chem., 49 (1977) 795.
3 T. Matsue, N. Kasai, M. Narumi, M. Nishizawa, H. Yamada and I. Uchida, J. Electroanal. Chem., 300 (1991) 111.
4 P. Janda and J. Weber, J. Electroanal. Chem., 300 (1991) 119.
5 Y. Kajiya, R. Tsuda and H. Yoneyama, J. Electroanal. Chem., 301 (1991) 155.
6 W. Schuhmann, R. Lammert, B. Uhe and H.L. Schmidt, Sensors Actuators, B1 (1990) 537.
7 J.R. Li, M. Cai, T.F. Chen and L. Jiang, Thin Solid Films, 180 (1989) 205.
8 M. Umana and J. Waller, Anal. Chem., 58 (1986) 2979.
9 N.C. Foulds and C.R. Lowe, J. Chem. Soc., Faraday Trans., 1 (1986) 82.
10 L.S. Clesceic, A.E. Greenberg, R. Rhodes Thussell, Standard Methods for the Examination of Water and Waste Water, American Public Health Association, Washington, DC, 17th edn., 1989.
11 S.B. Adeloju, S.J. Shaw and G.G. Wallace, Anal. Chim. Acta, 281 (1993) 621.

Analytica Chimica Acta, 281 (1993) 621–627
Elsevier Science Publishers B.V., Amsterdam

Polypyrrole-based potentiometric biosensor for urea

Part 2. Analytical optimisation

S.B. Adeloju and S.J. Shaw

Centre for Electrochemical Research and Analytical Technology, Department of Chemistry, University of Western Sydney, Nepean, P.O. Box 10, Kingswood, NSW 2747 (Australia)

G.G. Wallace

Intelligent Polymer Research Laboratory, Department of Chemistry, University of Wollongong, P.O. Box 1144, Wollongong, NSW 2500 (Australia)

(Received 22nd February 1993; revised manuscript received 26th April 1993)

Abstract

A novel potentiometric biosensor for urea, based on the entrapment of urease into a polypyrrole film, has been developed via galavanostatic film formation. The electrochemical polymerization was achieved by the application of a current density of 0.5 mA cm^{-2} to a working platinum disc electrode for 3 min in a solution containing 0.5 M pyrrole and 4000 $\mu g\ ml^{-1}$ urease. The optimum conditions for the reliable performance of this sensor were 1 mM phosphate buffer at pH 7.0 and 35°C. A Nernstian response was observed for increasing concentration of urea in the linear range of 0.5 to 100 mM. Trace concentrations of Hg^{2+} and K^+ were both found to inhibit the response of the biosensor.

Keywords: Biosensors; Potentiometry; Enzymatic methods; Enzyme electrode; Urea; Urease; Polypyrrole

Urea is a byproduct which is often monitored in blood to provide some indication of diagnosing kidney diseases [1]. The monitoring procedures for this substance usually involves the enzyme-catalysed decomposition of urea to ammonium ion and carbon dioxide. One of the decomposition products, usually ammonium ion, is measured to determine the concentration of urea in the sample. The enzyme urease which is often present in most biological systems plays a very important role in this process by catalysing the decomposition reaction.

Correspondence to: S.B. Adeloju, Centre for Electrochemical Research and Analytical Technology, Department of Chemistry, University of Western Sydney, Nepean, P.O. Box 10, Kingswood, NSW 2747 (Australia).

With the advent of enzyme based biosensors, several approaches for detecting urea have been proposed. Most of the early work in this area have involved the immobilization of urease on silicon–nonactin disc membranes which are sensitive to ammonium ions [2]. Since then several other approaches for the production of biosensors for urea based upon pH, air gap, ammonia gas and tungsten electrodes have been reported [3–5]. Most of these are based on the incorporation of the enzyme into polymer membranes such as PTFE, polymer gels, fluorocarbon, and indirect use of polypyrrole. Other recent approaches for the determination of urea include the use of a photometric fibre optics fluorescence detection system. Despite these developments there are several disadvantages and difficulties associated

with the existing biosensor for urea, particularly with the enzyme incorporation. Further development in the immobilization of urease on suitable sensing media is therefore necessary.

In Part 1 [6], we proposed a new approach for the incorporation of urease into a polypyrrole polymer backbone based on galvanostatic polymerization on both platinum and gold surfaces. The presence of the enzyme in the polypyrrole film was verified by scanning electron microscopy, amino acid analysis, cyclic voltammetry and x-ray photoelectron spectroscopy. However only a small amount of the enzyme was incorporated into the polypyrrole by this approach. The limitation in incorporating large quantities of urease has now been somewhat overcome by pretreatment of the enzyme prior to the electropolymerization.

In this paper, a novel potentiometric biosensor for urea based on the immobilization of urease in the polypyrrole film by galvanostatic polymerization is reported. The optimization performance of the sensor involved careful consideration of important factors such as urease and pyrrole concentration, magnitude of applied current density, temperature, pH, buffer concentration and choice of electrode substrate. Also, the influence of some organic and inorganic interferences were examined.

EXPERIMENTAL

Electropolymerization of the polypyrrole–urease film

Platinum, gold and glassy carbon electrodes were used as the substrate for the electropolymerization and entrapment of the enzyme; a 0.5 M pyrrole–4000 μg ml^{-1} urease solution was employed (unless otherwise stated). A three-electrode voltammetric cell was used for all electropolymerization. Platinum, gold and glassy carbon disc electrodes (diameter 3 mm) were used as the working electrodes and Pt and SCE were the auxiliary and reference electrode, respectively. A current density of 0.5 mA cm^{-2} was applied between the working and auxiliary electrode for a period of 3 min, unless otherwise stated.

Instrumentation

A potentiostat/galvanostat designed and built within the Faculty of Science and Technology at the University of Western Sydney, Nepean, was employed for the electropolymerization. The galvanostat was connected to a computer controller (Kaga monitor and Micro Bee keyboard) and an Epson LX-400 printer.

Chemicals and standard solutions

The pyrrole and urease were purchased from Sigma. Pyrrole was distilled under vacuum prior to use and was stored covered with aluminium foil in the refrigerator to prevent UV degradation. Urea and other reagents were of analytical reagent grade purity and 2.0 M stock solutions were prepared where necessary and later were diluted to give the required standard concentration. The urease solution was prepared by dissolving an appropriate amount into water and this solution was prefiltered through a 541 Whatman filter paper prior to use [6].

Procedure

The potentiometric measurements were performed with a working electrode (Pt coated polypyrrole–urease film) and a reference electrode (SCE). A TPS Lab Analyser (Model 440) connected to an ICI chart recorder (DP 600 Dual Pen Recorder) was used to monitor the potential change.

RESULTS AND DISCUSSION

Optimization of the biosensor for urea

Effect of urease and pyrrole concentration. Two types of effects were observed, as illustrated in Fig. 1, when increasing concentration of urease was used as the "counter ion" for the polymerization of polypyrrole. Bare platinum causes the maximum change in potential. As platinum responds to a large number of analytes, there is some advantage in covering the surface with polypyrrole–urease to improve the selectivity of the sensor for urea. Urease concentration of 200 and 500 μg ml^{-1} caused a decrease in potential change because of the limitation of diffusion by

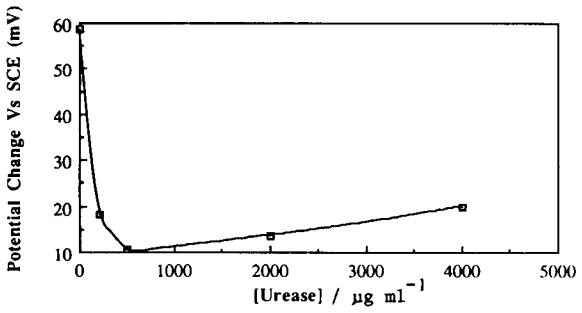

Fig. 1. Effect of the urease concentration. The following experimental conditions were maintained: [urea] = 57 mM in 1 mM phosphate buffer (pH 7 at 25°C) and the response time was 10 min. The polypyrrole films were formed with varying concentration of urease in 0.5 M pyrrole with a current density of 1 mA cm^{-2} for a period of 2 min.

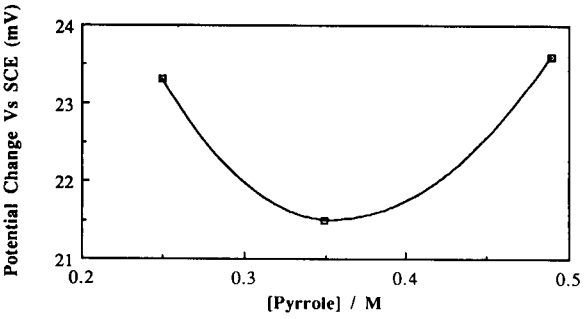

Fig. 2. Effect of pyrrole concentration on the potential change of the sensor. Experimental conditions were the same as Fig. 1 except the concentration of urease was 4000 mg l^{-1} and the pyrrole concentration was changed.

the polypyrrole–urease film on the platinum working electrode. The 500 μg ml^{-1} urease film produced a smaller increase in potential change compared to the 200 mg l^{-1} urease film. This may be due to the presence of a higher concentration of enzyme which balances the charge of the polypyrrole, thus enabling the formation of a thicker film. However, as the concentration of urease was increased to 4000 mg l^{-1} the change in potential decreased possibly due to an increase in film thickness. In contrast, the potential change increased with increasing concentration of urease due to an alteration in the conductivity of the film. The platinum disc electrodes were not completely covered with the polypyrrole–urease film when the electropolymerization was performed in solutions containing less than 500 mg l^{-1} urease. At lower urease concentration (200 mg l^{-1}) the films were much thinner and the response was not due to the conductivity changes in the polypyrrole film, but results mainly from the response of the bare platinum electrode to urea.

The increasing pyrrole concentration had very little effect between 0.25–0.50 M, as illustrated in Fig. 2. However, 0.50 M pyrrole was choosen as the optimum concentration because the enzyme and pyrrole in this solution could be reused up to 6 times. On the other hand, lower pyrrole concentrations did not enable the optimum reuse of the enzyme solution as many times.

Effect of current density and polymerization period. Figure 3 shows that the use of a current density of 0.5 mA cm^{-2} for the electropolymerization gave the best potentiometric response. At a current density of 0.6 mA cm^{-2} or greater, the potential change was lower, possibly because of the rapid polymerization process and the incorporation of less enzyme into the film. At lower current densities, the rate of polymerization was slow and the amount of enzyme incorporated into to the film was lower than the use of 0.5 mA cm^{-2}. A current density of 0.5 mA cm^{-2} was therefore employed for the electropolymerization.

The effect of polymerization time on the potentiometric response is illustrated in Fig. 4. Generally, polymerization periods less than 3 min resulted in an inadequate coverage of the platinum and the majority of the potential change

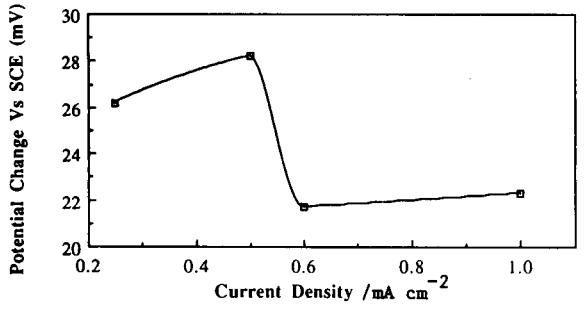

Fig. 3. Effect of current density for polypyrrole–urease film formation. Experimental conditions were the same as Fig. 2, except [pyrrole] = 0.50 M and the current density was varied.

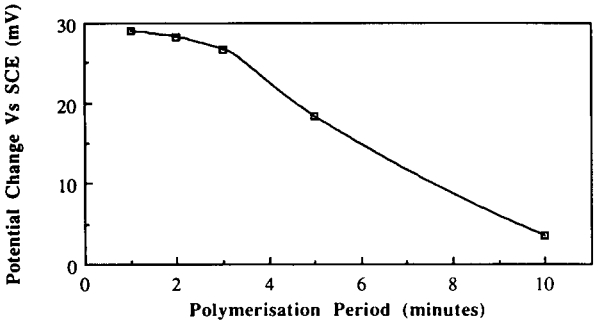

Fig. 4. Influence of polymerization period during film growth. The experimental conditions were the same as Fig. 3, except the polymerization period was varied and a constant current density f 0.5 mA cm^{-2} was maintained.

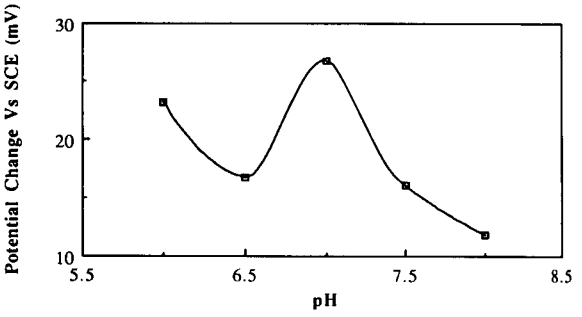

Fig. 5. Effect of pH. The following conditions were used for the polymerization procedure; 0.50 M pyrrole and 4000 mg l^{-1} urease dissolved in water. The film was galvanostatically formed with a current density of 0.50 mA cm^{-2} for 3 min. The potentiometric measurements were performed with a 1 mM phosphate buffer at 25°C with 57 mM urea in solutions with varied pH.

was produced by the bare electrode. Periods greater than 3 min provided adequate coverage of the platinum electrode with the polypyrrole–urease film. However, beyond a polymerization period of 3 min the resulting potential change decreased considerably. This was due to the creation of a diffusion barrier by the thicker polymer film, which caused a reduction in the potential change for urea. Therefore, a polymerization period of 3 min was employed for the electropolymerization of the polypyrrole–urea film.

Influence of pH. The pH of the medium used for measuring urea was altered and the resulting effect on the potential change of the biosensor is given in Fig. 5. The maximum potential change for urea was obtained at pH 7.0. This pH has been cited previously as optimum for the catalytic activity of urease in the conversion of urea to carbon dioxide [7,8]. Solutions buffered to pH 7.0 with phosphate buffer were used for all other measurements.

Effect of temperature. The effect of temperature on the performance of the biosensor was investigated and the resulting effect on the potential change is illustrated in Fig. 6. The optimum temperature was found to be 35°C, similar to that previously reported by other workers [9]. Generally, as the temperature increases the rate of the reaction also increases and hence the response increases. However, for enzyme systems at temperatures above the optimum temperature the protein can be denatured. This was evident in Fig. 6 where above 35°C the potential change was not as great. However, above 40°C the change in potential again increased possibly due to a change in the structure of the polypyrrole film at relatively high temperatures, i.e., a change in porosity of the conducting polymer. The optimum temperature of 35°C was therefore employed for the potentiometric measurements.

Effect of buffer concentration. Figure 7 illustrates the effect of the buffer concentration on the sensor response. The increasing buffer concentration resulted in a decrease in the potential change. It appears that the higher buffering capacity of the more concentrated buffer solution hinders the effect of the catalytic process in the sensor. Therefore, a very weak buffer was neces-

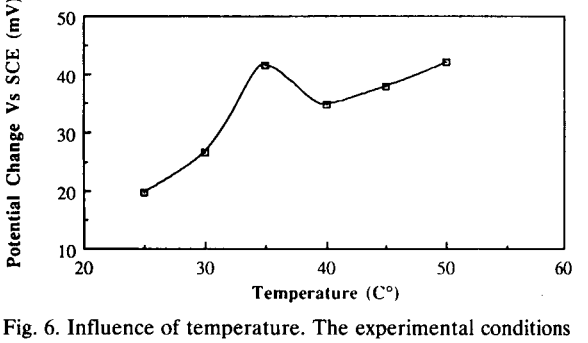

Fig. 6. Influence of temperature. The experimental conditions were the same as Fig. 5, except the temperature was varied and the pH was maintained at 7.0.

sary to enable the potentiometric response to be measured. Thus, the utilization of the lowest buffer concentration (1 mM) provided the best condition for the attainment of the maximum potential change. Lower concentrations of buffer were not investigated as the buffer capacity was not sufficient to cause a change in the electrode potential due to the alteration of the pH by the presence of other substances.

Choice of electrode substrate. The influence of the substrate on urea response was investigated for three different electrode surfaces covered with a polypyrrole–urease film. The best signal was obtained on a platinum-coated polypyrrole–urease electrode. Glassy carbon and gold-coated polypyrrole–urease films did not produce a significant change in potential. The urea response was about 8 times less sensitive on the glassy carbon electrode than on the platinum electrode, while the response for the gold electrode was about 13 times less sensitive. Platinum-coated polypyrrole–urease electrodes were therefore employed for all other experiments.

Influence of the urea concentration. The Nernstian behaviour of urea for the polypyrrole–urease biosensor at various concentrations was investigated. Figure 8a reveals that the potential change increased with increasing concentration of urea. There appeared to be a linear response within 0.5–500 mM. Upon further investigation a distinct linear response was observed between 0.5 and 100 mM urea, as illustrated in Fig. 8b. A potential change of 17.5 mV per decade was obtained, but it is difficult to predict the predominating redox reaction because the catalytic process is complex, involving the conversion of ammonia to ammonium ions, while simultaneously establishing an equilibrium between carbon dioxide, hydrogen carbonate ions and carbonate ions, as well as changes in conductivity occuring within the electroactive polypyrrole film.

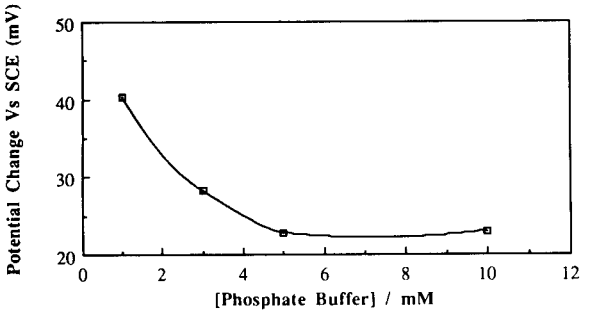

Fig. 7. Effect of buffer concentration as a function of the change in potential. The experimental conditions were the same as Fig. 6 except the phosphate buffer concentration was varied and the pH was maintained at 7.0.

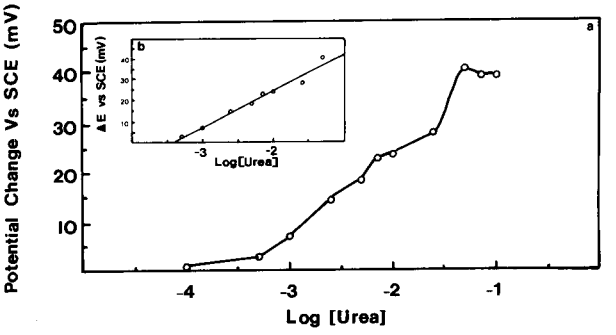

Fig. 8. Nernstian response for log [urea] as a function of potential change. The optimum conditions for polypyrrole–urease biosensor consists of; 0.5 mA cm^{-2} for 3 min in a 0.50 M pyrrole and 4000 mg l^{-1} urease solution. The potentiometric response was monitored in a 1 mM phosphate buffer, pH 7.0 at 35°C with varying concentration of urea. (a) Saturated response; (b) linear concentration range.

Interfering species

Effect of potassium and mercury(II) ions. Figure 9a shows that the presence of potassium ions drastically decreased the biosensor response to urea. Initially, it was assumed that the suppression was caused by the chloride ion from the potassium chloride employed in this study but it has been recently reported that both potassium and sodium ions inhibit the activity of urease [10]. The addition of 250 mg l^{-1} of KCl to a solution containing 57 mM urea decreased the response by 20%, but the same response remained fairly constant in the presence of greater than 500 mg l^{-1}. The use of the biosensor for the determination of urea in samples will therefore require the removal of potassium and sodium ions or the use of standard additions.

Also, it has been well known that mercury(II) ions and other heavy metal ions can inhibit the activity of urease [10]. Figure 9b illustrates the depressive influence of mercury(II) ions on the

response to urea. Evidently, trace levels of these ions decreased the response of the sensor to urea. The presence of 20 mg l^{-1} mercury(II) ions resulted in a 25% decrease in potential change, and the addition of 150 mg l^{-1} of mercury(II) ions produced a 92% suppression of the response. Furthermore, a linear relationship was observed between the extent of suppression and the mercury(II) concentration between 0 and 100 mg l^{-1}. It may therefore be possible to also use the urea biosensor for the determination of trace concentrations of mercury(II) ions, although other heavy metal ions, such as Ag^{+} and Cu^{2+} are likely to interfere.

Effect of proteins on the biosensor. The interference of a protein (human serum albumin, HSA) on the urea biosensor was investigated. Generally, proteins adsorb onto the polypyrrole/platinum surface and interfere by blocking the surface of the polymer. Such adsorption decreases the acccessibility of the polymer surface to other analytes. However, the presence of HSA up to 500 mg l^{-1} in the test solution did not interfere with the biosensor response to urea. It can therefore be assumed that other proteins would also not interfere.

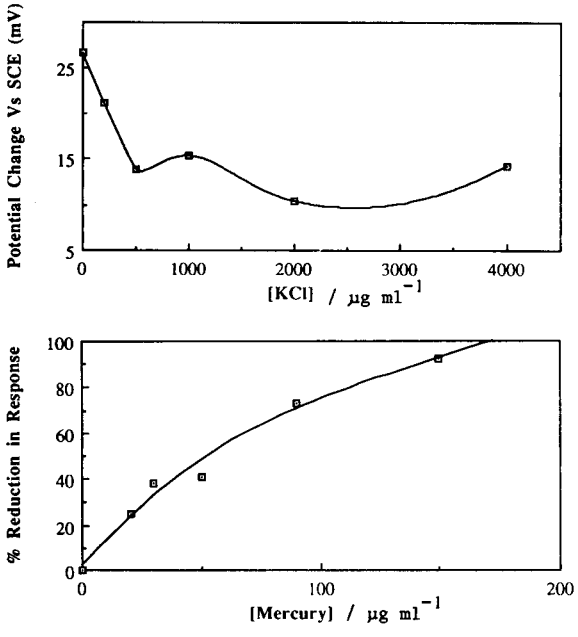

Fig. 9. Inhibitory effect of (top) potassium ions and (bottom) mercury(II) ions on the urea response. The experimental conditions were the same as Fig. 8, except a constant concentration of 57 mM urea was employed.

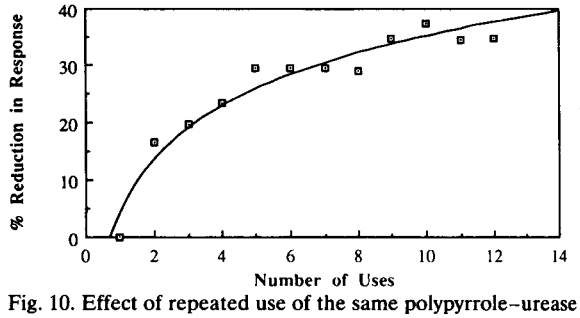

Fig. 10. Effect of repeated use of the same polypyrrole–urease electrode. The experimental conditions were the same as Fig. 9, except a constant concentration of urea was employed (57 mM).

Stability of the biosensor

Figure 10 illustrates the main disadvantage of the polypyrrole-based urea biosensor, viz. the inability to obtain the same response upon re-use of the same sensor. This may be due to poisoning of the polypyrrole–urea film by urea, which may bond strongly to the polymer and decrease the number of free active sites. Or it may reflect on the rate of consumption of the immobilised enzyme in the polpyrrole and hence indicate that less active enzyme is available for the subsequent measurement of urea. One way of increasing the lifetime of the immobilised enzyme is to use the biosensor in a flowing system so that the urea is only in contact with the polypyrrole film for short periods. This would result in less destruction of the biosensor and improve the ability to obtain similar response with further reuse. However, the use of the sensor in a flowing system will require either a more sensitive detection method or an array of sensors to enhance the response to urea.

Analytical applications

The potential application of the biosensor to the determination of urea in samples is highly dependent on the achievable limit of detection, linear concentration range, the recovery efficiency and possible interferences. Most of these have been discussed in earlier parts of this paper. Although, no attempts are reported in the pre-

TABLE 1

Recovery study for urea with the polypyrrole biosensor

Amount added (mg l^{-1})	Amount found by biosensor (mg l^{-1})	%Recovery [a]
0	0	100±1
12	12	100±3
24	24	100±4
48	49	102±5

[a] Mean±S.D., $n = 6$.

sent study to apply the biosensor to real samples, a reasonable indication of its suitability for such purpose can be gained by investigating the recovery efficiency in simulated samples.

The results in Table 1 indicate that the use of the potentiometric polypyrrole biosensor is adequate for the determination of 0–50 μg ml^{-1} urea. The % recoveries are in the 100–102% range and the standard deviation of 1–5% obtained for the various concentrations of urea in the solutions are reasonable. These results show that the biosensor can be used for the determination of urea in a simple matrix. However, in complex sample matrices such as blood, special consideration will need to be given to sample pretreatment. Such consideration can be extensive and complex, and this aspect is currently being investigated in our laboratory. The results will be reported in Part 3 [11].

Conclusions

A novel approach for the rapid construction of a biosensor for urea has been successfully demonstrated. The biosensor, based on the immobilisation of urease in a polypyrrole film, had a linear calibration range of 0.5 to 100 mM urea. Although, the response of the sensor to urea was inhibited by both mercury(II) and potassium ions, it was not affected by HSA. The advantage of this biosensor over previously developed sensors include ease of polymerization and enhanced electrical properties due to the conductive matrix.

The authors are grateful to the University of Western Sydney, Nepean for the provision of research support and an Australian Postgraduate Research Award for this project.

REFERENCES

1 J.H. Eckfeldt, A.S. Levine, C. Greiner and M. Kershaw, Clin. Chem., 28 (1982) 1500.
2 S. Butt and K. Cammann, Anal. Lett., 25 (1992) 1597.
3 R. Tor and A. Freeman, Anal. Chem., 58 (1986) 1042.
4 Y.J.Wang, C.H. Chen, G.H. Hsiue and B.C. Yu, Biotechnol. Bioeng., 40 (1992) 446.
5 G. Palleschi, M. Mascini, E. Martinez-Fabregas and S. Alegret, Anal. Lett., 21 (1988) 1115.
6 S.B. Adeloju, S.J. Shaw and G.G. Wallace, Anal. Chim. Acta, 281 (1993) 611.
7 L.C. de Faria, C. Pasquini and G. de Oliveria Neto, Analyst, 116 (1991) 357.
8 H.J. Moynihan, C.K. Lee, W. Clark and N.H.L. Wang, Biotechnol. Bioeng., 34 (1989) 951.
9 H.M. Abdulla, G.M. Greenway and A.E. Platt, Analyst, 114 (1989) 1575.
10 H. Zoliner, Handbook of Enzyme Inhibitors, VCH, Weinheim, 1989, pp. 102, 47, 45.
11 S.B. Adeloju, S.J. Shaw and G.G. Wallace, Anal. Chim. Acta, in preparation.

Analytica Chimica Acta, 281 (1993) 629–635
Elsevier Science Publishers B.V., Amsterdam

Multicomponent batch-injection analysis using an array of ion-selective electrodes

Dermot Diamond

School of Chemical Sciences, Dublin City University, Dublin 9 (Ireland)

Jianmin Lu, Qiang Chen and Joseph Wang

Department of Chemistry and Biochemistry, New Mexico State University, Las Cruces, NM 88003 (USA)

(Received 13th April 1993)

Abstract

Multicomponent batch-injection analysis is demonstrated for the first time using a multi-channel pipette and an array of three ion-selective electrodes. With this approach, simultaneous determination of species for which suitably selective sensors are available can be quickly and easily achieved. The number of sensors in the array can be easily expanded to match the number of channels in the multi-pipette (eight at present). Signals from the array are monitored with a multi-channel I/O card (Analog Devices RTI-815) fitted inside a 486-DX PC compatible computer. Data display and processing is achieved using routines written in Microsoft QuickBasic (version 4.5).

Keywords: Ion-selective electrodes; Sensors; Multicomponent batch-injection analysis

The ability to perform multicomponent assays is extremely attractive as it drastically reduces analysis times and expense. Ion-selective electrodes (ISEs) have been shown to be ideal devices for use in arrays, because of their excellent selectivity and stability over extended periods of intensive use [1]. Up to now, ISE arrays have been used in conventional batch measurements, flow-injection analysis (FIA) and in many clinical analysers. We now report the first application of the sensor array approach to batch-injection analysis, a relatively new analytical technique.

Arrays of standard sized sparingly-selective electrodes (electrodes which have very broad and overlapping selectivity) have been investigated previously using conventional steady-state batch measurements by Otto and Thomas (Ca^{2+}, Mg^{2+}, K^+, Na^+) [2], Beebe et al. (K^+, Na^+) [3] and Beebe and Kowalski (K^+, Na^+) [4]. Processing of the array data enabled the mixed response to multicomponent samples to be deconvoluted and the response to the individual components obtained. In these investigations, a single-channel meter with a manual switch was used to obtain the data from each sensor in the arrays sequentially. Forster et al [5] used an array of mini-sensors (1.0 mm o.d.) which consisted of three selective electrodes (K^+, Na^+ and Ca^{2+}) and one sparingly selective electrode. Data were simultaneously acquired from the four sensors using a multi-channel I/O card fitted inside a PC. Forster and Diamond [6] used three selective electrodes and a multiple-ionophore electrode (contains several selective ionophores within a single PVC membrane) in an FIA system.

Correspondence to: D. Diamond, School of Chemical Sciences, Dublin City University, Dublin 9 (Ireland).

Batch-injection analysis (BIA) is a recently developed technique [7] which involves injecting small sample volumes (10–100 μl typically) directly onto a flat sensor surface immersed in a relatively large volume dilution cell. Although BIA offers many of the advantages of FIA [8,9] compared to conventional steady-state measurements (high speed sample throughput, response measured relative to baseline leading to less problems with drift, precise sampling, microlitre sample volumes, etc.), the lack of a flow manifold precludes any sample processing on-line to remove interferents or to convert the analyte into a more easily detectable form. Consequently, BIA is, in its present form, restricted to situations where very selective sensors are available [10]. As injection is made via the top of the BIA cell, the sensors must be capable of being used in an inverted position, which is difficult with most liquid-filled ISEs due to the movement of air to the internal membrane boundary on inversion. Hence, until recently, only solid-state ion-selective electrodes (F^-, Cl^- and pH) have been used for BIA [11].

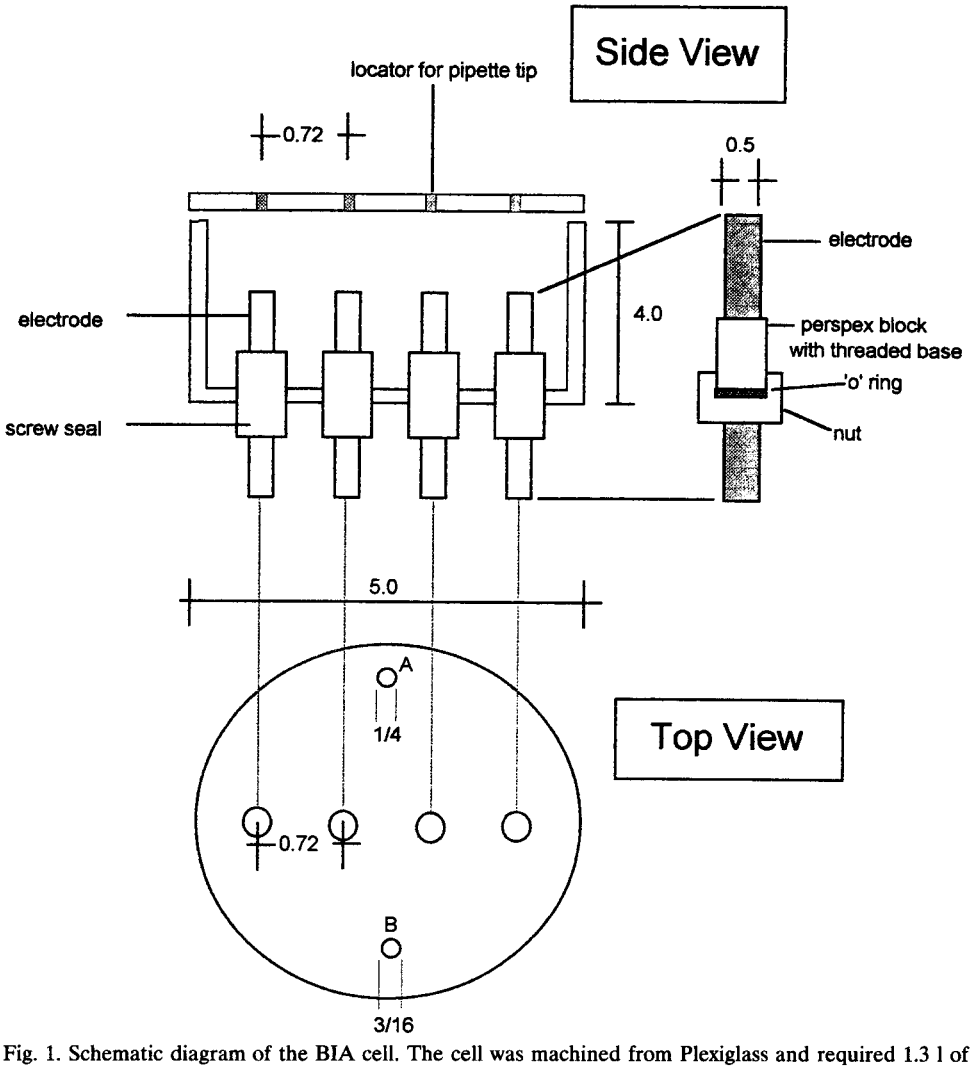

Fig. 1. Schematic diagram of the BIA cell. The cell was machined from Plexiglass and required 1.3 l of filling solution in order to adequately cover the electrodes. All dimensions are in inches.

We recently demonstrated modification of the usual ISE design of liquid-filled poly(vinylchloride) (PVC) membrane electrodes to give a form which could be successfully used for BIA in an inverted position over extended periods of use [12]. However, up to now, only single-component measurements have been made with BIA. In the following sections, we demonstrate that an array of inverted ion-selective electrodes can be used with a new multi-channel pipette and computer-based multichannel data acquisition system to perform multicomponent analysis in a BIA cell.

EXPERIMENTAL

Reagents

Selectophore® grade ionophores valinomycin (K^+) and ETH1001 (Ca^{2+}), membrane plasticiser *o*-nitrophenyloctyl ether (o-NPOE), membrane exchanger potassium tetra(*p*-chlorophenyl)borate (KTpClPB), tetrahydrofuran (THF) and high-molecular weight poly(vinylchloride) (PVC) were obtained from Fluka (New York). The sodium ionophore (methyl *p*-tert.-butylcalix[4]aryl acetate) [13] was synthesised and purified at Dublin City University as described previously [14]. Potassium (Fisher), sodium, lithium and calcium chloride (Baker) were of analytical grade. Mineral water samples (Evian Natural Spring Water and Gerolsteiner Sparkling Mineral Water) were obtained in a local supermarket and were used as received.

PVC membrane and electrode preparation

Sodium, potassium and calcium selective PVC membranes were prepared in the following manner. 10 mg of the ionophores and 2 mg of ion exchanger (KTpClPB) were dissolved in 1 g of plasticiser (o-NPOE) and 0.5 g of high-molecular-weight PVC added to give a slurry. THF was added dropwise until a clear solution was obtained and the resulting, slightly viscous solution poured into a glass petrie dish and left covered with a loosely fitting lid for 24 h. Evaporation of the THF left clear PVC membranes of approximately 0.2 mm thickness from which the sensor discs were cut. These discs were clipped in place on the electrode tip (1.0 cm diameter exposed surface). The electrode design was such that the body could be unscrewed in the middle to facilitate complete filling of the lower half (to the membrane) with the internal reference electrolyte (0.1 M solution of the primary ion). The upper half of the body (to the cable) was completely sealed with silicone polymer and epoxy resin. The electrode could thus be used in an inverted position in the BIA cell, which is necessary in order to obtain the reproducible wall-jet characteristics required for acceptable precision [12].

BIA cell design

The BIA cell used in this study is shown in Fig. 1. The design is such that the inverted electrode tips are diametrically opposite to every second channel of a new eight-channel pipette (Oxford Benchmate Multi-8, Fisher), giving a maximum of four possible electrode positions. Reduction of the electrode diameter would obviously make it possible to use all eight pipette channels with suitable modification of the cell design.

Data collection

Signals from the ISEs were fed through a home-made breakout-box to a multichannel data acquisition card (RTI-815, Analog Devices, Norwood, MA) fitted in an expansion slot of an Everex Tempo 486-33 PC compatible microcomputer. Data were displayed and processed using routines written in Microsoft QuickBasic [6]. A home-made motor-driven stirrer was used to ensure homogeneous mixing in the BIA cell and efficient wash-out of the sample from the ISE membrane diffusion layer after injection in order to prevent unacceptably long delays in return to baseline [12].

RESULTS AND DISCUSSION

In all of the following experiments, 0.1 M LiCl was used as cell filling solution (cell volume ca. 1.3 l). Samples and standards were made up with a background of 0.1 M LiCl to buffer the ionic strength. In accordance with previous optimisa-

tion studies [12], the pipette tip-to-ISE distance and the injection volume were fixed at 2.0 mm and 50 μl, respectively, for each electrode in the array.

Cross-talk between channels can be a problem in multi-sensor configurations [15,16]. Electronic cross-talk is not a problem with potentiometric arrays as the amount of additional circuitry external to the I/O card is minimal and screened cable is used to carry the individual ISE signals. Chemical cross-talk is a greater potential problem for a variety of reasons such as

(i) fluctuations in the reference electrode junction potential as the sample plugs are dispersed throughout the cell after injection (minimised by careful positioning of the reference electrode);

(ii) the well-known response of ISEs to interferents leading to spurious response signals (can be identified and corrected for by modelling the array characteristics).

Figure 2A shows the response obtained from the three-electrode BIA array to injections of 2.0 mM Ca^{2+}, 0.5 mM K^+ and 2.0 mM Na^+ (in 0.1 M LiCl ionic strength adjustment buffer, with 0.1 M LiCl as the cell filling solution). It should be noted that all three pipette tips in use are filled with the solution to be injected; i.e., each electrode tip experiences the same sample upon injection. The results confirm the excellent selectivity of each membrane used, with no cross-response being obtained in any case. Figure 2B shows the response of the array to alternating high-low injections of Ca^{2+} and K^+. Two mixed solutions (2.0×10^{-2} M Ca^{2+}, 5.0×10^{-4} M K^+ and 5.0×10^{-4} M Ca^{2+}, 4.0×10^{-3} M K^+) were alternatively injected onto the array. As before, all three pipette tips were filled with the same solution. From these results it is clear that

(i) there is no response from the sodium electrode to any of the injections, confirming the excellent selectivity of this membrane against K^+ and Ca^{2+};

(ii) there is no carryover of primary ion response from high to low concentrations with the calcium and potassium electrodes due to the efficient washout of sample. Hence, reproducibility can be expected to be good;

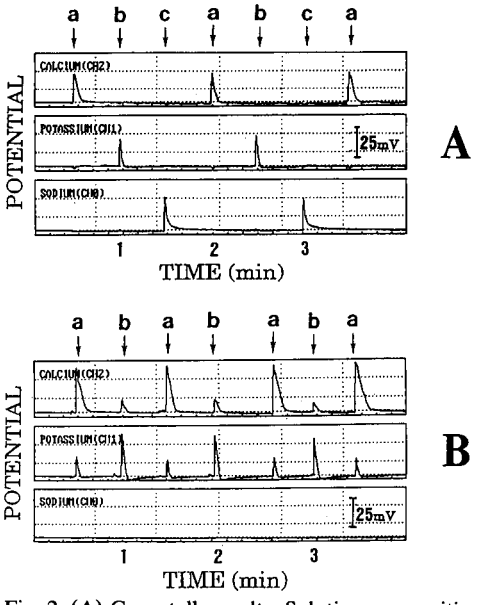

Fig. 2. (A) Cross-talk results. Solution compositions used. (a) 2.0 mM Ca^{2+}; (b) 0.5 mM K^+; (c) 2.0 mM Na^+; 2.0 mm pipette tip-to-electrode surface separation, 50 μl injection volume, 0.1 M LiCl used as background matrix in injection solutions and as cell filling solution. (B) Carryover investigations. Solutions compositions used: (a) 2.0×10^{-2} M $CaCl_2$, 5.0×10^{-4} M KCl, 0.1 M LiCl; (b) 5.0×10^{-4} M $CaCl_2$, 4.0×10^{-3} M KCl, 0.1 M LiCl. Other experimental details as for Fig. 2A.

(iii) there is no observable effect when a mixed solution containing a larger concentration of interferent is injected. Again, this confirms the excellent selectivity of the calcium and potassium membranes.

Figure 3 illustrates the reproducibility of the array response to a tertiary mixture (10.0 mM Ca^{2+}, 5.0 mM K^+ and 5.0 mM Na^+). The %R.S.D. ($n = 7$) was found to be 4.31% (Ca^{2+}), 3.46% (K^+) and 4.5% (Na^+). From these results, it is clear that the three ISEs respond rapidly and reproducibly to their primary ion in this mixture, and that the analytical result is obtained within a few seconds. The slightly higher Na^+ R.S.D. is due to an obviously low peak at 3 min. This particular peak contributes almost 50% of the total standard error of the sodium series and when it is removed from the calculations, the %R.S.D. drops to 2.21%. Such rogue responses occur occasionally because of slight differences in

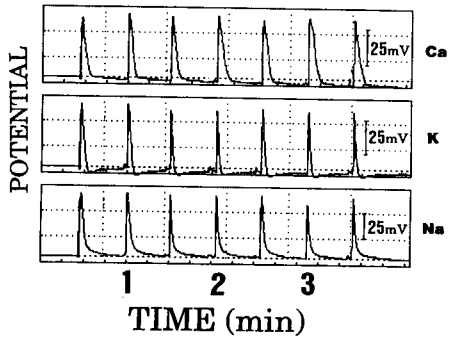

Fig. 3. Reproducibility of array response. Solution composition 10.0 mM Ca^{2+}, 5.0 mM K^+, 5.0 mM Na^+, 0.1 M LiCl. Other experimental details as for Fig. 2A. Calculated %R.S.D.s are 4.31% (Ca^{2+}), 3.46% (K^+) and 4.5% (Na^+) for $n = 7$ (the %R.S.D. for Na^+ is reduced to 2.21% if the obviously low peak at 3 min is removed from the calculation).

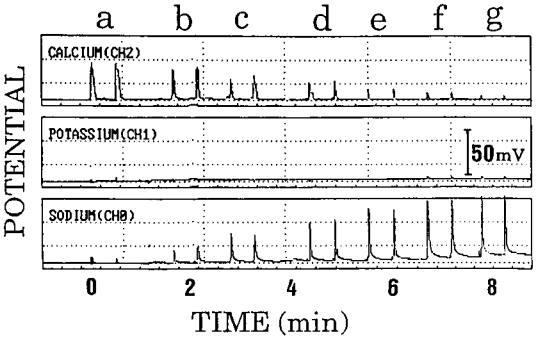

Fig. 4. Simultaneous calibration of Ca^{2+} and Na^+. For concentrations of primary ions in the calibration solutions see Table 1. 0.1 M LiCl used as ionic strength adjustment buffer, other experimental details as for Fig. 2A. Linear regression data: Na^+ curve (on five points b to f): slope 41.3 mV per decade, $r = 0.9915$; Ca^{2+} curve (on five points a to e): slope 25.00 mV, $r = 0.9986$.

the positioning of the pipette which affects the wall-jet hydrodynamics. This problem can be greatly reduced, and the precision correspondingly improved, by careful design of the pipette positioner on the cell lid, which should have holes tapered to fit the shape of the pipette tips. The figure also illustrates the excellent baseline stability offered by the BIA potentiometric measurements. It should be noted that in this illustration, the software autoscales the data to fit in each display window. Hence the mV range (sensitivity) is slightly different for each window. Note also the different shapes of the peaks at the individual ISEs, which illustrates the ability of the BIA sensor array approach to simultaneously explore the kinetic behaviour of different sensors.

Simultaneous calibrations for Ca^{2+} and Na^+ are illustrated in Fig. 4. Mixed solutions of Ca^{2+} (decreasing concentration) and Na^+ (increasing concentration) were used (see Table 1 for details). As before, a stable baseline is apparent and the injections have no effect on the K^+ ISE except for solutions f and g (high sodium concentration) where a small response can be discerned. The results indicated some curvature in the response in both cases, but more so with the Na^+ ISE, where curvature is apparent at both ends of the range. Linear regression on the five points b to f in the Na^+ ISE sequence yields a slope of 41.3 mV per decade and a correlation coefficient of 0.9915. Likewise, linear regression on the five points a to e in the Ca^{2+} ISE sequence yields a slope of 25.00 mV per decade and a correlation coefficient of 0.9986. The sub-Nernstian slopes are not surprising considering the speed of sample transport over the electrode membrane on injection. Indeed, in BIA, peak maxima are typically reached in a fraction of a second, and the membrane response often does not appear to reach a steady state. However, these kinetic-limited responses can still be used for analytical purposes because of the excellent reproducibility offered by the technique.

In order to demonstrate the rapid multicomponent capability of BIA sensor array approach, two mineral water samples were analysed for the three ions of interest (Evian natural spring water

TABLE 1

Composition of solutions used to generate results illustrated in Fig. 4

Solution	$[Ca^{2+}]$ (mol dm^{-3})	$[Na^+]$ (mol dm^{-3})
a	5.0×10^{-2}	1.0×10^{-4}
b	2.5×10^{-2}	5.0×10^{-4}
c	1.0×10^{-2}	1.0×10^{-3}
d	5.0×10^{-3}	2.5×10^{-3}
e	2.5×10^{-3}	5.0×10^{-3}
f	1.0×10^{-3}	1.0×10^{-2}
g	5.0×10^{-4}	2.5×10^{-2}

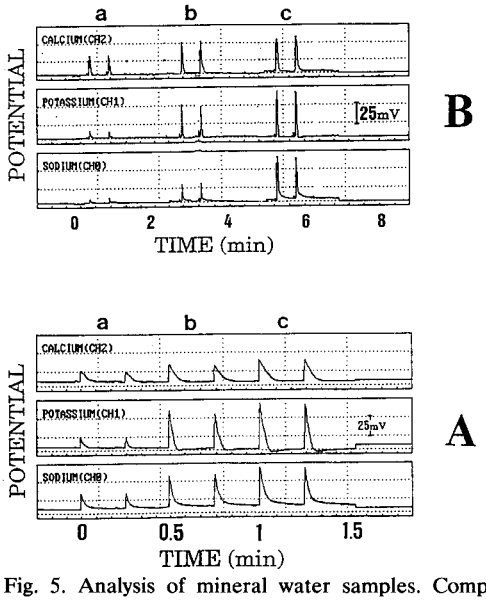

Fig. 5. Analysis of mineral water samples. Composition of solutions. (A) Evian natural spring water: (a) sample, 0.1 M. LiCl; (b) sample, 1.0×10^{-4} M NaCl, 2.5×10^{-3} M $CaCl_2$, 1.0×10^{-4} M KCl, 0.1 M. LiCl; (c) sample, 5.0×10^{-4} M. NaCl, 5.0×10^{-3} M $CaCl_2$, 5.0×10^{-4} M KCl, 0.1 M LiCl. (B) Gerolsteiner sparkling mineral water: (a) sample, 0.1 M LiCl; (b) sample, 1.0×10^{-2} M NaCl, 2.5×10^{-3} M $CaCl_2$, 1.0×10^{-4} M KCl, 0.1 M. LiCl; (c) sample, 2.0×10^{-2} M NaCl, 5.0×10^{-3} M $CaCl_2$, 5.0×10^{-4} M KCl, 0.1 M LiCl. Other experimental details as for Fig. 2A. See Table 2 for results.

and Gerolsteiner sparkling mineral water). Because of the importance of matrix matching standard additions were used. Two spiked samples were prepared (see Fig. 5 for details) and the samples and standards injected in duplicate. As before, the cell filling solution and all injection solutions had a fixed background of 0.1 M LiCl. The results show relatively good agreement (Table 2) with those obtained by flame atomic absorption spectroscopy (FAAS) and with the labelled quantities.

Conclusions

The above results demonstrate for the first time that multicomponent analysis is possible with BIA. With very selective sensors such as those used in this study, deconvolution is not necessary in order to achieve accurate data. The BIA array can be used without chemical or electronic crosstalk and high sample turnovers accomplished (typically 100–180 samples per hour). When combined with the multicomponent capability, rugged and simple cell design, and lack of mechanical parts, this makes BIA with selective sensor array detection an attractive method for routine quality control in many industrial situations. The BIA sensor array approach can be extended from that presented in this report to include other selective sensors as desired for various high-speed clinical and environmental assays. Typical examples would Include ISEs for pH, F^- and Cl^-, and certain amperometric sensors (e.g., redox sensors, O_2, etc.) and modified electrodes. Biosensors represent another interesting prospect because of the selective nature of enzyme- and antibody-based reactions. Multicomponent assays in a BIA cell with biosensor arrays should be possible although stability would be more critical than in disposable, single-shot type assays. Rapid testing of sensor batches in a manufacturing quality control situation would also be greatly facilitated by

TABLE 2

Results of mineral water analysis

Sample	Metal ion	Concentration (M)		
		BIA array	FAAS	Labelled
Evian	Ca^{2+}	1.64×10^{-3}	1.21×10^{-3}	1.95×10^{-3}
	K^+	3.56×10^{-5}	2.63×10^{-5}	n/a [a]
	Na^+	1.58×10^{-4}	2.40×10^{-3}	2.2×10^{-4}
Gerolsteiner	Ca^{2+}	3.61×10^{-3}	3.04×10^{-3}	n/a
	K^+	5.64×10^{-5}	2.83×10^{-5}	n/a
	Na^+	5.37×10^{-3}	4.54×10^{-3}	5.87×10^{-3}

[a] Not available.

the use of the BIA sensor array technique. There is no doubt that with this, and similar developments, BIA sensor array schemes will become practical tools for automated analysis.

We would like to thank T. Baker for carrying out the FAAS analysis of the mineral water samples. D.D. would also like to thank Dublin City University for providing leave of absence in order to carry out this research at NMSU.

REFERENCES

1 D. Diamond, Electroanalysis, 5 (1993) in press.
2 M. Otto and J.D.R. Thomas, Anal. Chem., 57 (1985) 2647.
3 K.R. Beebe, D. Uerz, J. Sandifer and B.R. Kowalski, Anal. Chem., 60 (1988) 66.
4 K.R. Beebe and B.R. Kowalski, Anal. Chem., 60 (1988) 2273.
5 R.J. Forster, F. Regan and D. Diamond, Anal. Chem., 63 (1991) 876.
6 R.J. Forster and D. Diamond, Anal. Chem., 64 (1992) 1721.
7 J. Wang and Z. Taha, Anal. Chem., 63 (1991) 1053.
8 J. Ruzicka and E. Hansen, Flow-Injection Analysis, Wiley, New York, 2nd edn., 1988.
9 M. Valcarcel and M. Luque deCastro, Flow-Injection Analysis, Ellis Horwood, Chichester, 1987.
10 A. Amine, J.-M. Kaufmann and G. Palleschi, Anal. Chim. Acta, 273 (1993) 213.
11 J. Wang and Z. Taha, Anal. Chim. Acta, 252 (1991) 215.
12 J. Lu, Q. Chen, D. Diamond and J. Wang, Analyst, (1993) in press.
13 D. Diamond, G. Svehla, E. Seward and M.A. McKervey, Anal. Chim. Acta., 204 (1988) 223.
14 A.M. McKervey, E.M. Seward, G. Ferguson, B. Ruhl and S.J. Harris, J. Chem. Soc. Chem. Commun., (1985) 388.
15 S.D. Kolev, J.H.M. Simons and W.E. van der Linden, Anal. Chim. Acta., 273 (1993) 71.
16 C.S. Cha, M.J. Shao and C.C. Liu, Sensors Actuators, B2 (1990) 239.

Analytica Chimica Acta, 281 (1993) 637–644
Elsevier Science Publishers B.V., Amsterdam

Room temperature phosphorescence optosensor for tetracyclines

Fausto Alava-Moreno, Marta Elena Díaz-García and Alfredo Sanz-Medel

Department of Physical and Analytical Chemistry, University of Oviedo, c / Julián Clavería 8, 33006 Oviedo (Spain)

(Received 7th December 1992)

Abstract

A flow-through optosensor for tetracyclines based on the tetracycline–europium chelate room temperature phosphorescence energy transfer is proposed. The sensor is developed in conjunction with a flow-injection analysis system and is based on the transient immobilization on a non-ionic resin (packed in a flow-through cell) of the tetracycline–europium chelate. The analytical performance characteristics of the proposed sensor for semiautomated analysis and control of very low levels of tetracycline were as follows: the detection limits for tetracycline, oxytetracycline and chlortetracycline were 0.25, 0.30 and 0.40 ng ml^{-1}, respectively, with a relative standard deviation of 1% for determination of 0.24 $\mu g\ ml^{-1}$ of each antibiotic ($n = 10$). Most of the common metal ions in biological samples did not interfere, except Fe(III) which caused serious interference and should be masked with 1,10-phenanthroline. The recommended method has been successfully tested for determination of tetracyclines in clinical samples (urine and pharmaceutical preparations).

Keywords: Flow injection; Phosphorimetry; Sensors; Optosensors; Tetracyclines

The tetracyclines (TCs) are broad spectrum antibiotics that exhibit high activity against nearly all gram-positive and gram-negative bacteria. Owing to their extensive use in infectious diseases therapy several procedures have been reported for their determination, both in pharmaceutical preparations and biological samples (fluids and tissues). The pharmacopoeia method for the determination of tetracyclines is a time-consuming and somewhat inaccurate biological assay not well suited for routine analysis [1]. A number of alternative chemical methods have also been proposed including spectrophotometry [2–4], spectrofluorimetry [5–7], chemiluminescence [8], liquid chromatography [9,10] and kinetic methods [11]. A potentiometric method based on the use of tetracyclinase and a CO_2 electrochemical sensor have also been developed [12].

The unique sensitized luminescence characteristics of certain lanthanide ions, notably europium(III), were first exploited for the determination of tetracyclines by Hirschy et al. [6]. In a recent report, Wenzel et al. [13] studied the use of Eu(III) as a fluorogenic reagent for post-column LC and flow-injection (FI) detection of tetracyclines.

In aqueous solution, free europium ions do not luminesce efficiently, since any excited-state species are relaxed by vibrionic energy transfer to the aqueous solvent shell [14]. In order to observe luminescence and to avoid radiationless relaxation mechanisms the water should be removed

Correspondence to: A. Sanz-Medel, Department of Physical and Analytical Chemistry, University of Oviedo, c/ Julián Clavería 8, 33006 Oviedo (Spain).

or at least this solvent shell replaced by other ligands.

Typically, luminescence is enhanced by the use of micelle-forming reagents and water exclusion ligands such as trioctylphosphine oxide [15]. Very recently Duggan [10] studied this approach for LC with post-column liquid room temperature phosphorescence (LRTP) detection of tetracyclines. Unlike molecular phosphorescence, sensitized lanthanide luminescence occurs readily in liquid solution at room temperature. Because energy transfer from the organic triplet state of the ligand to the emitting level of the lanthanide ion is an intramolecular process, the luminescence is not quenched by oxygen [6].

Very recently the combined use of FIA and solid substrate (SS)-RTP optosensing detection in an aqueous carrier used as a continuous flow stream has been demonstrated for ultratrace aluminium determination [16]. In the same vein, we report here the combined use of FIA and SS-RTP europium optosensing detection to determine tetracyclines at very low concentrations. The method is based on the transient immobilization (onto a non-ionic resin packed in a flow-through cell) of the Eu(III)–tetracycline complex, which exhibits RTP. The sensitivity was four-fold better than that of the solution batch method [6] and offers the advantage of being simpler than the micellar enhanced technique [10].

EXPERIMENTAL

Reagents

The hydrochlorides of tetracycline (TC), chlortetracycline (CTC) and oxytetracycline (OTC) were purchased from Sigma (St Louis, MO). Europium chloride hexahydrate was purchased from Fluka.

The chelating resin Chelex 100 (BioRad), the strongly acid cation exchanger SP-Sephadex (Sigma), Amberlite IRA-118H (Sigma) and Dowex 50 × 2-100 (Sigma), the weakly acidic cation exchanger Amberlite IRC-50 (Sigma) and the non-ionic resin Amberlite XAD-2 (Sigma) were packed in columns and cleaned by passing 2 M HCl until no atomic absorption signals for iron were obtained in the effluents.

Analytical reagent grade chemicals were employed for the preparation of all the solutions. Freshly prepared ultrapure water (Milli-Q/Milli-Q2 system, Millipore) was used in all the experiments both for sample and standard solutions.

The carrier solution used in the FIA experiments consisted of 0.07 M *N,N,N′,N′*-tetramethylethylenediamine (TEMED, Merck)–0.1 M HCl (pH 7.5, μ = 0.25 M adjusted with NaCl).

Instrumentation

Phosphorescence emission measurements were carried out with a Perkin-Elmer LS5 luminescence spectrometer, which employs a xenon-pulsed (10 s half-width, 50 Hz) excitation source and is equipped with a Perkin-Elmer 3600 data station. The delay times used were typically 0.03 ms and the gate time was 2 ms. Instrument excitation and emission slits were set at 10 and 20 nm, respectively, throughout this study. Steady-state phosphorescent signals were recorded with a Perkin-Elmer 560 chart recorder.

Figure 1 illustrates the simple optosensing FIA manifold used. A conventional Hellma flow-cell (Model 176.52) of 25 μl volume was used. At the bottom of the flow cell, a small piece of nylon net was placed to prevent particle displacement by the carrier. The resin was loaded with the aid of a syringe and the other end of the flow cell was kept free [16]. The cell was then connected to the

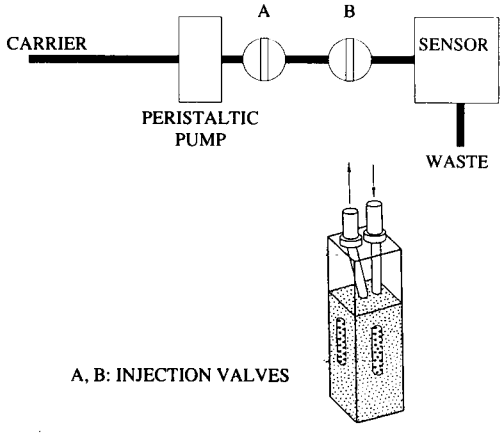

Fig. 1. FIA manifold for the proposed sensor.

flow system and 10 min allowed for the particles to settle. In order to secure that the complex first retained by the packing solid material was in the light path, the resin level was maintained 1 mm lower than that of the cell window. The resin packed in this way could be used for four months or even longer with satisfactory RTP readings.

A four-channel Gilson Minipuls-2 peristaltic pump was used to generate the flowing streams. Omnifit 1106 rotary valves were used for sample introduction (valve A in Fig. 1) and for the retained chelate elution (valve B). PTFE tubing (0.8 mm i.d.) and fittings were used for connecting the flow-through cell, the rotary valves and the carrier solution reservoirs.

pH measurements were made with a WTW pH meter (Wiss. Tech. Werkstatten, Weilheim) and a Radiometer GK-2401-C combination glass-saturated calomel electrode.

General procedure

Samples or standards (1 ml) were injected via valve A and pumped through the flow system. The Eu(III)–TC complex formed (see below) went through the flow cell where it was retained on the resin. The high SS-RTP of the complex on the solid support was measured at the spectral maxima, $\lambda_{ex} = 390$ nm, $\lambda_{em} = 622$ nm. Once the RTP measurement was taken, 2 ml of 0.5 M HCl was injected via valve B (to strip the Eu–TC chelate retained on the solid phase), before proceeding with the next sample injection.

For injection in this flow-through sensor standards and samples were prepared as follows. An appropriate aliquot of the TC standard solution (or the sample) was transferred into a 10-ml standard flask and 25 μl of the Eu(III) solution (6.6×10^{-2} M) was added before the solution was brought up to the mark with the carrier solution.

For urine analysis, to 5 ml of sample 25 μl of Eu(III) (6.6×10^{-2} M) and 0.1 ml of aqueous 1,10-phenanthroline (5×10^{-3} M) solution (in order to prevent interference from the possible presence of iron in the samples) were added. The solution was diluted to 10 ml with 0.15 M TEMED solution of pH 7.5.

For pharmaceutical preparations, 1 g of the sample was accurately weighted and dissolved by adding 60 ml of 0.2 M HCl and 20 ml of ethanol. The resulting solution was transferred to a 100-ml volumetric flask and made up to volume with ultrapure water. Then an appropriate aliquot of this solution was further diluted by placing it in a 10-ml standard flask and 0.1 ml of 1,10-phenanthroline (5×10^{-3} M) solution and 25 μl of Eu(III) solution were added. The solution was brought to volume with the carrier solution.

Reagent blanks were prepared and measured following the same procedure.

RESULTS AND DISCUSSION

Selection of the sensor phase

Tetracyclines are known to form luminescent metal chelates with doubly and triply charged metal cations [17]; it has been suggested that the complexation takes place through the β-diketone oxygens on rings C and D (Fig. 2) readily forming six-membered rings with metal ions. The benzoyl moiety is believed to be involved in possible energy transfer processes [10,17].

For the sensor phase selection, tetracycline was initially studied and preliminary studies were carried out with the strong cation exchanger Chelex 100, loaded with different metal ion species, packed into the flow cell. Tetracycline immobilization onto the solid support should be then produced by complexation with the metal ion (mixed complex) according to the reaction scheme proposed in Fig. 2.

Results indicated that the TC–metal complexes immobilized onto the Chelex 100 exhibited enhanced fluorescence when compared with the corresponding complexes in solution. The TC complexes in solution had fluorescence maxima within the 508–514 nm range, while they are generally blue-shifted when retained on the resin (see Table 1). This could be explained by taking into account that species in solution may have a different TC–metal stoichiometric ratio than those immobilized on the solid support. Detection limits were evaluated for all the metals in the presence of Chelex 100 support. As shown in

TABLE 1

Spectral luminescence properties of metal–tetracycline chelates

Metal ion	Solution		Immobilized onto Chelex 100		
	λ_{ex}	λ_{em}	λ_{ex}	λ_{em}	DL [a] (ng ml^{-1})
Eu^{3+}	390	615	390	622	7
Ca^{2+}	395	514	383	504	25
Mg^{2+}	400	512	383	504	30
Sr^{2+}	375	508	387	501	10
Al^{3+}	416	510	381	505	200
In^{3+}	400	514	381	501	150
Zn^{2+}	385	512	395	512	27

[a] Detection limit.

Table 1, Eu^{3+} detection limits were lowest, being significantly better than those for Al^{3+} and In^{3+}.

The luminescence properties of the TC–Eu^{3+} chelate retained onto the Chelex 100 are particularly well suited for room temperature phosphorimetry. The TC molecule absorbs the excitation radiation and transfers the excited energy through its triplet state to the lowest resonance level of Eu^{3+}, whereafter the ion undergoes a radiative transition resulting in an line-type emission characteristic of the ion. The ion-specific emission appears as long wavelengths (615–622 nm) with a large Stokes' shift (around 200 nm). The most important feature in this context is the long luminescence lifetime which makes it possible to apply time-resolved detection for the effective background elimination and to enhance sensitivity.

Although the luminescence emission originates from the europium ion, the surroundings have proved to play a very important role in the process [6]. This could explain the shorter wavelength emission and lower intensity observed for the TC–Eu chelate in solution as compared with the complex immobilized on the solid support. The "rigidly held" mechanism should account for the higher intensity observed when the TC–Eu complex is retained on the solid [18].

As a result of this preliminary search for a sensitive luminescent sensor phase for tetracycline, the Chelex 100–Eu solid support was selected for further study.

Substrate studies

The solid support for flow-injection RTP optosensing should ideally be translucent so that reflected or absorbed light entering or leaving the probe would be negligible.

Preliminary experiments using the chelating resin Chelex 100, loaded with Eu^{3+}, packing the flow-cell showed that the continuous carrier flow over the solid phase gradually released the Eu^{3+} ions from its surface (the same phenomenon was observed for the other ions studied in Table 1) bringing about decreased luminescence signals. Therefore, an alternative flow approach was ad-

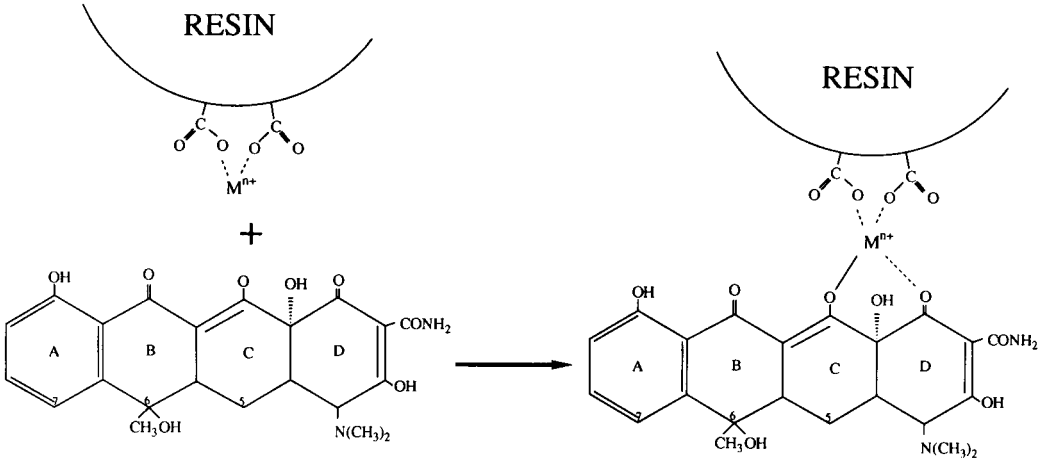

Fig. 2. Proposed response mechanism for the sensor using Chelex 100–Eu as solid support.

dressed: the transient immobilization on different exchange resins of preformed TC–Eu complex.

SP-Sephadex, Dowex 50 × 2-100, Amberlite IRA 118H and Amberlite IRC, all cation exchanger polymers supplied as spheres, were tested to retain the positively charged Eu–TC chelate [6]. Because of the important lipophilic moiety of the complex, its retention on the non-ionic resin Amberlite XAD-2 was also studied.

Table 2 summarizes the analytical characteristics obtained at pH 8 with the different supports. SP-Sephadex (cation exchanger) and Amberlite XAD-2 (non-ionic resin) offered the best performance. It seemed clear from these results that both driving forces, electrostatic and hydrophobic interactions may retain the complex on the solid support. Thus, Amberlite XAD-2 was used in subsequent experiments. Figure 3 shows RTP spectra at different delay times for the TC–Eu chelate immobilized onto the Amberlite XAD-2 support and Fig. 4 shows the probable response mechanism for the proposed sensor.

Chemical requirements and experimental conditions

The study of the influence of pH on the luminescence of the different chelates with three tetracyclines: Eu–TC, Eu–OTC and Eu–CTC adsorbed on the Amberlite XAD-2 resin showed that the optimum pH for the retention/detection occurred at pH 7.5 in all cases. The luminescence signal was not appreciably quenched by oxygen, probably because the emission process involves intra- rather than inter-molecular energy transfer [6].

TABLE 2

Influence of solid support on analytical performance

Solid support	Upper limit of linear range (M)	R.S.D. [a] (%)	DL [b] (ng ml^{-1})
Chelex 100	8×10^{-7}	1.8	7
SP-Sephadex	8×10^{-7}	1.6	4
Amberlite IRA 118H	10^{-6}	1.3	13
Amberlite IRC 50	10^{-6}	2.9	42
Dowex 50×2-100	10^{-6}	1.7	20
Amberlite XAD 2	8×10^{-7}	1.2	2

[a] 5 Measurements of 0.24 μg ml^{-1} TC. [b] Detection limit.

The influence of Eu(III) concentration for optimum complex formation was also studied using different TC concentrations in the range 0–10^{-6} M. Concentrations of Eu(III) higher than 1.3×10^{-4} M had no influence on the luminescence signal. Thus, in order to secure complete TC–Eu complex formation 1.7×10^{-4} M of Eu(III) was used in further studies.

Elution of the Eu–TC chelate from the solid support was studied by using HCl, H_2SO_4 and Na_2SO_4 at different concentrations, as leaching agents. Acids were preferred to Na_2SO_4, and HCl and H_2SO_4 provided similar results. HCl was selected finally in order to keep resin shrink-

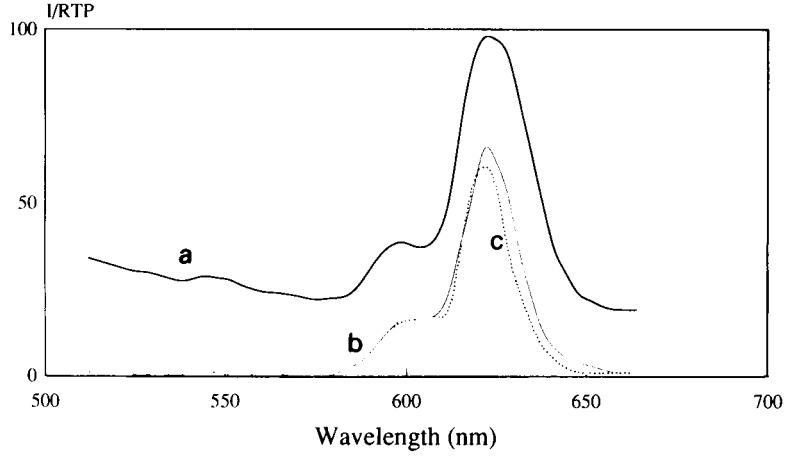

Fig. 3. RTP spectrum of the immobilized complex at different delay times. (a) 0.01 ms; (b) 0.03 ms; (c) 0.05 ms.

TABLE 3

Effects of diverse ions on the determination of 0.24 μg of each tetracycline

Ion	conc. (μg ml^{-1})	Recovery [a]		
		TC	CTC	OTC
–	–	100.0	100.0	100.0
Na^+	7000	98.5	99.5	97.9
K^+	400	100.5	100.5	100.0
Ca^{2+}	200	101.0	101.0	99.5
Mg^{2+}	50	99.0	100.5	99.0
Sr^{2+}	50	100.5	101.0	99.5
Cu^{2+}	2	98.5	99.0	99.0
Fe^{3+}	2	58.0	53.0	45.0
	2 [b]	100.3	99.7	101.3
Zn^{2+}	2	100.5	100.0	99.0
Al^{3+}	2	100.5	100.0	99.5
Cl^-	7000	99.0	100.0	99.5
1,10-Phen.		100.0	99.5	100.5

[a] Mean of 3 determinations. [b] 20 μg ml^{-1} 1,10-phenanthroline was added.

ing problems at a minimum (the same anion composition in the carrier and in the eluent). It was verified that 2 ml of 0.5 M HCl completely washed the complex out of the resin, and allowed the reuse of the latter.

As expected, the analytical signal decreased slightly as the carrier flow-rate increased. Thus, a flow-rate of 0.75 ml min^{-1} was finally selected for subsequent work as a compromise between sensitivity and sample throughput.

Selectivity of the RTP sensor

The selectivity study for this RTP flow-through sensor for tetracyclines was focused first on those inorganic components potentially present in the samples to be analyzed (e.g., Na^+, K^+, Mg^{2+}, Ca^{2+}, Cl^-). The results for the determination of 0.24 μg of the different tetracyclines studied following the recommended procedure are summarized in Table 3.

Na^+, K^+, Ca^{2+}, Mg^{2+} and Cl^-, at twice the concentration levels normally present in serum, did not interfere in the determination of the tetracyclines. The effect was also checked, of other cations such as Cu^{2+}, Fe^{3+}, Zn^{2+} and Al^{3+} that could be present in these samples as impurities and displace Eu(III) from the TC chelate. As shown in Table 3, the only interference was produced by Fe(III). It was found, however, that the quenching influence from Fe(III) could be eliminated by masking it with 1,10-phenanthroline.

Analytical performance characteristics

The analytical figures of merit of the proposed sensor were evaluated. Calibration graphs were prepared from the results of triplicate 1-ml injections of the corresponding TC–Eu chelate stan-

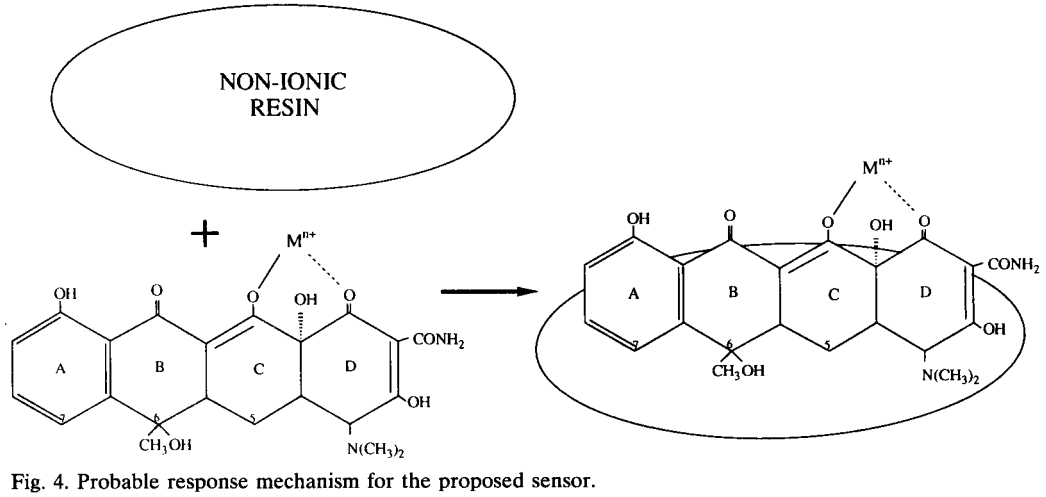

Fig. 4. Probable response mechanism for the proposed sensor.

TABLE 4

Analytical characteristics for each tetracycline

Tetracycline [a]	R.S.D. [b] (%)	DL [c] (ng ml^{-1})
Tetracycline	1.0	0.25
Chlortetracycline	1.0	0.40
Oxytetracycline	0.9	0.30

[a] Upper limit of linear range was 8×10^{-7} M in each instance. [b] 5 Measurements of 0.24 μg ml^{-1}. [c] Detection limit.

dard solutions. The detection limit, using the $3\sigma_B$ criterion (σ_B being the standard deviation of the blank) and the observed relative standard deviation were evaluated for the three tetracyclines under investigation. The results obtained are summarized in Table 4.

Analytical applications

Following the procedure detailed in the Experimental section, the proposed RTP sensor was applied to the determination of tetracycline in spiked urine and a pharmaceutical preparation. Three different urine samples were spiked with a known amount of tetracycline and analyzed using direct aqueous calibration and the standard addition technique. No pretreatment of samples was necessary. As shown in Table 5 results by both techniques compared favorable with those expected. Tetracycline recovery was within $\pm5\%$ of the spiked amount at nM levels. Also a pharmaceutical preparation (Terramycin, Pfizer) was analyzed according to the procedure stated in the Experimental section. The results obtained using the proposed optosensor were 30.1 ± 0.1 mg g^{-1} ($n = 6$) which compared favorably with that reported by the manufacturer (30 mg g^{-1}).

TABLE 5

Analysis of urine samples [a]

Sample	Direct calibration (nM)	Standard addition (nM)	Conc. spiked (nM)
1	197 ± 1	191 ± 2	200
2	150 ± 1	148 ± 3	150
3	250 ± 1	243 ± 1	250

[a] Results are the mean $\pm$ std. dev. of 3 determinations.

Conclusions

The RTP-based optosensor developed for the tetracycline antibiotic group has proved to be accurate and suitable for the assay of tetracyclines added to urine and present in a pharmaceutical formulation. It does not suffer from interferences due to inorganic compounds, proteins (present in urine) or excipients. It is worth mentioning that the sensor is characterized by a reproducible and repetitive return of the readout to the baseline after each single measurement cycle is completed. The RTP sensor responds almost instantantly to the presence of the tetracycline–metal complex, enabling a large number of samples to be measured in sequence without deterioration. A sampling frequency of 10–12 h^{-1} can be achieved.

The analytical future of RTP optosensing [18] appears bright both from a practical and from a fundamental stand-point: from a practical point of view the intrinsically high spectral selectivity of phosphorescence can be substantially improved by measuring other related optical properties of the complexes (lifetime, light polarization, etc.) for multivariate analysis. In this way new sensing schemes could be exploited and their application to real sample multicomponent analysis should be easier, particularly when aided by chemometrics. Work in this direction is currently in progress in our laboratory as significant differences were observed in the lifetimes of the three studied TC–Eu immobilized complexes. As few compounds can bind to the solid support used and transfer excitation energy to Eu^{3+} the use of time-resolved luminescence would increase even further the selectivity for a single or group of structurally analogous compounds (e.g., tetracyclines). From a basic point of view, time-resolved luminescence optosensing offers great potential, as yet unexploited, for fundamental studies on new sensing mechanisms and for the development and design of flow-through and probe-type fiber optical sensors for (bio)-chemical species using delayed fluorescence and RTP measurements [18].

Financial support from Fundación de Investigaciones Sanitarias de la Seguridad Social (FISss) Project 90/0842 and Fundación para el Fomento en Asturias de la Investigación Científica y Aplicada (FICYT) are gratefully acknowledged.

REFERENCES

1 British Pharmacopeia, HMSO, London, 1980.
2 M.M. Abdel-Khalek and M.S. Mahrous, Talanta, 30 (1983) 792.
3 A.A. Alwarthan, S.A. Al-Tamrah and S.M. Sultan, Analyst, 116 (1991) 183.
4 S.M. Sultan, F.E.O. Suliman, S.O. Duffnaa and I.I. Abu-Abdoun, Analyst, 117 (1992) 1179.
5 H. Poiger and Ch. Schlatter, Analyst. 101 (1976) 808.
6 L.M. Hirschy, E.V. Dove and J.D. Winefordner, Anal. Chim. Acta, 147 (1983) 311.
7 W.B. Chang, Y.B. Zhao, Y.X. Li and L.Y. Hu, Analyst, 117 (1992) 1377.
8 A.A. Alwarthan and A. Townshend, Anal. Chim. Acta, 196 (1987) 135.
9 W.J.J. Blanchflower, R.J. McCracken and D.A. Rice, Analyst, 114 (1989) 421.
10 J.X. Duggan, J. Liquid Chromatogr., 14 (1991) 2499.
11 M.A.H. Elsayed, M.H. Barary and H. Mehgoub, Anal. Lett., 18 (1985) 1357.
12 Y.S. Zhou, S. Jing and N. Li-Hua, Talanta, 36 (1989) 849.
13 T. Wenzel, L. Colette, D. Dahlen, S. Hendrikson and L. Yarmaloff, J. Chromatogr., 433 (1988) 149.
14 W. De, W. Horrocks, Jr. and D.R. Sidnik, Acc. Chem. Res., 14 (1981) 384.
15 J. Hemmilä, S. Dakubu, V.M. Mukkala, H. Siitari and T. Lovgren, Anal. Biochem., 137 (1984) 335.
16 R. Pereiro García, Y.M. Liu, M.E. Díaz García and A. Sanz-Medel, Anal. Chem., 63 (1991) 1759.
17 K.W. Kohn, Anal. Chem., 33 (1961) 863.
18 A. Sanz-Medel. Solid Surface Room Temperature Phosphorescence and Flow Analysis: a happy marriage. Plenary Lecture presented at ISM'92. Córdoba, Anal. Chim. Acta, 283 (1993) in press.

Analytica Chimica Acta, 281 (1993) 645–653
Elsevier Science Publishers B.V., Amsterdam

Covalent immobilisation of glucose oxidase on methacrylate copolymers for use in an amperometric glucose sensor

C.E. Hall and E.A.H. Hall

University of Cambridge, Institute of Biotechnology, Tennis Court Road, Cambridge CB2 1QT (UK)

(Received 4th March 1993; revised manuscript received 24th April 1993)

Abstract

Glucose oxidase was covalently immobilised on the surface of copolymers of methyl and glycidyl methacrylates. The enzyme modified polymers were deposited from dichloromethane solutions onto platinum electrodes to form an amperometric glucose sensor based on the electrochemical measurement of hydrogen peroxide. The enzyme has been shown to retain its activity throughout the immobilisation and casting procedure, and the influence of various experimental variables have been explored for optimum analytical performance.

Keywords: Amperometry; Sensors; Covalent immobilization; Glucose sensors; Glucose oxidase; Methacrylate copolymers

Many methods have been used as immobilisation systems for the biologically active component of biosensor devices. These methods have included covalent attachment, adsorption, and physical entrapment [1]. However, the transfer of these technologies to large scale production of a sensor device is often costly because of the multiple steps involved in the process, and because the process does not lend itself easily to existing industrial mass-fabrication techniques. Indeed, there are few examples of a successful transfer of laboratory technology to microchip scale devices [2]. It is the aim of this paper to address this problem by investigating polymers, already employed as photoresist materials in microstructure fabrication procedures, as immobilisation matrices for enzymes.

A typical photoresist material contains photosensitisers, photocross-linkable groups, together with the bulk polymer, either as individual components or covalently attached to the polymer backbone [3]. Traditionally, the vast majority of polymers employed as photoresists are copolymers based on methyl methacrylate [4]. More recently, Nishikubo et al. [5–7] reported the use of photoresist materials based on copolymers of methyl and glycidyl methacrylates. Significantly, glycidyl groups have been employed for a number of years as a means of covalently binding enzymes and cells [8], and a similar copolymer has previously been employed to prepare catalyst beds consisting of enzyme coated polymer heads [9].

In this paper a glucose sensitive electrode has been prepared from a glucose oxidase modified

Correspondence to: E.A.H. Hall, University of Cambridge, Institute of Biotechnology, Tennis Court Road, Cambridge CB2 1QT (UK).

copolymer of methyl and glycidyl methacrylates which has been cast from dichloromethane solution onto a platinum substrate. Additionally, parameters which may effect the operation of the electrode were evaluated to provide both a reliable fabrication routine and a reproducible response to glucose. To our knowledge such an electrode has not been investigated before.

EXPERIMENTAL

Materials

Glucose oxidase E.C.1.1.3.4 (type X-S from *Aspergillus Niger*) was supplied by Sigma. Buffer solutions were prepared from AnalaR grade reagents (BDH) and deionised water. The polymers were prepared and purified in the manner described below using HPLC-grade solvents. The monomers, methyl methacrylate and glycidyl methacrylate were obtained from Aldrich, as was the initiator, benzoyl peroxide (70%).

Polymer preparation

A number of polymers have been prepared during the optimisation of this sensor. The following is a typical recipe for the preparation of a 1:1 copolymer of glycidyl and methyl methacrylate within this class of polymers, modified from the work of Nishikubo et al. [5].

Methyl methacrylate (4.0 g, 0.4 mol l^{-1}) and glycidyl methacrylate (5.68 g, 0.4 mol l^{-1}) were added to dry benzene (95 ml) and thoroughly degassed with nitrogen. The solution was heated to 70°C and benzoyl peroxide (0.693 g, 2×10^{-2} mol l^{-1}) in benzene (5 ml) was added. The mixture was stirred at 75°C for five hours before cooling and precipitating with methanol (1000 ml). The precipitate was filtered and dried under vacuum before being reprecipitated from dichloromethane solution (1 g per 10 ml). The reprecipitated polymer was freeze-dried for four hours on an Edwards Freeze Dryer Modulyo before being modified with glucose oxidase.

The molecular weights of the polymers were determined by GPC (quoted in polystyrene units) by RAPRA Technology.

Enzyme immobilisation on polymers

The covalent immobilisation of enzymes to a substrate has been extensively reviewed [1,8]. In this instance the methods of Winquist and Danielsson [10] and Hannibal-Freidrich et al. [9] for epoxide containing polymers have been modified to provide the following protocol.

The co-polymer (125 mg) was mixed with enzyme solution (5 ml of 1 mg ml^{-1} of 0.05 M sodium phosphate buffer pH 7.0) and shaken for 96 h at 4°C. The modified polymer was filtered and washed with buffer solution (2×10 ml) and then shaken for a further 24 h at 4°C with glycine solution (5 ml, 1 mmol in buffer). The polymer was filtered and then washed sequentially with buffer solution (2×10 ml), NaCl solution (2×5 ml, 0.5 M in buffer), and finally buffer solution (2×10 ml) before drying for one hour under reduced pressure.

A method for the absolute determination of the amount of enzyme immobilised on the polymer could not be made, but a relative estimate was obtained by difference between the concentration of the enzyme solution used and the total enzyme concentration of the collected washings. The protein determination was carried out using Coomassie Protein Reagent, Sigma, on a Perkin-Elmer Lambda 5 UV–Visible spectrophotometer. The method is claimed to have a lower detection limit of 1 μg ml^{-1}, however in practice, the limit was found to be 10 μg ml^{-1} and known concentration protein solutions could be fitted to a standard curve with an error of $\pm 15\%$, so that measurements made using this method can only be treated as approximate.

Electrode preparation

Electrodes were prepared by coating platinum wire electrodes (length 1.5 cm, diameter 0.05 cm; area 0.25 cm^2) with the enzyme modified polymer. This was achieved by dripping a dichloromethane solution of the polymer (5 mg per 150 μl) down the length of the electrode, giving a 'pear-shaped' coating. In this way coatings of modified polymer of either approximately 0.5 mg or 1 mg were obtained with reproducible activity/response. Before use the electrodes were soaked in buffer solution (0.05 M potassium per-

chlorate–0.05 M potassium phosphate pH 5.5) for 24 h.

Electrochemical measurements

In this study the electrochemical determination of hydrogen peroxide, and hence glucose, has been carried out at a potential of 0.65 V (vs. SCE) in 0.05 M potassium perchlorate–0.05 M potassium phosphate buffer solution at pH 5.5, using electrodes coated with enzyme modified polymer. The electrochemical measurements were made using an EG&G 273A potentiostat/galvanostat in conjunction with a Gould Y-t recorder.

$$\beta\text{-D-glucose} + GOD_{2FAD} \rightarrow$$

$$\beta\text{-D-gluconolactone} + GOD_{2FADH_2}$$

$$GOD_{2FADH_2} + O_2 \rightarrow GOD_{2FAD} + H_2O_2$$

$$H_2O_2 \rightarrow O_2 + 2H^+ + 2e^-$$

Alternatively a lower measuring potential could be employed by using an artificial electron acceptor or by reacting the hydrogen peroxide with a redox active species with a lower redox potential [8].

RESULTS AND DISCUSSION

Response of GOD modified polymer

The response to glucose, measured as described via the anodic oxidation of H_2O_2, at an electrode coated with the GOD-modified polymer, is shown in Fig. 1. It has an extended linear response range compared with the soluble enzyme, where the classic Michaelis-Menten enzyme kinetics generally control the reaction pathway, typically with a quoted K_m of ≤ 5 mM [11]. The response is linear over the first 10 mmol glucose added and saturates at a concentration in excess of 50 mM. This seems likely to be the result of diffusional limitations imposed by the polymer.

Optimisation of the response from this GOD-modified polymer is influenced by both the polymer loading and conditioning time in aqueous media.

Conditioning time. Figure 2a shows that the magnitude of the response to glucose improves with conditioning time. An enzyme-linked reaction mechanism is controlled by the kinetics of the enzyme reaction and the diffusion of the substrate to the enzyme. The signal recorded from measuring a product of the reaction will thus show a linear concentration response only below the range where the enzyme kinetics exceed the substrate diffusion. If the diffusion coefficient for the substrate is decreased the signal will show an extended linear range, but a smaller signal (scaled by the change in diffusion coefficient). The data here does not show any change of this nature, but only in magnitude. This data would be consistent with changes in the diffusion of product in the polymer or an increase in enzyme "concentration", "activity" or availability, which may be correlated to the uptake of water and electrolyte from the buffer solution into the polymer during conditioning. The improvement tends to a maximum after 3–4 h, with only small further differences recorded up to 26 h. Conditioning times above 48 h led to erratic responses and ultimately an overall decrease in response, which seems to be due to detachment of the polymer from the electrode.

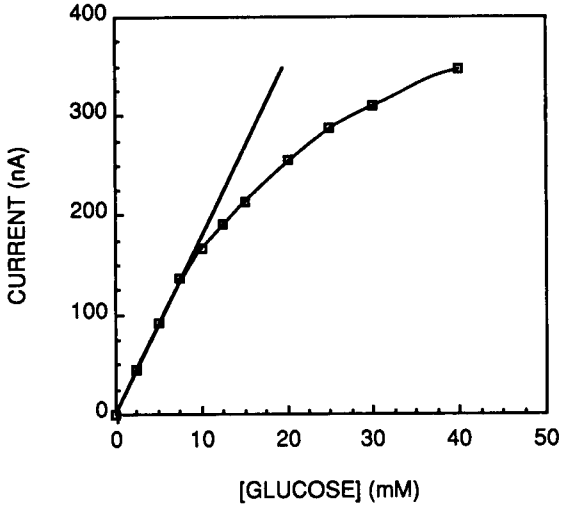

Fig. 1. Plot of current versus glucose concentration for glucose oxidase modified polymer coating on a platinum wire electrode, recorded at 0.65 V vs. SCE at pH 6.5.

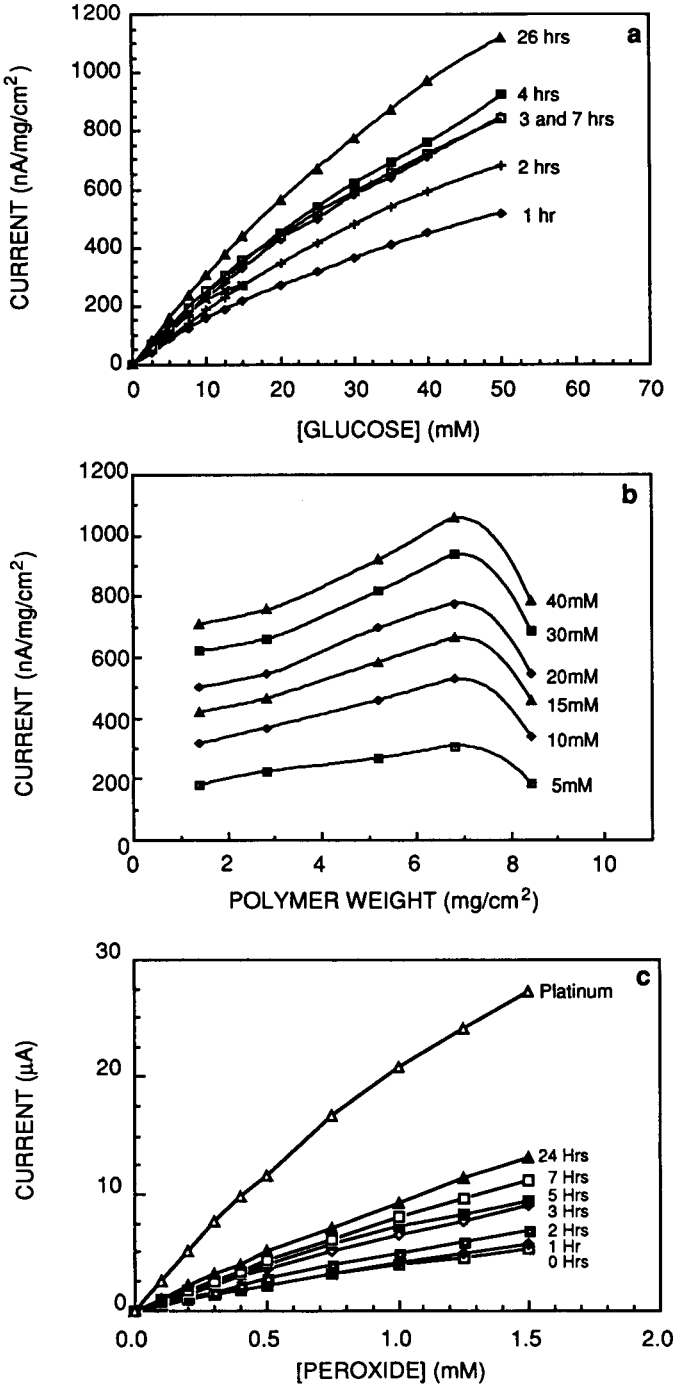

Fig. 2. (a) Plot of current versus glucose concentration for various conditioning times for 50G50M1E. (b) Plot of current response versus polymer weight at various glucose concentrations after 24 h conditioning. (c) Plot of current versus hydrogen peroxide concentration at platinum, and enzyme modified polymer coated electrodes after different conditioning times.

The changes bear resemblance to the effect of partitioning of hydrogen peroxide in the film which can be demonstrated in unmodified polymer (Fig. 2c). Even for very low polymer loadings (i.e., thin films, 2 mg cm^{-2}), the electrochemical measurement of hydrogen peroxide in solution at a platinum electrode coated with polymer is significantly reduced compared with the uncoated electrode. The magnitude of the signal increases with conditioning time from which it can be deduced that the concentration of H_2O_2 (and thus the current signal) increases in the polymer layer. The partioning properties of the polymer toward H_2O_2 cannot therefore be dismissed as a source of the signal enhancement with conditioning time in the enzyme modified polymer.

Polymer loading. The current response to glucose is also influenced by the polymer loading per unit area. Obviously the enzyme loading will increase in line with the weight of polymer deposited, but the current due to H_2O_2 recorded following additions of glucose goes through a maximum at around 6.8 mg cm^{-2} of polymer (Fig. 2b), and even below this amount, the signal is not directly proportional to the weight of polymer (i.e., twice the weight of polymer does not give double the signal).

The increase in polymer deposited on the electrode, however, also results in an increase in the thickness of the polymer coating. The thickness of the 'unwetted' layer of polymer is a function of conditioning time and within the first 24 h will thus increase with total polymer thickness for a given conditioning time. In general, however, the signal magnitude is increased by greater polymer loading, but decreased by greater thickness due to the limitations on the diffusion of substrate and product through the polymer. In the electrode geometry used here, which describes a 'pear shaped' polymer coating, these opposing contri-

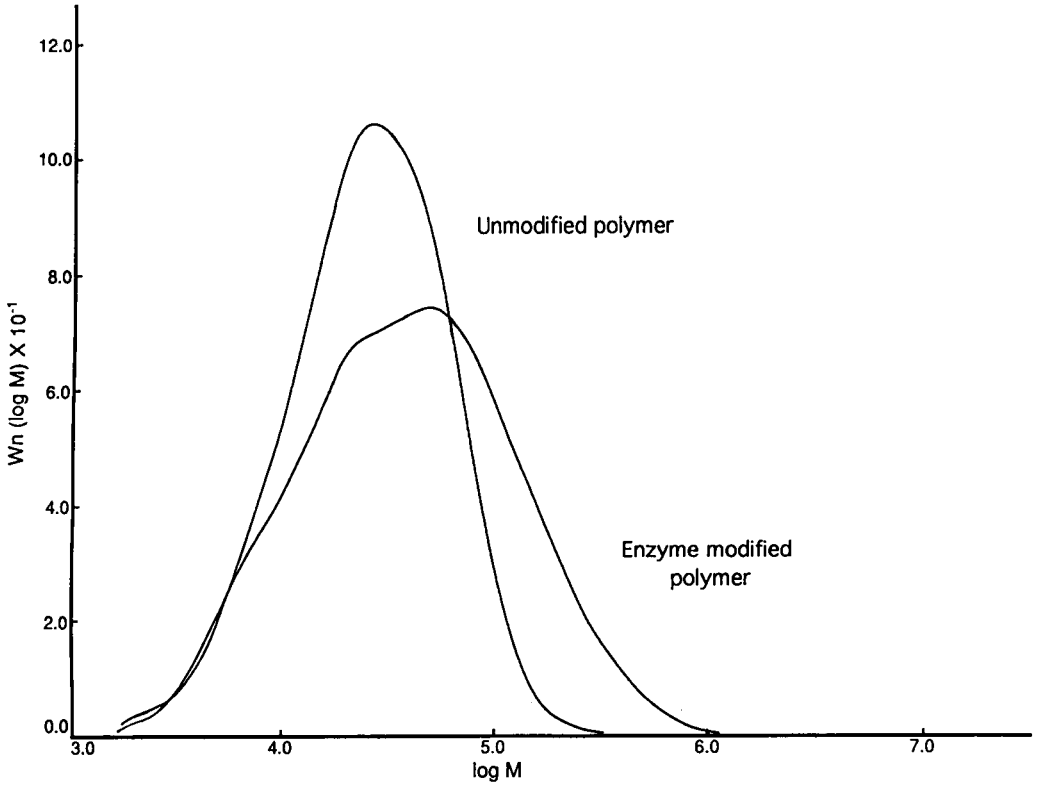

Fig. 3. Molecular weight distributions for polymer 50G50M, and the enzyme modified 50G50M.

butions reach a compromise at an averaged loading of 6.8 mg cm^{-2}.

The current response of the electrode can therefore become limited by enzyme availability (rather than total enzyme deposited) and/or the rate of diffusion of either the substrate (glucose) to the enzyme, or the product (hydrogen peroxide) to the electrode. Above 6.8 mg cm^{-2} plots of glucose against current response indicate that the rate determining step in the process is diffusion, whilst below this there is mixed enzyme and diffusion control and the magnitude of the signal is modulated primarily by water uptake or swelling processes associated with the conditioning procedure, and varying the availability or "activity" of the enzyme.

Copolymer composition. The electrochemical response to glucose obtained with the glucose oxidase-modified polymer electrode should also be sensitive to the total amount of enzyme immobilised on the polymer and to the molecular weight of the polymer, which influences the rate of diffusion through the polymer layer.

Table 1 contains molecular weight data and approximate enzyme immobilisation efficiencies for methyl-glycidyl methacrylate copolymers. In these copolymers, maximum enzyme immobilisation is achieved up to 25% methyl–75% glycidyl copolymer, so it is not immediately clear what parameter is limiting the reaction with the protein since its appears to become independant of epoxide concentration and reaches a maximum as found by Nishikubo et al. [5]. From the molecular weight data for the enzyme modified polymer (e.g., 50G50M1E in Table 1 and Fig. 3) it is indicated that the number average molecular weight (M_n), which has a relation to the number of chains initiated in the polymerisation, remains fairly constant and the weight average molecular weight (M_w) doubles during the enzyme immobilisation procedure. It would be expected that the covalent attachment of an enzyme to existing polymer chains would increase the molecular weight as can be seen from Fig. 3, but the greater dispersity in this sample must reflect the heterogeneity of the immobilisation mechanism and is probably a function of available surface area as well as glycidyl groups.

TABLE 1

Molecular weight and enzyme modification data for a series of copolymers of methyl and glycidyl methacrylates

Polymer [a]	Yield (%)	M_w	M_n	M_w/M_n	Immob. Effic. [b] % (±3)	Bound Enzyme [c] % (±0.15)
50G50M1	91.9	38950	20950	1.85	–	–
50G50M1E	80	75500	21900	3.65	22.0	0.85
100M1	50.9	92150	45000	2.05	0.0	0.00
10G90M1	61.4	62950	27100	2.35	20.9	0.91
25G75M1	76.9	37500	21900	1.7	24.5	1.00
50G50M2	87.8	30700	14850	2.05	27.0	1.16
75G25M1	91.2	31350	12950	2.45	28.2	1.18
100G1	93.1	13400	8845	1.5	26.2	1.05

[a] Designation denotes monomer composition; M = methyl methacrylate, G = glycidyl methacrylate, E = enzyme modified. [b] Based on the uptake of enzyme from a solution containing 1.0 mg ml^{-1} GOD. [c] Calculated from the mass of enzyme consumed divided by the mass of polymer used.

The yields of polymers prepared with different monomer ratios increased with glycidyl methacrylate concentration which is in line with the greater reactivity of this monomer. Furthermore the molecular weights of the polymers decreased with increase in glycidyl methacrylate concentration, which probably reflects the lower solubility of the homopolymer of glycidyl methacrylate. The yields and molecular weight distributions of the copolymers were also shown to be modulated by reaction time and control of the initiation reaction, but in a separate study [12] it was found that these caused only minor changes in the estimation of bound enzyme. Nevertheless, the consistency in the enzyme immobilisation yield was not reflected by a similar invariant signal response in the presence of glucose.

The response to glucose of electrodes prepared from these polymers consistently reached a maximum at 25% glycidyl methacrylate (Fig. 4). If this maximum reflects only enzyme loading, copolymers with greater than 25% glycidyl methacrylate would be expected to show an equivalent or greater electrochemical current response to additions of glucose. However, the data shows a drop in this response which must also be a function of the polymer composition. With changed glycidyl concentration the molecular weight distributions of the resultant copolymers

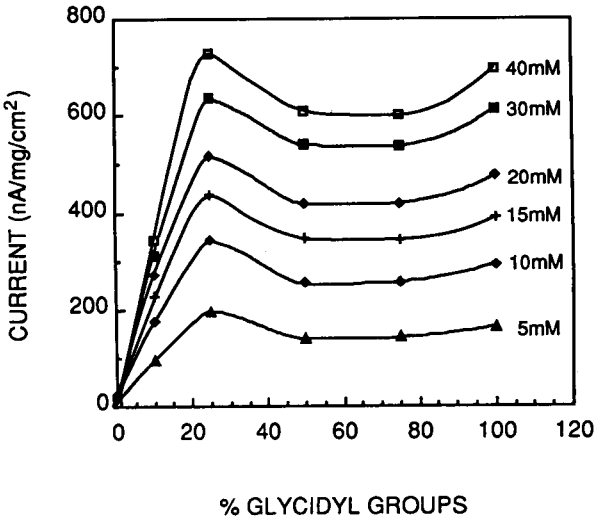

Fig. 4. Plot of current response versus %glycidyl groups in the copolymerisation mix at various glucose concentrations.

can give a matrix with different diffusion properties and thus cause an altered current signal; on the other hand, the number of glycidyl groups may affect the orientation of the enzyme with respect to the polymer surface and hence its later activity or availability. Since the electrochemical response to peroxide is independant of the polymer composition and only dependent on conditioning time, the latter explanation is the most likely cause of this ambiguity.

Storage and stability

One major drawback with enzyme-based detection systems has often been the activity and lifetime of the enzyme component, even after covalent immobilisation.

4°C Storage of GOD modified polymer. The enzyme modified polymer was stored as prepared at 4°C. Electrodes were cast from this material at periodic intervals and the response to glucose was measured after 24 h conditioning time. After an initial stabilisation period, following polymerisation and enzyme modification, newly cast electrodes showed little deterioration, even after some months.

Storage of cast polymer films in buffer solution. Three electrodes were prepared and then stored in buffer at 4°C for different time periods. The electrochemical response to glucose of these electrodes was measured first after 3 days and then during the storage period of four weeks; it was similar throughout. This is in contrast to the long term experiments on conditioning time at room temperature which suggested that the activity of the enzyme modified polymer became erratic after long time periods in buffer solution. In the latter case, the deterioration appeared to be associated with detachment of the film from the electrode.

Multiuse stability. The response to glucose of a single electrode used once every day then washed and stored at 4°C in buffer solution between

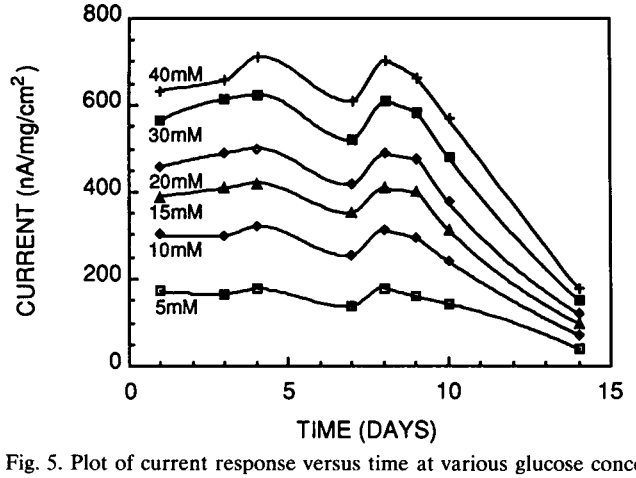

Fig. 5. Plot of current response versus time at various glucose concentrations for an electrode in continous use.

measurements demonstrates reasonable reproducibilty for eight days and then a gradual decline until zero activity was found on day 17 (Fig. 5). This result can be compared with that reported above for an electrode stored without use in buffer solution at 4°C. The decline of the electrode signal could be due to the physical deterioration of the electrode coating, but since it was not seen above, it seems more likely that it was enhanced by slow poisoning of the enzyme by the hydrogen peroxide produced during the enzyme reaction with glucose. In a separate experiment it was observed that peroxide was retained by the polymer, even when stored in buffer solution for long periods.

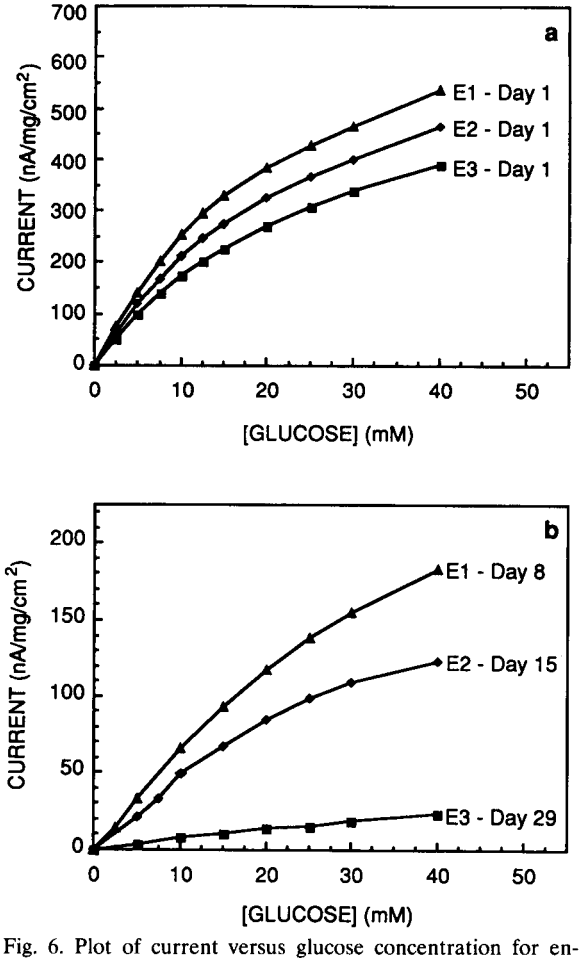

Fig. 6. Plot of current versus glucose concentration for enzyme modified polymer during dry storage as cast electrodes. (a) First measurement, (b) second measurement.

Dry storage of cast polymer films. Figure 6a shows the response to glucose of three electrodes after 24 h conditioning. These electrodes are prepared using the same mass of polymer film. The differences between the samples represent the 'manufacturing' error in the manual drop coating technique that was used. Figure 6b (note the different current scales) shows the response of the same three electrodes following 7, 14, and 28 days of dry storage at 4°C, after being dried for four hours at room temperature and subsequent reconditioning for 24 h. This figure confirms that the activity of the polymer decreases rapidly during these wetting and drying processes, which is in sharp contrast to the stability of the same polymer stored prior to electrode preparation or after film fabrication if stored in buffer. This again seems to be a result of poor adherence between the polymer and the electrode and strain produced in the film by the repeated wetting and drying procedures.

Conclusions

The electrochemical response of the glucose oxidase modified polymer coated electrode was promising in both the magnitude of the signal and its linearity over the first 10 mM range of glucose additions. Compared with the same assay employing glucose oxidase in solution, considerable diffusional control is introduced into the assay, even for very thin polymers. The diffusion element was further highlighted by the film thickness and weight experiments which showed that diffusion control dominated in thick films. It was also shown that the increased response with longer conditioning times after the polymer had been swollen by water and electrolyte could be associated with changes in the partioning characteristics for H_2O_2 or enzyme activity.

The composition of the co-polymer had only minor effect on the protein immobilisation levels above 25% glycidyl methacrylate; the electrochemical response of the system also reached a maximum at 25% glycidyl groups but decreased slightly for greater glycidyl ratios.

The long term stability of the glucose oxidase-

modified polymer was excellent, although cast films stored in buffer, suffered from deterioration, apparently as a result of polymer integrity and adherence. Dry storage of cast electrodes once they had been conditioned in buffered solution, did not improve the stability, but this was expected since the wetting and drying procedures introduce strains in the polymer film. Greater signal deterioration was observed if electrodes were in long term use or exposed to glucose, which is consistent with peroxide poisoning of the enzyme [13].

Perhaps the most encouraging result of all is that the enzyme is apparently not deactivated by dissolution in dichloromethane in film casting, during the preparation of the electrode. While quantitative reinforcement of this conclusion is difficult, a rough estimate which compares 10 μl of an aqueous enzyme solution (0.1 mg ml^{-1}) immobilised in thin film behind a dialysis membrane, produces a current signal (normalised to nA μg^{-1} enzyme) in response to 5 mM glucose which is of the same order as that obtained from 0.5 mg of enzyme modified polymer. The robustness of this immobilised enzyme is possibly due to an inherent property of its method of preparation in aqueous solution, such that a "film" of water around the enzyme is left from the enzyme immobilisation procedure. It has been shown that a "microlayer" of water is required to retain protein activity [14] and indeed some decrease in conditioning time could be achieved for the polymer described here, if water-saturated dichloromethane was used in the casting process.

These observations allows the polymer to be considered for development as a material for thin layer deposition manufacturing techniques. The major limitations highlighted by this study are concerned with the stability and adherence of the host polymer rather than enzyme and these factors are being addressed in current work. The methacrylate family is easily modified to change the surface properties to improve adherence. Photolithographic polymers, emulsion polymers and others with special characteristics can also be developed from this basic system for particular manufacturing processes.

Future uses for this polymer may also extend well beyond this application, as long as the biological component of the material is sufficiently resistant to damage during the processing stages.

We are grateful to the U.K. Science and Engineering Research Council for the financial support for this project.

REFERENCES

1 J.F. Kennedy, C.A. White and E.H.M. Melo, Chimiaoggi–Maggio, 21 (1988) 21.
2 D.F.G. Moore, ERASMUS Course On Molecular Sensor Technology, Cambridge, 1991.
3 C. Roucoux, C. Loucheux and A. Lablache-Combier, J. Appl. Polym. Sci., 26 (1981) 1221.
4 E. Reichmanise and L.F. Thompson, Ann. Rev. Mater. Sci., 17 (1987) 235.
5 T. Nishikubo, T. Iizawa, M. Yamada and K. Tsuchiya, J. Polym. Sci. Polym. Chem., 21 (1983) 1025.
6 T. Nishikubo, T.Iizawa, E. Takahashi and F. Nono, Polym. J., 16 (1984) 371.
7 T. Nishikubo and T. Iizawa, Polym. Prepr. Am. Chem. Soc., 25 (1984) 315.
8 E.A.H. Hall, Biosensors, Open University Press, Milton Keynes, 1990.
9 O. Hannibal-Friedrich, H. Chun and M. Sernetz, Biotechnol. Bioeng., 22 (1980) 157.
10 F. Winquist and B. Danielsson, in E.A.G. Cass (Ed.) Biosensors, I.R.L. Press, Oxford, 1990, p. 181.
11 B.E.P. Swobada and V. Massay, J. Biol. Chem., 290 (1965) 2209.
12 C.E. Hall and E.A.H. Hall, unpublished results.
13 S. Krishnaswamy and J.R. Kittrell, Biotechnol. Bioeng., 20 (1978) 821.
14 T. Yamane, Biocatalysis, 2 (1988) 1.

Analytica Chimica Acta, 281 (1993) 655–661
Elsevier Science Publishers B.V., Amsterdam

An amperometric enzyme electrode for bile acids

W. John Albery, R. Bruce Lennox [1], Edmond Magner [1] and Girish Rao [1]

Unit of Metabolic Medicine, St. Mary's Hospital Medical School, Paddington, London W2 1PG (UK)

David Armstrong [1], R. Hermon Dowling and Gerard M. Murphy

Gastroenterology Unit, Division of Medicine, United Medical and Dental Schools of Guy's and St. Thomas's Hospitals, London SE1 9RT (UK)

(Received 22nd December 1992; revised manuscript received 15th April 1993)

Abstract

An amperometric enzyme electrode for the detection of bile acids using 3-α-hydroxysteroid dehydrogenase coupled to an *N*-methyl phenazinium tetracyanoquinodimethanide electrode (NMPTCNQ) is described. Kinetic analysis shows that the rate limiting step is the transport of substrate through the membrane. The response time of the electrode is less than 5 min and it has a detection limit of 1 μM. The electrode has the advantage over conventional methods of being able to detect the amount of free bile acid in solution. It has been tested in clinically derived samples of gastric aspirate. Excellent agreement has been found between the enzyme electrode and the more cumbersome conventional assay which involves incubation and the spectrophotometric determination of enzymatically produced NADH. The enzyme electrode has also been used to measure bile acid concentrations in plasma.

Keywords: Kinetic analysis; Amperometry; Sensors; Bile acids; Enzyme electrodes

In previous papers [1–3], the theory and development of a number of amperometric enzyme electrodes in which the enzyme is trapped behind a membrane have been described. Electrodes manufactured from the conducting organic salt *N*-methyl phenazinium tetracyanoquinodimethanide (NMPTCNQ) have been shown to efficiently oxidize the ubiquitous cofactor NADH [3–5].

Correspondence to: E. Magner, Massachusetts Institute of Technology, Department of Chemistry, Room 16-210, Cambridge, MA 02139 (USA).

[1] Present addresses: Department of Chemistry, McGill University, Montreal, PQ, H3A 2K6 (Canada) (R.B.L.); Department of Chemistry, Room 16-210, Massachusetts Institute of Technology, Cambridge, MA 02139 (USA) (E.M.); Department of Pharmaceutical Chemistry, University of California, San Fransisco, CA 94143 (USA) (G.R.); Faculty of Medicine, McMaster University, Hamilton, Ontario, L8S 4M1 (Canada) (D.A.).

Coupling of this reaction with a hydroxysteroid dehydrogenase enzyme as in the scheme below

$$SH_2 + NAD^+ \xrightarrow[\text{dehydrogenase}]{\text{Hydroxysteroid}} S + NADH + H^+$$

$$NADH \xrightarrow{NMPTCNQ} NAD^+ + H^+ + 2e^-$$

allows for the selective determination of bile acids (SH_2). The enzyme, 3-α-hydroxysteroid dehydrogenase, catalyses the oxidation of the 3-α-hydroxy group to a carbonyl group. The structures of the four bile acids studied are shown in Fig. 1.

Due to their amphipathic nature, bile acids play an important role in the digestion process; they are involved in the intestinal absorption of fatty acids and lipids [6] and are believed to be involved in duodeno-gastric reflux [7] and in gallstone formation [8]. Disturbance of bile acid metabolism is an important feature of many hu-

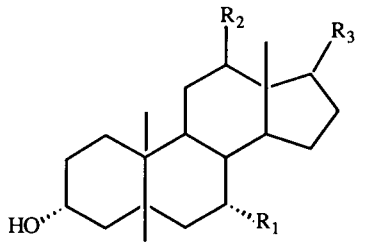

TC, $R_1 = R_2 = OH$, $R_3 = C_3H_6CONH(CH_2)_2SO_3^-$
CDC, $R_1 = H$, $R_2 = OH$, $R_3 = C_4H_8CO_2^-$
TDC, $R_1 = H$, $R_2 = OH$, $R_3 = C_3H_6CONH(CH_2)_2SO_3^-$
TCDC, $R_1 = H$, $R_2 = OH$, $R_3 = C_3H_6CONH(CH_2)_2SO_3$

Fig. 1. Structure of bile acids used.

man diseases, e.g. liver dysfunction [9]. Consequently, the measurement of bile acid concentrations can be used as a diagnostic marker for a number of pathological conditions [7–9].

At concentrations above ca. 1 mM, bile acids form micelles. Unlike small-molecular-weight amphiphiles such as sodium dodecyl sulfate, aggregation occurs over a wide range of concentrations rather than at a single concentration. In vivo, the physiologically important parameter is the concentration of the monomer species [10].

Bile acid concentrations are currently determined using ion-exchange chromatography followed by coupled gas chromatography–mass spectrometry [11] or by spectrophotometric monitoring of NADH in an enzymatic assay [12]. Both of these methods measure the total concentration of bile acids, and are not capable of measuring the monomer concentration. In this paper, the development of a sensor for the in vitro measurement of bile acid concentrations is reported where the sensor detects the concentration of monomeric bile acid using a simple electrochemical setup.

EXPERIMENTAL

Cavity electrodes (1 mm in diameter, 0.3 mm depth) of a paste of silicone oil (Aldrich) and NMPTCNQ [3], a saturated calomel electrode and a strip of platinum gauze were used as the working, reference and counter electrodes respectively. In analyzing clinical samples, a three-in-one electrode [working electrode (1.5 mm diameter cavity, 0.3 mm depth), reference electrode (Ag/AgCl in saturated NaCl)] and counter electrode (platinum disc, 1 mm diameter) was used. The working electrode was potentiostatted at 0 V (SCE) in all experiments. Experiments were peformed using an in-house apparatus and the current was recorded on a Bryans 60000 $X - Y$ chart recorder.

CHES buffer [2-(*N*-cyclohexylamino)ethane sulfonic acid, 0.15 M, pH 8.9 (Sigma)] was used unless otherwise stated. The background electrolyte also contained 10 mM NAD^+ (Sigma, grade III) and sodium chloride (0.1 M). The enzymes used, 3-α- and 7-α-hydroxysteroid dehydrogenase [*Pseudomonas testoronii* (EC 1.1.1.150 and EC 1.1.1.159) respectively] were purchased from Sigma. Human serum albumin and all of the bile acids [taurocholate (TC), chenodeoxycholate (CDC), taurochenodeoxycholate (TCDC), taurodeoxycholate (TDC) and deoxycholate (DC)] used were also from Sigma. The bile acids were used as received. All other chemicals were of Analar grade. Dialysis membranes (SpectraPor) were purchased from Pierce and Warriner. Unless otherwise stated, all experiments used SpectraPor 2 membrane (MW cutoff 12–14 kD). Deionised water (Elgastat or Milli-Q) was used throughout. Plasma used was obtained from one of the authors.

Methanolic extracts of gastric aspirates were prepared using Amberlite XAD-2 and the bile acid extraction procedure as described in the literature [13]. Following this procedure the samples were diluted with background electrolyte containing NaCl, CHES and NAD^+ as described above until the concentration of bile acids lay in the range 0.1 to 2 mM. In the electrochemical assay, the membrane electrode was dipped into a 10-ml sample of the solution and after 5 min a steady current was observed. In the spectrophotometric assay, after dilution, the sample was incubated with enzyme for 30 min at 37°C. The total amount of NADH formed was then measured spectrophotometrically at 340 nm.

When measuring the response of the sensor in plasma, the electrode was placed in a 1.0-ml

solution of sodium phosphate buffer (0.1 M, pH 7.4). To this was added 1.0 ml of plasma. An increase in current resulted which can be ascribed to the oxidation of ascorbate present in the plasma. A known quantity of bile acid was then added, with no change in current being observed. Addition of NAD^+ produces a second rise in the observed current, which can be attributed to the oxidation of bile acid. This method filters out any interferences as the observed increase in current after addition of NAD^+ can only come from bile acids present in solution.

A 0.25-ml solution of bile acid and albumin was made up to 0.75 ml with ethanol in Eppendorf tubes. This procedure precipitates the albumin which was subsequently removed by centrifugation (60 s pulse at 13 500 rpm (9000 *g*) using a microcentrifuge). A 100-μl aliquot was then added to the electrochemical cell and the resulting current compared with that obtained from an aliquot from a similar solution to which no albumin had been added.

RESULTS AND DISCUSSION

It is desirable that an amperometric sensor of the type used here operates such that the response of the electrode is governed by transport of the substrate through the membrane. The first task was therefore to find a membrane that was sufficiently permeable to bile acids whilst retaining the enzyme in the electrolyte layer between the membrane and the electrode. A number of membranes were used, after which it was found that membranes with a MW cutoff of greater than ca. 1.5 kD were required in order to be able to measure any response. This apparently high cutoff is required because bile acids, due to their shape, tend to behave like molecules with a molecular weight of 1–1.5 kD rather than the typical value of ca. 0.4 kD.

For each of the four bile acids studied, the same variation of current with bile acid concentration was obtained; an initial linear region followed by saturation of the response. There are two different explanations for the latter behavior. For taurocholic acid (Fig. 2A), as shown below,

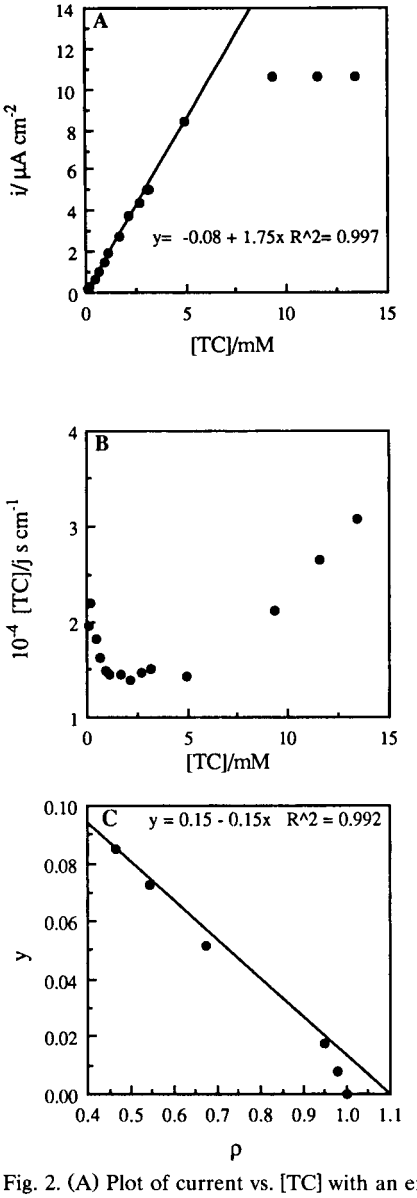

Fig. 2. (A) Plot of current vs. [TC] with an enzyme concentration of 30 units/ml; (B) Hanes plot and (C) ρ plot of data in (A).

there is a switch from the response being governed by transport of the bile acid across the membrane to it being controlled by enzyme kinetics. For the three other bile acids, saturation is caused by the formation of micelles. The porosity of the membrane is such that only monomer can diffuse through the membrane, thereby excluding the micelles.

Typical results for the variation of current density (i) with the concentration of taurocholic acid are shown in Fig. 2A. A good linear response is obtained up to ca. 2 mM, after which the response saturates. A response time (100%) of 5 min was observed. The kinetic analysis described previously [3] is used to ascertain the rate limiting step. From the Hanes type plot (Fig. 2B) of $[S]/j$ vs. [S], where [S] is the concentration of bile acid and j is the flux, a ρ plot [3] of the data is constructed (Fig. 2C) where s_∞ is the bulk bile acid concentration, k_s is the mass transfer rate constant

$$y = \frac{\rho^{-1} - 1}{s_\infty} = \frac{1}{K_{ME}}\left[1 - \frac{\rho k'_{ME}}{k_s}\right]$$

and

$$\rho = \frac{[j/s_\infty]}{[j/s_\infty]_0} \leq 1$$

for the transport of substrate through the membrane, K_{ME} is equivalent to the Michaelis Menten constant (K_M) in homogeneous enzyme kinetics and k'_{ME} is the effective electrochemical rate constant for the enzyme electrode at low substrate concentrations. A linear plot is obtained with ρ_0, the x intercept, being equal to unity, indicating that the response of the electrode is governed by transport of bile acid through the membrane. This conclusion is further reinforced by the fact that decreasing the pore size of the membrane (SpectraPor 3, MW cutoff of 3.5 kD) decreases the magnitude of the response in the linear region (by 45%), which can be ascribed to a decrease in k_s. The y intercept on the Hanes plot yields a value of 6.6×10^{-5} cm s^{-1} for k'_{ME}. From the y intercept of the ρ plot a value of 6.7 mM is obtained for K_{ME}. This value compares with the solution value of ca. 10 μM for K_M [14], showing one of the advantages of a membrane electrode where the dynamic range of the electrode can be greatly enhanced through judicious use of the appropriate membrane.

A similar value of k'_{ME} ($\pm 10\%$) (in the initial linear region) to that obtained for taurocholate is obtained for each of the other bile acids. For taurocholic acid increasing the enzyme concentration leads to a proportional increase in the limiting current, further demonstrating that the rate determining step in the saturated region involves enzyme kinetics. With the other three bile acids such as chenodeoxycholic acid, changing the enzyme concentration does not alter the limiting current. This is a result of the fact that the bile acid monomers begin to aggregate, limiting the pool of bile acid available for detection. This aspect of the chemistry of bile acids can be used to advantage as, with the electrode described here, it is now possible to measure the physiologically important free bile acid concentration. The use of the electrode to study the micellization of bile acids will be presented in a future paper [15].

The fact that the response of the electrode is controlled by mass transport of the analyte means that, as long as this condition is fulfilled, factors such as enzyme loading and the composition and pH of the buffer are not important. The lifetime of the electrode was found to be one day, as after continuous use for ca. 12 h followed by overnight storage in buffer, the response of the electrode above ca. 20 μM is determined by enzyme kinetics. Consequently, a new electrode was prepared each day using a fresh solution of enzyme.

It should be noted that the enzyme adsorbs readily on to the surface of the electrode. With adsorbed enzyme (no membrane), a plot of current density vs. concentration of bile acid is initially linear, but with a sensitivity which is only 10% of that of the membrane electrode. The response levels off after a concentration of 100 μM. This saturation is probably due to enzyme kinetics becoming rate limiting.

Determination of bile acids in extracts of gastric aspirate

Patients with a defective pyloric sphincter between the stomach and the duodenum may suffer from duodeno-gastric reflux, a condition where bile from the duodenum enters the stomach and may digest the stomach wall. As noted above, the bile acid content of gastric aspirate is currently analyzed spectrophotometrically following incubation at 37°C for 30 min. A faster method of analysis is thus desirable. Figure 3 compares typi-

cal results for the electrochemical assay with those obtained using the spectrophotometric assay. Excellent agreement between the two methods is obtained. In the spectrophotometric assay, the increase in absorbance at 340 nm due to production of NADH is equivalent to the total concentration of bile acid. In the electrochemical assay, the steady state current is a measure of the total bile acid concentration as the differences in k_s for the different bile acids are small.

Determination of bile acids in plasma

Elevated levels of bile acids in blood are thought to be an early indication of liver dysfunction [9]. In the blood, bile acids are transported to and from the intestine and the liver. Transport is effected by albumin to which bile acids are strongly bound [10]. The binding constants for a number of bile acids have been determined [10]. There appear to be two classes of binding sites; strongly binding sites which bind from two to six bile acid molecules per molecule of albumin and weakly binding sites which can bind up to twenty molecules of bile acid. At bile acid concentrations less than 1 mM, only the high affinity sites are of importance. In normal healthy individuals, the concentration of bile acids is typically 2–3 μM [10]. In patients suffering from liver dysfunction, the concentration of bile acids can be as high as 250 μM. Thus a necessary requirement for any bile acid sensor for plasma samples is the ability to measure low levels of bile acid, down to 2 μM.

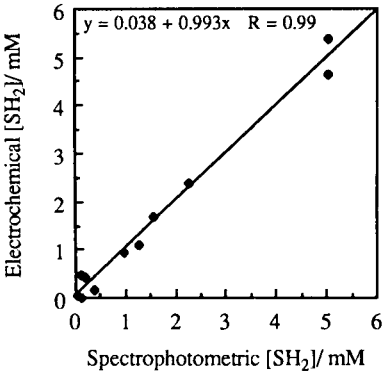

Fig. 3. Comparison of electrochemical assay vs. spectrophotometric assay of bile acids in gastric aspirate extracts.

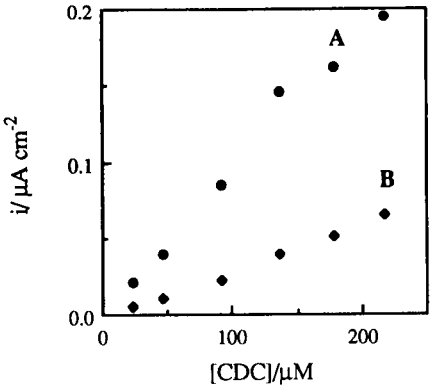

Fig. 4. Comparison of electrode response to added CDC in buffer (A) to that in plasma (B) at an enzyme concentration of 250 units/ml.

A good linear plot ($y = 0.002 + 0.0016 \cdot$ [CDC], $R^2 = 0.999$) is obtained in the region 2–50 μM. The limit of detecttion of the electrode under these conditions was found to be 1 μM, the concentration of bile acid at which the signal-to-noise ratio has a value of 3. At the pH used (7.4), the response of the electrode is still linear (Fig. 4A), though the limiting current at higher concentrations (greater than 500 μM) decreases as expected from the pH profile of the enzyme [14].

As albumin has a molecular weight of ca. 68 kD [16], any bile acid molecules bound to it are effectively screened off from detection by the membrane entrapped enzyme. Thus, only unbound ("free") bile acid can be detected. Addition of bile acids to plasma shows a much diminished response compared (Fig. 4B) with a simple calibration plot in buffer (Fig. 4A). This carries the advantage that what is being measured is the active bile acid concentration, an advantage that is unique to this electrode. The electrode however will not be able to detect bile acid which is present in normal concentrations as, using chenodeoxycholate as an example, for a total concentration of 2 μM only ca. 0.04 μM will be free in solution [10]. Thus, while it would be desirable to be able to measure free bile acid concentration, it is not possible to do so unless the total concentration of bile acid is elevated, to approximately 50 μM.

Two approaches were taken in an attempt to overcome the problem of measuring the concentration of bile acid in the presence of albumin. The first involved blocking the binding sites of bile acids on albumin. The second approach involved destruction of the albumin binding capability through the use of various denaturants. Using the first approach, a variety of substances which bind to albumin were added to a solution of bile acid and albumin in an attempt to release the bound bile acid. These substances included Cibracon Blue [17], Evans Blue and oleic acid [18]. No increase in current and hence no measurable displacement of the bile acid was observed. An alternative method was to use a bile acid which lacks the 3-α-hydroxy group so that the 7-α-hydroxysteroid dehydrogenase could be used instead. As for the 3-α-enzyme, the response at low substrate concentration is determined by transport through the membrane. Deoxycholic acid has no 7-α-hydroxy group and binds to albumin with a binding constant of 4×10^4 M^{-1} [10]. Addition of a large excess of deoxycholic acid to a solution of chenodeoxycholic acid and albumin gives rise to a small increase in currrent, but does not restore the current to the level expected. The reasons for this are unclear. While deoxycholic acid does not possess a 7-α-hydroxy group, it is possible that it acts as a competitive inhibitor for the 7-α-hydroxysteroid dehydrogenase enzyme.

Using the second approach, classical denaturing techniques such as heating, addition of base/acid, urea, guanidine, sodium dodecyl sulfate and ammonium sulfate failed to liberate the bound bile acids. The only method that yielded quantitative results was that used by Cohn et al. [19] to produce fatty acid free albumin. Using this methodology it is possible to recover 96% of the added bile acid (Fig. 5).

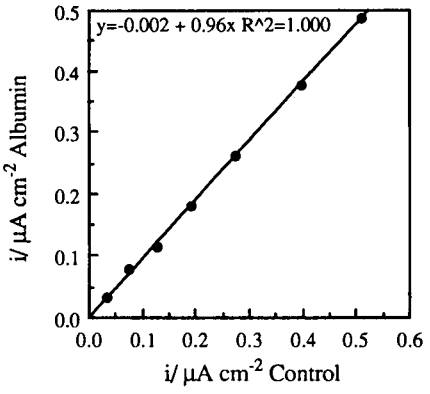

Fig. 5. Comparison of response from taurocholate recovered from a solution containing albumin (40 g dm^{-3}) to the response from a control solution containing no albumin. Enzyme concentration as in fig. 4.

Conclusions

An enzyme electrode for the determination of bile acids has been developed which has a number of advantages compared with the spectrophotometric assay that is conventionally used. A significant advantage of this enzyme electrode is the fact that the clinically important quantity, the free bile acid concentration is measured. Furthermore, the long incubation period involving the consumption of expensive enzyme is not necessary using the enzyme electrode. The dynamic range of the measurement is increased by two orders of magnitude and finally, the equipment used is much cheaper than that required for the spectrophotometric assay. Both the electrochemical and spectrophotometric assays share the disadvantage of being able to measure just the total concentration of all 3-α-hydroxysteroids and not the concentrations of individual bile acids.

Professor Desmond Johnston is gratefully acknowledged for the provision of laboratory space and his assistance during the course of this work. R.B.L. acknowledges the award of a postdoctoral fellowship from NATO.

REFERENCES

1 W.J. Albery and P.N. Bartlett, J. Electroanal. Chem., 194 (1985) 211.
2 W.J. Albery, Y.N. Kalia and E. Magner, J. Electroanal. Chem., 325 (1992) 83.
3 W.J. Albery, P.N. Bartlett, A.E.G. Cass and K.W. Sim, J. Electroanal. Chem., 218 (1987) 127.
4 K. McKenna, S.E. Boyette and A. Brajter-Toth, Anal. Chim. Acta, 206 (1988) 75.
5 S. Zhao, U. Korell, L. Cuccia and R.B. Lennox, J. Phys. Chem., 96 (1992) 5641.
6 A.F. Hofmann and B. Borgstrom, J. Clin. Invest., 43 (1964) 247.

7 H.W. Davenport, Gastroenterology, 54 (1968) 175.
8 S.N. Marcus and L.W. Heaton, Gut, 29 (1988) 522.
9 M.G. Korman, A.F. Hofmann and W.H. Summerskill, N.E. J. Med., 290 (1974) 1399.
10 F. Scagnolari, A. Roda, A. Fini and B. Grigolo, Biochem. Biophys. Acta., 791 (1984) 274.
11 K.V. Wood, Y. Sun and R.G. Elkin, Anal. Chem., 63 (1991) 247.
12 G.M. Murphy, B.H. Billing and D.N. Baron, J. Clin. Path., 23 (1970) 594.
13 P. Talalay and P.I. Marcus, J. Biol. Chem., 218 (1956) 675.
14 S. Barnes and A. Chitranukroh, Ann. Clin. Biochem., 14 (1977) 237.
15 G. Rao, Ph.D. thesis, University of London, 1990.
16 A.L. Lehninger, Biochemistry, Worth, New York, 2nd edn., 1975, p. 176.
17 R.J. Leatherbarrow and P.D.G. Dean, Biochem. J., 189 (1980) 27.
18 D.S. Goodman, J. Am. Chem. Soc., 80 (1958) 3892.
19 E.J. Cohn, L.E. Strong, W.L. Hughes, D.J. Mulford, J.N. Ashworth, M. Melin and H.L. Taylor, J. Am. Chem. Soc., 68 (1946) 459.

Analytica Chimica Acta, 281 (1993) 663–671
Elsevier Science Publishers B.V., Amsterdam

Preparation and characterization of a multi-cylinder microelectrode coupled with a conventional glassy carbon electrode and its application to the detection of dopamine

Wenfeng Peng and Erkang Wang

Laboratory of Electroanalytical Chemistry, Changchun Institute of Applied Chemistry, Chinese Academy of Sciences, Jilin 130022 (China)

(Received 13th January 1993; revised manuscript received 27th April 1993)

Abstract

A multi-cylinder microelectrode coupled with a conventional glassy carbon disc electrode (MCM/GC) was prepared and characterized using cyclic voltammetry and chronoamperometry. It was demonstrated that in the same way as one observed a steady-state current at closely spaced microelectrodes when redox recycling takes place, the same effect can be obtained with the MCM/GC device. The experimental results obtained with $K_3Fe(CN)_6$ solutions were compared with a previously developed theory. Further, it was demonstrated that with a carbon fibre MCM/GC device, the voltammetric behaviour of dopamine is greatly improved by virtue of redox recycling, hence giving high sensitivity. The steady-state collection current was linearly related to dopamine concentration in the range 1×10^{-4} to 5×10^{-7} mol l^{-1}, and the detection limit was 2×10^{-7} mol l^{-1}. The influence of coexisting ascorbic acid was also investigated. This device was applied successfully in the determination of dopamine hydrochloride in pharmaceutical preparations.

Keywords: Amperometry; Voltammetry; Chronoamperometry; Dopamine; Multi-cylinder microelectrode; Pharmaceuticals

Owing to the improvement in signal-to-noise characteristics micrometre-scale amperometric electrodes have advantages over conventional electrodes [1]. However, the currents delivered by individual microelectrodes are very small and this has an adverse effect on their detectability. For instance, a small-scale microdisc electrode may give a steady-state diffusion current after a few seconds of electrolysis in static solution, but this electrode usually has sensitivity of a few pA (μmol l^{-1})$^{-1}$, limiting the determination of electroactive species to low micromolar concentrations with sensitive current-measuring instrumentation [2].

Great emphasis has been placed on the development of regular or irregular arrangements of microelectrodes in an attempt to amplify the current output [3–21]. As a consequence of these studies, two typical devices have emerged which are now considered to have particular value for trace microchemical determinations: the regular microdisc array electrode (DAE) and the interdigitated microband array electrode (IDE). The former is a simple microelectrode ensemble, as all units with suitable distances are electrically connected and operated at the same potential and the total current is the sum of the individual

Correspondence to: E. Wang, Laboratory of Electroanalytical Chemistry, Changchun Institute of Applied Chemistry, Chinese Academy of Sciences, Jilin 130022 (China).

currents [3,9,10,12]. For example, a 1 mm^2 device with disc radius of 5 μm and disc density of 100 mm^{-2} would have a theoretical steady-state current output of the order of 100 pA $(\mu mol\ l^{-1})^{-1}$. With such a device, submicromolar determinations in static solution are feasible.

By comparison, IDE has received more attention in recent years [5,6,15–17,20]. This is a two-electrode device consisting of an anode and a cathode; each electrode is composed of a series of microscopic band connections and alternate anode and cathode microbands are separated by an insulation gap a few micrometres wide. The IDE operates by recycling a reversible redox species between the anode and the cathode and this process generates an amplified and stable current that is tens of times greater than for macroscopic electrodes, with a sensitivity of the order of tens of nA $(\mu mol\ l^{-1})^{-1}$ and detection limits at nanomolar concentration levels [16]. Interest in "redox recycling" microelectrode devices has steadily increased not only owing to their high sensitivity, but also because of the working mechanism which promises applications in kinetic studies in electrochemistry [11,22–24].

In this paper, a multi-cylinder microelectrode coupled with a conventional glassy carbon disc electrode (MCM/GC) is proposed. This device combines features of both DAE and IDE and delivers a fast and enhanced steady-state response with a sensitivity similar to that of IDE. In comparison with other "redox recycling" devices, it has the advantage of facile fabrication. As most microelectrode materials take the shape of a cylinder, the MCM/GC device can be prepared very cheaply, whereas other devices are made by sophisticated methods such as microlithography [5,6,15–17] and screen printing technology [20], which require instrumentation and expertise not usually found in an electrochemical or analytical laboratory. A further advantage is that carbon fibre can be used as the electrode material. This material has proved to have a low background over a wide positive potential range [25] and is especially advantageous for the electrochemical oxidation of organic compounds.

A theoretical treatment of the mass transport process at a multi-cylinder microelectrode coupled with a parallel planar electrode has recently been attempted, and the following expression was derived for the steady-state diffusion current [26]:

$$i = 2\pi mnFDlC^b/\cosh^{-1}(w/r + 1) \quad (1)$$

where D is the diffusion coefficient and C^b the bulk concentration of the analyte, n the number of electrons, F the Faraday constant, r, l and m the cylinder radius, length and number, respectively, and w the distance from the microcylinders to the plane electrode. This paper presents some experimental results that demonstrate its practical validity.

Voltammetric detection of catecholamines has attracted considerable attention in biomedical applications such as liquid chromatography, biosensors and in vivo measurements of neurotransmitters [27–30]. Among various electrodes used, pretreated carbon fibre [31,32] and carbon fibre array [33] electrodes have proved to be of high sensitivity. In this work, the MCM/GC device was further evaluated in the detection of dopamine.

EXPERIMENTAL

Chemicals and materials

Potassium hexacyanoferrate(II) (Beijing Chemical Factory), dopamine (Sigma, St. Louis, MO, USA) and ascorbic acid (Beijing Chemicals) were of analytical-reagent grade. Dopamine and ascorbic acid solutions were freshly prepared in 0.2 mol l^{-1} Na_2HPO_4–KH_2PO_4 buffer (pH 7.1); as the two species are fairly readily oxidized, the phosphate buffer was degassed for 10 min by nitrogen purging immediately before use. Potassium hexacyanoferrate(III) solutions were made using potassium chloride (Chantou Chemical Factory) as the supporting electrolyte. Other chemicals used for interference experiments were of analytical-reagent grade. All solutions were prepared with doubly distilled water.

Microscopic platinum wires of diameters 10, 20 and 30 μm were purchased from Goodfellow (UK). Carbon fibres of diameter 14.5 μm (99% carbon) (Hysol Grafil, UK) was a kind gift from Professor H.B. Mark, Jr., during a visit to Wuhan

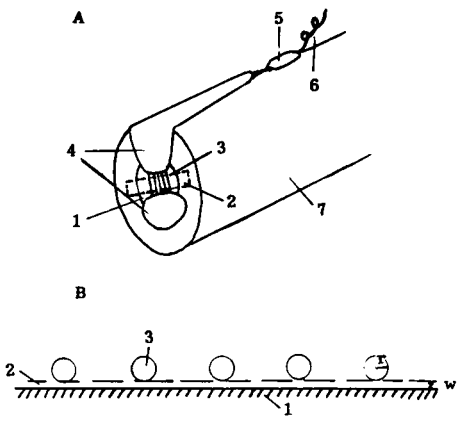

Fig. 1. (A) Illustration of multi-cylinder microelectrode coupled with a glassy carbon disc electrode (MCM/GC). 1 = GC disc electrode; 2 = PTFE band; 3 = platinum microwires or carbon fibres; 4 = epoxy resin; 5 = silver conducting paint; 6 = copper lead; 7 = PTFE rod. (B) Cross-section at the centre.

University. Polyester sheets of thickness 0.5 mm and PTFE films of thickness 2, 10 and 30 μm were supplied by the Laboratory of Polymer Chemistry of this Institute. Dongfeng AD-U epoxy resin and DH-1 silver conducting paint were produced by Dongfeng Chemical Plant, Guangzhou, and Science Equipment Company of China, respectively.

Preparation of MCM / GC device

The MCM/GC device was constructed by a micromanipulation technique developed in this laboratory. Prior to fabrication, platinum wires and carbon fibres were washed thoroughly with water, acetone and 2-propanol and were examined by optical microscopy for imperfections. A GC disc electrode of diameter 4 mm was polished carefully with alumina slurries of 1 and 0.5 μm and residual polishing material was removed from the surface by sonication in a doubly distilled water-bath for 5 min. As illustrated in Fig. 1, an extremely thin PTFE band (ca. 0.5 mm wide) was extended on the GC surface and was pressed tight to ensure close contact, and the micrometre-scale wires or fibres were then placed across the band in a coplanar parallel geometry. A drop of semi-cured epoxy resin was applied to either side of the band for electrode positioning and insulation. The distances between individual wires or fibres were adjusted under a conventional optical microscope using a fine sewing needle (ca. 50 μm tip diameter). After 24 h, the resin hardened and the PTFE band was carefully drawn off. Electrode contact to individual or multiple wires or fibres was achieved using silver conducting paint.

The distance between the microcylinders and the GC surface, w, was obtained in terms of the thickness of the spacing PTFE band. The average cylinder length, l, and the distances between microcylinders were measured with an optical microscope fitted with a calibrated vernier at high magnification. The device was not ready for use until an electrical examination had been made; the purpose of this procedure is to ensure that electrical short-circuiting does not occur. For a qualified MCM/GC device the resistance between the microcylinder electrode and the GC electrode was found to be typically > 20 MΩ.

The MCM/GC device was electrolytically preconditioned before application. The treatment given here for platinum electrodes was to apply a cyclic potential sweep of 100 mV s^{-1} in 0.5 mol l^{-1} H_2SO_4 electrolyte in the range -1.0 to $+1.0$ V vs. Ag/AgCl. The carbon fibre microelectrodes was activated by anodic conditioning in phosphate buffer solution (pH 7.1); the potential was scanned at the same rate from 0.0 to $+1.5$ V vs. Ag/AgCl for over ten cycles.

Instrumentation and measurements

Experiments were carried out using a bipotentiostatic voltammeter (CMBP-1; Jiangsu Electroanalytical Instrument Factory), a picoamperometer (Model 902-PA, developed by Wuhan University) and an x–y–t two-pen recorder (Model 3033; Yokogawa Hokushin Electric). As the voltammeter had a current measuring range from hundreds of mA to a few μA and could not be used for very low concentration measurements with microelectrodes, a picoamperometer was fitted to it simply by connecting the output "grounds" of the two instruments. The picoamperometer employed was of high sensitivity: a vacuum static electronic tube of input impedence $> 10^{15}$ Ω was used for

current-to-voltage (I/V) conversion [34]. Voltammetry and chronoamperometry were performed mainly in three modes: (1) the GC is kept at open circuit so that, as in a conventional three-electrode configuration, the microelectrode is the only working electrode; (2) the microelectrode works as generator electrode to which a potential sweep or step is applied, while the GC maintains a constant potential and works as a collector electrode; (3) in contrast to (2), the microelectrode works as a collector electrode and the GC as a generator electrode. The specific conditions are given in the figure captions. All experiments were carried out at room temperature (18–20°C).

RESULTS AND DISCUSSION

Cyclic voltammetry

Figure 2A shows the cyclic voltammetric behaviour of the multiple microscopic platinum wire electrode for the reduction of $Fe(CN)_6^{3-}$ in aqueous KCl solution. For a five-cylinder microelectrode with $r = 10$ μm and distances between adjacent cylinders exceeding 0.5 mm, a peak-shaped voltammogram is obtained at a sweep rate of 20 mV s^{-1}. When a GC disc electrode is coupled with these cylinders in a parallel geometry with a 2-μm gap (i.e. $w = 2$ μm), bipotentiostatic voltammetry can be performed with the microelectrode as a generator electrode or collector electrode. The two operational modes produce well defined steady-state currents at the multi-cylinder microelectrode which are much larger than those when the GC is not working (i.e. the GC is left at open circuit), as shown in Fig. $2B_2$ and $2C_1$, where ca. 2.7- and 2.3-fold amplifications are found, respectively.

For the above multi-cylinder microelectrode coupled with a GC disc electrode where the individual cylinders are wide apart, similar voltammetric behaviour to that of individual cylinder electrodes is exhibited in terms of wave features. Figure 2C shows a steady-state current of 3.56 μA for the microelectrode composed of five cylinders, whereas the currents obtained in the same way at individual cylinders add up to 3.60 μA. This agreement implies that the individual cylinders in the MCM/GC device work independently and have no mutual influences on the amperometric response. Therefore, from the viewpoint of increasing the current output, more microcylinders can be arranged in an MCM/GC device.

However, this conclusion does not apply when the distances between cylinders are small with respect to their diameters. The MCM/GC device

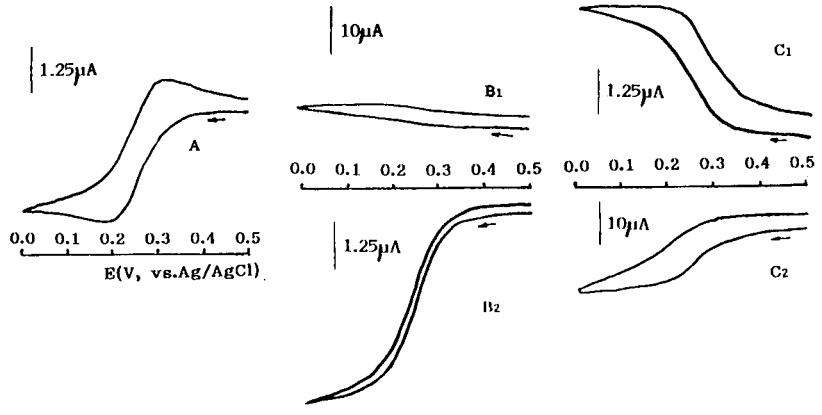

Fig. 2. Cyclic voltammograms of 1.67×10^{-3} mol l^{-1} $K_3Fe(CN)_6$ in 0.2 mol l^{-1} KCl solution obtained with a platinum MCM/GC device. Dimensions of the device: $r = 10$ μm; $w = 2$ μm; $l = 0.74$ mm; $m = 5$. Potential sweep from 0.0 to +0.5 V vs. Ag/AgCl at 20 mV s^{-1}. (A) cylinder microelectrode only working (GC kept at open circuit); (B_1, B_2) generator–collector mode, GC (B_1) kept at +0.5 V vs. Ag/AgCl; (C_1, C_2) as B_1, B_2, microelectrode (C_1) at +0.5 V vs. Ag/AgCl.

used in Fig. 3 involves only two microcylinders with a distance of 5 μm ($r = 15$ μm, $w = 10$ μm); the total steady-state current at the dual-cylinder microelectrode is 70% of that obtained by doubling the individual currents (comparisons are made between Fig. 3C and E and Fig. 3D and F). Except for the current amplitude, pronounced peaks are observed on the *i–E* waves. These probably result from interaction of the diffusion fields established between individual cylinder electrodes and the GC electrode or, in other words, diffusion shielding exists between co-potentiostated microcylinders. The diffusion shielding phenomenon is further demonstrated in Fig. 3B where the coupled GC is not working. Figure 3A shows that the increase in the steady-state current is less than twice the single electrode value, in addition to giving rise to an *i–E* wave with more pronounced peak characteristics.

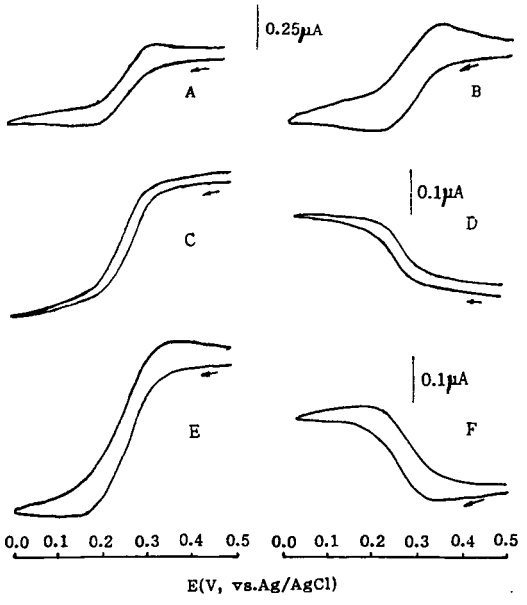

Fig. 3. Cyclic voltammograms of $K_3Fe(CN)_6$ obtained with an MCM/GC device with $r = 15$ μm, $w = 10$ μm, $l = 1.18$ mm, $m = 2$ and a distance between dual cylinders of 5 μm. Other conditions as in Fig. 2. (A) Single-cylinder microelectrode; (B) dual-cylinder microelectrode; (C) A, as generator (GC collector); (D) A, as collector (GC generator); (E) B, while GC is at +0.5 V vs. Ag/AgCl; (F) B, as collector at +0.5 V vs. Ag/AgCl.

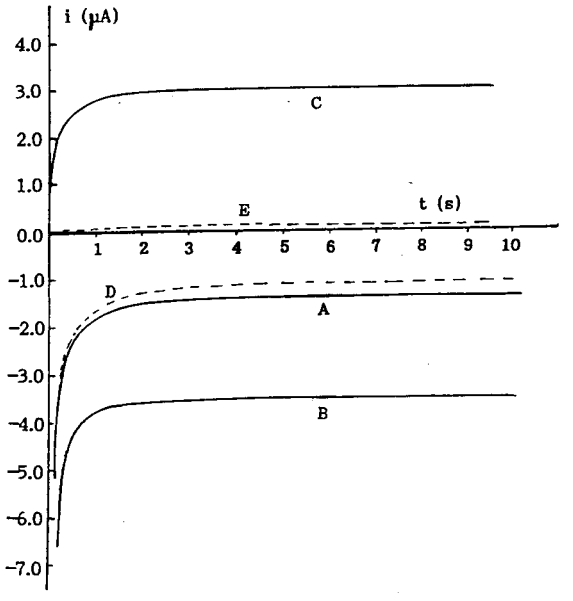

Fig. 4. Chronoamperometric curves of MCM/GC device. Concentrations of $K_3Fe(CN)_6$ and ascorbic acid: 1.01×10^{-3} and 5.20×10^{-4} mol l^{-1}, respectively. Potential steps are from +0.5 to 0.0 V for the former and vice versa for the the latter. Other conditions as in Fig. 2. (A) multi-cylinder microelectrode only working; (B, D) microelectrode works as generator, GC as collector; (C, E) microelectrode as collector, GC as generator. Solid lines, potassium hexacyanoferrate(III); dashed lines, ascorbic acid.

Chronoamperometry

Chronoamperometry for the reduction of $Fe(CN)_6^{3-}$ at the multi-cylinder platinum microelectrode, shown in Fig. 4, illustrates the effects of GC coupling on the *i–t* response. The time-dependent behaviour of the diffusion current at the five-cylinder microelectrode follows a short Cottrell response when the diffusion layer is small relative to the electrode radius. When the GC is coupled and works as generator or collector electrode, the *i–t* curve shows large changes in terms of magnitude and speed of response; in this instance a response time of ca. 2 s to reach the steady state is estimated for the device with $r = 10$ μm and $w = 2$ μm.

It is obvious that the current amplitude of the microelectrode in the collection mode is not the same as that in the generation mode. For practical devices with $r = 10$ μm and $w = 30$, 10 and 2 μm, the ratios of the two currents were found to

be 4.0%, 25.3% and 81.3%, respectively. From this trend, current ratios approaching unity can be expected with devices with even smaller w values. The inequality of the currents obtained in the two operational modes can be ascribed to mass exchange with the bulk solution, i.e., 100% collection efficiency is not achieved in the present devices. As the $w = 2$ μm devices proved to have high current ratios, they were used to demonstrate the validity of the above-mentioned theory. Table 1 compares the steady-state current values calculated from Eqn. 1 with the experimental data, and shows that the theoretical predictions agree with the experiment to within $\pm 25\%$. It should be pointed out that the theory was developed based on a total mass recycling model [26].

The chronoamperometric behaviour of an irreversible redox species, ascorbic acid, is demonstrated in Fig. 4. Compared with hexacyanoferrate(III) of the same concentration, the steady-state currents are much smaller and, in particular, the multi-cylinder microelectrode working as a collector electrode gives essentially a background response. These results show that the MCM/GC device shows excellent selectivity for reversible redox species over the irreversible type. As will be demonstrated further, this selective property is especially favourable for low-concentration measurements, as coexisting impurities such as oxygen are no longer sensitive at the collector microelectrode.

Detection of dopamine

The mechanism of the electrochemical oxidation of dopamine is well established. Following the electrode reaction, the intermolecular cyclization of oxidized dopamine, the open-chain *o*-quinone, to the substituted indole takes place [36]. Figure 5 shows the voltammetric behaviour of dopamine at a preconditioned multi-cylinder carbon fibre microelectrode. At a sweep rate of 20 mV s^{-1}, a virtually sigmoidal voltammogram with a half-wave potential of +0.32 V vs. Ag/AgCl is obtained for the oxidation of dopamine. However, the cathodic wave appearing at +0.30 V vs. Ag/AgCl is drawn out, and the cathodic current (i_c) is small compared with the

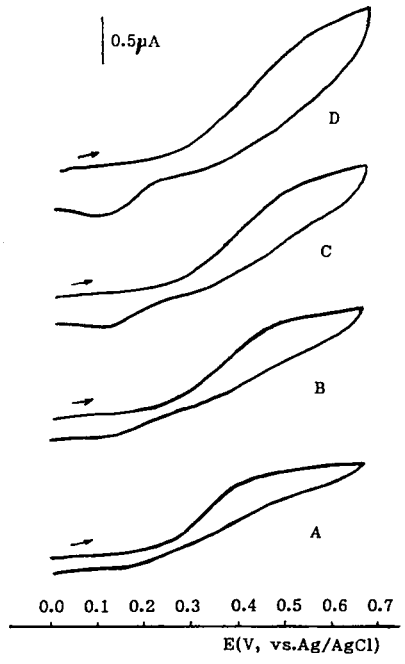

Fig. 5. Cyclic voltammograms of 1.56×10^{-3} mol l^{-1} dopamine in 0.2 mol l^{-1} phosphate buffer (pH 7.1) obtained with a multi-cylinder carbon fibre microelectrode with $r = 7.25$ μm, $m = 4$ and scan rate (A) 20, (B) 50, (C) 100 and (D) 200 mV s^{-1}.

TABLE 1

Verification of theory [26] by comparison with experimental results for 1.67×10^{-3} mol l^{-1} $K_3Fe(CN)_6$ in 0.2 mol l^{-1} KCl [a]

Device No.	r (μm)	w (μm)	l (mm)	m	i_g (μA)	i_c (μA)	i_t (μA)	$(i_g/i_t) \times 100$ (%)	$(i_c/i_t) \times 100$ (%)
1	10	2	0.74	5	4.38	3.56	3.92	111.7	90.8
2	12.5	2	0.85	4	4.35	3.42	4.01	108.5	85.3
3	15	2	1.04	4	5.25	4.05	5.37	97.8	75.4

[a] i_g and i_c are steady-state currents at the same multi-cylinder microelectrode when it works as a generator and collector electrode, respectively; i_t is the theoretical current calculated from Eqn. 1, taking $D = 6.5 \times 10^{-10}$ m^2 s^{-1} [35].

anodic current (i_a). As the potential scan rate increases, the ratio of the two currents, i_c/i_a, increases (see Table 2), suggesting that the oxidized form of dopamine can be detected by a fast sweep potential before it changes into the indole form, which is unreducible at the applied potential.

The reduction behaviour of oxidized dopamine was examined using a carbon fibre MCM/GC device with $r = 7.25$ μm, $w = 2$ μm and $m = 4$. When the GC works as a generator electrode where the above reactions proceed, oxidized dopamine can be collected at the carbon fibre microelectrode at 0.0 V vs. Ag/AgCl. As shown in Fig. 6B, the carbon fibre electrode displays a well defined sigmoidal voltammagram, indicating that the cyclization reaction is suppressed and the electrochemical reversibility of dopamine is improved. This result can be explained by the working mechanism of the MCM/GC device. Because the diffusion time of the oxidized dopamine from the generator electrode to the closely spaced collector electrode is shorter than its lifetime, a high percentage of the transient intermediate can be collected before it changes into the indole form and hence the redox recycling is enhanced.

As a consequence of high redox recycling of the dopamine–oxidized dopamine couple, high sensitivity is achieved with the MCM/GC device. The steady-state collection current at the carbon fibre microelectrode was found to be directly proportional to dopamine concentration from 1×10^{-4} to 5×10^{-7} mol l^{-1}, with a correlation coefficient of 0.996. The detection limit was 2×10^{-7} mol l^{-1} (signal-to-noise ratio = 3). For repeated measurements of 5×10^{-5} and 5×10^{-6} mol l^{-1} dopamine in phosphate buffer solutions,

TABLE 2

Dependence of cathodic/anodic current ratio on potential sweep rate (according to Fig. 5)

Current	Sweep rate (mV s^{-1})			
	20	50	100	200
i_a (μA)	0.80	0.875	1.00	1.20
i_c (μA)	0.05	0.125	0.25	0.45
i_c/i_a	0.063	0.143	0.250	0.375

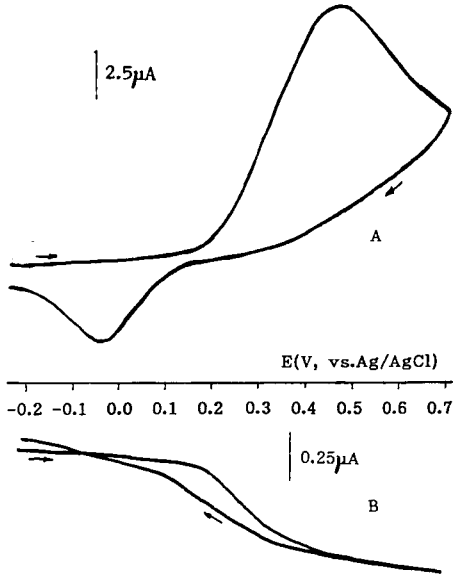

Fig. 6. Cyclic voltammograms of 1.56×10^{-3} mol l^{-1} dopamine obtained with a carbon fibre MCM/GC device at a scan rate of 20 mV s^{-1}. Dimensions of the device: $r = 7.25$ μm; $w = 2$ μm; $l = 0.83$ mm; $m = 4$. (A) and (B) represent GC and carbon fibre electrode working as generator and collector, respectively. The potential of carbon fibre electrode is 0.0 V vs. Ag/AgCl.

the relative standard deviations were 2.8% and 6.4% ($n = 7$), respectively. It should be mentioned that although the device has good reproducibility in low-concentration measurements, the current gradually decreases with use for dopamine concentrations above 10^{-3} mol l^{-1}; this may be a result of slight adsorption of the reaction products at the electrode surfaces. For this reason, after ten successive measurements the MCM/GC device must be reactivated by the electrochemical treatment procedure mentioned above.

As demonstrated by chronoamperometry, ascorbic acid itself gives virtually a baseline current at the collector microelectrode owing to its irreversibility. However, the acid is likely to reduce the oxidized dopamine in the redox recycling and decrease the current. The influence of ascorbic acid on the detection of dopamine was tested by adding ascorbic acid at fixed concentrations to dopamine solutions with a 10-μl syringe. As shown in Table 3, the steady-state current of 1.56 mmol

l^{-1} dopamine at the carbon fibre microelectrode remains independent of ascorbate concentration up to 0.75 mmol l^{-1}. When 1.0×10^{-4} mol l^{-1} ascorbic acid coexists in dopamine of the same concentration, only a 10% decrease in the collection current is observed, and for dopamine of even lower concentration, 1.0×10^{-5} mol l^{-1}, about a fourfold amount ascorbic acid hardly interferes. These results imply that most of the oxidized dopamine molecules are collected before the homogeneous reduction takes effect. Although the selectivity shown here cannot be considered very high, the method can be of value as the voltammetric detection of dopamine in an ascorbic acid-containing background continues to be an important topic owing to its applications in neuroscience [29,30].

Other interferants were also tested. Twenty-fold amounts of citric acid and tartaric acid and metal ions such as 100-fold amounts of Mg^{2+}, Ca^{2+}, and fivefold amounts of Ni^{2+}, Co^{2+}, Sn^{2+}, Zn^{2+}, Pb^{2+} and Cu^{2+} had no effect on detection. Equal amounts of Fe^{3+} and other catecholamines such as epinephrine, norepinephrine and dihydroxyphenylanine seriously interfered as they showed the same voltammetric behaviour.

TABLE 3

Results of effect of coexisting ascorbic acid on the steady-state collection current of dopamine [a]

Ascorbic acid concentration (mmol l^{-1})	Dopamine concentration (mmol l^{-1})	Collection current (μA)
0.0	1.56	0.55
0.30	1.56	0.54
0.75	1.56	0.51
1.00	1.56	0.45
1.50	1.56	0.38
3.00	1.56	0.15
0.0	0.101	0.040
0.100	0.101	0.036
0.200	0.101	0.030
0.400	0.101	0.025
0.0	0.010	0.0042
0.020	0.010	0.0040
0.040	0.010	0.0038
0.060	0.010	0.0035

[a] Data were obtained using a carbon fibre MCM/GC device with $r = 7.25$ μm, $w = 2$ μm, $l = 0.83$ mm and $m = 4$. Conditions as in Fig. 6.

TABLE 4

Results of determination of dopamine hydrochloride in injection solutions

Sample No. [a]	Labelled amount (mg per 2 ml)	Amount found [b] (mg per 2 ml)		Recovery [c] (%)
		This method	Reported method [37]	
1	20	19.65	19.70	104.5
2	20	19.90	19.88	97.0
3	20	20.22	20.18	98.0

[a] Produced by Tianjing Pharmaceutical Factory at different times. [b] Each value is an average of three individual determinations. [c] Obtained with this method after addition of dopamine.

Using the calibration graph method, the above device was applied to the determination of dopamine hydrochloride in pharmaceutical preparations. The samples were appropriately diluted with 0.2 mol l^{-1} phosphate buffer to bring the dopamine concentration to 100 μg ml^{-1} and the electrochemical measurements were followed. UV spectrophotometry was performed simultaneously for comparison. The results are given in Table 4.

Conclusions

The multi-cylinder microelectrode coupled with a GC disc electrode is a novel "redox recycling" device. The device is cheap, easy to fabricate and robust in electrochemical measurements. As demonstrated in cyclic voltammetry and chronoamperometry, the MCM/GC device displays a steady-state response for reversible redox species within 2 s electrolysis with a sensitivity of a few μA per millimolar concentration. By virture of fast redox recycling between the narrowly spaced microelectrode and GC electrode, electrogenerated species can be collected at the multi-cylinder microelectrode before competitive homogeneous reactions take place. Therefore, the MCM/GC device also shows high sensitivity for catecholamines, which are usually considered as quasi-reversible because of instability of the products of electrode reactions, and for the same

reason good selectivity is obtained in the presence of electrochemically irreversible substances.

This project was supported by the National Natural Science Foundation of China.

REFERENCES

1 M.D. Ryan and J.Q. Chambers, Anal. Chem., 64 (1992) 79R.
2 J.W. Bixler, A.M. Bond, P.A. Lay, W. Thormann, P. Van Den Bosch, M. Fleischmann and B.S. Pons, Anal. Chim. Acta, 187 (1986) 67.
3 W.L. Caudill, J.O. Howell and R.M. Wightman, Anal. Chem., 54 (1982) 2532.
4 K. Stulik, V. Pacakova and M. Podolak, J. Chromatogr., 298 (1984) 225.
5 D.G. Sanderson and L.B. Anderson, Anal. Chem., 57 (1985) 2388.
6 K.R. Wehmeyer, M.R. Deakin and R.M. Wightman, Anal. Chem., 57 (1985) 1913.
7 T. Hepel and J. Osteryoung, J. Electrochem. Soc., 133 (1986) 752.
8 C.J. Miller and M. Majda, J. Electroanal. Chem., 207 (1986) 49.
9 K. Aoki, K. Tokuda and H. Matsuda, J. Electroanal. Chem., 199 (1986) 69.
10 R.M. Penner and C.R. Martin, Anal. Chem., 59 (1987) 2625.
11 A.J. Bard and T.V. Shea, Anal. Chem., 59 (1987) 2101.
12 J. Wang and J.M. Zadeii, J. Electroanal. Chem., 249 (1988) 339.
13 J.E. Bartelt, M.R. Deakin, C. Amatore and R.M. Wightman, Anal. Chem., 60 (1988) 2167.
14 H.A.O. Hill, N.A. Klein, I.S.M. Psalti and N.J. Walton, Anal. Chem., 61 (1989) 2200.
15 O. Niwa, M. Morita and H. Tabei, J. Electroanal. Chem., 267 (1989) 291.
16 B.J. Seddon, H.H. Girault and M.J. Eddowes, J. Electroanal. Chem., 266 (1989) 227.
17 M.S. Harrinton and L.B. Anderson, Anal. Chem., 62 (1990) 546.
18 J. Wang, A. Brennsteiner and A.P. Sylwester, Anal. Chem., 62 (1990) 1102.
19 D.E. Tellman and S.L. Petersen, Electroanalysis, 2 (1990) 499.
20 D.H. Craston, C.P. Jones, D.E. Williams and N.El Murr, Talanta, 38 (1991) 17.
21 W. Peng, B.J. Seddon, X. Zhou and Z. Zhao, Fenxi Huaxue, 20 (1992) 857.
22 B.J. Feldman and R.M. Murray, Anal. Chem., 58 (1986) 2844.
23 C.E. Chidsey, B.J. Feldman, C. Lundgren and R.W. Murray, Anal. Chem., 59 (1986) 601.
24 J.J. Miasik, A. Hooper and B.C. Tofield, J. Chem. Soc., Faraday Trans. 1, 82 (1986) 1117.
25 T.E. Edmonds, Anal. Chim. Acta, 171 (1985) 1.
26 W. Peng and E. Wang, Anal. Chem., in press.
27 O. Magnusson, L.B. Nilsson and D. Winsterlund, J. Chromatogr., 164 (1979) 41.
28 R.N. Adams, Anal. Chem., 48 (1976) 1126A.
29 R.M. Wightman, L.J. May and A.C. Michael, Anal. Chem., 60 (1988) 769A.
30 R.M. Wightman, C. Amatore, R.C. Engstrom, P.D. Hale, E.W. Kristensen, W.G. Kukr and L. May, J. Neurosci., 25 (1988) 513.
31 A.G. Ewing, M.A. Dayton and R.M. Wightman, Anal. Chem., 53 (1981) 1842.
32 K.F. Martin, C.A. Marsden and F. Crespi, Trends Anal. Chem., 7 (1988) 334.
33 J. Mattusch and G. Werner, Pharmazie, 44 (1989) 39.
34 W. Peng, P. Li, Z. Chen, C. Wang and G. Lin, Anal. Instrum., 95 (1993) 10.
35 H.A.O. Hill, N.A. Klein, I.S.M. Psalti and N.J. Walton, Anal. Chem., 61 (1989) 2200.
36 M.D. Hawley, S.V. Tatawawadi, S. Piekarski and R.N. Adams, J. Am. Chem. Soc., 89 (1967) 447.
37 C.S. Sastry, V.G. Das and K.E. Rao, Analyst, 110 (1985) 395.

Analytica Chimica Acta, 281 (1993) 673–679
Elsevier Science Publishers B.V., Amsterdam

Micro-choline sensor for acetylcholinesterase determination

Eriberta N. Navera, Masayasu Suzuki, Kenji Yokoyama, Eiichi Tamiya, Toshifumi Takeuchi and Isao Karube

Research Center for Advanced Science and Technology, University of Tokyo, 4-6-1-Komaba, Meguro-ku 153 (Japan),

Junko Yamashita

Jikei University, 3-19-18 Nishi-Shinbashi, Minato-ku 105 (Japan)

(Received 13th January 1993; revised manuscript received 28th April 1993)

Abstract

A micro-choline sensor was developed using a carbon fibre working electrode for the determination of acetylcholinesterase activity in rat serum samples. The mechanism is based on the measurement of hydrogen peroxide generated from choline which is produced by the enzymatic hydrolysis of acetylcholine. The fabrication of the electrode is described. The sensor is polarized at 1.2 V. Enzyme is entrapped in a PVA–SbQ photocross-linkable polymer [poly(vinyl alcohol) containing styrylpyridinium] and covered with Nafion (perfluorosulphonated membrane), which has permselectivity characteristics, so that the access of ascorbate, a common interfering species, to the electrode surface is blocked. Using this sensor, the esterase activity was determined. The slope values showed a fast response time between 1 and 3 min and a high enzyme activity in the serum samples. The calibration graph for the choline sensor was linear between 0.05 and 5.0 mM. The operational and long-term stability of the sensor demonstrated good quality performance. The procedure for preparing this type of coated electrode indicates some attractive prospects for its use especially for the determination of organophosphorus pesticides in human serum.

Keywords: Amperometry; Biosensors; Enzymatic methods; Carbon fibre electrode; Choline; Enzyme electrodes; Serum

Esterases play an important role in re-establishing the original state of the post-synaptic membrane. They are responsible for the hydrolysis of acetylcholine, a neurotransmitter operating in the cholinergic synapses. Cholinesterase (ChE) in serum is an important indicator of liver disease [1]. In humans, the determination of serum ChE activity plays an important role in anaesthesiology [2]. Recently much attention has been focused on organophosphorus insecticides, having a common mechanism of acute toxic action, the inhibition of acetylcholinesterase (AchE) [3].

In spite of the rapid advances in protein and macromolecular chemistry during the last 15 years, and the increasing insight into the crucial role of macromolecules in cellular functions, very little information is available on the properties of ChE. In this respect, voltammetric and electrochemical studies are important. Microelectrodes have a number of features that are beneficial for electrochemical studies. The reduced area of the electrode results in a diminished charging current and allows the extension of electroanalytical techniques to samples of lower concentration and

Correspondence to: I. Karube, Research Center for Advanced Science and Technology, University of Tokyo, 4-6-1-Komaba, Meguro-ku 153 (Japan).

smaller size. The objective of this work was to fabricate a microcholine sensor capable of measuring AchE activity. Carbon fibre was used as the working electrode. Carbon fibre is a flexible electrode material combining good stimulation properties with excellent recording behaviour during in vitro and in vivo test [4].

Several physico-chemical methods are available for the determination of AchE, including spectrophotometric, conductimetric, radiometric, liquid chromatographic and microdialysis methods. However, these methods are time consuming, involve complicated procedures and require expensive equipment. In addition, colour reaction measurements are affected by chromogenic interferents. Histochemical and immunocyto-chemical studies have also been reported, but such methods can only monitor distribution patterns of centrifugal AchE-containing fibers [5]. In other work biosensors have been used, but with different electrode materials and size [6].

This paper describes a micro-choline sensor based on amperometric detection of H_2O_2 using immobilized choline oxidase (ChO) and its application to serum samples for the determination of AchE activity. The detection of H_2O_2 is already an established approach to the construction of biosensors based on electrodes containing immobilized oxidases. In addition, amperometric detection at constant potential is the most common mode of measurement because it offers the best sensitivity, requires relatively simple instrumentation and provides considerable selectivity through judicious selection of the applied potential. Before measurement the electrodes were covered with nafion, a perfluorosulphonated polymer, in order to prevent interfering signals from ascorbic acid and other anionic metabolites. The formation of H_2O_2 is based on the equation

$$\text{acetylcholine} \xrightarrow{\text{AchE}} \text{acetate} + \text{choline}$$

$$\text{choline} + O_2 \xrightarrow{\text{ChO}} H_2O_2 + \text{betaine}$$

The results presented in this paper clearly illustrate the effectiveness of the sensor in measuring AchE activity in a volume of 10 μl within a response time of 2 min with no interferences.

EXPERIMENTAL

Apparatus

Voltammetric measurements and diagnostic amperometry were carried out using a potentiostat (Hokuto Denko HB 104) and an *X–Y* recorder (Graphtec WX 2400). The electronic signal from the amperometric detection of H_2O_2 was recorded on a strip-chart recorder. A conventional three-electrode system using a platinum wire as the counter electrode, carbon fibre (100–200 μm diameter) as the working electrode and Ag/AgCl as the reference electrode. Most of the experiments were done in stirred solutions using a 1.5-cm magnetic stirrer. The batch method was employed throughout.

Reagents

ChO (EC 1.1.3.17 101, IU mg^{-1}, from *Alcaligenes* sp.), AchE (EC 3.1.1.7, 1000 IU mg^{-1}, from electric eel), and stock solutions (0.1 M) of choline chloride and acetylcholine chloride (all from Sigma) were used as substrates. Serum AchE was from mice (ICR strain), obtained from Jikei University. PVA–SbQ [poly(vinyl alcohol containing styrylpyridinium] polymer membrane was obtained from Toyo Gosei Co. Nafion (5 wt.% solution in a mixture of lower aliphatic alcohols) was provided by DuPont. Bovine serum albumin (BSA), was purchased from Wako. 2-(*N*-Morpholino)ethanesulphonic acid monohydrate (MES) buffer (pH 7.1) was used. Other reagents were of analytical-reagent grade and were used as received.

Preparation of the sensor

Electrode fabrication and pretreatment method. The carbon fibre electrode was fabricated as shown in Fig. 1 by the method of Ponchon et al. [7] with a slight modification. A sensor was prepared by mounting a carbon fibre (Toho-Beslon HA.7) with a tip diameter of ca. 100–200 μm in a glass capillary with silver paste and epoxy resin. Prior to immobilization and Nafion coating, the fabricated carbon fibre was first washed thoroughly with ethanol and distilled water and then oven-dried for 5 min at 60°C. The same carbon fibre was used as the working electrode and was

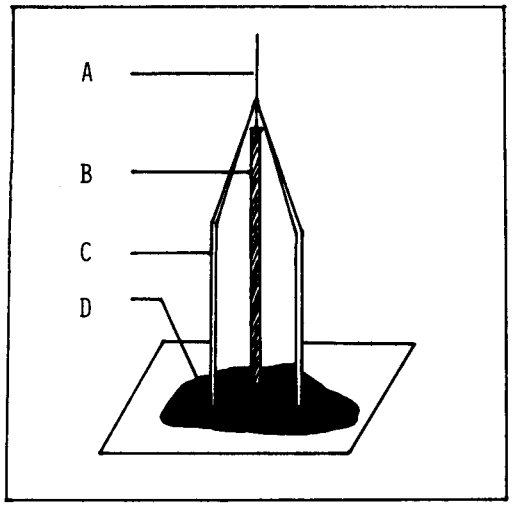

Fig. 1. Schematic diagram of carbon fibre electrode. A = Carbon fibre (100–200 μm diameter); B = lead wire; C = glass capillary; D = epoxy resin.

electrochemically pretreated at 1.2 V. First the background current was observed and then, when the applied current had increased anodically for 15 min, pretreatment was stopped to avoid anodic damage and the electrodes were oven-dried again for 5 min in preparation for the immobilization of enzymes.

Enzyme immobilization. ChO (5 U) and 2 mg of BSA were dissolved in 500 μl of water and 0.2 g of an 11% solution of PVA–SbQ was added. The electrodes were dipped into the solution for 10 min. The electrodes were exposed to fluorescent light for 15 min in order to entrap the enzymes within the polymer.

Nafion coating to remove interfering signal from ascorbic acid. Ascorbic acid is an electroactive substance that can interfere with the electronic signal output from choline or acetylcholine when using biological samples [8], hence it is important to discriminate each signal.

A Nafion coating was applied after the immobilization procedure, by dip-coating the electrode in 5% Nafion solution for 10 s three times and air drying for 15 min. The coated electrode was viewed under a scanning electron microscope to ensure that the Nafion coating was complete. The film thickness was not determined.

Serum sample preparation

Mice were anaesthesized with nembutal (50 mg ml^{-1}), followed by extraction of whole blood from the heart. The blood samples were allowed to clot and were centrifuged at 3000 *g* for 10 min, after which the supernatant was transferred into a propylene tube and capped. All samples were stored at −40°C.

Characterization of acetylcholine and choline electrodes

Before application to the serum samples, the electrodes were characterized as shown in Table 1. When using the biosensor, the performance of the working electrodes needs to be assessed before application to biological samples. Table 1 shows that with the batch of three sets of acetylcholine and choline electrodes, the highest current obtained was 0.70 μA, linearity range 0.2–1 m*M*, a correlation coefficient (*R*) of 0.990 and a

TABLE 1

Characterization of acetylcholine and choline sensors

Sensor	Highest current (μA)	Linearity range (mM)	*R*	S.D. [a]	R.S.D. (%) [a]
Ach	0.70	0.2–1 mM	0.990	0.15	2.25
Ach	0.70	0.2–1 mM	0.984	0.14	2.0
Ach	0.70	0.2–1 mM	0.998	0.19	3.0
Ch	0.70	0.2–1 mM	0.977	0.16	2.56
Ch	0.70	0.2–1 mM	0.999	0.12	1.44
Ch	0.70	0.2–1 mM	0.994	0.17	3.4

[a] $n = 3$

relative standard deviation of < 3.0. These data served as standard data for comparison after application to serum samples. Acetylcholine characterization was included because when a choline sensor is applied to the serum it is in effect an acetylcholine sensor [9].

Measurement of AchE by amperometric method

Preliminary experiments were conducted using purified AchE. However, prior to amperometric measurements the cholinesterase was assayed by the method of Whittaker [10]; the thiocholine liberated was detected by its chromogenic reaction with DTNB (5,5′-dithio-bis(2-nitrobenzoic acid). All amperometric measurements were made in a cell with a working volume of 20 ml using 0.1 M MES buffer (pH 7.1). The potential was poised at 1.2 V and the temperature was maintained at 30°C with a thermostated water-circulation bath. Using the choline sensor the AchE activity for a saturated level amount was measured by adding an equivalent amount of acetylcholine chloride substrate (0.1 M) and the initial slope was calculated in terms of the change in current divided by change in time. On injection of the sample, the current rapidly increased and reached a steady-state response in less than 2 min with the choline sensor. Serum AchE activity was measured in the same manner as that of the purified enzymes. Acetylcholine was added to the buffer solution several minutes before the enzyme assay in order to minimize its non-enzymatic decomposition.

RESULTS AND DISCUSSION

Electrochemical pretreatment and nafion coating

In this work electrochemical pretreatment was used merely to enhance the sensitivity of carbon fibres. The pretreatment of all carbon surfaces prior to an electrochemical is vital for obtaining consistent, reproducible results [11]. The Nafion coating prevents interference from the ascorbic acid signal [12]. Figure 2 illustrates the effect of ascorbic acid on the electronic output signal of choline. As shown, at the same concentrations of ascorbic acid and choline, taking the difference between their current signals indicates how much ascorbic acid could affect the choline sensor.

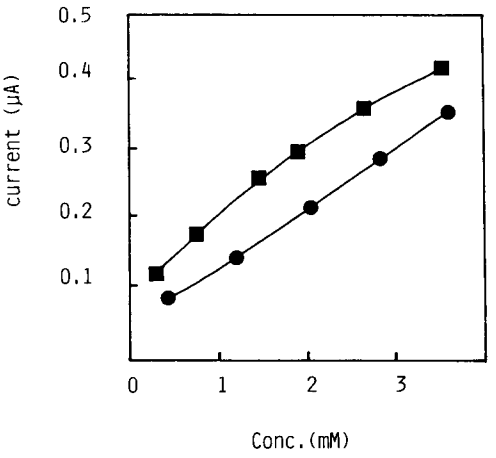

Fig. 2. Effect of ascorbic acid on choline sensor in 0.1 M MES buffer at pH 7.1. Ascorbic acid (final conc. 3 mM); choline (final conc. 3 mM). ■ = Ascorbic acid response; ● = choline response.

The unusual transport and selectivity properties of Nafion have been ascribed to its structure. On a molecular scale, it consists of a hydrophobic fluorocarbon phase and hydrophilic sulphonic acid phase [13]. In addition with the Nafion coating there was a decrease in the high background current coming from the working electrodes.

Immobilization procedure

ChO was entrapped in the photopolymer network via a cross-linking method by exposing the polymer to light of wavelength 300–460 nm, when it was insolubilized by cyclodimerization of the styrylpyridinium group. The principle involved in the immobilization of enzymes as developed by Ichimura and Watanabe [14] using PVA–SBQ to entrap bioactive material (see Fig. 3) is of particular interest because, owing to the mild conditions for network formation of the polymer matrix, no change in pH or temperature is necessary. Above all, this type of immobilization can preserve the native properties of the entrapped biocatalyst, as there is no chemical change to the biocatalyst molecule. Albumin was used because it serves well as a macromolecular support for enzyme immobilization.

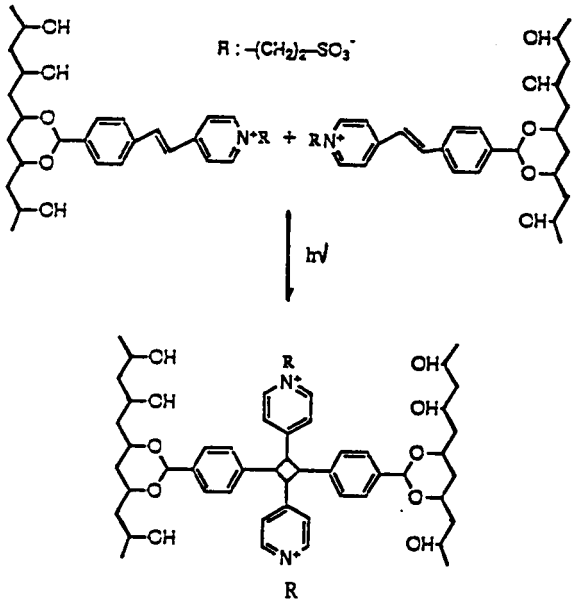

Fig. 3. Structure of PVA–SbQ, a photocross-linkable polymer containing poly(vinyl alcohol) with styrylpyridinium groups.

Calibration graph for choline sensor

Typical calibration graphs were obtained using serum samples (Fig. 4). It can be seen that the current is a linear function of acetylcholine concentration between 0.05 and 3 mM in 10 μl of serum as a source of AchE activity. The linearity range corresponds to the K_m value for ChO of 1.2 mM. Concentrations of the analyte from 0.05 to 5 mM could be detected. The increase in the detection range compared with the in vitro characterization of electrodes is due to the Nafion coating, which has the capability of reducing the high background current that occurred when the PVA–SbQ was used [15].

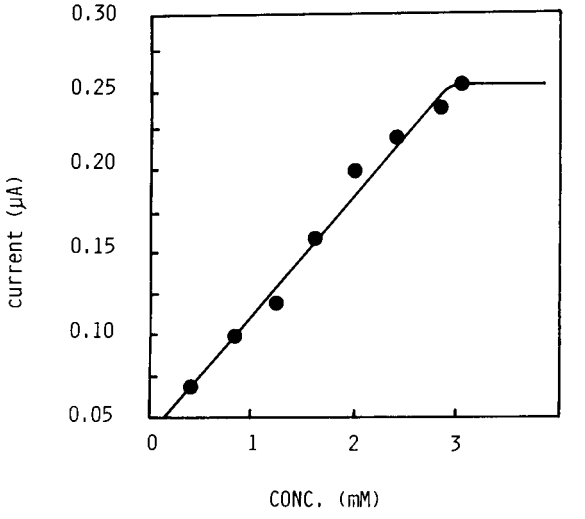

Fig. 4. Typical calibration graph for the choline sensor in a supporting electrolyte of 0.1 M MES buffer (pH 7.1) containing 10 μl of serum as source of esterase activity and with 3 mM acetylcholine chloride substrate concentration.

Determination of esterase activity

The enzyme activity of purified AchE was first measured as a control in the determination of AchE in serum. It should be noted that AchE is considered to be the true cholinesterase in blood. With a small volume of only 10 μl the enzymatic reaction was measured in terms of current versus time. Using the fabricated choline sensor the initial slope, expressed as μA min^{-1}, was calculated against AchE activity equivalent to the volume of the purified enzymes injected into the system, and of which an equivalent amount of acetylcholine substrate was made to react. As an example, with an initial slope of 0.14 μA per 5 min, it gave an equivalent of 10 U of AchE (Fig. 5). This value was set as the standard for comparison for the biological samples. For serum with the same volume it gave 25 U of AchE (Fig. 5b). The AchE activity was calculated in international units (U) per litre of serum, where 1 U is defined as the amount that forms 1 μmol of choline per minute under the present conditions. A straight line was obtained when the activity was plotted against the slope (current increase per minute). Table 2 compares the present method and the spectrophotometric method. The results demonstrate that the present system gives high performance in terms of relative sensitivity.

A typical response curve is shown in Fig. 6. The response time is faster than that of previously fabricated sensors. Figure 6 also shows that AchE is the rate-determining step of the catalytic reaction. The amperometric response using serum samples from rat gave a high activity. Interference from the ascorbic acid signal could be discounted owing to the use of the Nafion coating. This is essentially due to the structure of Nafion,

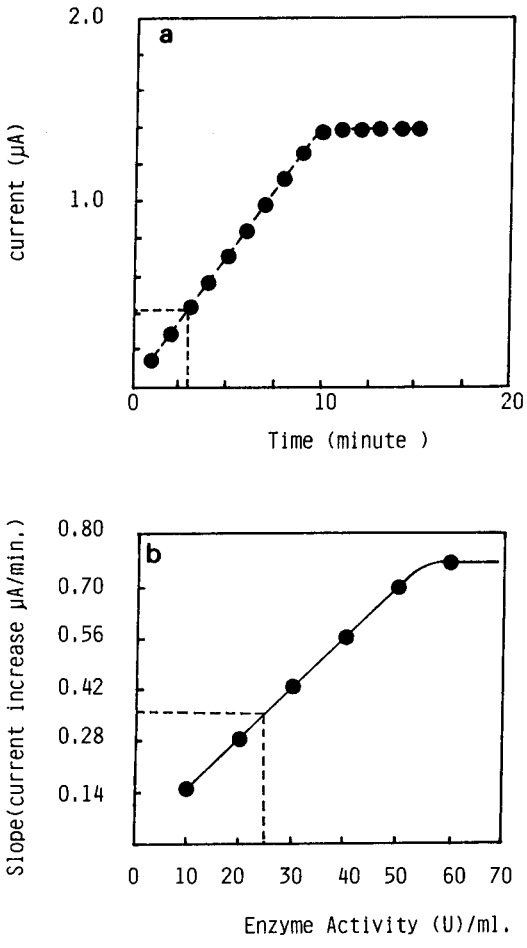

Fig. 5. (a) Enzyme-catalysed reaction of purified AchE expressed as current increase versus time, obtained using a carbon fibre immobilized with ChO using PVA–SbQ with a sample volume of 10 μl and with an initial slope value of 0.14 μA min^{-1}, giving an equivalent amount of 10 U. (b) Calibration graph for the relationship between AchE (purified) and slope (current increase per minute) in 0.1 M MES buffer (pH 7.1).

which can extract cationic species and preconcentrate them in the film [16]. Overlapping of oxidation potentials is also avoided.

Stability of the sensor

In a typical biosensor experiment, either be operational or long-term stability can be important. In terms of operational stability, in a batch-wise procedure the sensor showed no difference in activity after the first and twentieth time of use. The long-term stability was good; when the enzyme film was stored at 5°C, no decrease in activity was observed after 1.5 months.

TABLE 2

Comparison between the present method and the spectrophotometric method

Serum No.	Activity of AchE in serum (U) [a]	
	Biosensor	Spectrophotometric method
1	25	20
2	28	26
3	30	28

[a] 1 U will hydrolyse 1.0 μmol of acetylcholine to choline per minute at pH 8.0 at 37°C.

Conclusion

The present micro-choline sensor described here could provide a new assay for determining ChE levels in serum with a small volume of 10 μl. The enzymic–amperometric method has the clear advantage over the spectrophotometric method that it can be used when the solutions to be analysed are turbid or coloured. Determination of AchE activity in biological fluids still requires both sensitive and easy to perform methods, and

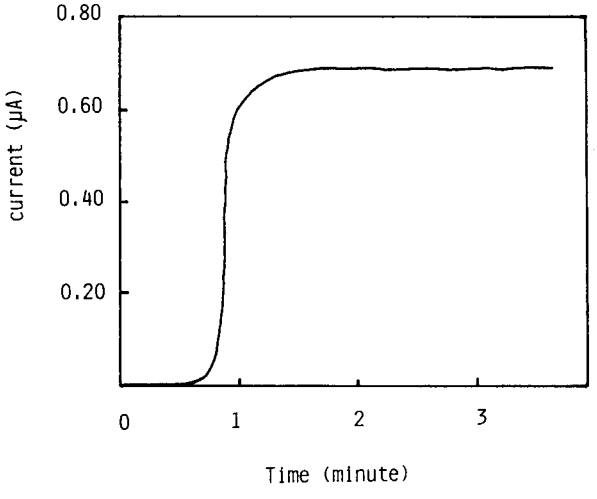

Fig. 6. Amperometric response profile of choline sensor after reaching a steady-state current with injection of 0.1 mM acetylcholine chloride in 20 ml of MES buffer solution (pH 7.1).

in this respect biosensors are attractive devices. The extension of this work to the determination of organophosphorus compounds in human serum will undoubtedly lead to a very useful sensor.

The authors are grateful to Mr. Aristotle Malay Coronel for assistance with the manuscript.

REFERENCES

1 T. Yao, Anal. Chim. Acta, 153 (1983) 169.
2 G. Palleschi, M.G. Lavagnini, D. Moscone and R. Pilloton, Biosensors Bioelectron., 5 (1990) 27.
3 K. Harlin and P.F. Ross, J. Assoc. Off. Anal. Chem., 73 (1990) 616.
4 A.J.M. Starrenburg and G.C. Burger, IEEE Trans. Biomed. Eng., BME-29 (1982) 352.
5 L. Jeune and F. Jourdan, J. Comp. Neurol., 314 (1991) 383.
6 M.G. Garguilo, N. Huynh, A. Proctor and A.C. Michael, Anal. Chem., 65 (1993) 523.
7 J.L. Ponchon, R. Cespuglio, F. Gonon and M. Jouvet, Anal. Chem., 51 (1979) 1483.
8 G. Nagy, M. Rice and R. Adams, Life Sci., 31 (1982) 2611.
9 M. Mascini and D. Moscone, Anal. Chim. Acta, 179 (1986) 439.
10 M. Whittaker, in Methods of Enzymatic Analysis, Vol. 4, 1984, pp. 15–74.
11 D. Wise, Applied Biosensors, Butterworth, Boston, 1989, pp. 1–37.
12 E.N. Navera, M. Suzuki, E. Tamiya, T. Takeuchi and I. Karube, Electroanalysis, 5 (1993) 17.
13 J. Jeddy and N. Vanderbor, J. Electroanal. Chem., 235 (1987) 299.
14 K. Ichimura and S. Watanabe, J. Polym. Sci., 22 (1984) 439.
15 E.N. Navera, K. Sode, E. Tamiya and I. Karube, Biosensors Bioelectron., 6 (1991) 675.
16 G.A. Gerhardt, Brain Res., 290 (1984) 390.

ANALYTICA CHIMICA ACTA, VOL. 281 (1993)

AUTHOR INDEX

Analytica Chimica Acta, 281 (1993) 686
Elsevier Science Publishers B.V., Amsterdam

Errata

Anal. Chim. Acta, 277 (1993) 205–214
The name of the second author was accidentally omitted. The authors of the paper are A. Singh *and* F.C. Garner.

Anal. Chim. Acta, 276 (1993) 335–340
Page 339, Fig. 6, the legend should read: "Relationship of H_2O_2/O_2 *P* ratio with membrane pore radius for uncoated (•) and organosilane coated (○) polycarbonate membranes". The ordinate of Fig. 6 should be labelled: "Ratio of H_2O_2/O_2 *P* values".

PUBLICATION SCHEDULE FOR 1994

	S'93	O'93	N'93	D'93	J	F						
Analytica Chimica Acta	281/1 281/2 281/3	282/1 282/2 282/3	283/1 283/2	283/3 284/1 284/2	284/3 285/1 285/2	285/3 286/1 286/2						
Vibrational Spectroscopy		6/1			6/2							

INFORMATION FOR AUTHORS

Detailed "Instructions to Authors" for *Analytica Chimica Acta* was published in Volume 256, No. 2, pp. 373–376. Free reprints of the "Instructions to Authors" of *Analytica Chimica Acta* and *Vibrational Spectroscopy* are available from the Editors or from: Elsevier Science Publishers B.V., P.O. Box 330, 1000 AH Amsterdam, The Netherlands. Telefax: (+31-20) 5862845.

Manuscripts. The language of the journal is English. English linguistic improvement is provided as part of the normal editorial processing. Authors should submit three copies of the manuscript in clear double-spaced typing on one side of the paper only. *Vibrational Spectroscopy* also accepts papers in English only.

Abstract. All papers and reviews begin with an Abstract (50–250 words) which should comprise a factual account of the contents of the paper, with emphasis on new information.

Figures. Figures should be prepared in black waterproof drawing ink on drawing or tracing paper of the same size as that on which the manuscript is typed. One original (or sharp glossy print) and two photostat (or other) copies are required. Attention should be given to line thickness, lettering (which should be kept to a minimum) and spacing on axes of graphs, to ensure suitability for reduction in size on printing. Axes of a graph should be clearly labelled, along the axes, outside the graph itself. All figures should be numbered with Arabic numerals, and require descriptive legends which should be typed on a separate sheet of paper. Simple straight-line graphs are not acceptable, because they can readily be described in the text by means of an equation or a sentence. Claims of linearity should be supported by regression data that include slope, intercept, standard deviations of the slope and intercept, standard error and the number of data points; correlation coefficients are optional.

Photographs should be glossy prints and be as rich in contrast as possible; colour photographs cannot be accepted. Line diagrams are generally preferred to photographs of equipment.

Computer outputs for reproduction as figures must be good quality on blank paper, and should preferably be submitted as glossy prints.

Nomenclature, abbreviations and symbols. In general, the recommendations of the International Union of Pure and Applied Chemistry (IUPAC) should be followed, and attention should be given to the recommendations of the Analytical Chemistry Division in the journal *Pure and Applied Chemistry* (see also *IUPAC Compendium of Analytical Nomenclature, Definitive Rules*, 1987).

References. The references should be collected at the end of the paper, numbered in the order of their appearance in the text (*not* alphabetically) and typed on a separate sheet.

Reprints. Fifty reprints will be supplied free of charge. Additional reprints (minimum 100) can be ordered. An order form containing price quotations will be sent to the authors together with the proofs of their article.

Papers dealing with vibrational spectroscopy should be sent to: Dr J.G. Grasselli, 150 Greentree Road, Chagrin Falls, OH 44022, U.S.A. Telefax: (+1-216) 2473360 (Americas, Canada, Australia and New Zealand) or Dr J.H. van der Maas, Department of Analytical Molecule Spectrometry, Faculty of Chemistry, University of Utrecht, P.O. Box 80083, 3508 TB Utrecht, The Netherlands. Telefax: (+31-30) 518219 (all other countries).

0003-2670/93/$06.00

This issue is printed on acid-free paper.

PRINTED IN THE NETHERLANDS

COAL

Typology - Physics - Chemistry - Constitution

Third, Completely Revised Edition

By **D.W. van Krevelen**

The first edition of the book *"Coal: Typology - Chemistry - Physics - Constitution"* appeared in 1961. In 1981 a new edition was published in which the text was unaltered proving that after 20 years the book was still considered a standard work in its field. The enormous activities in the 80's in the field of coal conversion processes (especially gasification and liquefaction) and the equally amazing development of instrumental techniques of observation and analysis prompted a complete revision and update of the book. The present edition contains almost 1000 pages compared to the 514 pages of its predecessors of 1961 and 1981. The number of illustrations has greatly increased from 253 to 574 and that of the tables from 76 to 208. These figures amply testify to the increase in coal research.

Compared with its former editions, the present book treats a considerable number of new subjects: modern concepts of geotectonics and of organic geochemistry; the problem of pseudohomogeneity of vitrinite; developments of the classification and systematics of coals and coal components (macerals); an exposé on electron microscopy and the most important instrumental physical methods of analysis (FTIR, NMR, ESCA and analytical pyrolysis combined with gas chromatography and mass spectroscopy); the principles of physical-statistical structure analysis based on the concept of additivity of a large number of molar functions; a revision of Seyler's ideas of discrete steps in coalification; an essay on coal fluorescence; and the survey on magnetic properties - magnetic susceptibility and magnetic resonance - is considerably enlarged. completely new chapter is added on cohesion and adhesion phenomena as found in coals. The chapter on solvent extraction and solubilisation is significantly enlarged and new concepts are discussed. The actions of hydrogen, molecular oxygen and oxidising agents on coal are updated and a newly written chapter treats the *"grand processes"* of coal conversion (combustion, gasification, carbonisation and liquefaction). Coal constitution in its diverse aspects is revised with a practically complete survey of many proposed coal models. Essays on synthetic coal analogues and on the simulation of natural coalification are added. Also new is the compendium, a set of comprehensive tables, containing the most important numerical data of this book in a fully comparative form.

Every chapter has its own bibliography, divided into general references (leading books on the treated subject) and special references, which are quotations of scientific papers discussed in the text. The extensive subject index, complete index of names and the compendium are provided in order to facilitate usage as an encyclopedic work.

Contents:

© 1993 Hardbound
Price: Dfl. 695.00 (US $ 397.00)
ISBN 0-444-89586-8

ORDER INFORMATION

For USA and Canada
ELSEVIER SCIENCE PUBLISHERS
Judy Weislogel, P.O. Box 945
Madison Square Station
New York, NY 10160-0757
Fax: (212) 633 3880

In all other countries
ELSEVIER SCIENCE PUBLISHERS
P.O. Box 330
1000 AH Amsterdam
The Netherlands
Fax: (+31-20) 5862 845

US$ prices are valid only for the USA & Canada and are subject to exchange rate fluctuations; in all other countries the Dutch guilder price (Dfl.) is definitive. Customers in the European Community should add the appropriate VAT rate applicable in their country to the price(s). Books are sent postfree if prepaid.

ELSEVIER
SCIENCE PUBLISHERS

0003-2670(19930924)281:3;1-5